Stress-Induced Mitochondrial DJ-1: Role of Parkin, Pink1 and VDAC1

Sarah Hewitt

Thesis submitted to the Faculty of Graduate and Postdoctoral Studies in partial fulfillment of the requirements for a doctoral degree in Neuroscience

Department of Cellular and Molecular Medicine

Faculty of Medicine

University of Ottawa

Table of Contents **Page number**

Abstract

Parkinson's disease (PD) is the second most common neurodegenerative disease and is characterized by motor symptoms such as tremor, rigidity, akinesia and postural instability. Approximately 90% of the cases are due to unknown causes however a familial inheritance has been shown for about 10% of cases. Loss-of-function mutations in DJ-1 cause early-onset PD. Originally identified as an oncogene, DJ-1 has since had many functions attributed to it but its major role in the cell seems to be oxidative stress handling. We have previously demonstrated that DJ-1 deficiency results in hypersensitivity of cells to oxidative stress. Additionally, mitochondria from DJ-1 null mice are fragmented and produce more ROS. To better understand the relationship between DJ-1, cell survival and mitochondria, we investigated the possible interaction between DJ-1 and the mitochondrial protein voltage dependent anion channel 1 (VDAC1). Here we show mitochondrial translocation of DJ-1 following oxidative stress in murine embryonic fibroblasts (MEFs) and primary cortical neurons, a process dependent on Pink1 and Parkin. Additionally, we confirm that DJ-1 and VDAC1 interact and that stress-induced mitochondrial translocation of DJ-1 depends on VDAC1. Deficiency of VDAC1 in primary cortical neurons results in decreased survival, increased ROS production following extended stress, fragmented mitochondria and decreased mitochondrial ATP production. We also demonstrate that there is substantially less matrix-localized DJ-1 in VDAC1 deficient cells. Finally, we demonstrate that decreased mitochondria ATP production can signal for DJ-1 translocation to mitochondria. Taken together, we suggest that mitochondrial translocation of DJ-1 is a two-step process. First, a signal, perhaps decreased mitochondrial ATP production, induces DJ-1 translocation to

mitochondria. Second, DJ-1 localizes to the matrix in a VDAC1-dependent manner. Our work suggests that stress-induced mitochondrial localization of DJ-1, specifically to the matrix, is regulated by VDAC1 to promote survival possibly by promoting ATP production.

Acknowledgements

This dissertation exists due to the significant time and effort put into the project by both myself and numerous other individuals during my time in Dr. David Park's laboratory at the University of Ottawa, Department of Cellular and Molecular Medicine.

I would like to first thank my supervisor. Dr. David Park, for his continued support throughout my graduate studies. I am eternally grateful for his guidance, expertise and wisdom. I also want to extend my appreciation to my graduate advisory committee members – Dr. Ruth Slack, Dr. Michael Schlossmacher, and Dr. Heidi McBride – for their support and advice throughout the years.

I would like to thank my family and friends for their continued love, support and patience throughout my graduate studies. Every step, no matter how hard, they have been there to keep me inspired and to keep me motivated.

I would like to thank the current and former members of the Park and Slack laboratories. To Dr. Isabella Irrcher, for mentoring me in the beginning and introducing me to the world of mitochondria. To Dr. Alvin Joselin, for a great collaboration and important part of this dissertation. To Dr. Mireille Khacho, for invaluable input into all aspects of my project. To Dr. Maxime Rousseaux, Dr. Hossein Aleyasin, Dr. Mohammad Parsanejad, Paul Marcogliese and Katie Don-Carolis for being part of the 'DJ-1 Team' and providing so much support and assistance. A special thank you to Dr. Yasmilde Rodriguez Gonzalez for the help in editing of this dissertation. Thank you to Steve Callaghan, for all his technical support and for keeping the experiments (and the lab!) running smoothly.

I would like to thank the staff of the Department of Cellular and Molecular Medicine and Neuroscience Program as well as the staff at the Faculty of Medicine for their assistance throughout my graduate studies.

Finally I would like to thank my funding sources: Parkinson Society Canada (Graduate Student Award); Ontario Graduate Scholarship; and Canadian Institute of Health Research (Doctoral Award).

If you can imagine it, you can achieve it

If you dream it, you can become it

– *William Arthur Ward*

List of Manuscripts

I. ROS-dependent regulation of Parkin and DJ-1 localization during oxidative stress in neurons.

Joselin AP[#], **Hewitt SJ**[#], Callaghan SM, Kim RH, Chung YH, Mak TW, Shen J, Slack RS, Park DS.

Human Molecular Genetics. 2012 Nov 15;21(22):4888-903. Epub 2012 Aug 7.

#Authors contributed equally

II. VDAC1 is important for sub-mitochondrial localization of DJ-1.

Hewitt SJ, Callaghan SM, Brini M, Craigen WJ, Figeys D, Slack RS, Park DS.

This manuscript is in preparation for submission.

Appended Articles:

I. DJ-1 protects the nigrostriatal axis from the neurotoxin MPTP by modulation of the AKT pathway.

Aleyasin H[#], Rousseaux MW[#], Marcogliese PC, **Hewitt SJ**, Irrcher I, Joselin AP, Parsanejad M, Kim RH, Rizzu P, Callaghan SM, Slack RS, Mak TW, Park DS.

Proceedings of the National Academy of Science USA. 2010 Feb 16;107(7):3186-91. Epub 2010 Jan 26.

#Authors contributed equally

II. Loss of the Parkinson's disease-linked gene DJ-1 perturbs mitochondrial dynamics.

Irrcher I, Aleyasin H, Seifert EL, **Hewitt SJ,** Chhabra S, Phillips M, Lutz AK, Rousseaux MW, Bevilacqua L, Jahani-Asl A, Callaghan S, MacLaurin JG, Winklhofer KF, Rizzu P, Rippstein P, Kim RH, Chen CX, Fon EA, Slack RS, Harper ME, McBride HM, Mak TW, Park DS.

Human Molecular Genetics. 2010 Oct 1;19(19):3734-46. Epub 2010 Jul 16.

III. Progressive dopaminergic cell loss with unilateral-to-bilateral progression in a genetic model of Parkinson disease.

Rousseaux MW, Marcogliese PC, Qu D, **Hewitt SJ**, Seang S, Kim RH, Slack RS, Schlossmacher MG, Lagace DC, Mak TW, Park DS.

Proceedings of the National Academy of Science USA. 2012 Sep 25;109(39):15918-23. Epub 2012 Sep 10.

List of Tables **Page number**

List of Figures **Page number**

Abbreviations

AAV	Adeno-Associated Virus
AD	Autosomal Dominant
ADP	Adenosine DiPhosphate
AIF	Apoptosis-Inducing Factor
ANOVA	ANalyis Of VAriance
ANT	Adenine-Nucleotide Transferase
Apaf-1	Apoptosis activating factor 1
AR	Autosomal Recessive
ARe	Androgen Receptor
ATP	Adenosine TriPhosphate
ATPβ	ATP synthase, β subunit
Bcl-2	B-cell lymphoma-2
Bcl-x_L	B-cell lymphoma-eXtra Large
Ca^{2+}	Calcium
CCCP	Carbonyl Cyanide m-Chloro Phenyl hydrazine
CM-H2DCFDA	5-(and-6)-ChloroMethyl-2', 7'-dichlorodiHydroFluorescin DiAcetate
CNS	Central Nervous System
COXI	Cytochrome c OXidase subunit I
COXV	Cytochrome c OXidase subunit V
DBS	Deep Brain Stimulation
DIABLO	Direct Inhibitor of Apoptosis Binding protein with LOw pI
DIV	Days *In Vitro*

DNA	DeoxyriboNucleic Acid
Drp1	Dynamin-related protein 1
ER	Endoplasmic Reticulum
ETC	Electron Transport Chain
FBS	Fetal Bovine Serum
Fis1	Mitochondrial Fission protein 1
GBA	β-GlucocereBrosidAse
GFP	Green Fluorescent Protein
GPe	Globus Pallidus external segment
GPi	Globus Pallidus internal segment
GSH	reduced Glutathione
GSSG	oxidized Glutathione
GST	Glutathione S-Transferase
HDAC1	Histone DeACetylase 1
HEK293	Human Embryonic Kidney 293 cell line
HRP	HorseRadish Peroxidase
IMM	Inner Mitochondrial Membrane
IMS	Inner Mitochondrial membrane Space
Kb	Kilo base pairs
KDa	KiloDalton
Keap1	Kelch-like ECH-associated protein 1
KO	KnockOut
LB	Lewy Body

LC	Locus Coeruleus
LC3	microtubule-associated protein Light Chain 3
L-DOPA	LevoDOPA
LHON	Leber's Hereditary Optic Neuropathy
LN	Lewy Neurite
LRRK2	Leucine Rich Repeat Kinase 2
MEFs	Mouse Embryonic Fibroblasts
Mff	Mitochondrial fission factor
Mfn	Mitofusin
MOI	Multiplicity Of Infection
mnSOD	manganese SuperOxide Dismutase
MPP^+	1-Methyl-4-PhenylPyridinium ion
MPPP	1-Methyl-4-Phenyl-4-Propionoxy Piperidine
mPTP	mitochondrial Permeability Transition Pore
MPTP	1-Methyl-4-Phenyl-1,2,5,6-TetrahydroPyridine
MQC	Mitochondrial Quality Control
mRNA	messenger Ribosomal Nucleic Acid
mtDNA	mitochondrial DNA
mtHSP70	mitochondrial Heat Shock Protein 70
NAC	N-Acetyl-Cysteine
NDUFA9	39kDa subunit of Complex I
Nrf2	Nuclear factor erythroid 2-related factor
$O_2^{\cdot -}$	superOxide

$OH^{\cdot}$	HydrOxyl radical
OMM	Outer Mitochondrial Membrane
Opa1	Optic atrophy 1
PBS	Phosphate Buffered Saline
PD	Parkinson's Disease
PERK	Pancreatic ER Kinase
PGC-1α	Peroxisome proliferator-activated receptor-γ Co-activator 1α
PIAS	Protein Inhibitor of Activated Signal transducers and activators of transcription
Pink1	PTEN-induced putative kinase 1
PSF	Pyramidine tract-binding protein-associated Splicing Factor
PTEN	Phosphatase and TENsin homolog
PVDF	PolyVinyliDene Fluoride
REM	Rapid Eye Movement
ROS	Reactive Oxygen Species
SDS	Sodium Dodecyl Sulfate
SEM	Standard Error of the Mean
SNc	Substantia Nigra pars compacta
SNr	Substantia Nigra pars reticulata
STN	SubThalamic Nucleus
TFAM	Mitochondrial Transcription Factor A
TH	Tyrosine Hydroxylase
Tom20	Translocator of the outer mitochondrial membrane 20

TSPO	TranSlocator PrOtein
UPDRS	Unified Parkinson's Disease Rating Scale
UPR	Unfolded Protein Response
VDAC	Voltage Dependent Anion Channel
VSP35	Vacuolar protein Sorting-associated Protein 35
VTA	Ventral Tegmental Area
WT	WildType

CHAPTER 1

General Introduction

1.1 Parkinson's Disease Etiology

Parkinson's disease (PD), the second most common neurodegenerative disease, affects approximately 1% of the population over 60 years of age and up to 4% of the population over 80 years old (de Rijk et al., 1995; Bower et al., 1999; de Lau and Breteler, 2006; Alves et al., 2008). The first medical description of the disease came from James Parkinson, who termed it 'shaking palsy', however this disease has been mentioned even earlier, by Leonardo da Vinci in the late 13th or early 14th century and even in 1350-1200 BCE by Egyptians (Parkinson, 1817; Forno, 1996). In the almost 200 years since the initial medical characterization, the complexity of this disease has been revealed – with patients showing variability in age of onset, symptoms, and responsiveness to therapies. As such, official diagnosis of this disease does not occur until autopsy, although a skilled neurologist can detect over 90% of cases (Hughes et al., 2002). Additionally, treatment is limited to symptomatic relief, due to the multifactorial nature of PD combined with an unknown cause in the majority of cases.

1.1.1 Idiopathic PD

Approximately 90% of all cases of PD are of unknown cause (idiopathic) and are most likely due to environmental factors (Alves et al., 2008). Numerous studies have suggested age as the number one risk factor for developing PD (Tanner and Langston, 1990; de Rijk et al., 1995; Bower et al., 1999; de Lau and Breteler, 2006). Although correlative at best, studies indicate that pesticide exposure, heavy metal exposure, well water consumption and rural living may contribute to idiopathic PD (Tanner and Langston, 1990; Gorell et al., 1998; Priyadarshi et al., 2001; Dick et al., 2007).

Interestingly, both cigarette smoking and coffee consumption have been linked to decrease incidence of PD (Ross et al., 2000; Hernán et al., 2002; Ritz et al., 2007).

Additionally, certain epigenetic changes, such as DNA methylation, chromatin remodelling and histone modification, may mediate susceptibility to these environmental factors (Urdinguio et al., 2009; Portela and Esteller, 2010; Jakovcevski and Akbarian, 2012; Feng et al., 2014). Most likely, pathogenesis of the disease occurs due to a combination of environmental and genetic factors.

1.1.2 Familial PD

Almost 20 years ago, the first study showing familial linkage in cases of PD emerged (Polymeropoulos et al., 1997). The development of stronger tools has allowed for identification of numerous genes linked with either autosomal dominant (AD) or autosomal recessive (AR) PD as well as several susceptibility genes (Hardy, 2010; Peeraully and Tan, 2012; Bras et al., 2015). Through the use of these genetic tools, 11 genes have been identified as having a causative role in development of monogenic typical or atypical PD (Table 1.1) (Klein and Westenberger, 2012; Bonifati, 2014; Bras et al., 2015). Genes including *α-synuclein*, *leucine-rich repeat kinase 2* (*LRRK2*), *vacuolar protein sorting-associated protein 35* (*VPS35*), *Parkin*, *PTEN-induced putative kinase 1* (*PINK1*), and *DJ-1* have been shown to be involved in familial PD.

Table 1.1. Summary of confirmed genes having a causative role in Parkinson's disease (PD). Here the confirmed genes responsible for familial PD are summarized with locus, onset, type of inheritance and classification of symptoms. Onset varies in familial PD, with juvenile (<20 years old), early (<40 years old), and late (>50 years old) types. There are two methods of inheritance encountered - autosomal dominant (AD) and autosomal recessive (AR). Genetic forms of PD can either be classified as classical, in which symptoms are similar to idiopathic PD, or atypical, in which additional symptoms may exist.

Gene (Locus)	Onset	Inheritance	Type	References
α-SYNUCLEIN (*PARK1,4*)	Early to late	AD	Aggressive	(Polymeropoulos et al., 1997)
PARKIN (*PARK2*)	Early	AR	Slow	(Kitada et al., 1998)
PINK1 (*PARK6*)	Early	AR	Slow	(Valente et al., 2004)
DJ-1 (*PARK7*)	Early	AR	Slow	(Bonifati et al., 2003)
LRRK2 (*PARK8*)	Late	AD	Typical	(Zimprich et al., 2004)
ATP13A2 (*PARK9*)	Juvenile	AR	Atypical	(Ramirez et al., 2006)
PLA2G6 (*PARK14*)	Juvenile	AR	Atypical	(Paisán-Ruíz et al., 2009)
FBXO7 (*PARK15*)	Juvenile	AR	Atypical	(Shojaee et al., 2008)
VPS35 (*PARK17*)	Late	AD	Typical	(Vilariño-Güell et al., 2011; Zimprich et al., 2011)
DNAJC6 (*PARK19*)	Juvenile	AR	Atypical	(Edvardson et al., 2012)
SYNJ1 (*PARK20*)	Juvenile	AR	Atypical	(Krebs et al., 2013)

The well-characterized *α-synuclein* and *LRRK2*, as well as the more recently discovered *VPS35*, show AD inheritance, in which only one mutated allele is required to elicit an effect. Mutations in *α-synuclein* include point mutations as well as gene multiplication events (two or three copies) and account for ~2% of all familial PD cases (Polymeropoulos et al., 1997; Krüger et al., 1998; Chartier-Harlin et al., 2004; Ibáñez et al., 2004; Ibáñez et al., 2009; Nuytemans et al., 2010). There appears to be a dosage effect with *α-synuclein*, as individuals with four copies of the gene show early-onset PD (<50 years old at age of onset) and faster disease progression, compared to individuals with three copies who show late-onset PD (Chartier-Harlin et al., 2004; Fuchs et al., 2007). Mutations in *LRRK2* occur in 2-40% of both the late-onset AD as well as sporadic PD, depending on the population (Lesage et al., 2006; Ozelius et al., 2006). Over 80 mutations in LRRK2 have been identified, with 6 of them showing pathological involvement in PD (Zimprich et al., 2004; Nuytemans et al., 2010). Individuals with these mutations typically show mid-to-late onset with slow disease progression, and some mutations show an age-dependent penetrance (Healy et al., 2008). Mutations in *VPS35* were identified by two separate groups concurrently (Vilariño-Güell et al., 2011; Zimprich et al., 2011). Both groups demonstrated that these patients have a missense mutation in *VPS35* that results in typically late-onset of the disease (Vilariño-Güell et al., 2011; Zimprich et al., 2011). Further investigation has shown relatively similar symptoms to idiopathic PD but with increased incidence of depression, although the sample size is quite limited (Struhal et al., 2014).

Parkin, *Pink1*, and *DJ-1* mutations resulting in PD are all inherited in an AR manner. The second identified gene to cause PD and the first to be AR-associated was

Parkin (Kitada et al., 1998). Mutations in this gene are responsible for ~10-20% of all early-onset PD and up to 77% of cases with age of onset <30 years old (Lücking et al., 2000; Klein and Lohmann-Hedrich, 2007). An impressive 887 mutations in *Parkin* have been identified, resulting in 147 unique changes to the protein (Klein and Westenberger, 2012). *Parkin* mutations typically result in PD that is early-onset and with slow disease progression (Kitada et al., 1998; Lücking et al., 2000; Lohmann et al., 2003; Klein and Lohmann-Hedrich, 2007). The second most common gene associated with early-onset PD is *Pink1*, with approximately 1-9% of this group carrying mutations for this gene (Rogaeva et al., 2004; Valente et al., 2004; Bonifati et al., 2005). Mutations in *DJ-1* are by far the most rare mutations for early-onset PD, counting for only 1-2% of these cases (Abou-Sleiman et al., 2003; Bonifati et al., 2003; Pankratz et al., 2006). These mutations of *DJ-1* will be more thoroughly discussed in Section 1.7.2.

Additional loci have been linked to PD, however no specific genes within these regions have been identified as yet (Bras et al., 2015). Additionally, one risk gene and 24 risk loci have been identified (Bras et al., 2015). The risk gene, *β-glucocerebrosidase* (*GBA*), is particularly interesting, as over 300 mutations in it are associated with the lysosomal storage disorder Gaucher disease (Hruska et al., 2008). Homozygous or heterozygous mutations in *GBA* are also found in up to 15% of autopsy-confirmed PD cases (Goker-Alpan et al., 2004; Lwin et al., 2004; Sidransky et al., 2009). *GBA* mutations occur 5 times more frequently in PD patients than controls (Sidransky et al., 2009). While mutations in this gene and other loci are associated with a medium to low risk of developing PD, they help give insight into the potential various pathways involved in the disease pathogenesis.

1.2 Parkinson's Disease Phenotypes

1.2.1 Motor Symptoms

The hallmark symptoms of PD include resting tremor, rigidity of limbs, akinesia and postural instability (Parkinson, 1817; Hoehn and Yahr, 1967; Lang and Lozano, 1998; Samii et al., 2004; Jankovic, 2008; Massano and Bhatia, 2012). Resting tremor is an involuntary rhythmic oscillatory movement that occurs during rest and disappears with active movement (Samii et al., 2004; Jankovic, 2008; Massano and Bhatia, 2012). It is the most easily identifiable and most common symptom in PD, with at least 70% of patients experiencing it (Hoehn and Yahr, 1967; Hughes et al., 1993; Samii et al., 2004; Jankovic, 2008). Resting tremor in PD typically occurs in extremities, especially the hands in a "pill rolling" type of movement (Samii et al., 2004; Jankovic, 2008; Massano and Bhatia, 2012). It occasionally involves the jaw, chin and lips but never the head/neck in PD patients (Jankovic, 2008; Massano and Bhatia, 2012). Rigidity of limbs refers to increased resistance and stiffness that persists throughout a range of movements involving both distal and proximal joints (Samii et al., 2004; Jankovic, 2008; Massano and Bhatia, 2012). A "cogwheel" motion is often observed in PD patients, where muscles respond with jerky movements due to the force used to move limbs (Samii et al., 2004; Jankovic, 2008; Massano and Bhatia, 2012). Akinesia (or bradykinesia) is the slowness in movement, particularly in planning, initiating and executing movement (Berardelli et al., 2001; Samii et al., 2004; Jankovic, 2008; Massano and Bhatia, 2012). Considered to be the most disabling of the cardinal symptoms, at least in early stages of PD, akinesia affects fine motor tasks such as handwriting and doing up buttons (Samii et al., 2004). Postural instability is an impairment in balance due to loss of properly functioning

postural reflexes (Samii et al., 2004; Jankovic, 2008; Massano and Bhatia, 2012). It is often absent in early stages of PD, particularly in younger patients (Samii et al., 2004; Jankovic, 2008). Postural instability leads to an increased risk of falling, and the frequency of falls is linked to disease severity (Koller et al., 1989; Samii et al., 2004; Williams et al., 2006; Jankovic, 2008; Massano and Bhatia, 2012).

These symptoms are thought to arise due to the selective loss of dopaminergic neurons in the *substantia nigra pars pacta* (SNc) and thus disruption of basal ganglia circuitry. These neurons are important in motor control, particularly in initiation of voluntary movement. The *substantia nigra* is part of the basal ganglia-thalamocortical circuitry, in which "direct" and "indirect" signalling pathways from the SNc lead to activation of the primary motor cortex and supplementary motor area via the thalamus (Figure 1.1).

Figure 1.1. Effect of Parkinson's disease on basal ganglia signalling. Simplified overview of signalling involved in both "direct" and "indirect" circuits originating from substantia nigra *pars compacta* (SNc). Loss of dopaminergic neurons in the SNc ultimately leads to enhanced inhibition of the thalamus by the globus pallidus internal segment (GPi), loss of cortical activation and loss of initiation of voluntary movement. Thickness of arrow indicates strength of transmission. SMA, supplementary motor area; M1, primary motor cortex; STN, subthalamic nucleus; GPe, globus pallidus external segment; SNr, substantia nigra *pars reticulata*.

A

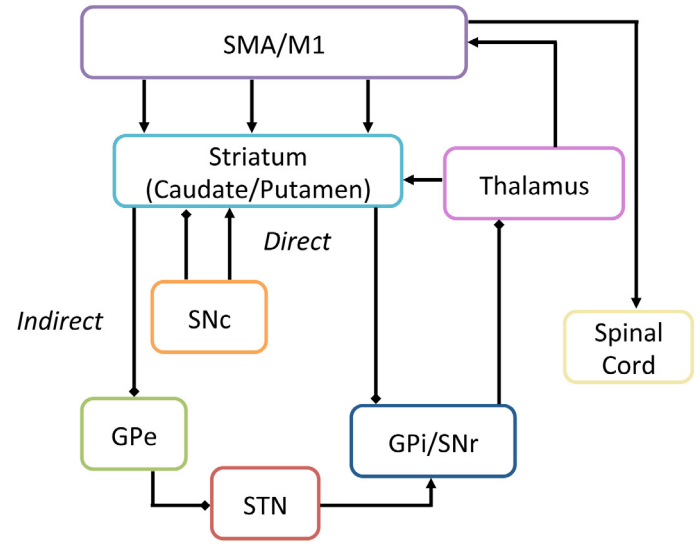
Normal Basal Ganglia Signaling
SMA/M1
Striatum
(Caudate/Putamen)
Thalamus
Direct
Indirect
SNc
Spinal
Cord
GPe
GPi/SNr
STN

B

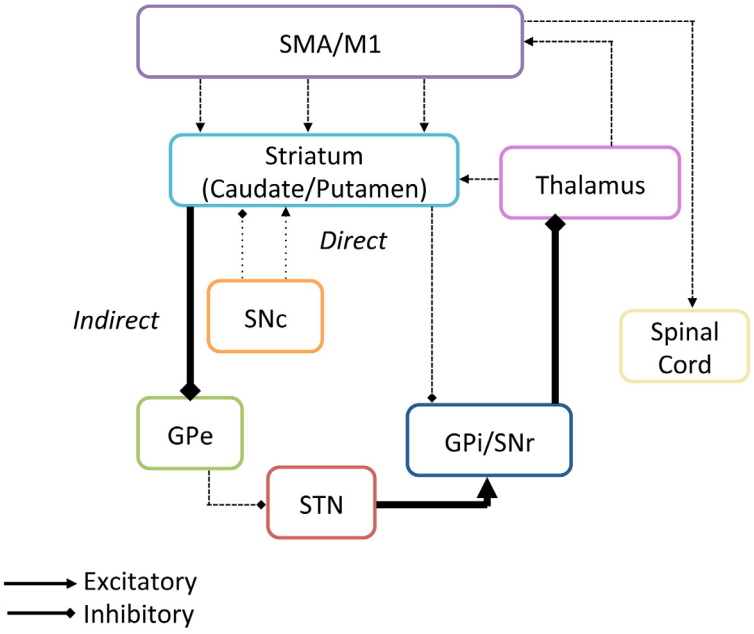
PD Basal Ganglia Signaling
SMA/M1
Striatum
(Caudate/Putamen)
Thalamus
Direct
Indirect
SNc
Spinal
Cord
GPe
GPi/SNr
STN
Excitatory
Inhibitory

The striatum, made up of the putamen and caudate, consists mostly (~95%) of medium spiny neurons that are rich in dopamine receptors (Kringelbach et al., 2007). In the "direct" circuit, a subset of these striatal neurons are activated by the dopaminergic transmission from the SNc, which in turn inactivate the globus pallidus internal segment (GPi), allowing for activation of the primary motor cortex (M1) and supplementary motor area (SMA) as the thalamus is no longer inhibited. In the "indirect" circuit, a separate subset of the striatal neurons are inhibited by the dopaminergic transmission from the SNc, which prevents the inhibition of the globus pallidus external segment (GPe), and stops the activation of the GPi via the subthalamic nucleus (STN). Loss of input from the SNc leads to an overall increase in inhibition of the thalamus, via loss of inhibition of the GPi by the direct pathway and inhibition of the GPe by the indirect pathway. Loss of thalamus signalling leads to loss of cortical activation and consequently loss of initiation of voluntary movement.

1.2.2 Non-Motor Symptoms

PD patients exhibit various non-motor symptoms throughout the stages of their disease. These symptoms include alterations in neuropsychiatric, sleep, autonomic, and sensory functions (Samii et al., 2004; Chaudhuri and Naidu, 2008; Jankovic, 2008; Poewe, 2008). Almost 40% of PD patients have dementia, with a 2-6 times higher risk versus the general population (Marder et al., 1995; Aarsland et al., 2001). Approximately 30-40% of PD patients suffer from depression (Poewe, 2008; Blonder and Slevin, 2011). The majority of PD patients encounter night time awakenings, at a rate three times higher than the general population (Stacy, 2002; Porter et al., 2008). A wide range of autonomic

symptoms are encountered by PD patients, such as constipation, bladder hyperactivity, erectile dysfunction and excessive sweating, which worsen with disease progression (Edwards et al., 1991; Singer et al., 1992; Sakakibara et al., 2001; Swinn et al., 2003; Verbaan et al., 2007; Jankovic, 2008; Poewe, 2008). Olfactory dysfunction affects anywhere from 70-100% of PD patients (Chaudhuri and Naidu, 2008; Simuni and Sethi, 2008).

Two early occurring symptoms, gastro-intestinal dysfunction and anosmia (loss of sense of smell), are thought to occur years before motor symptoms (Doty et al., 1988; Abbott et al., 2001; Braak et al., 2003; Braak et al., 2004; Ponsen et al., 2004; Poewe, 2008; Haehner et al., 2011). Additionally, rapid eye movement (REM) sleep behaviour disorder is frequently encountered and even considered to be a risk factor for PD (Schenck et al., 1996; Gagnon et al., 2006). With some non-motor symptoms occurring before the motor symptoms, they are ideal early indicators of the disease.

1.3 Pathology

1.3.1 Substantia Nigra Pars Compacta (SNc)

The most visible hallmark of PD in the post-mortem human brain is the striking loss of pigmented cells in the SNc, located in the basal ganglia (Parkinson, 1817; Greenfield and Bosanquet, 1953; Hoehn and Yahr, 1967; Bernheimer et al., 1973; Gaspar and Gray, 1984; Hughes et al., 1993). It is proposed that at least 30% of these neurons are lost by the time clinical symptoms arise (Fearnley and Lees, 1991; Hilker et al., 2005; Greffard et al., 2006). These dopaminergic neurons contain melanin, a naturally dark substance and hence are easily identifiable and their absence is quickly detected visually

during post-mortem analysis (Hughes et al., 1993; Lang and Lozano, 1998). Additionally, loss of dopamine terminals and decreased dopamine levels in the striatum have been observed (Foix and Nicolesco, 1925; Bernheimer et al., 1973; Nyberg et al., 1983; Scherman et al., 1989; Wilson et al., 1996).

Fritz Heinrich Lewy first described the presence of intracytoplasmic protein aggregates called Lewy Bodies (LBs) and Lewy Neurites (LNs) in PD post-mortem brains (Greenfield and Bosanquet, 1953; Okazaki et al., 1961; Forno, 1996; Lang and Lozano, 1998; Holdorff, 2002). These aggregates appear to have a dense core, surrounded by filamentous material and contain α-synuclein and ubiquitin (Okazaki et al., 1961; Forno, 1996; Spillantini et al., 1997; Baba et al., 1998). It is unclear as to whether these aggregates are a protective mechanism or damage-inducing in the cell. It is proposed that oligomers and fibrils of α-synuclein as well as the aggregation process itself are neurotoxic, whereas LBs are protective (Maries et al., 2003; Ross and Poirier, 2005).

1.3.2 Locus Coeruleus (LC)

There is also select degeneration in non-dopaminergic areas such as the *locus coeruleus* (LC) (Greenfield and Bosanquet, 1953; Gaspar and Gray, 1984; Cash et al., 1987; Chan-Palay and Asan, 1989; German et al., 1992; Zarow et al., 2003), which may account for some of the non-motor symptoms observed in many patients. The LC is responsible for the physiological response to stress or panic and therefore its degeneration is thought to be responsible for sleep disturbances, especially during the REM sleep cycle of PD patients (García-Lorenzo et al., 2013).

1.3.3 Ventral Tegmental Area (VTA)

Adjacent to the SNc is a group of dopaminergic neurons termed the ventral tegmental area (VTA). There are mixed reports on the involvement of the VTA in PD pathology, however the consensus appears to be that this area is significantly less affected than the SNc in PD (Uhl et al., 1985; German et al., 1989; German et al., 1992; Dymecki et al., 1996; Alberico et al., 2015). Interestingly, some of the non-motor symptoms such as depression and anxiety found in some PD patients could be related to VTA dysfunction (Russo and Nestler, 2013; Alberico et al., 2015).

1.3.4 Braak Hypothesis

Thorough investigation of the central nervous system (CNS) for the presence of LBs demonstrated a progressive invasion of these proteinaceous inclusions that start in lower brain regions and spread upwards (Braak et al., 2002; Braak et al., 2004). Studying the areas of the brain and nervous system that exhibit LB pathology, together with the timing in which these LBs appeared in accordance to the progression of the disease, led Dr. Heiko Braak to propose a staging system to PD (Braak et al., 2002; Braak et al., 2004). As such, the Braak hypothesis suggests that in PD, the SNc is actually affected at the mid-way point of the disease, at which point the patients are clinically diagnosed (Braak et al., 2002; Braak et al., 2004). In the earlier stages, more caudal parts of the brain are affected by LB pathology and the disease progresses rostrally (Braak et al., 2002; Braak et al., 2004). It is proposed that only once LBs reach the midbrain, do patients become symptomatic (Braak et al., 2002). The more areas affected by LB

pathology, the higher the stage and thus the more severe the stage of the disease (Braak et al., 2002; Braak et al., 2004).

1.3.5 Disease Scale in Parkinson's Disease

PD is a degenerative disease, and as time passes, the symptoms of the disease worsen. Hoehn and Yahr were first to propose a scale in which severity of PD was ranked on a scale of 1-5, with 1 being the least and 5 being the most severe (Hoehn and Yahr, 1967). They did so to highlight the differences in symptoms between patients, in what seemed to be a fairly homogeneous disease population (Hoehn and Yahr, 1967). This study was the first to demonstrate how widely varied symptoms (and severity of these symptoms) were within the PD population. Numerous staging models have since been created and employed, making it difficult to compare assessments between the different models (Disease, 2003). As such, a more universal scale was created, termed the Unified Parkinson's Disease Rating Scale (UPDRS) (Disease, 2003). The UPDRS is comprised of four components – providing a comprehensive assessment of both motor and non-motor symptoms as well as additional complications with these symptoms (Disease, 2003). The stage of PD and identification of the most predominant symptoms often dictates the direction in which treatment is taken.

1.4 Current Therapies

Current therapy for PD consists of managing symptoms caused by the loss of dopaminergic neurons – while effective short-term, there is no long-term single medical

therapy for PD. The complexity of this disease leads to increasing difficulties in treatment, as one therapy could work for one patient but not another.

1.4.1 Dopamine Replacement

The most common drug administered for treatment of PD is levodopa (3,4-dihydroxyphenylalanine; L-DOPA), a precursor of dopamine (Lang and Lees, 2002; Goetz et al., 2005; Connolly and Lang, 2014). Dopamine cannot be administered directly as it does not cross the blood brain barrier. By increasing the amount of precursor available, the remaining dopaminergic neurons can produce more dopamine and thus the SNc neurons can compensate for the loss of cortical activation by the thalamus. Other pharmacological strategies that revolve around boosting available dopamine levels include dopamine agonists and monoamine oxidase inhibitors, which prevent degradation of dopamine (Lang and Lees, 2002; Goetz et al., 2005; Jankovic, 2008; Connolly and Lang, 2014).

PD patients go through "ON" and "OFF" phases in which they experience relief and subsequently no relief from the symptoms despite pharmacological treatment (Lang and Lees, 2002; Goetz et al., 2005; Connolly and Lang, 2014). Over time, the amount of "OFF" time increases as the effectiveness of treatment decreases (Chase, 1998; Ahlskog and Muenter, 2001; Jankovic, 2005; Jankovic, 2008; Connolly and Lang, 2014). Dosages can be adjusted to accommodate patients; however, within a few years of initial treatment, motor fluctuations as well as dyskinesia, or involuntary movement, develop and can become severely debilitating (Chase, 1998; Ahlskog and Muenter, 2001; Lang and Lees, 2002; Goetz et al., 2005; Jankovic, 2005; Jankovic, 2008; Connolly and Lang,

2014; Sharma et al., 2015). These unwanted motor symptoms are most likely partially due to the fact that physiological levels of dopamine transmission are not restored, and go through constant fluxes (Chase, 1998), nonetheless, the full molecular mechanism of L-DOPA-induced dyskinesia is not fully understood (Jenner, 2008; Sharma et al., 2015). Typically within 10 years of L-DOPA treatment, the negative side effects outweigh the benefits from the pharmacological treatment and the patient must seek alternative treatment options (Lang and Lees, 2002; Goetz et al., 2005; Cenci, 2007; Jenner, 2008; Connolly and Lang, 2014; Sharma et al., 2015).

1.4.2 Surgical Treatments

During the 1940s-1960s, specific lesioning techniques were employed to treat a variety of neurological issues, including PD (Meyers, 1940; Cooper, 1956). While the technique of lesioning the thalamus in PD patients proved to be successful, it was often marred by unwanted side effects from the invasiveness of the procedure, or from accidental lesioning of non-target tissue (Matsumoto et al., 1984; Tasker, 1998). The irreversible nature of this procedure also contributed to the possible negative outcome of this technique. It was in the late 1980s that a reversible lesioning technique was introduced in this context – deep brain stimulation (DBS) (Benabid et al., 1987). This technique opened the door for a safer option for treating PD outside of pharmacological methods.

The results from the first DBS procedure for treatment of PD was published by Dr. Benabid in 1987 and involved placement of electrodes in the ventral intermediate thalamic nucleus of the patient (Benabid et al., 1987). It had been discovered that

applying a frequency over 100Hz actually caused *inhibition* of the surrounding tissue, versus activation when the frequency was below 100Hz (Benabid et al., 1987; Kringelbach et al., 2007). This discovery led to the development of a reversible lesioning technique in which tissue did not have to be physically destroyed. Numerous targets in the basal ganglia that had previously been the focus of permanent lesioning techniques were now the main focus for the development of DBS to treat PD.

Unfortunately it still remains that only treatment, but no cure, exists for PD. In order to cure and even prevent this degenerative disease, we need to better understand the causes of the disease itself.

1.5 Parkinson's Disease Pathogenesis

1.5.1 Protein Aggregation

Proteinaceous bodies found throughout the cell body (LBs) and neurites (LNs) were found to contain aggregated α-synuclein and ubiquitin, amongst other proteins (Okazaki et al., 1961; Forno, 1996; Spillantini et al., 1997; Baba et al., 1998). The endoplasmic reticulum (ER) is responsible for the proper folding of proteins following their translation (Kaufman, 1999). The Unfolded Protein Response (UPR) is an ER stress mechanism, activated typically when an accumulation of unfolded and/or misfolded proteins occurs (Kaufman, 1999). Activation of this pathway leads to an overall reduction in translation and therefore less protein burden on the ER, while specifically upregulating translation of stress-response proteins (Kaufman, 1999). Various experimental models of PD have shown ER stress and activation of the UPR *in vitro* (Ryu et al., 2002). Post-mortem analysis of PD patients has also shown an increase in markers of ER stress and

induction of the UPR – specifically increased levels of phosphorylated pancreatic ER kinase (PERK) and its downstream target eukaryotic initiation factor 2α (eIF2α) in the SNc (Hoozemans et al., 2007).

Additionally, the PD-related Parkin is an E3 ubiquitin ligase that mediates proteasomal degradation of its targets following ubiquitination (Imai et al., 2000). The UPR increases levels of both Parkin mRNA and protein and overexpression of Parkin can protect against UPR-induced death (Imai et al., 2000). Loss of Parkin leads to an accumulation of its target proteins and this could play a role in the pathogenesis of the disease (Imai et al., 2000). The protein product of another PD gene, α-synuclein, is shown to aggregate, especially when mutated (Narhi et al., 1999). Expression of mutant α-synuclein *in vitro* increases ER stress and leads to significantly higher cell death compared to WT α-synuclein (Smith et al., 2005). Interestingly, transplant of embryonic nigral neurons to PD patients results in LB-like pathology of the transplanted tissue years later (Alves et al., 2008; Kordower et al., 2008). These findings suggest that PD-like pathology can propagate from the host tissue to the donor tissue, possibly via α-synuclein (Alves et al., 2008; Kordower et al., 2008). There are recent studies that indicate aggregated α-synuclein may indeed cause aggregation of soluble α-synuclein, in a similar fashion to the prion protein in prion disease (Volpicelli-Daley et al., 2011; Angot et al., 2012; Luk et al., 2012).

1.5.2 Inflammation

In addition to the proteinaceous inclusions throughout the brain, post-mortem studies of PD patients have found increased markers of inflammation and activated

microglia specifically localized to the *substantia nigra* and striatum (McGeer et al., 1988; Mogi et al., 1994; Mogi et al., 1996; Banati et al., 1998; Hunot et al., 1999; Imamura et al., 2003). The central nervous system was considered "immune privileged" due to the strict regulations of the blood brain barrier – limiting entry of molecules via tight junctions and monitoring by specific astrocytes and microglia (Hanisch and Kettenmann, 2007; Heneka et al., 2014). In the brain, microglia are considered the resident macrophages and are constantly surveying their environment (Hanisch and Kettenmann, 2007; Heneka et al., 2014). When activated, microglia are responsible for clearing dead or dying cells, as well as releasing various trophic factors (Batchelor et al., 1999; Hanisch and Kettenmann, 2007; Heneka et al., 2014). While a moderate level of activation is beneficial, extended periods of microglial activation can be harmful to otherwise healthy cells, due to the generation of reactive oxygen species (ROS) and cytokines (Hanisch and Kettenmann, 2007; Heneka et al., 2014).

Additionally, induction of inflammation either locally or systemically by the bacterial endotoxin lipopolysaccharide, causes specific loss of dopamine neurons in the *substantia nigra* (Herrera et al., 2000; Qin et al., 2007). The proof of concept that suppression of the immune system can be protective in an animal model of PD was shown by our group in two different studies, in which loss of components required for an immune-mediated inflammation response protects dopaminergic neurons in the *substantia nigra* against oxidative stress (Mount et al., 2007; Lira et al., 2011). It has been proposed that early stages of microglial activation is protective however over time this activation can become dysfunctional – it is this aberrant and extended activation of microglia that can cause neuronal death (Mosley et al., 2012; Heneka et al., 2014).

1.5.3 Oxidative Stress and Mitochondrial Dysfunction

It has been suggested that oxidative stress plays a role in dopaminergic cell death, with the finding that there is a decrease in the electron transport chain (ETC) complex I activity in addition to the presence of ROS-damaged end products in the *substantia nigra* of post-mortem PD patients (Dexter et al., 1989; Schapira et al., 1989; Lang and Lozano, 1998). As well, post-mortem examination of the frontal cortex of PD patients shows mitochondrial respiratory impairments, a modest decrease in complex I activity and an increase in oxidation products of protein and phospholipids (Navarro et al., 2009). While these findings are supportive of the notion of the role of oxidative stress in PD, they do not determine if in fact ROS is a cause for degeneration or simply a consequence. Interestingly, Parkinson-like symptoms have been observed in numerous patients following the administration of the heroin analogue 1-methyl-4-phenyl-4-propionoxy piperidine (MPPP) contaminated with 1-methyl-4-phenyl-1,2,5,6-tetrahydropyridine (MPTP) (Davis et al., 1979; Langston et al., 1983). Similarly, administration of MPTP to rodents results in the loss of dopamine and its metabolites in the nigrostriatal pathway as a result of dopaminergic cell death (Heikkila et al., 1984; Heikkila et al., 1985). Importantly the metabolite of MPTP, 1-methyl-4-phenylpyridinium ion (MPP^+), is a substrate for the dopamine transporter where it is targeted to mitochondria and inhibits complex I (Betarbet et al., 2000).

Another complex I inhibitor, rotenone, often found in pesticides, can cause progressive nigrostriatal dopaminergic degeneration in rats (Heikkila et al., 1985; Betarbet et al., 2000). Inhibition of complex I can lead to deregulated Ca^{2+} levels as well as decreased ATP synthesis (Sherer et al., 2002). Disruption of the ETC can also result

in increased levels of ROS that lead to oxidation of lipids, DNA and proteins (Sherer et al., 2002). An increase in ROS can induce damage to mitochondria when antioxidant defenses have been exhausted (Choi et al., 2006). Through a cycle of mitochondria dysfunction, decreased antioxidant potential, and increased ROS production, cell death is inevitable (Sherer et al., 2002; Choi et al., 2006).

Of the familial PD genes identified, DJ-1, Parkin and Pink1 all have strong association with mitochondria. DJ-1 is a multi-functional protein, most notably involved in sensing reactive oxygen species (Canet-Avilés et al., 2004; Shendelman et al., 2004). DJ-1 partially localizes to mitochondria upon induction of stress and this localization protects cells against further damage (Canet-Avilés et al., 2004; Junn et al., 2009). DJ-1 deficient mice are hypersensitive to oxidative stress and have fragmented mitochondria that produce higher levels of reactive oxygen species (Kim et al., 2005b; Aleyasin et al., 2010; Krebiehl et al., 2010). A more in depth look at DJ-1 will be discussed in section 1.7. Loss of Parkin in mammalian cells causes mitochondrial dysfunction (Palacino et al., 2004). Pink1 is a serine/threonine kinase that contains a mitochondrial targeting motif (Valente et al., 2004; Silvestri et al., 2005; Zhou et al., 2008). Pink1 deficient mammalian cells have dysfunctional mitochondria and are hypersensitive to oxidative insult (Haque et al., 2008; Wood-Kaczmar et al., 2008; Dagda et al., 2009; Liu and Lu, 2010).

There is much controversy surrounding the link between mitochondrial dysfunction and PD – whether the damage to mitochondria is a cause or result of the disease, and if it is a cause, why are only specific areas of the brain affected? There are other diseases in which mitochondrial dysfunction is a key factor. For example, Leber's hereditary optic neuropathy (LHON) is characterized by decreased complex I activity

(Parker et al., 1989). This decrease is most often caused by one of three single point mutations in mitochondrial-encoded subunits of complex I (Schrier and Falk, 2011). Individuals with LHON develop progressive blindness most likely due to thickening of the retinal nerve fibres as well as loss of retinal ganglion cells in the optic nerve (Schrier and Falk, 2011). Despite this complex I dysfunction, there is no apparent correlation between this disease and risk of Parkinson's disease, however it is interesting to note the specificity of degeneration also observed in LHON.

In contrast, mutations leading to defects in the ETC (most commonly in subunits of complex I) in Leigh's disease lead to necrotizing lesions in the basal ganglia, brain stem, diencephalon or cerebellum (Finsterer, 2008). While typically early childhood-onset, it can also develop in young adults however most patients die by 5 years of age (Finsterer, 2008). Some of these patients have lesions involving the substantia nigra (Medina et al., 1990), which supports the role of mitochondrial dysfunction in neurodegeneration. However, this disease has a much more rapid onset compared to PD, and not all the same areas in the brain are affected.

Interestingly, mice in which an essential component of mitochondrial function, mitochondrial transcription factor A (TFAM), was removed from dopaminergic neurons, exhibit a slow degeneration of these neurons as well as progressive motor deficits (Ekstrand and Galter, 2009). TFAM is essential in maintaining the integrity of mitochondrial DNA (mtDNA), and its loss increases the rate of mutations occurring in the mtDNA, thereby affecting the function of mitochondria (Larsson et al., 1998; Ekstrand and Galter, 2009). This mouse model further implicates the role of mitochondrial dysfunction in the pathology of PD. However it does not explain why

dopaminergic neurons in the substantia nigra degenerate while neighbouring dopaminergic neurons in the VTA are relatively spared.

Interestingly, it has been shown that neurons in the SNc are constantly firing, even in absence of synaptic input (Chan et al., 2007; Chan et al., 2010). The SNc pacemaking is rather unique as it uses Ca^{2+}channels, specifically the L-type Ca^{2+} channel $Ca_V1.3$ (Chan et al., 2007; Chan et al., 2010). It is proposed that this ATP-dependent process results in accelerated aging of these neurons, compared to neighbouring neurons, such as in the VTA, that do not use $Ca_V1.3$ channels for pacemaking (Chan et al., 2010). In further support of the idea that these $Ca_V1.3$ channels cause the selective vulnerability of SNc neurons, blockade of these channels using the Ca^{2+} channel inhibitor isradipine prevents cell death in two *in vivo* rodent models of PD (Chan et al., 2007; Chan et al., 2010). Additionally, SNc neurons seem to have more oxidative stress than VTA neurons, and treatment with isradipine considerably reduces these levels (Guzman et al., 2010). Given these findings, a newly discovered inhibitor specific to $Ca_V1.3$ channels is a potential therapeutic option for PD patients (Kang et al., 2012). By reducing Ca^{2+} mediated pacemaking activity of these neurons, there is less demand for ATP production and therefore less stress on mitochondria, which could in turn prevent the early aging of these neurons (Chan et al., 2010; Kang et al., 2012).

1.6 Mitochondria

1.6.1 Structure and Function

Believed to have originated as engulfed prokaryotes and establishing an endosymbiotic relationship in eukaryotes, mitochondria exist in most eukaryotic cells and

are considered the "power house" of the cells (Gray et al., 1999, 2001). With its own genetic code, mitochondria are able to produce a major source of energy in a cell, ATP, via oxidative phosphorylation. Additionally, mitochondria store and regulate Ca^{2+} and are essential in many signalling pathways, such as cell death (Duchen, 1999; Butow and Avadhani, 2004; Duchen, 2004; Green and Kromer, 2004).

Mitochondria are double membrane bound organelles, with an outer mitochondrial membrane (OMM), inner mitochondrial membrane space (IMS), inner mitochondrial membrane (IMM) and matrix. Invaginations of the inner membrane, termed cristae, largely increase the overall surface area of the IMM and are the site for oxidative phosphorylation.

Embedded within and on the surface of the IMM are the five complexes – termed the electron transport chain (ETC) due to the shuttling of electrons along these complexes. The shuttling of electrons facilitates ATP production via metabolism of glucose and other sugars. Also known as oxidative phosphorylation, this process uses pyruvate (sourced from glucose breakdown by glycolysis) and succinate (mainly sourced from the citric acid cycle) as substrates. Electrons travel through the complexes in a series of redox reactions to finally be accepted by O_2 to create H_2O, driving protons from the matrix across the IMM to the IMS. This drive creates an electrochemical gradient in which the IMS has a higher concentration of protons versus the matrix. ATP synthase, the final complex of the ETC, uses the proton-motive force of this gradient to pump protons back into the matrix, thus driving ATP synthesis.

1.6.2 Dynamics

Mitochondria are not static organelles – they are highly dynamic, undergoing constant fission (breaking apart) and fusion (joining together). This process is mediated by numerous factors, including the fission protein dynamin-related protein 1 (Drp1) and the fusion proteins mitofusins 1 and 2 (Mfn1, 2) and optic atrophy 1 (Opa1) (Chen and Chan, 2004; Detmer and Chan, 2007; Lackner, 2014). Fission occurs when Drp1 is recruited to the OMM and forms a ring-like structure at the site to be fissed. Mitochondrial fission protein 1 (Fis1) and mitochondrial fission factor (Mff) actively target Drp1 to the OMM. This site is also in contact with the endoplasmic reticulum (ER), which marks the site for the actual break in the mitochondrion. Fusion of the OMM is regulated by mitofusin-1 (Mfn1) and mitofusin-2 (Mfn2) while IMM fusion is mediated by optic atrophy 1 (OPA1). Mfn1/2 act as tethers – they bind with other Mfn1/2 on the OMM of other mitochondria to initialize fusion.

The dynamic changes of mitochondria allow for mixing of genomic and matrix content and dilution of oxidized and/or damaged proteins and mtDNA (Fischer et al., 2012). Furthermore, fusion enhances ER-mitochondria communication and allows for more efficient movement of mitochondria throughout the cell (Csordás et al., 2006; Rowland and Voeltz, 2012). Disruption of the balance between fission and fusion, more notably towards a fragmented state, is indicative of mitochondrial stress/damage and is implicated in numerous diseases (Chen and Chan, 2006; Chen and Chan, 2009; Archer, 2013; Lackner, 2014).

1.6.3 Reactive Oxygen Species (ROS)

Mitochondria are a major source of energy for cells by oxidative phosphorylation. A by-product of cellular respiration is the creation of ROS, mainly by complex I and III of the ETC (Muller, 2000; Turrens, 2003; Murphy, 2009; Zorov et al., 2014). Multiple components of the cell produce ROS, and the exact contribution of mitochondrial-produced ROS is difficult to determine, but this contribution is accredited to numerous diseases (Halliwell and Whiteman, 2004; Balaban et al., 2005; Beal, 2005; Lin and Beal, 2006; Rhoads et al., 2006; Chinta and Andersen, 2008; Zorov et al., 2014). High levels of ROS can be detrimental to the cell, however there are multiple processes by which the cell can remove excess oxidative stress by converting harsher radicals to less damaging forms (Sherer et al., 2002; Chinta and Andersen, 2008).

One source of ROS is superoxide ($O_2^{\cdot -}$), which is formed by the addition of an electron to molecular oxygen, mainly at the site of the ETC in mitochondria. Manganese superoxide dismutase (mnSOD) converts superoxide to hydrogen peroxide (H_2O_2) in the mitochondrial matrix and catalase can then convert the H_2O_2 to H_2O. Glutathione cycles between a reduced state (GSH) and oxidized state (GSSG), and during this cycling allows for conversion of H_2O_2 to H_2O. Superoxide is highly reactive, and can reduce Fe^{2+} to catalyze the Fenton reaction, in which H_2O_2 is converted to the hydroxyl radical ($OH^{\cdot}$). Excessive ROS can eventually cause DNA damage and lipid peroxidation (Sherer et al., 2002; Chinta and Andersen, 2008).

It is important to note that ROS plays a physiological role in the cell, and cannot be eliminated completely, without detrimental effects (Sena and Chandel, 2012). Low levels of ROS can serve to activate cell signalling pathways and immune responses (Sena

and Chandel, 2012). However, sustained levels of oxidative stress can be damaging to mitochondria, especially when anti-oxidant defenses have been exhausted (Chinta and Andersen, 2008). Additionally, damaged mitochondria can release ROS, further contributing to oxidative stress in the cell (Chinta and Andersen, 2008). Mitochondrial DNA is especially sensitive to oxidative damage, which leads to loss of essential components of the electron transport chain (Larsson et al., 1998). Damaged, dysfunctional mitochondria inefficiently produce energy, have disrupted regulation of dynamics, and can induce apoptosis (Detmer and Chan, 2007; Mattson et al., 2008).

1.6.4 Mitochondrial Quality Control (MQC)

Mitochondrial quality control (MQC) exists at various levels, depending on the degree of damage in the cell. Regulation occurs at the molecular, organellar and cellular level (Tatsuta and Langer, 2008; Ashrafi and Schwarz, 2012; Fischer et al., 2012). Maintenance of the ETC minimizes excessive ROS production and is achieved by proteolytic and protein regulation (Detmer and Chan, 2007; Tatsuta and Langer, 2008; Ashrafi and Schwarz, 2012; Fischer et al., 2012). Damaged mitochondria can be selectively degraded through a type of autophagy, termed mitophagy.

Two PD genes, Parkin and Pink1, have been recently implicated in mediating mitophagy. Parkin, an E3 ubiquitin ligase, translocates to damaged mitochondria to facilitate their clearance via mitophagy (Narendra et al., 2008; Geisler et al., 2010). Recent findings have also implicated Parkin-mediated ubiquitination of outer mitochondrial membrane proteins as a signal for degradation by mitophagy (Geisler et al., 2010; Narendra et al., 2010a; Poole et al., 2010). Additionally, upon induction of

stress, Pink1 is stabilized in the mitochondria – a process required for Parkin recruitment (Kim et al., 2008; Geisler et al., 2010; Narendra et al., 2010b).

This process allows for mitochondria to be removed in order to prevent further damage to the mitochondrial network (Tatsuta and Langer, 2008; Ashrafi and Schwarz, 2012; Fischer et al., 2012). If damage is too severe to fix, mitochondria can signal for apoptosis and this prevents the damaged cell from adversely affecting surrounding cells (Tatsuta and Langer, 2008; Ashrafi and Schwarz, 2012; Fischer et al., 2012).

The existence of Parkin-mediated MQC in neurons, especially *in vivo*, is still highly debated. The major issue is the fact that the majority of studies investigating MQC employ overexpression techniques and harsh, non-physiological stressors (Grenier et al., 2013). Notably, one group did not observe *in vivo* Parkin-mediated MQC in a dopaminergic neuron-specific mitochondrial damage model (Sterky et al., 2011). It is important to note that this mitochondrial damage model has not been fully characterized, and there may be complications in the model, in which Parkin is unable to localize to mitochondria (Grenier et al., 2013). Despite this, MQC is still argued to have an essential function in neurons (Rugarli and Langer, 2012).

1.7 DJ-1

1.7.1 Structure

The human *PARK7* gene consists of 8 exons over a span of 24 kilo base pairs (Kb), located on chromosome 1p36. It encodes for a 189 amino acid protein called DJ-1. Human DJ-1 tertiary structure consists of a six-strand parallel β-sheet flanked by α-helical arrangements, and is typically found in dimeric form (Abou-Sleiman et al., 2003;

Honbou et al., 2003; Huai, 2003; Macedo et al., 2003; Tao and Tong, 2003; Wilson et al., 2003). This structure places DJ-1 in the highly conserved DJ-1/ThiJ/PfpI superfamily of proteins. The archetypical bacterial ThiJ and PfpI proteases contain similar structural domains to DJ-1. Interestingly, DJ-1 has a warped catalytic triad and a blocked putative active site, thus rendering it non-proteolytic (Abou-Sleiman et al., 2003; Honbou et al., 2003; Huai, 2003; Wilson et al., 2003; Shendelman et al., 2004).

DJ-1 undergoes a shift in its isoelectric point during oxidative stress, becoming more acidic (Mitsumoto et al., 2001; Taira et al., 2004). Based on its structure, DJ-1 has two highly reactive cysteine residues – at position 53 and 106. It is believed that oxidation of one residue in particular, cysteine 106 (C106), is responsible for the shift in its isoelectric point (Canet-Avilés et al., 2004). Some studies have suggested that C53 also plays a role in this shift (Taira et al., 2004). The cysteine residue can be oxidized to sulfinic acid (via sulfenic acid) or even to sulfonic acid with prolonged exposure to oxidative stress (Abou-Sleiman et al., 2003; Canet-Avilés et al., 2004; Zhou et al., 2006). Highly oxidized DJ-1 has been found in both sporadic PD and Alzheimer's disease patients' brains (Choi et al., 2006).

1.7.2 Mutations Causing Parkinson's Disease

Over 10 years ago, two loss of function mutations in *PARK7* were linked to early-onset PD. The first mutation was identified in a Dutch family, where exons 1-5 of the gene as well as 4Kb of the promoter were deleted (Bonifati et al., 2003). This deletion mutation led to no detectable protein level (Macedo et al., 2003; Irrcher et al., 2010). The second mutation was identified in an Italian family, where a single point mutation in exon

7 lead to leucine 166 becoming a proline (L166P) (Bonifati et al., 2003). This substitution leads to loss of dimerization and consequently destabilization of the protein (Macedo et al., 2003). Additional PD-causing mutations that alter amino acid sequence have been identified, including M26I (exon 2), E64D (exon 3), E163K (exon 7), A104T (exon 5), and D149A (exon 7) (Abou-Sleiman et al., 2003; Clark et al., 2004; Hering et al., 2004; Annesi et al., 2005). It is estimated that mutations in *PARK7* account for approximately 1-2% of early-onset PD (Abou-Sleiman et al., 2003; Pankratz et al., 2006).

1.7.3 Functions

1.7.3.i Oncogene

DJ-1 was originally identified as an oncogene, as in co-operation with H-ras or C-myc, it can transform mouse cells (Nagakubo et al., 1997). While able to minimally transform cells by itself, a combination of DJ-1 and ras or myc causes exponential transformation (Nagakubo et al., 1997). Additionally, DJ-1-expressing cells induce significantly more tumour formation in nude mice (Kim et al., 2005b). Notably, increased levels of DJ-1 have been observed in various types of cancer. In breast cancer, even in early detected cases, DJ-1 expression is increased and thought to be a potential biomarker for this cancer (Le Naour et al., 2001). Additionally, elevated levels of DJ-1 have been detected in lung cancer and are correlated to poor outcome (Kim et al., 2005b; Fan et al., 2015). In astrocytomas, loss of DJ-1 localized to the nucleus is suggestive of poor prognosis (Miyajima et al., 2010).

1.7.3.ii Chaperone

The *Escherichia coli* molecular chaperone Hsp31 is also a member of DJ-1/ThiJ/PfpI superfamily of proteins, and shares structural resemblance to DJ-1 (Abou-Sleiman et al., 2003). This similarity suggests that DJ-1 too could possess a chaperone-like activity, which has been confirmed by various studies (Shendelman et al., 2004; Zhou et al., 2006). The chaperone function of DJ-1 is redox-dependent as this function is lost in a reducing environment (Shendelman et al., 2004; Zhou et al., 2006). This chaperone activity depends on the highly reactive C53 but not C106 in one study (Shendelman et al., 2004) and C106 but not C53 in another study (Zhou et al., 2006). Additionally, the PD-mutant L166P does not possess any chaperone activity (Shendelman et al., 2004). Moderately oxidized DJ-1, but not the L166P mutant, is able to prevent aggregation of α-synuclein (Shendelman et al., 2004; Zhou et al., 2006). Interestingly, highly oxidized DJ-1 is unable to prevent fibrillation of α-synuclein (Zhou et al., 2006).

1.7.3.iii Transcription Regulator

DJ-1 has been implicated as a co-factor in regulation of numerous genes. The first interactor of DJ-1 identified was the protein inhibitor of activated signal transducers and activators of transcription (PIAS)x-α (Takahashi et al., 2001). DJ-1 positively regulates the androgen receptor (ARe) by binding PIASx-α, which normally inhibits this receptor – a process dependent on sumoylation of DJ-1 at lysine 130 (Takahashi et al., 2001; Shinbo et al., 2006). Overexpression of DJ-1 increases ARe activity ~20-fold whereas DJ-1

knockdown decreases the activity by ~5-10-fold (Tillman et al., 2007). Furthermore, DJ-1 increases tyrosine hydroxylase (TH) transcription via the ARe (Jeong et al., 2006). Notably, the PD-associated mutant L166P does not interfere with binding to PIASx-α (Macedo et al., 2003). However both this mutant as well as the K130R mutant show improper sumoylation and can not protect cells against UV radiation-induced death (Shinbo et al., 2006).

Pyramidine tract-binding protein-associated splicing factor (PSF), which has a co-repressor function on the TH promoter, interacts with DJ-1 (Tanner et al., 2005; Ishikawa et al., 2010). This interaction prevents the inhibitory effect on TH transcription by stopping the sumoylation of PSF and thus preventing recruitment of histone deacetylase 1 (HDAC1) (Zhong et al., 2006; Ishikawa et al., 2010). PD-associated mutants M26I, D149A and L166P as well as the exon 1-5 deletion DJ-1 demonstrate higher levels of PSF sumoylation (Zhong et al., 2006). PSF also inhibits transcription of peroxisome proliferator-activated receptor-γ co-activator 1α (PGC-1α), a master regulator of mitochondrial biogenesis and stress response (Zhong and Xu, 2008). DJ-1 prevents sumoylation of PSF, thereby releasing inhibition of PGC-1α and allowing for transcription of MnSOD (Zhong and Xu, 2008). Interestingly, highly oxidized DJ-1 is unable to prevent sumoylation of PSF and therefore MnSOD levels are reduced (Zhong and Xu, 2008).

Overexpressed DJ-1 protects dopaminergic neuronal cultures against oxidative stress by upregulating biosynthesis of glutathione (Kim et al., 2005b). DJ-1 increases both glutamate cysteine ligase transcription and activity (Kim et al., 2005b). Blocking glutathione synthesis abolishes the protective effects of DJ-1 overexpression (Kim et al.,

2005b). In addition, DJ-1 regulates the stability of a master anti-oxidant transcription factor, nuclear factor erythroid 2-related factor (Nrf2) (Clements et al., 2006). DJ-1 binds to Nrf2, preventing interaction with Kelch-like ECH-associated protein 1 (Keap1), its inhibitor protein that leads to Nrf2 ubiquitination and subsequent degradation (Clements et al., 2006).

1.7.3.iv Pro-Survival

Previous research in our laboratory has shown that loss of DJ-1 leads to hypersensitization to MPTP and oxidative stress and that its reintroduction can promote survival in the same paradigms (Kim et al., 2005a). Overexpressed WT DJ-1, but not PD-associated mutant L166P, protects against various stressors in numerous cell models (Junn et al., 2005; Kim et al., 2005b; Shinbo et al., 2006). A study showed that part of this pro-survival role of DJ-1 is through the Akt pathway, as DJ-1 negatively regulates phosphatase and tensin homolog (PTEN) (Kim et al., 2005b). Overexpressed DJ-1 was able to protect against PTEN-induced cell death, but interestingly DJ-1 provides protection in a PTEN-dependent manner (Kim et al., 2005b). Akt phosphorylation, and thus activation, is reliant on DJ-1 (Kim et al., 2005b; Aleyasin et al., 2010). Our group further explored this link, demonstrating that Akt requires DJ-1 in order to be activated during times of stress, and DJ-1 is only protective in the presence of Akt (Aleyasin et al., 2010). Additionally, there is noticeably less Akt activation with the PD-associated L166P mutant (Aleyasin et al., 2010).

Another study demonstrated that DJ-1, but not L166P mutant DJ-1, interacts with the cell death-inducing protein Daxx (Junn et al., 2005). Upon stimulation, Daxx

translocates from the nucleus to the cytoplasm to activate apoptosis signal-regulating kinase 1 (Ask1). DJ-1 binds to Daxx, sequestering it into the nucleus and thus preventing activation of Ask1 and halting the subsequent cell death pathway (Junn et al., 2005).

1.7.3.v Oxidative Stress Sensor

It has been speculated that DJ-1 acts directly as an anti-oxidant, and the C53A and C106S cysteine mutants, as well as the PD-associated L166P mutant, lack this ability (Taira et al., 2004; Andres-Mateos et al., 2007). It was also demonstrated that WT DJ-1 but not C53A, C106S/A or L166P mutants could undergo a shift in isoelectric point and additionally protect against cell death (Canet-Avilés et al., 2004; Taira et al., 2004; Blackinton et al., 2009). This role is controversial, as a study has shown DJ-1 to have too low of a direct anti-oxidant function to be protective (Shendelman et al., 2004; Yang et al., 2005; Andres-Mateos et al., 2007). It is instead suggested that oxidation of DJ-1 serves to indicate increased levels of oxidative stress in the cell (Canet-Avilés et al., 2004).

1.7.3.vi Role in Mitochondrial Health

Previous studies demonstrate that DJ-1 can localize to mitochondria to exert its antioxidant effects (Canet-Avilés et al., 2004; Blackinton et al., 2005; Zhang et al., 2005; Shinbo et al., 2006; Andres-Mateos et al., 2007; Hayashi et al., 2009; Junn et al., 2009; Xiong et al., 2009). It is believed that oxidation of one residue in particular, cysteine 106 (C106) is essential for it to translocate to mitochondria and exert its protective role (Canet-Avilés et al., 2004). Some studies question the necessity of C106 oxidation (Maita

et al., 2013), however DJ-1 targeted specifically to mitochondria provide the highest protection against oxidative stress, compared to nuclear targeted or WT DJ-1 (Junn et al., 2009).

More recent work in our laboratory, as well as others, has demonstrated that DJ-1 deficiency both *in vitro* and *in vivo* results in fragmented mitochondria that produce more ROS (Irrcher et al., 2010; Krebiehl et al., 2010). Treatment with the anti-oxidant N-acetyl cysteine (NAC) rescues this mitochondrial morphological effect (Irrcher et al., 2010). Mfn1, one of the regulators of OMM fusion, is decreased with loss of DJ-1 and inhibition of fission by expression of a dominant-negative Drp1 can reverse the hypersensitivity of DJ-1 null neurons *in vitro* (Irrcher et al., 2010). Loss of DJ-1 negatively impacts mitochondrial health.

1.8 Voltage Dependent Anion Channel (VDAC)

1.8.1 Structure and Function

The voltage-dependent anion channel (VDAC) is a pore-forming protein that resides predominantly in the OMM (Colombini, 1980; Roos et al., 1982; Lindén and Gellerfors, 1983; Ludwig et al., 1986; Peng et al., 1992; Rostovtseva et al., 2000). This transmembrane protein is capable of oligomerization and has multiple, distinct isoforms in humans, mice and rats (Colombini, 1980; Lindén and Gellerfors, 1983; Sampson et al., 1997; Shi et al., 2003; Shoshan-Barmatz et al., 2004; Zalk et al., 2005; Shoshan-Barmatz et al., 2006; Bayrhuber et al., 2008; Shoshan-Barmatz et al., 2010). VDAC is approximately 31kDa in size and consists of a single β-barrel that spans the membrane and an α-helix at the N-terminus that sits horizontally in the middle of the pore

(Bayrhuber et al., 2008; Hiller et al., 2008; Ujwal et al., 2008). The diameter of the monomer VDAC channel is estimated at 0.9 – 3nm (Ludwig et al., 1986; Colombini, 1987; Benz, 1994; Bayrhuber et al., 2008; Hiller et al., 2008; Ujwal et al., 2008). The α-helix has a high degree of flexibility and is thought to move in and out of the pore, allowing for either an 'open' or 'closed' status, which accounts for the larger variability in pore diameter measured (Bayrhuber et al., 2008; Ujwal et al., 2008; Mertins et al., 2012).

This voltage-dependent channel has the highest conductance at low potentials, when it allows for the passage anions such as adenine nucleotides, chloride, phosphate, succinate and pyruvate (Colombini, 1980; Roos et al., 1982; Ludwig et al., 1986; Rostovtseva and Colombini, 1997; Shoshan-Barmatz et al., 2006; Mertins et al., 2012). The size of the channel become reduced with higher positive or negative potentials, and VDAC becomes almost impermeable to ATP and ADP (Ludwig et al., 1986; Benz et al., 1988; Benz et al., 1990; Liu and Colombini, 1992; Gellerich et al., 1993; Lee et al., 1994; Rostovtseva and Colombini, 1997; Shoshan-Barmatz et al., 2006). In this relatively 'closed' state, VDAC becomes more preferential to cations and mitochondrial function decreases significantly (Ludwig et al., 1986; Benz et al., 1988; Benz et al., 1990; Liu and Colombini, 1992; Gellerich et al., 1993; Lee et al., 1994).

1.8.2 Ca^{2+} Regulation

The translocation of Ca^{2+} into and out of the mitochondria is partially regulated through VDAC (Gincel et al., 2001; Rapizzi et al., 2002; Bathori et al., 2006). Ca^{2+} is a universal messenger that regulates many cellular processes such as cellular structure,

muscle contraction, synaptic transmission of neurotransmitters and even cell death (Bennett and Weeds, 1986; Trump and Berezesky, 1995; Crompton, 1999; Berchtold et al., 2000; Friel, 2000; Verkhratsky, 2005; Clapham, 2007; Kostyuk, 2007). Cytoplasmic Ca^{2+} levels are significantly lower than extracellular Ca^{2+} levels. A large influx of Ca^{2+} into the cell can occur rapidly and the cell must return cytosolic Ca^{2+} to resting levels in order to prevent activation of various messengers (Pounds and Rosen, 1988; Friel, 2000; Verkhratsky, 2005). Two Ca^{2+} 'sinks' exist to help maintain Ca^{2+} homeostasis in the cytosol – the ER and mitochondria (Bernardi, 1999; Friel, 2000; Verkhratsky, 2005). VDAC contains Ca^{2+} binding sites, and may regulate mitochondria-dependent apoptosis (Gincel et al., 2001). Increased Ca^{2+} levels induce an 'open' conformation of VDAC, which could allow for rapid entry of Ca^{2+} into mitochondria (Bathori et al., 2006). Additionally, VDAC enhances the permeability of Ca^{2+} at mitochondria-ER contact points (Rapizzi et al., 2002). Increased mitochondrial Ca^{2+} levels can enhance metabolism, however sustained high levels of Ca^{2+} can also lead to mitochondrial dysfunction and eventually apoptosis (Hunter and Haworth, 1979; Jouaville et al., 1999; Boustany et al., 2002; Pivovarova and Andrews, 2010). By regulating permeability of Ca^{2+} to mitochondria, VDAC plays a role in regulating various cellular processes (Rapizzi et al., 2002; Bathori et al., 2006).

1.8.3 Role in Cell Death

There are various models in which mitochondria have been implicated in inducing apoptosis, chiefly by releasing the pro-apoptotic factor cytochrome *c* (Green and Reed, 1998; Shoshan-Barmatz et al., 2006). Upon accumulation of excessive mitochondrial

Ca^{2+}, mitochondria can undergo a sudden permeability transition (Massari and Azzone, 1972; Haworth and Hunter, 1979; Hunter and Haworth, 1979; Bernardi, 1999; Bernardi et al., 2006; Shoshan-Barmatz et al., 2008). This change in permeability can cause a loss of mitochondrial membrane potential, efflux of Ca^{2+} into the cytosol, and release of cytochrome *c* (Haworth and Hunter, 1979; Hunter and Haworth, 1979; Newmeyer and Ferguson-Miller, 2003; Green and Kromer, 2004; Ekert and Vaux, 2005; Shoshan-Barmatz et al., 2008). Together with cytochrome *c*, other proteins such as direct inhibitor of apoptosis binding protein with low pI (DIABLO), apoptosis-inducing factor (AIF) and cleaved optic-atrophy 1 (OPA1) are also released from permeabilized mitochondria into the cytoplasm (Li et al., 1997; Susin et al., 1999; Verhagen et al., 2000; Newmeyer and Ferguson-Miller, 2003; Green and Kromer, 2004; Arnoult et al., 2005; Ekert and Vaux, 2005). These proteins trigger a chain of reactions, leading to apoptosis via apoptosis activating factor 1 (Apaf-1) activation and subsequently caspase activation (Green and Kromer, 2004; Ekert and Vaux, 2005; Youle and Strasser, 2008).

The mitochondrial permeability transition pore (mPTP) has been proposed to contain VDAC, adenine-nucleotide transferase (ANT), cyclophilin D (CypD) and translocator protein (TSPO) (Halestrap and Davidson, 1990; Szabó et al., 1993; Szabó and Zoratti, 1993; Baines et al., 2005; Sileikyte et al., 2011). The essential participation of ANT, CypD and TSPO in the mPTP has since been refuted, as cells deficient for each of these components still can undergo mitochondrial permeability (Kokoszka et al., 2004; Basso et al., 2005; Šileikytė et al., 2014). The voltage-dependence and diameter of the mPTP is similar to VDAC, and thus it was suggested that VDAC was in fact the mPTP (Szabó et al., 1993; Szabó and Zoratti, 1993; Bernardi et al., 2006). Despite the

similarities, cells deficient for all three VDAC isoforms can undergo permeabilization of the OMM and are inducible for apoptosis (Baines et al., 2007). While not an essential component, further investigation into VDAC1 specifically, suggests that regulation of its N-terminus can promote either cell-survival or apoptosis, depending on the interactor (Shi et al., 2003; Azoulay-Zohar et al., 2004; Abu-Hamad et al., 2009; Arbel and Shoshan-Barmatz, 2010; Arbel et al., 2012).

1.8.4 Interactors

Hexokinase, a key enzyme in glycolysis, has been shown to localize to mitochondria in an Akt-dependent manner to promote survival (Pastorino et al., 2005). It interacts with VDAC1 to reduce the conductance of the channel and promote survival (Azoulay-Zohar et al., 2004; Abu-Hamad et al., 2008). This interaction and subsequent decrease in channel conductance is reliant on specifically the N-terminus of VDAC1 (Azoulay-Zohar et al., 2004; Abu-Hamad et al., 2009). Interaction of VDAC and hexokinase is also dependent on the phosphorylation status of VDAC – phosphorylated VDAC does not bind hexokinase, thereby losing its protective effect (Pastorino et al., 2005).

VDAC1 has been shown to interact with various members of the B-cell lymphoma-2 (Bcl-2) family of protein. Bcl-2 proteins regulate both cell survival and death (Youle and Strasser, 2008). The anti-apoptotic Bcl-2 protein is the founder protein for the Bcl-2 family of proteins and its deregulation is associated with development of lymphomas (Tsujimoto et al., 1985; Vaux et al., 1988). It interacts with VDAC1, lowering conductance of the channel and preventing cell death (Arbel and Shoshan-

Barmatz, 2010). This interaction is dependent on several domains of VDAC1, including its N-terminus (Abu-Hamad et al., 2009; Arbel and Shoshan-Barmatz, 2010).

Another family member, B-cell lymphoma-extra large (Bcl-x_L), resides in mitochondria and prevents apoptotic cell death (Boise et al., 1993). Bcl-x_L interacts with VDAC1, however the functional outcome of this interaction is controversial. One group demonstrated that this interaction induced closing of VDAC1 and prevented cytochrome *c* release into the cytosol (Shimizu et al., 1999). However another group showed that the interaction promoted the open state of VDAC, allowing for passage of metabolites (Vander Heiden et al., 2001). Additional studies have shown that Bcl-x_L interacts specifically within the N-terminal region of VDAC1, causing reduced conductance of the channel and preventing apoptosis (Shi et al., 2003; Arbel et al., 2012). More recently it has been suggested that this interaction appears to allow for increased Ca^{2+} uptake into the mitochondrial matrix (Huang et al., 2013).

The pro-apoptotic proteins Bax and Bak, also Bcl-2 family members, have both been implicated in an alternative mechanism for mediating release of cytochrome *c* from mitochondria following membrane permeabilization (Kluck et al., 1999; Kuwana et al., 2002; Green and Kromer, 2004; Youle and Strasser, 2008). It has been proposed that Bax and/or Bak can oligomerize and form a pore that allows for release of proteins from the OMM such as cytochrome *c* (Kuwana et al., 2002). Additionally, Bax appears to interact with VDAC1 and enhances the opening of this channel, leading to increased release of cytochrome *c* (Shimizu et al., 1999; Shi et al., 2003). This interaction appears to depend on the N-terminus of VDAC1 (Shi et al., 2003).

In collaboration with the laboratory of Dr. Daniel Figeys (Institute of Systems Biology, University of Ottawa), an interaction screen was performed. This screen, in which FLAG-VDAC1 was overexpressed in HEK293 cells, interacting proteins were co-immunoprecipitated and identified by mass spectrometry, showed that DJ-1 interacts with VDAC1 (Dr. Figeys, personal communication). The convergence of both DJ-1 and VDAC1 on promoting survival during oxidative stress via mitochondrial function, together with this possible interaction, has led us to investigate the possible interaction between these two factors.

1.9 Statement of Research Hypothesis and Objectives

The Parkinson's disease-linked DJ-1 is a pro-survival protein that can protect against oxidative stress and inhibit cell death, especially when targeted to mitochondria. The outer mitochondrial membrane protein VDAC1 is also a key factor in regulating cell survival during stress.

We hypothesize that *VDAC1 mediates entry of DJ-1 into mitochondria during stress to promote survival*. To address this theory, we outlined the following objectives to study for this dissertation:

1) Assess stress-induced localization of DJ-1 to mitochondria
2) Confirm physical/functional interaction between DJ-1 and VDAC1
3) Determine effect of VDAC1 deficiency on cortical neuron mitochondrial health
4) Elucidate sub-mitochondrial localization of DJ-1
5) Identify signal inducing DJ-1 translocation to mitochondria

CHAPTER 2

ROS-dependent regulation of Parkin and DJ-1 localization during oxidative stress

Human Molecular Genetics. 2012 Nov 15;21(22):4888-903. Epub 2012 Aug 7.

Alvin P. Joselin[#], **Sarah J. Hewitt**[#], Steve M. Callaghan, Raymond H. Kim, Young-Hwa Chung, Tak W. Mak, Jie Shen, Ruth S. Slack and David S. Park

#Authors contributed equally

Statement of Author Contributions

Sarah J. Hewitt and Dr. Alvin P. Joselin designed and conducted all experiments. **Sarah J. Hewitt** carried out all experiments investigating DJ-1 translocation and Dr. Alvin P. Joselin carried out all experiments investigating Parkin translocation. Steve M. Callaghan made all viruses utilized and provided general technical assistance. DJ-1 transgenic mice were made in the laboratory of Dr. Tak W, Mak, by Dr. Raymond H. Kim. Pink1 transgenic mice were made in the laboratory of Dr. Jie Shen. Dr. Young Hwa-Chung gave insight into experimental design. **Sarah J. Hewitt**, Dr. Alvin P. Joselin and Dr. David S. Park analyzed data, wrote the manuscript and edited the manuscript.

ROS-dependent regulation of Parkin and DJ-1 localization during oxidative stress in neurons

Alvin P. Joselin[1#], **Sarah J. Hewitt**[1#], Steve M. Callaghan[1], Raymond H. Kim[2], Young-Hwa Chung[4], Tak W. Mak[2], Jie Shen[3], Ruth S. Slack[1] and David S. Park[1,4]

#Authors contributed equally

1 Department of Cellular and Molecular Medicine, University of Ottawa, 451 Smyth Road, Ottawa, Ontario, Canada K1H 8M5

2 Campbell Family Cancer Research Institute, Ontario Cancer Institute, University Health Network, 620 University Avenue, Toronto, Ontario, Canada M5G 2C1

3 Center for Neurologic Diseases, Department of Neurology,
Brigham and Women's Hospital, Harvard Medical School, 77 Avenue Louis Pasteur, Boston, MA 02115, USA

4 Department of Cogno-Mechatronics Engineering, Pusan National University, Geumjeong GU, Busan 609 735, South Korea

Abstract

Mutations in several genes, including *Parkin*, PTEN-induced kinase 1 (*Pink1*) and *DJ-1*, are associated with rare inherited forms of Parkinson's disease (PD). Despite recent attention on the function of these genes, the interplay between DJ-1, Pink1 and Parkin in PD pathogenesis remains unclear. In particular, whether these genes regulate mitochondrial control pathways in neurons is highly controversial. Here we report that Pink1-dependent Parkin translocation does occur in mouse cortical neurons in response to a variety of mitochondrial damaging agents. This translocation only occurs in the absence of antioxidants in the neuronal culturing medium, implicating a key role of reactive oxygen species (ROS) in this response. Consistent with these observations, ROS blockers also prevent Parkin recruitment in mouse embryonic fibroblasts. Loss of DJ-1, a gene linked to ROS management, results in increased stress-induced Parkin recruitment and increased mitophagy. Expression of wild-type DJ-1, but not a cysteine-106 mutant associated with defective ROS response, rescues this accelerated Parkin recruitment. Interestingly, DJ-1 levels increase at mitochondria following oxidative damage in both fibroblasts and neurons, and this process also depends on Parkin and possibly Pink1. These results not only highlight the presence of a Parkin/Pink1-mediated pathway of mitochondrial quality control (MQC) in neurons, they also delineate a complex reciprocal relationship between DJ-1 and the Pink1/Parkin pathway of MQC.

Introduction

Parkinson's disease (PD), a neurodegenerative movement disorder, is characterized by loss of dopaminergic (DA) neurons in the substantia nigra *pars compacta* (Dauer and Przedborski, 2003). Growing evidence has implicated mitochondrial quality control (MQC) pathways. Mitochondrial defects have been noted in PD patients (Schapira et al., 1989; Navarro and Boveris, 2009). Moreover, exposure to drugs that inhibit mitochondrial complex I mimic certain aspects of PD (Greenamyre et al., 1999; Betarbet et al., 2000; Jenner, 2001). Interestingly, a number of recessive, early-onset PD genes are implicated in the maintenance of mitochondrial homeostasis. Pink1 is a serine/threonine kinase containing an N-terminal mitochondrial-targeting motif (Valente et al., 2004). Pink1 localizes to mitochondria (Valente et al., 2004; Silvestri et al., 2005; Zhou et al., 2008) and its loss leads to increased oxidative stress and sensitization to death (Haque et al., 2008; Wood-Kaczmar et al., 2008). Parkin, another PD gene, possesses E3 ligase activity (Rankin et al., 2001). At least in select tumor lines in response to carbonyl cyanide m-chloro phenyl hydrazone (CCCP)-induced mitochondrial depolarization, Parkin translocates to mitochondria and participates in clearance of dysfunctional mitochondria (Narendra et al., 2008) in a Pink1-dependent manner (Kim et al., 2008; Vives-Bauza et al., 2010). Whether this is true in primary neurons is unclear. Critically, recent reports have indicated that neither CCCP (Van Laar et al., 2010), nor mitochondrial damage caused by mitochondrial transcription factor A (TFAM) loss (Sterky et al., 2011) induce Parkin translocation in neurons, seriously undermining the relevance of the Pink1/Parkin mitochondrial quality control pathway in neurodegeneration.

DJ-1, a third PD recessive PD gene, is critical in oxidative stress response (Mitsumoto et al., 2001; Canet-Avilés et al., 2004; Kim et al., 2005a) and modulates various survival pathways (Yang et al., 2005; Görner et al., 2007; Aleyasin et al., 2010). We and others have shown that that DJ-1 loss results in hypersensitization of neurons to oxidative damage (Kim et al., 2005a; Manning-Boğ et al., 2007). How this sensitivity occurs is unclear. Recently, we demonstrated that DJ-1 deficiency leads to a fragmented mitochondrial phenotype, which can be rescued, by Parkin or Pink1 (Irrcher et al., 2010). However, while DJ-1 consistently appears to modulate oxidative stress responses (Mitsumoto et al., 2001; Kim et al., 2005a), Parkin translocation is reported to not involve ROS (Narendra et al., 2008). These inconsistencies led us to more carefully examine whether DJ-1 participates in the Pink1/Parkin mitochondrial quality control pathway. In summary, two central questions have emerged: a) does DJ-1 interact with the Pink1/Parkin mediated pathway of mitochondrial quality control and b) are these pathways relevant in primary neurons.

Presently, we show that DJ-1 integrates into the classical Pink1/Parkin pathway by both modulating Parkin translocation/mitophagy and responding to Pink1/Parkin by increasing its level at mitochondria during oxidative stress. Moreover, we provide critical evidence that Parkin translocation to mitochondria does occur in primary neurons in a ROS-dependent manner. Taken together, we provide a model by which DJ-1 acts in a complementary fashion to regulate a ROS-dependent Pink1/Parkin-mediated mitochondrial quality control pathway in neurons.

Results

Loss of DJ-1 results in earlier Parkin recruitment to mitochondria in MEFs

Specific Parkin recruitment to mitochondria has been documented in response to mitochondrial depolarization following CCCP (Narendra et al., 2008) or valinomycin (Rakovic et al., 2010) treatment and hydrogen peroxide treatment (Rakovic et al., 2010) in a number of cell lines. Previous reports from our lab (Irrcher et al., 2010) and others (Canet-Avilés et al., 2004) have also established a role for DJ-1 in the regulation of ROS and maintenance of mitochondrial dynamics. Accordingly, we first examined if the loss of DJ-1 affects Parkin recruitment to the mitochondria. DJ-1 deficient mouse embryonic fibroblasts (MEFs) were transfected with GFP-Parkin and treated with the mitochondrial uncoupler CCCP for various durations and analyzed for formation of Parkin puncta as previously described (Narendra et al., 2008). Within 1h of 10μM CCCP treatment, we observed noticeable mitochondrial translocation of wild-type (WT) Parkin (Figure 2.1A and 2.1B) but not the PD-related mutant C431F (Figure 2.1C) in WT MEFs. In the absence of DJ-1, however, the amount of cells displaying Parkin translocation was significantly higher after 1hr of CCCP treatment (Figure 2.1A and Figure 2.1B). This data demonstrates that DJ-1 deficient mitochondria are hypersensitized to depolarization-induced stress and recruit Parkin earlier.

Figure 2.1: Parkin translocation occurs earlier in the absence of DJ-1. (A) DJ-1 wildtype (WT) and knockout (KO) MEFs were transfected with GFP-Parkin and were either left untreated or treated with 10μM CCCP for 1h. Following treatment, cells were fixed, permeabilized and the mitochondria labeled using TOM20 antibody. Representative confocal images are presented. (B) Quantification of CCCP-induced Parkin translocation in DJ-1 WT and KO MEFs. GFP-Parkin transfected DJ-1 WT and KO MEFs were treated with 10μM CCCP for the indicated duration. Fixed cells were stained using TOM20 antibody and the number of cells displaying Parkin co-localization with mitochondrial staining quantified. (C) WT MEFs were infected with AAV encoding either WT GFP-Parkin or the C431F mutant. Cells were treated with 10μM CCCP and samples prepared for confocal analysis as mentioned before. (B and C) Results show the mean ± SEM values of triplicates with an average of 200 cells counted per condition. n.s., not significant; $^{**}P<0.01$; *t*-test for related samples.

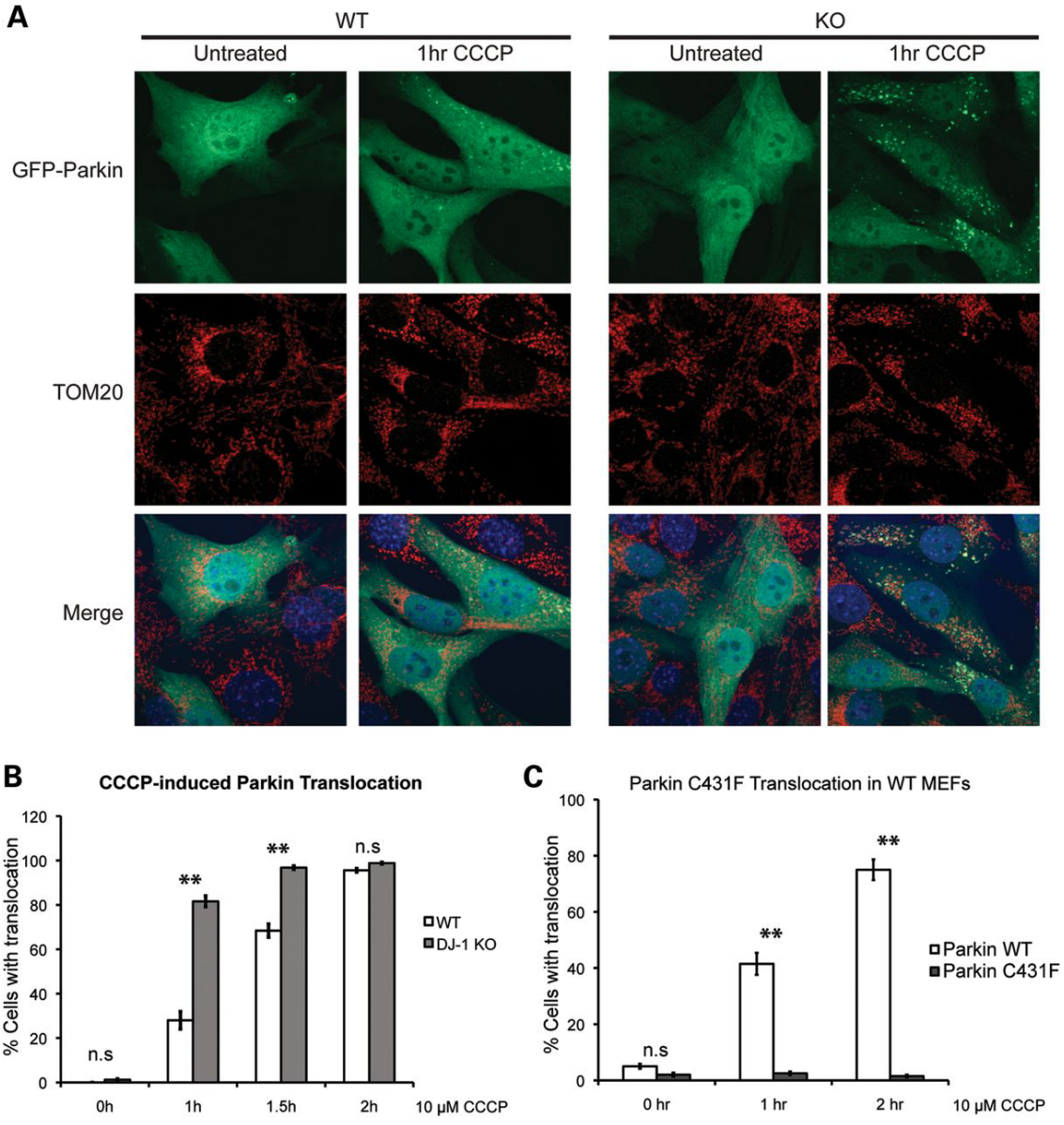
A
WT
KO
Untreated
1hr CCCP
Untreated
1hr CCCP
GFP-Parkin
TOM20
Merge
B
CCCP-induced Parkin Translocation
% Cells with translocation
120
100
80
60
40
20
0
n.s
**
**
n.s
WT
DJ-1 KO
0h
1h
1.5h
2h
10 μM CCCP
C
Parkin C431F Translocation in WT MEFs
% Cells with translocation
100
80
60
40
20
0
n.s
**
**
Parkin WT
Parkin C431F
0 hr
1 hr
2 hr
10 μM CCCP

DJ-1 is known to regulate ROS (Mitsumoto et al., 2001; Canet-Avilés et al., 2004). In addition, absence of DJ-1 leads to increased ROS under a number of conditions (Irrcher et al., 2010; Thomas et al., 2011). Accordingly, a plausible explanation for the observed earlier recruitment of Parkin to mitochondria in the absence of DJ-1 is increased oxidative stress. However, previous reports in HeLa cells indicated that ROS was not involved in mediating Parkin translocation (Narendra et al., 2008). We questioned whether there was something unique about HeLa cells that made them unresponsive to ROS. To address this discrepancy, we more carefully examined the requirement of ROS in our present studies in MEFs. WT MEFs were pre-treated with the antioxidants N-acetyl cysteine (NAC; 2mM) or TIRON (100μM) for 3h before the addition of CCCP. As evident from Figure 2.2A, Parkin translocation was noticeably inhibited by both NAC and TIRON even after 2h of CCCP treatment. Consistent with previous reports, we observed that NAC treatment, however, failed to prevent Parkin translocation in HeLa cells (Figure 2.2B, 2.S1). To further support the importance of ROS in Parkin translocation, we tested whether WT DJ-1 or a cysteine-106 (C106A) mutant of DJ-1, known to be deficient in response to oxidative stress, could alter Parkin translocation kinetics. Importantly, earlier translocation of Parkin observed in DJ-1 deficient MEFs was restored to WT levels by exogenously expressing WT DJ-1, but not the mutant C106A DJ-1 (Figure 2.2D). Consistent with previous reports in other cell types, Parkin translocation in MEFs was observed to be Pink1-dependent since Parkin translocation did not occur in a Pink1 deficient background (Figure 2.2E). Finally, in line with previously published results (Rakovic et al., 2010), Parkin translocation was also induced by 5h of 100μM hydrogen peroxide (H_2O_2) treatment in WT MEFs (Figure 2.S2). Taken together,

our results indicate that the ROS environment (known to be regulated by DJ-1) is an essential regulator of Pink1-mediated Parkin translocation, at least in non-transformed cell types.

Figure 2.2: Parkin translocation is ROS dependent in MEFs. GFP-Parkin transfected WT MEFs (A) or HeLa cells (B and C) were pretreated with either 2mM NAC or 100μM TIRON in the case of MEFs and only NAC in the case of HeLa cells, for 3h before treating the cells with 10μM CCCP for 2h. Cells were fixed, stained and the number of cells displaying Parkin translocation quantified (A and C). (D) DJ-1 WT or KO MEFs were co-transfected with GFP-Parkin and either vector control (Empty Vector), WT-DJ-1, or DJ-1 C106A (C106A) and were treated with vehicle (0h) or 10μM CCCP for 2h. GFP-positive cells were scored for the presence of Parkin puncta. (E) GFP-Parkin transfected WT or Pink1 deficient MEFs (Pink1 KO) were treated with 10μM CCCP for the indicated duration and Parkin translocation quantified. Bar graphs A, C, D and E show the mean ± SEM values of triplicates with an average of 200 cells counted per condition. **P*<0.05 and ****P*<0.001; n.s., not significant; *t*-test for related samples.

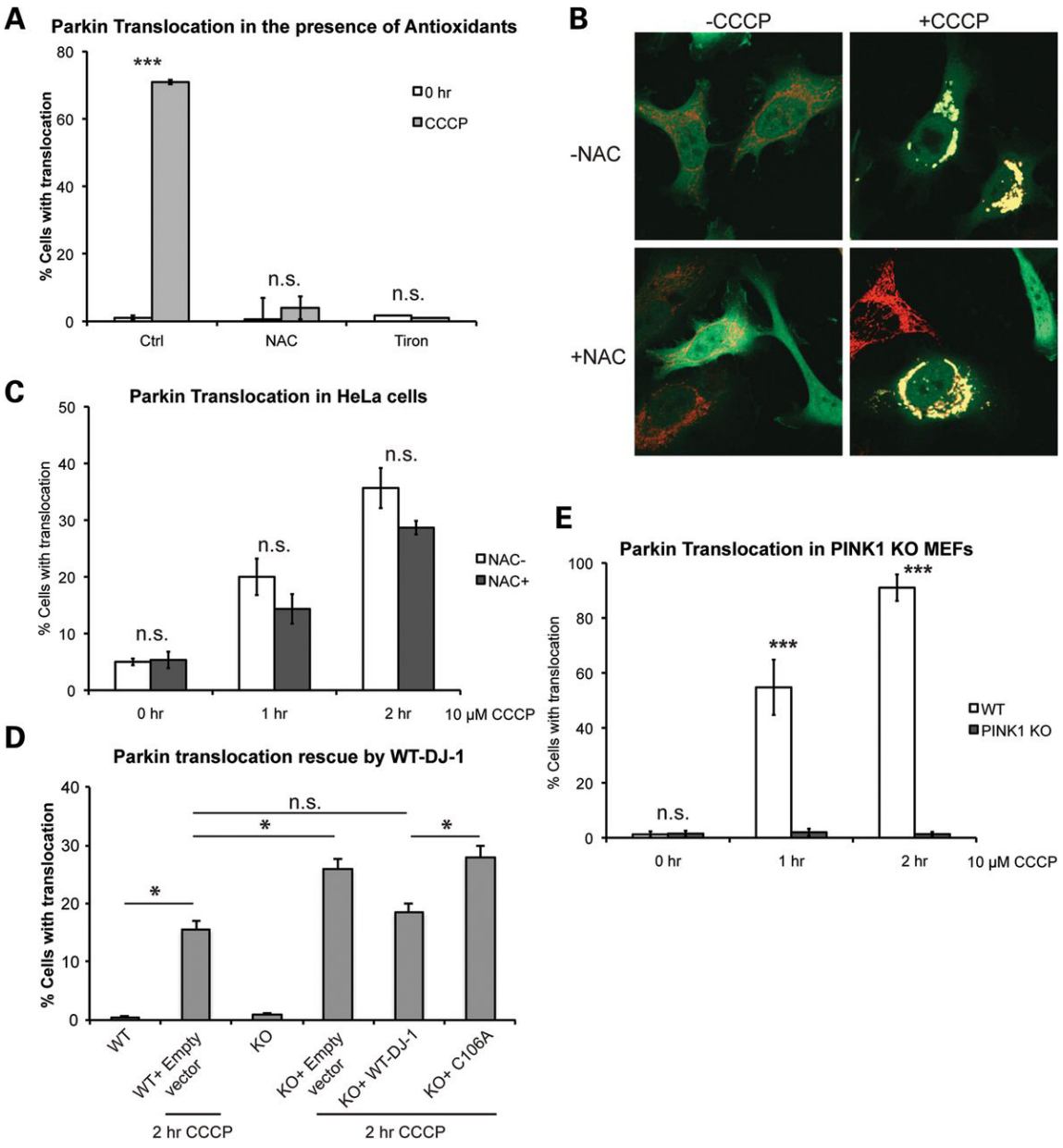
A
Parkin Translocation in the presence of Antioxidants
% Cells with translocation
0 hr
CCCP
***
n.s.
n.s.
Ctrl
NAC
Tiron
B
-CCCP
+CCCP
-NAC
+NAC
C
Parkin Translocation in HeLa cells
% Cells with translocation
NAC-
NAC+
n.s.
n.s.
n.s.
0 hr
1 hr
2 hr
10 μM CCCP
D
Parkin translocation rescue by WT-DJ-1
% Cells with translocation
n.s.
*
*
*
WT
WT+ Empty vector
KO
KO+ Empty vector
KO+ WT-DJ-1
KO+ C106A
2 hr CCCP
2 hr CCCP
E
Parkin Translocation in PINK1 KO MEFs
% Cells with translocation
WT
PINK1 KO
n.s.
***
***
0 hr
1 hr
2 hr
10 μM CCCP

It has been reported previously (Narendra et al., 2008) that once recruited to mitochondria, Parkin selectively mediates the clearance of these damaged mitochondria by activating mitophagy. To test if mitochondrial clearance was also heightened in DJ-1 knockout (KO) MEFs, we analyzed the total mitochondria per cell, both in Parkin-overexpressing WT and DJ-1 KO MEFs after treatment with 10μM CCCP for 6h (Figure 2.3). Compared to vehicle treated cells (0h), a noticeable decrease in the number of mitochondria was observed after 6h of CCCP treatment both in WT and DJ-1 KO MEFs. Interestingly, mitochondrial-staining intensity after CCCP treatment was significantly lower in DJ-1 deficient MEFs compared to WT MEFs (Figure 2.3B). These results suggest that earlier recruitment of Parkin in DJ-1 deficient cells is also accompanied by faster clearance of the damaged mitochondria.

Figure 2.3: Mitochondrial clearance is enhanced in DJ-1 deficient MEFs. (A) Representative confocal photomicrographs of GFP-Parkin transfected WT or DJ-1 KO MEFs treated with 10μM CCCP for 6h. Fixed cells were stained for mitochondrial marker COX 1. (B) Quantification of mitochondrial fluorescence intensity. Mitochondrial fluorescence of GFP positive cells was measured using ImageJ from confocal photomicrographs, as described in materials. Bar diagram represent ± SEM values of at least 25 cells per conditions. Results are representative of two independent experiments. $^{**}P<0.01$ and $^{***}P<0.001$; *t*-test for related samples.

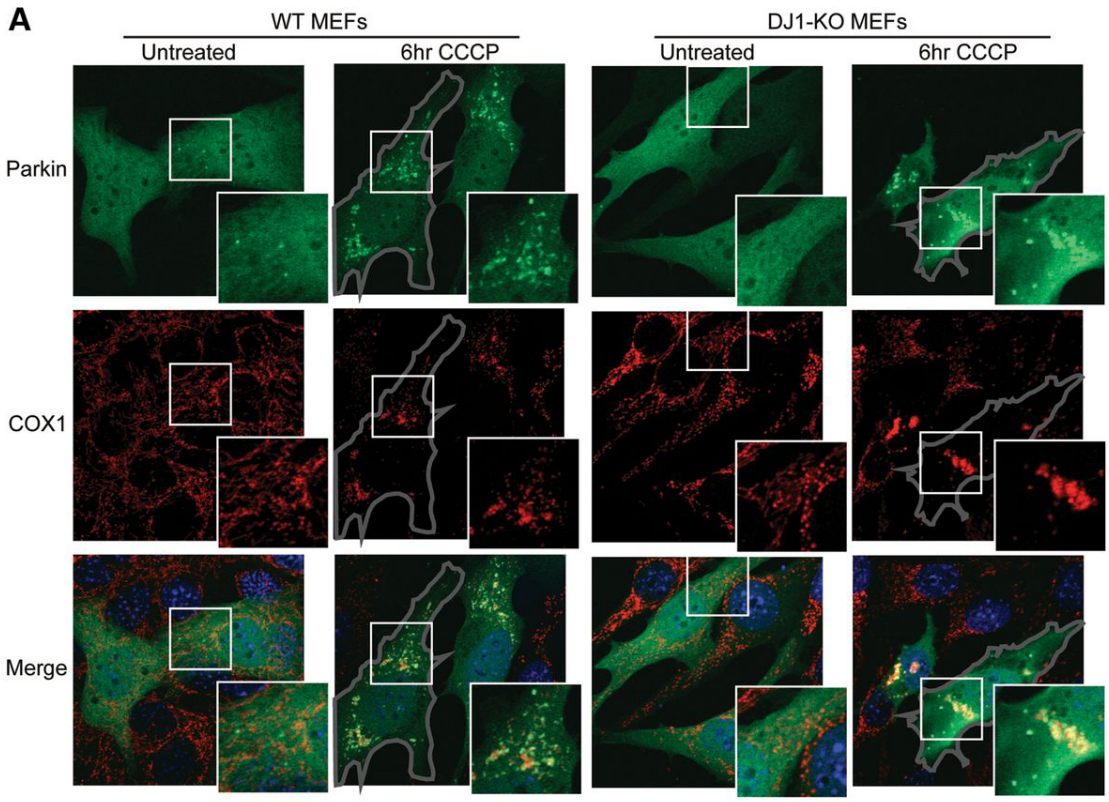
A
WT MEFs
DJ1-KO MEFs
Untreated
6hr CCCP
Untreated
6hr CCCP
Parkin
COX1
Merge

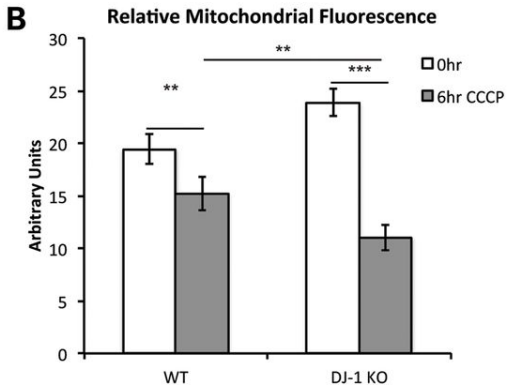
B
Relative Mitochondrial Fluorescence
Arbitrary Units
30
25
20
15
10
5
0
**
**
***
0hr
6hr CCCP
WT
DJ-1 KO

Stress-induced increase of mitochondrial DJ-1 is dependent upon Parkin/Pink1 in MEFs

The results above indicate that DJ-1 loss leads to earlier Parkin translocation, suggesting a critical role for DJ-1-mediated ROS regulation in Parkin function. We next determined whether the converse may be true, i.e. whether any function of DJ-1 may be impacted by Parkin/Pink1. Previous evidence indicated that the level of mitochondrial DJ-1 increases in response to H_2O_2-induced oxidative stress in SK-N-BE(2)C human neuroblastoma cells (Junn et al., 2009) and paraquat-induced stress in M17 neuroblastoma cells (Canet-Avilés et al., 2004). Accordingly, we explored how this increase may be impacted by Parkin/Pink1 deficiency. To determine levels of DJ-1 at mitochondria upon induction of oxidative stress in our present system, WT MEFs were treated with 100μM H_2O_2 for up to 6h and the cytoplasmic and mitochondrial-enriched fractions were separated by sub-cellular fractionation for analysis by immunoblot (Figure 2.4). Equal amounts (10μg) of mitochondrially-enriched fractions from each time point were loaded and a whole cell lysate from DJ-1 KO MEFs was included as a negative control. Following 1h of H_2O_2 treatment, a significant increase (Figure 2.4A) in the level of DJ-1 was observed at mitochondria and this augmented level was maintained at both 3h and 6h post-treatment. Immunoblotting against the 39kDa subunit of Complex I (NDUFA9) or mitochondrial heat shock protein 70 (mtHSP70) was performed as a loading control. Additionally, we noted no substantial increase in whole cell levels of DJ-1 with H_2O_2 treatment indicating that the observed increased levels of DJ-1 in the mitochondrial-enriched fraction is not simply due to increased global levels of DJ-1 in the cell (Figure 2.S3A). We also noticed endoplasmic reticulum (ER) contamination, as observed by the ER marker calnexin in our mitochondrial-enriched fractions (Figure

2.S4A). Accordingly, we could not rule out DJ-1 at the ER (however see data for neurons below). We next determined whether oxidative stress-mediated increase in mitochondrial DJ-1 might in turn be mediated by Parkin and/or Pink1. Importantly, the stress-induced increase of mitochondrial DJ-1 in WT MEFs is absent with Parkin deficiency (Figure 2.4A). This lack of increase in mitochondrial DJ-1 indicates that Parkin is required for stress-induced response of DJ-1 to mitochondria increase. While Pink1 deficiency resulted in higher basal DJ-1 levels at the mitochondria, mitochondrial DJ-1 level did not further increase with oxidative stress (Figure 2.4). Pink1 or Parkin deficiency did not induce any notable change in total basal DJ-1 levels (Figure 2.S3D). Taken together, this evidence indicates that the relationship of DJ-1 and Parkin is reciprocal; DJ-1 modulates stress-induced Parkin recruitment while Parkin and Pink1 activity is required for stress-induced increase of mitochondrial DJ-1.

Figure 2.4: Oxidative stress-induced increase in mitochondrial DJ-1 is dependent upon Parkin and Pink1 in MEFs. Wild-type (WT), Pink1-null and Parkin-null MEFs were treated with 100μM H_2O_2 for indicated time points. Mitochondria-enriched fractions were obtained through sub-cellular fractionation and were analyzed by immunoblot. (A) Quantification of densitometry using Image J software (NIH). Data represent mean ± SEM (n=3-4). n.s, not significant; *P<0.05 and **P<0.01; t-test for related WT samples; two-way ANOVA for WT vs. KO samples. (B) Representative blots for DJ-1 and mitochondrial loading control (NDUFA9 or mtHSP70). K, DJ-1 KO sample.

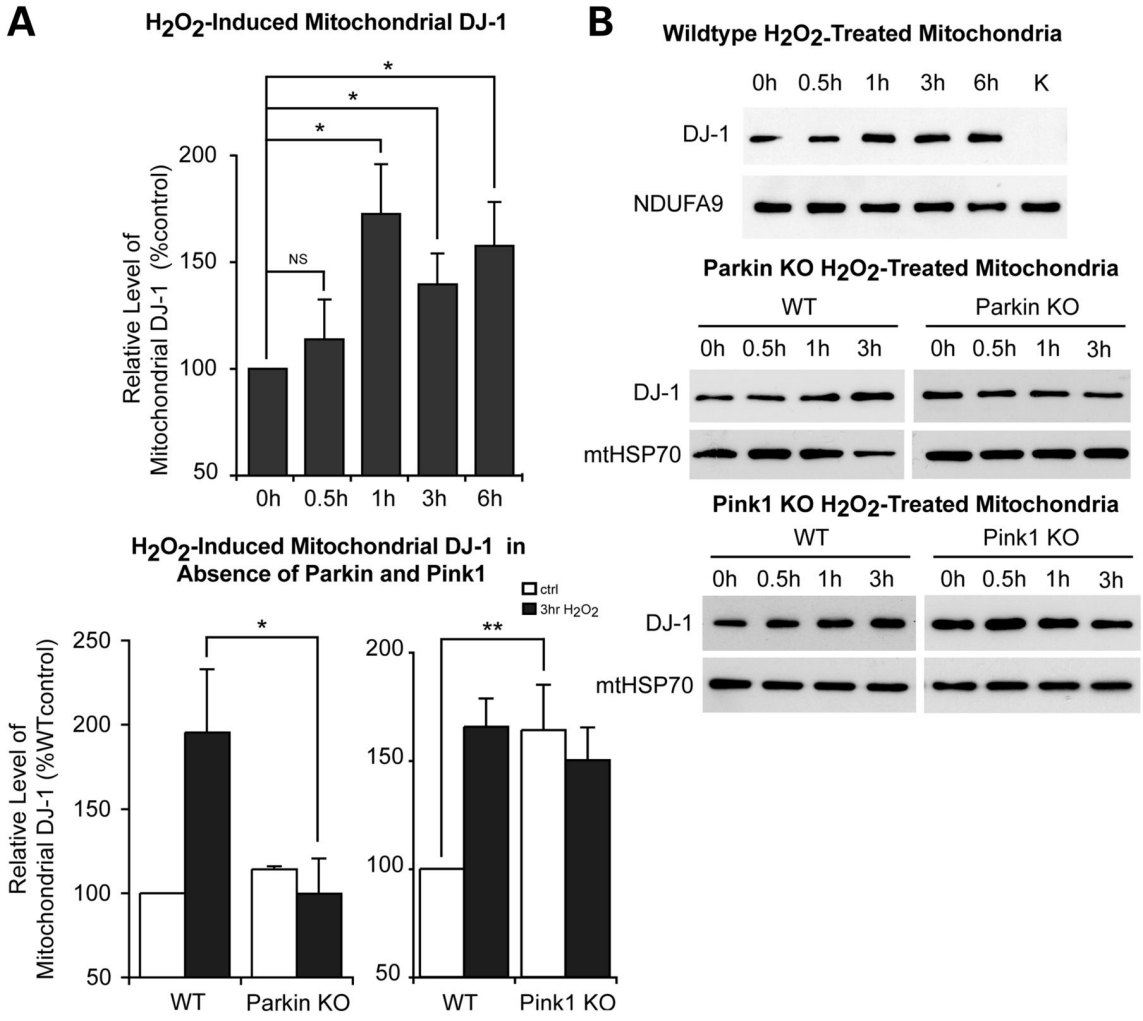
A
H_2O_2-Induced Mitochondrial DJ-1
Relative Level of Mitochondrial DJ-1 (%control)
200
150
100
50
NS
*
*
*
0h 0.5h 1h 3h 6h
H_2O_2-Induced Mitochondrial DJ-1 in Absence of Parkin and Pink1
ctrl
3hr H_2O_2
Relative Level of Mitochondrial DJ-1 (%WTcontrol)
250
200
150
100
50
*
**
WT
Parkin KO
WT
Pink1 KO
B
Wildtype H_2O_2-Treated Mitochondria
0h 0.5h 1h 3h 6h K
DJ-1
NDUFA9
Parkin KO H_2O_2-Treated Mitochondria
WT
Parkin KO
0h 0.5h 1h 3h 0h 0.5h 1h 3h
DJ-1
mtHSP70
Pink1 KO H_2O_2-Treated Mitochondria
WT
Pink1 KO
0h 0.5h 1h 3h 0h 0.5h 1h 3h
DJ-1
mtHSP70

Punctate Parkin staining in neurons in response to CCCP, rotenone and MPP^+ treatment

As stated previously, Parkin translocation to mitochondria is well established in HeLa cells, in other cultured cell types, and as presently reported in MEFs. In neurons however, Parkin translocation in the presence of classic Parkin-recruiting stimuli such as CCCP (Van Laar et al., 2010) or in the absence of TFAM (Sterky et al., 2011) does not appear to occur in neurons. This is a critical issue when it comes to determining whether or not MQC may be involved in degeneration observed in PD. Under routine culture conditions in media containing B27 supplement used for cortical neurons, we also failed to observe any Parkin translocation following induction of mitochondrial damage. To analyze for this translocation in neurons, we infected E15.5 mouse cortical neurons with an Adeno-associated virus (AAV) encoding the human *Parkin* gene fused to emerald-GFP. Parkin expression, observable as diffuse GFP fluorescence throughout the neuronal cell body, could be seen after 6 to 7 days of infection. With extended time courses and dosing ranges of CCCP, 1-methyl-4-phenylpyridinium (MPP^+) or rotenone, we could not observe any Parkin translocation. Interestingly, however, we could detect mitochondrial fragmentation within 1h of CCCP treatment or 9h of MPP^+ treatment indicating that the agents utilized were having an effect on mitochondria (Figure 2.5).

Figure 2.5: Antioxidant-dependent Parkin translocation in mouse primary cortical neurons. Representative confocal photomicrographs of primary cortical neuronal cultures infected with GFP-Parkin AAV were cultured under routine cortical culture conditions in the presence of B27. Cells were either treated with vehicle (0h) or with 5μM CCCP for 1h. GFP-Parkin localization was analyzed after staining for mitochondria.

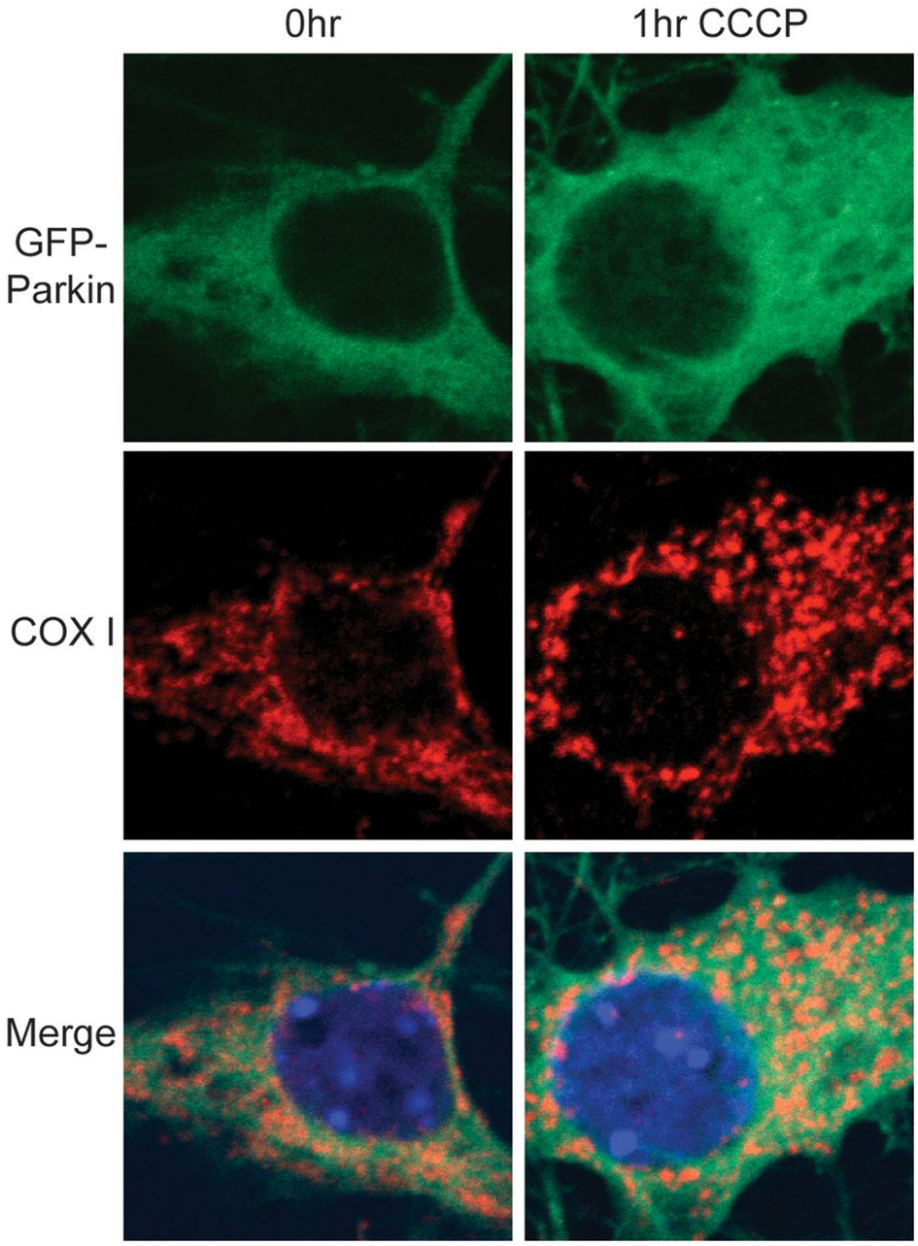
0hr
1hr CCCP
GFP-
Parkin
COX I
Merge

Our previous data in MEFs, however, suggested that ROS is a critical mediator of Parkin translocation. The supplement B27 contains numerous antioxidants including reduced glutathione, vitamin E (dl-α-tocopherol), catalase and superoxide dismutase. Accordingly, we reasoned that perhaps translocation was not observed in neurons because of the antioxidant-enriched media. To test this, we compared cells cultured in the presence or absence of B27 supplement. Initial experiments using poly-D-lysine only coated coverslips resulted in detachment of majority of neurons during drug treatments and subsequent staining procedure. For this reason, cortical neurons derived from WT CD-1 E15.5 mice embryos were plated on acid-treated coverslips, coated with poly-D-lysine and laminin. Indeed, a comparison of Parkin localization in cortical neurons cultured in the presence or absence of B27 revealed appearance of intense punctate Parkin staining in the cell bodies of the neurons after 5μM CCCP, 0.05μM rotenone or 20μM MPP^+ treatment (Figure 2.6A). Quantification of the number of neurons displaying punctate Parkin staining revealed a statistically significant increase in cells displaying Parkin puncta after oxidative stress (Figure 2.6B and 2.6C). We should note that the time course of CCCP and MPP^+-induced Parkin translocation differs likely due to delayed mitochondrial damage as observed by fragmentation. These observations not only demonstrate a change in Parkin translocation following oxidative damage in neurons, but also suggest that Parkin translocation is ROS-dependent.

Figure 2.6: Differential Parkin translocation in CCCP-treated mouse cortical neurons. (A) GFP-Parkin AAV infected cortical neurons were changed to media without B27 (-B27). Cells were either treated with vehicle (0h) or treated with 0.05μM rotenone for 3h or 20μM MPP+ for 24h or 5μM CCCP for 3h. Fixed and permeabilized cells were co-stained to label mitochondria using TOM20 antibody. (B and C) Quantification of number of neurons displaying GFP-Parkin translocation. Primary mouse cortical cultures infected with GFP-Parkin AAV were either changed to fresh media with or without B27 at least 24h before treating with 5μM CCCP or 0.05μM rotenone for the indicated durations. Neurons displaying punctate Parkin staining were quantified under fluorescence microscope. Bar graph represents the mean ± SEM values of triplicates with an average of 200 cells counted per condition. Quantification is representative of at least 3 independent experiments. n.s, not significant; **P*<0.05 and ***P*<0.001; *t*-test for related samples.

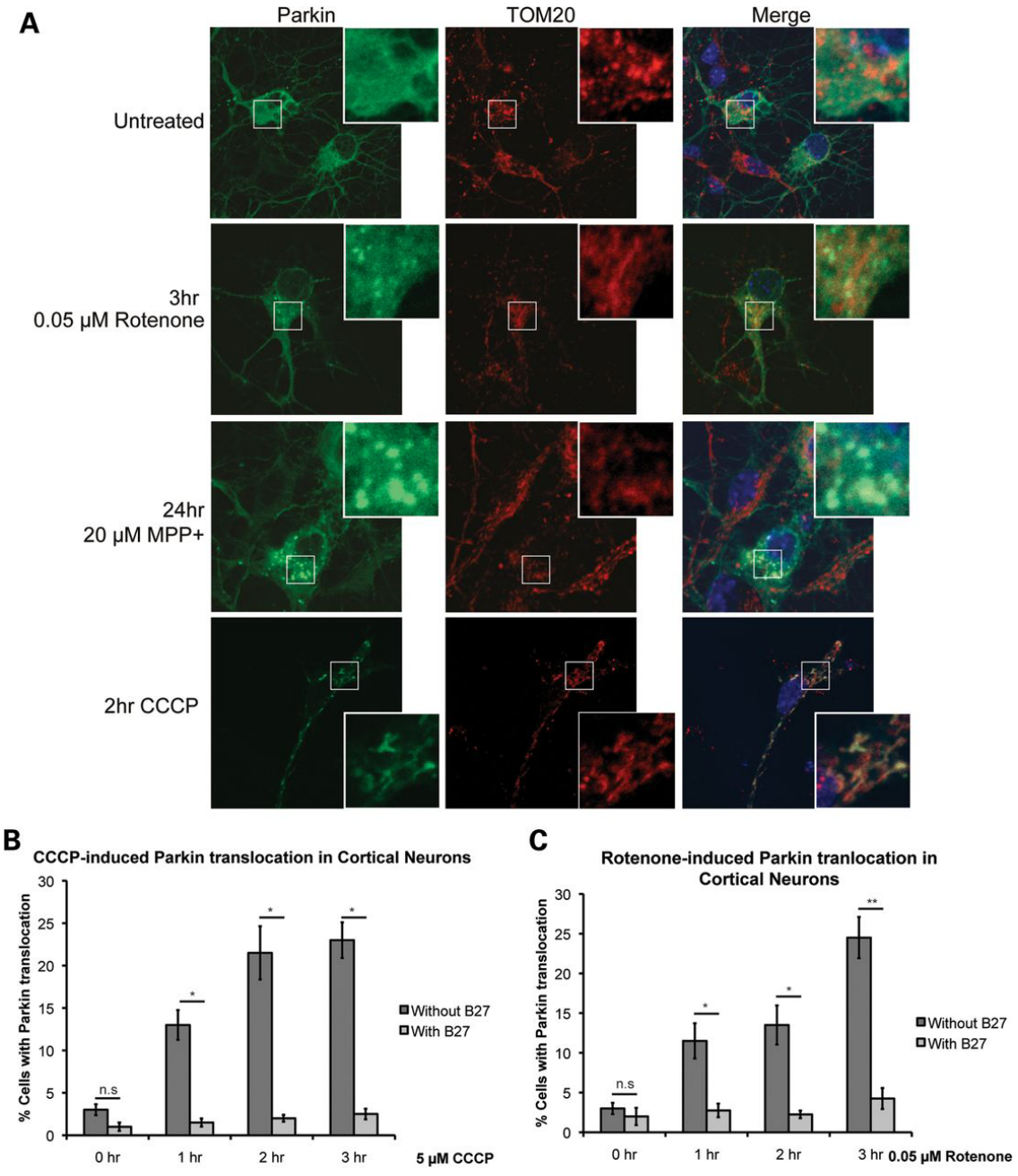
A
Parkin
TOM20
Merge
Untreated
3hr
0.05 μM Rotenone
24hr
20 μM MPP+
2hr CCCP
B
CCCP-induced Parkin translocation in Cortical Neurons
% Cells with Parkin translocation
30
25
20
15
10
5
0
n.s
*
*
*
0 hr
1 hr
2 hr
3 hr
5 μM CCCP
Without B27
With B27
C
Rotenone-induced Parkin tranlocation in Cortical Neurons
% Cells with Parkin translocation
30
25
20
15
10
5
0
n.s
*
*
**
0 hr
1 hr
2 hr
3 hr
0.05 μM Rotenone
Without B27
With B27

Parkin translocation in cortical neurons and mitophagy

To analyze the localization of the Parkin puncta, we performed co-labeling immunofluorescence studies. Cortical neurons from E15.5 mouse embryos were infected with GFP-Parkin encoding AAV and treated with 0.05μM rotenone after 7 days of culture. We first tested whether these puncta co-localized with mitochondrial markers. All mitochondrial markers used, such as TOM20, Complex IV subunit 1, Complex V and an artificial mitochondrial matrix cargo Oct4-dsRed (data not shown) all exhibited partial co-localization with the Parkin puncta in cells treated with MPP^+ (Figure 2.7A). However, the co-localization pattern was clearly different than that observed in CCCP-treated neurons (compare Figure 2.6A rotenone and MPP^+-treated with CCCP-treated), those previously shown in MEFs (Figure 2.1), and those reported in other cell types where there was more prominent overlap with mitochondrial staining.

Parkin is an E3-ubiquitin ligase and translocated Parkin has been shown to enhance ubiquitination at the clustering mitochondria in HeLa cells (Geisler et al., 2010; Matsuda et al., 2010). We were curious as to whether the punctate Parkin observed in the neurons overlap in any way with ubiquitination. To test this, we co-stained rotenone-treated, Parkin over-expressing cortical neurons with an antibody recognizing ubiquitin (Figure 2.7B). A diffuse cytoplasmic staining of ubiquitin was observed in control cells. Interestingly, rotenone-treated cells exhibited notable overlap of ubiquitin staining with Parkin puncta consistent with enhanced ubiquitination reported previously (Ding et al., 2010; Geisler et al., 2010; Matsuda et al., 2010).

We also performed co-staining for endogenous LC-3 as a marker for autophagy. LC-3 attaches to early autophagic vesicles during autophagosome biogenesis and is

widely used as a marker for autophagy induction (Klionsky et al., 2008). Since previous reports (Narendra et al., 2008) had demonstrated that in cell lines, Parkin translocation precedes mitochondrial clearance by autophagic vesicles by a process termed mitophagy, we investigated if the Parkin puncta observed in cortical neurons could also be mitophagic in nature. Some overlap of Parkin puncta with the endogenous LC-3 staining was observed (Figure 2.7C). These observations indicate that there are indeed MQC processes occurring in primary neurons in a ROS-dependent fashion. However, this process appears to be qualitatively quite different than those observed in other cell types.

Figure 2.7: Parkin co-localization with cellular organelle markers. (A) Confocal photomicrographs of GFP-Parkin infected primary cortical neurons treated with 20μM MPP^+ for 24h in the absence of B27 co-stained with TOM20. (White arrowheads, co-localized; purple arrowheads, not co-localized.). (B) and (C) Primary cortical neurons treated with 0.05 μM rotenone were analyzed for co-localization with ubiquitin (B) and LC3 (C).

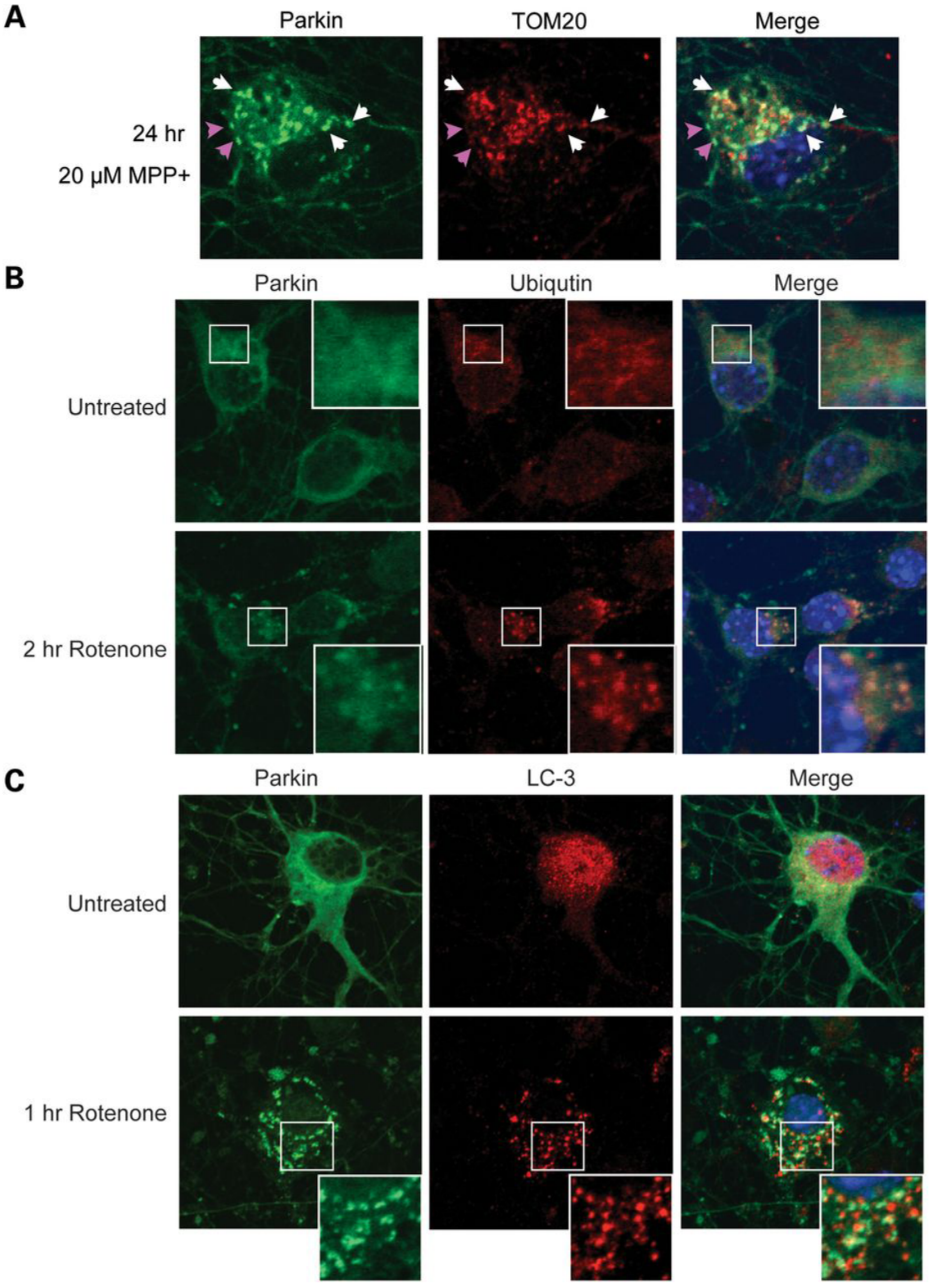
A
Parkin
TOM20
Merge
24 hr
20 μM MPP+
B
Parkin
Ubiqutin
Merge
Untreated
2 hr Rotenone
C
Parkin
LC-3
Merge
Untreated
1 hr Rotenone

Parkin translocation in DJ-1 or PINK1 deficient neurons

We next determined whether the observed aggregation of Parkin in primary neurons was dependent upon Pink1 and DJ-1, as we have explored in MEFs. Cortical neurons derived from WT and Pink1 deficient E15.5 mice embryos were plated on acid-treated coverslips, coated with poly-D-lysine and laminin. The neurons were infected with GFP-Parkin expressing AAV at the time of plating. Seven days post-plating, the media was changed to fresh growth media lacking B27, as mentioned before, followed by drug treatments. Within 2h of 5μM CCCP treatment, significant increase in cells displaying mitochondrially-translocated Parkin could be observed (Figure 2.8A) in WT cortical neurons. However, consistent with observations in Pink1 KO MEFs, no punctate Parkin staining was observed in Pink1 deficient neurons, even after 4h of CCCP treatment. These results indicate the presence of an active Pink1/Parkin pathway in primary neurons in response to mitochondrial damage.

Furthermore, similar experiments were performed in primary cortical neuronal cultures from DJ-1 deficient mice. We observed that, in comparison to WT neurons, Parkin translocation was accelerated in the absence of DJ-1, following treatment with either 5μM CCCP or 20μM MPP^+ (Figure 2.8B). We also investigated whether the observed Parkin translocation phenotype in DJ-1 deficient neurons could be rescued by overexpressing WT-DJ-1 (Figure 2.8D). Similar to MEFs, exogenously expressed WT-DJ-1 but not C106A mutant could restore CCCP-induced Parkin translocation levels to those observed in WT neurons. These results provide further evidence of sensitization of DJ-1 deficient cells to mitochondrial damage and therefore suggest an earlier activation of the Pink1/Parkin pathway of mitochondrial damage control.

An important consequence of the activation of the Pink1/Parkin pathway of mitochondrial clearance would be increased survival of cells that can more efficiently clear damaged mitochondria. To test if Parkin overexpression and therefore increased MQC does confer a survival advantage to cells under oxidative stress conditions, we analyzed the survival status of cells overexpressing WT Parkin or the E3-ubiquitin ligase mutant C431F after 6h of 0.05μM rotenone or 48h of 20μM MPP^+ treatment (Figure 2.8E). Under both oxidative stress conditions, overexpression of wild type Parkin offered a modest but significant increase in survival when compared to the C431F mutant. These observations provide further support for a functional Pink1/Parkin pathway in neurons. However, care must be taken in interpreting these survival results since the E3 ligase activity of Parkin may have other functions than regulating MQC.

Figure 2.8: Parkin translocation in Pink1 and DJ-1 deficient cortical neurons.

Primary mouse cortical cultures from wild-type (WT) or Pink1 deficient (Pink1 KO) (A) or DJ-1 deficient (DJ-1 KO) (B) embryos infected with GFP-Parkin AAV were treated with 20μM MPP^+ for the indicated durations. Number of cells displaying Parkin puncta were quantified. (C) Representative confocal images of Parkin translocation in CCCP-treated wild-type (DJ-1 WT) and DJ-1 knockout (DJ-1 KO) cortical neuronal cultures. (D) WT or DJ-1 deficient (DJ-1 KO) cortical neurons were infected with GFP-Parkin and either control (Ctrl) or FLAG-WT DJ-1 or FLAG-C106A DJ-1 AAV at the time of plating. Upper panel; expression levels of WT and C106A DJ-1 as illustrated by FLAG staining. Lower panel; Quantification of cells displaying Parkin puncta. (E) Survival of primary cortical neurons from CD1 embryos infected with either GFP- Parkin or GFP-C431F Parkin AAV after treatment with 20μM MPP^+ for 48h. All bar graphs are mean ± SEM vales of triplicates with an average of 200 cells counted per condition. *P<0.05 and **P<0.001; t-test for related samples and representative of at least 2 independent experiments.

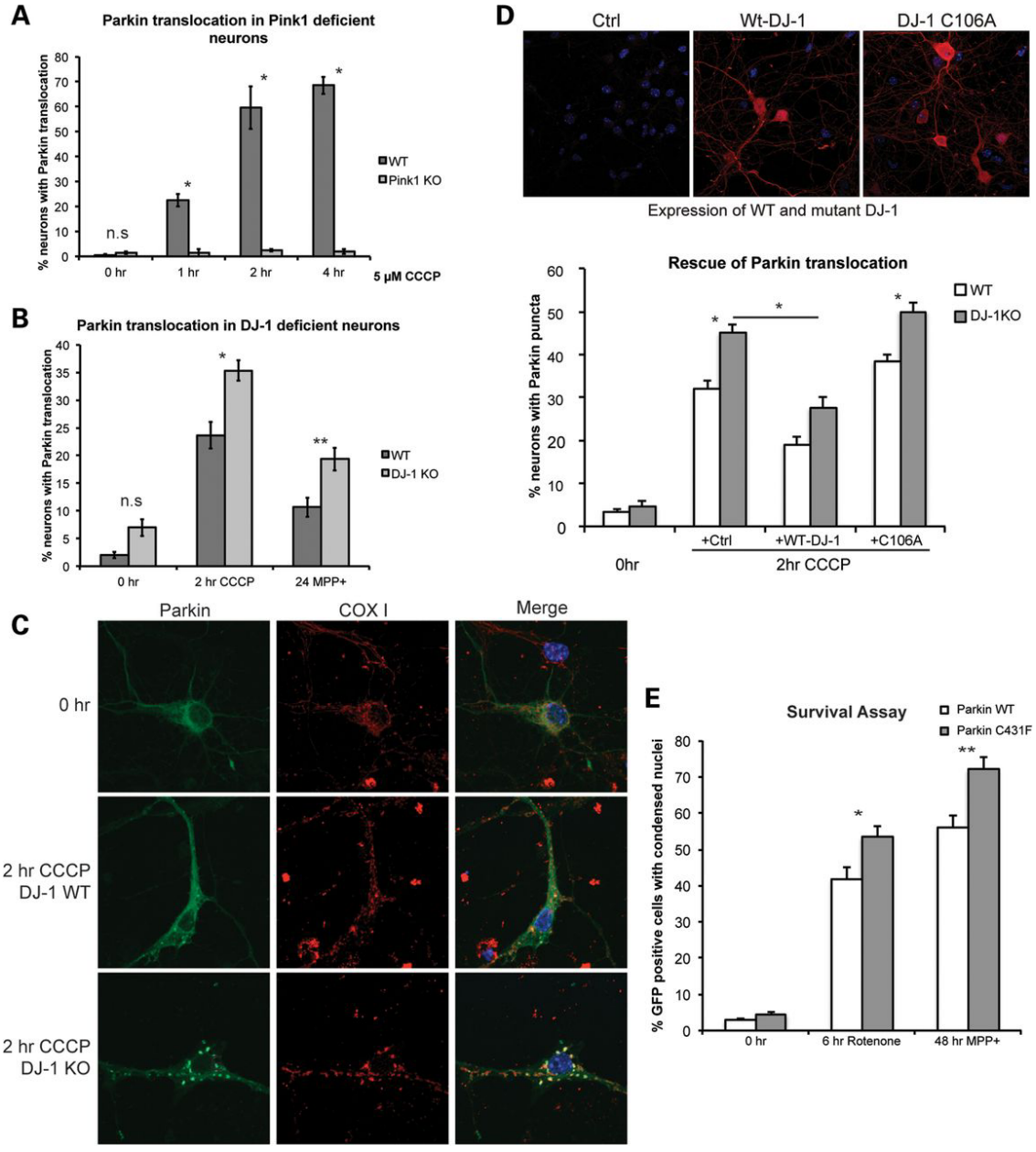
A
Parkin translocation in Pink1 deficient neurons
% neurons with Parkin translocation
WT
Pink1 KO
n.s
0 hr
1 hr
2 hr
4 hr
5 μM CCCP
B
Parkin translocation in DJ-1 deficient neurons
% neurons with Parkin translocation
WT
DJ-1 KO
n.s
0 hr
2 hr CCCP
24 MPP+
C
Parkin
COX I
Merge
0 hr
2 hr CCCP DJ-1 WT
2 hr CCCP DJ-1 KO
D
Ctrl
Wt-DJ-1
DJ-1 C106A
Expression of WT and mutant DJ-1
Rescue of Parkin translocation
% neurons with Parkin puncta
WT
DJ-1KO
0hr
+Ctrl
+WT-DJ-1
+C106A
2hr CCCP
E
Survival Assay
Parkin WT
Parkin C431F
% GFP positive cells with condensed nuclei
0 hr
6 hr Rotenone
48 hr MPP+

Increase of mitochondrial DJ-1 in primary neurons with oxidative stress

The above results further implicate DJ-1 in MQC. We next explored whether increased mitochondrial DJ-1 also occurs in primary neurons and whether this was dependent upon Pink1 similar to that observed in MEFs. WT primary cortical neurons from E14.5-15.5 were treated with 30μM H_2O_2, 10μM MPP^+, or 10μM CCCP in absence of antioxidants on DIV 6 (Figure 2.9). Equal amounts (10μg) of mitochondrially-enriched fractions from each time point were loaded. At 1h of H_2O_2 treatment, a significant increase (Figure 2.9A) in the level of DJ-1 at mitochondria was observed in cortical neurons. Sustained maintenance of these DJ-1 levels was also observed until 6h of H_2O_2 treatment. Similarly, by 3h treatment with MPP^+ and 1hr treatment with CCCP, the level of mitochondrial DJ-1 was significantly increased (Figure 2.9). Similar to MEFs, we also noted no significant increase in whole cell levels of DJ-1 with any treatment (Figure 2.S3B, C). These results demonstrate increased levels of DJ-1 at mitochondria in primary cortical neurons in response to oxidative stress by various agents, most notably the PD-linked drug MPP^+.

Figure 2.9: The PD-related MPP^+ as well as other oxidative stressors increase level of DJ-1 at mitochondria in cortical neurons. Wild-type (WT) cortical neurons harvested from E14.5-15.5 embryos were treated with 30μM H_2O_2, 10μM MPP^+ or 10μM CCCP for indicated time points in absence of antioxidants. Mitochondrial-enriched fractions were obtained through sub-cellular fractionation and were analyzed by immunoblot. A) Quantification of densitometry using Image J software (NIH). Data represent mean ± SEM (n=3-4 H_2O_2 and CCCP; n=6 MPP^+). n.s, not significant; **P*<0.05 and ***P*<0.01 B) Representative blots for DJ-1 and mitochondrial loading control (either NDUFA9 or mtHSP70).

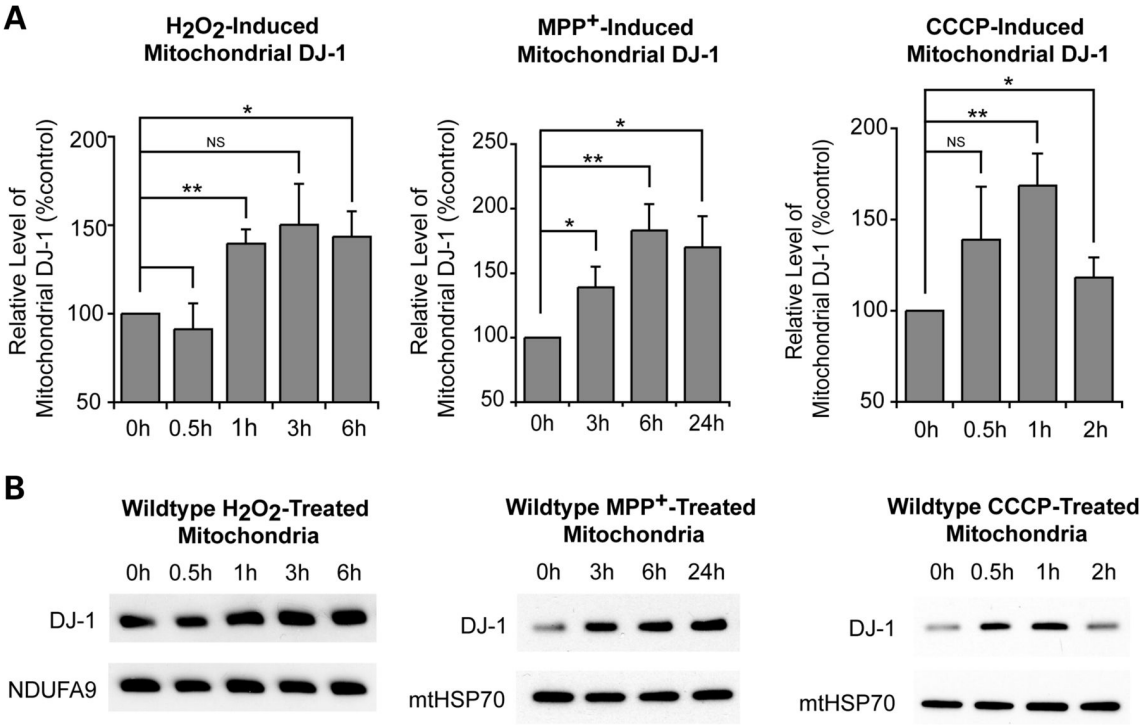
A
H2O2-Induced Mitochondrial DJ-1
MPP+-Induced Mitochondrial DJ-1
CCCP-Induced Mitochondrial DJ-1
Relative Level of Mitochondrial DJ-1 (%control)
NS
*
**
0h 0.5h 1h 3h 6h
0h 3h 6h 24h
0h 0.5h 1h 2h
B
Wildtype H2O2-Treated Mitochondria
Wildtype MPP+-Treated Mitochondria
Wildtype CCCP-Treated Mitochondria
DJ-1
NDUFA9
mtHSP70

To further confirm DJ-1 increase at the mitochondria and to rule out changes in DJ-1 levels due to contaminating ER (Figure 2.S4B), we investigated changes in mitochondrial DJ-1 using immunofluorescence. WT cortical neurons obtained as previously mentioned were plated onto poly-D-lysine-coated coverslips at a density of 100,000 cells per well of a 24-well dish. These neurons were treated, in absence of antioxidant supplementation, on DIV 6 with either 10μM MPP^+ (6h) or 10μM CCCP (1h). Neurons were stained for endogenous DJ-1 and a mitochondrial marker, mtHSP70. Control neurons exhibited mostly ubiquitous staining for DJ-1 while neurons treated with either MPP^+ or CCCP showed punctate DJ-1 staining that partially co-localizes with mitochondrial staining (Figure 2.S5, white arrows). Due to the large amount of cytoplasmic staining of DJ-1 as well as the large amount of mitochondria in the cell body, we focused on the neuronal processes for demonstrating DJ-1 punctate staining. These observations further support our previous findings using cellular fractionation that DJ-1 levels increase at mitochondria following oxidative stress in neurons.

Importantly, increased mitochondrial DJ-1 was dependent upon Pink1 just as observed in MEFs (Figure 2.10). It is also important to note that again, basal DJ-1 seems to be higher at mitochondria with Pink1-deficiency (Figure 2.10), perhaps due to an increase in basal ROS known to occur with Pink1 deficiency (Wood-Kaczmar et al., 2008). Unlike in the MEFs, Pink1 deficiency increased basal levels of total DJ-1 in cortical neurons, perhaps accounting for the increased basal level of mitochondrial DJ-1 in this cell type (Figure 2.S3E). Unfortunately, we could not obtain breeding from Parkin KO mice pairings required to test for Parkin involvement in DJ-1 translocation in neurons.

Figure 2.10: MPP^+-induced increase in mitochondrial DJ-1 is dependent upon Pink1 in primary cortical neurons. Wild-type (WT) and Pink1 cortical neurons harvested from E14.5-15.5 embryos were treated with 10μM MPP^+ for indicated time points in absence of antioxidants. Mitochondrial-enriched fractions were obtained through sub-cellular fractionation and were analyzed by immunoblot. A) Quantification of densitometry using Image J software (NIH). Data represent mean ± SEM (n=2-4). **P*<0.05; two-way ANOVA for WT vs. KO samples. B) Representative blots for DJ-1 and mitochondrial loading control (mtHSP70).

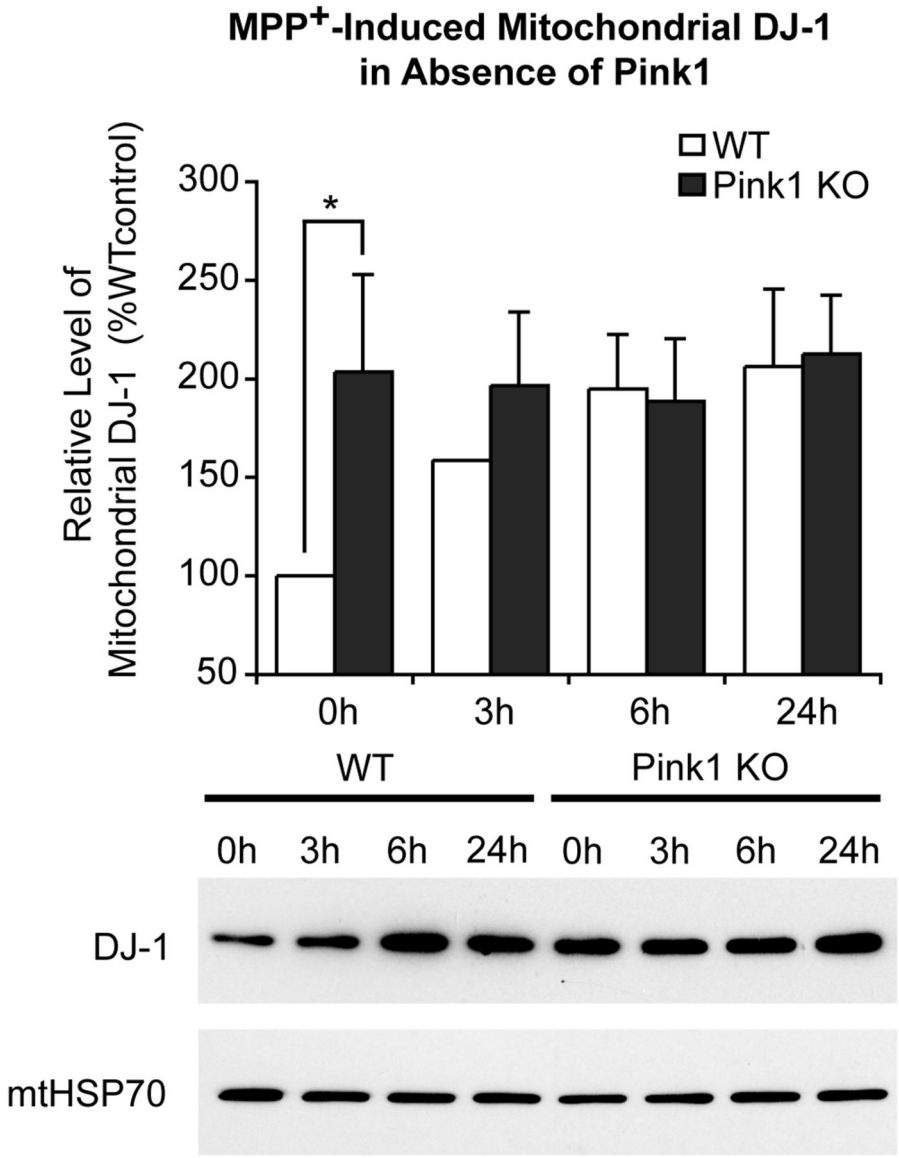
MPP+-Induced Mitochondrial DJ-1
in Absence of Pink1
WT
Pink1 KO
Relative Level of
Mitochondrial DJ-1 (%WTcontrol)
300
250
200
150
100
50
*
0h
3h
6h
24h
WT
Pink1 KO
0h 3h 6h 24h 0h 3h 6h 24h
DJ-1
mtHSP70

Discussion

Numerous recent studies have reported the individual roles of DJ-1, Parkin, and Pink1 in the regulation of mitochondrial function (Narendra et al., 2008; Hao et al., 2010; Vives-Bauza et al., 2010; Thomas et al., 2011). However, how these proteins relate to each other under situations of oxidative stress and the relevance of this interplay in PD pathogenesis is not completely clear.

Our present work addresses two critical questions in relation to the molecular and functional interactions between these PD-associated genes, namely: does DJ-1 have any significance in the Pink1/Parkin mitochondrial quality control pathway; and secondly, is oxidative stress central to Parkin translocation?

Although the role of Pink1 and Parkin in mitochondrial quality control has been well described, the role of DJ-1 at mitochondria remains less certain. Previous work from our laboratory (Irrcher et al., 2010) and others (Thomas et al., 2011) has shown that loss of DJ-1 leads to basally increased levels of ROS and deregulated mitochondrial dynamics suggesting a loss of mitochondrial quality control. Furthermore, loss of mitochondrial integrity would cause cells to be sensitized to additional oxidative stress, which we have previously observed with DJ-1 deficiency both *in vitro* and *in vivo* (Kim et al., 2005a). However, how and whether DJ-1 associates to mitochondrial quality control pathways is unknown.

Presently, we provide critical evidence that DJ-1 does indeed impact the Parkin translocation-mediated pathway of MQC both in MEFs and neurons in response to CCCP. DJ-1-deficiency enhances Parkin translocation. Interestingly, this result is dissimilar from a previous report in which transient knockdown of DJ-1 in HeLa cells did

not have any significant effect on Parkin translocation (Vives-Bauza et al., 2010). Although the reason for this is unclear, it may involve the peculiarities of HeLa cells in regards to what we have observed with their response to ROS. Interestingly, HeLa cells usually lack endogenous levels of Parkin and may have activation of compensatory mechanisms to deal with damaged mitochondria.

The potential reason for DJ-1 regulation of Parkin translocation in response to abrupt depolarization is unclear. While there are a number of functions attributed to DJ-1 including transcription regulation and chaperone abilities (Nagakubo et al., 1997; Hod et al., 1999; Quigley et al., 2003; Tao and Tong, 2003), the most prominent is the ability of DJ-1 to manage ROS. Mitochondria deficient in DJ-1 are reported to produce more ROS (Irrcher et al., 2010). This increase occurs through numerous potential mechanisms including regulation of Nrf2 (Clements et al., 2006), a master antioxidant regulator, and the pro-survival Akt pathway (Aleyasin et al., 2010). It is possible that increased ROS leads to increased mitochondrial damage, which increases the need for Parkin-initiated MQC. This would also suggest that ROS plays a central role in signaling and/or mediating mitochondrial damage resulting in specific Parkin activation. Indeed our present work would support this hypothesis.

While the evidence above suggests that DJ-1 influences Parkin recruitment, the reciprocal also appears to be true, i.e., stress-induced increase of mitochondrial DJ-1 is mediated by Parkin. Whether this is dependent upon Parkin recruited at mitochondria or Parkin in the cytoplasm, is unknown. Additionally, it is important to note that in this scenario, the role of Pink1, while clear for Parkin translocation, is less clear for DJ-1. While no oxidative stress-induced increase in DJ-1 at mitochondria was detected with

Pink1 loss, increased total DJ-1 expression and increased level of mitochondrial DJ-1 was observed under basal conditions. This basal increase of DJ-1 is reasonable given that Pink1 loss is also reported to increase the ROS environment (Wood-Kaczmar et al., 2008) and perhaps accounts for the increased levels of DJ-1 at the mitochondria. Stress-mediated increase in mitochondrial DJ-1, however, appears to also involve Pink1 since no further increase in DJ-1 levels was observed following oxidative stress in Pink1 deficient cells. Finally, it is important to note that we have not ascertained the source of the increased mitochondrial DJ-1. However, our data suggest that it is not due to a global increase in DJ-1.

What is the potential role of mitochondrial DJ-1? Previous work has demonstrated that this mitochondrial translocation promotes survival of cells in response to oxidative stress (Junn et al., 2009). How survival is affected is unknown. Our unpublished data suggests that DJ-1 loss reduces PGC1-α levels, a key mediator of mitochondria biogenesis, which was shown to be regulated by DJ-1 activity (Zhong and Xu, 2008). In addition, DJ-1 deficiency decreases fusion rates, which predisposes cells to death (Irrcher et al., 2010). Whether these mechanisms are facilitated by only mitochondrial DJ-1 is unclear. Taken together, these data fit a model by which a Parkin-mediated signal induced by oxidative damage initiates a survival response of increased DJ-1 at mitochondria, perhaps to limit oxidative damage - although this has yet to be directly tested. Presumably, as our data would suggest, cells lacking DJ-1 would not be able to initiate this survival response at mitochondria, and the resulting increased mitochondrial damage would promote an even greater translocation of Parkin to further activate mitochondrial quality control (see Figure 2.11 for summary).

Figure 2.11: Schematic representation of DJ-1 and Pink/Parkin interplay during oxidative stress. The Pink1/Parkin MQC pathway is activated by increased ROS levels due to oxidative stress and/or mitochondrial damage in order to maintain mitochondrial health. Stress-induced DJ-1 requires Pink1/Parkin to help maintain mitochondrial health, possibly through inhibiting ROS directly or through other unknown MQC pathways in parallel to Pink1/Parkin.

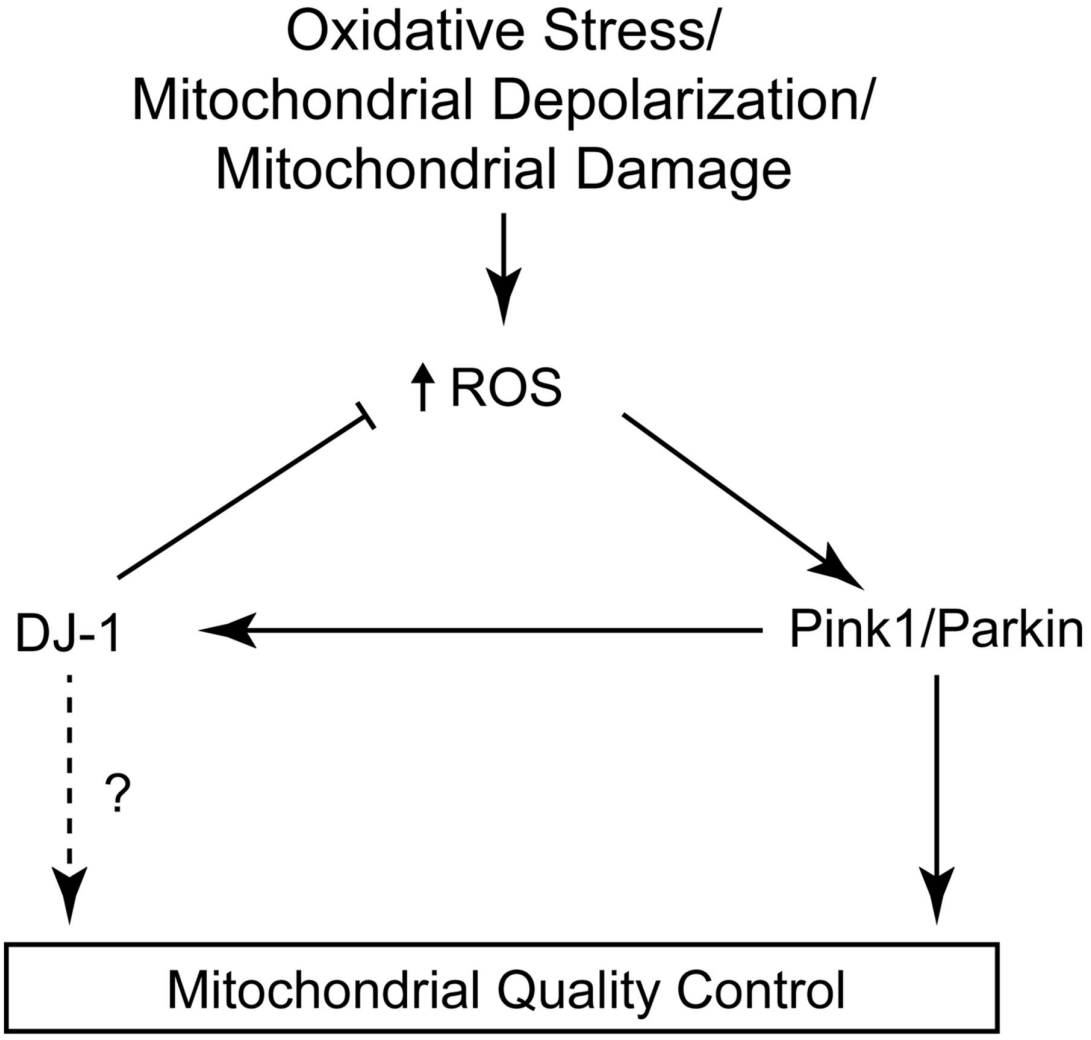
Oxidative Stress/
Mitochondrial Depolarization/
Mitochondrial Damage
↑ ROS
DJ-1
Pink1/Parkin
?
Mitochondrial Quality Control

While the above evidence presents a model of reciprocal relationship between DJ-1 and Parkin, its physiological relevance is unclear. There is controversy at least on two levels. First, most work on Parkin translocation has focused on CCCP. How biologically relevant this artificial and robust method of rampant and complete depolarization of mitochondria is to the neurodegenerative process remains unknown. Second, whether this translocation occurs in any robust fashion in neurons is also unclear. Previous reports indicate that it does not, at least with CCCP (Van Laar et al., 2010) and TFAM loss (Sterky et al., 2011). In support of this, we initially had difficulty detecting any Parkin translocation with CCCP or any other mitochondrial-damaging agents in cultured neurons under routine culture conditions. However, we observed that treatment with these agents did induce depolarization and massive mitochondrial fragmentation (Figure 2.5). These results indicated that the lack of Parkin translocation was not due to lack of biological effect of these agents and that Parkin translocation can be separated from fission events. The latter is particularly interesting since recent reports suggest an active role for Parkin in maintaining mitochondrial morphology (Gegg et al., 2010; Ziviani et al., 2010). Importantly, it has been shown that Parkin can ubiqutinate Mitofusin 1 and 2 (Gegg et al., 2010), key molecules regulating mitochondrial fusion, leading to the degradation of these molecules and increasing mitochondrial fission. Results presented here, however, suggest that recruitment of Parkin to mitochondria occurs after induction of mitochondrial fission. It is therefore unlikely that fission events are directly related to Parkin translocation.

Based on our observations of ROS-dependency in MEFs, we reasoned that perhaps the lack of translocation in neurons might be due to the presence of antioxidants in the culture media. Indeed we showed that depletion of such supplements revealed

translocation induced by mitochondrial toxins including CCCP, MPP^+ and rotenone. These results suggest that Parkin translocation mediated by depolarization of mitochondria or inhibition of mitochondrial complex I require, at least in neurons (and in MEFs), the generation of ROS. However, care must be taken in interpreting the specifics of the ROS mediated signal. Indeed, the source and localization of ROS is known to be critical for any particular biological outcome (Valko et al., 2007; Novo and Parola, 2008).

Interestingly, CCCP treatment induced qualitatively different translocation than that with H_2O_2 in MEFs or MPP^+ or rotenone in neurons, which produced only partial Parkin translocation to mitochondria. Why this difference occurs is unknown. However, CCCP induces complete depolarization of mitochondria while MPP^+ is known to activate multiple death pathways both mitochondrial and independent of its role as a mitochondrial complex I inhibitor (Choi et al., 2008). It should be noted that Parkin puncta observed in neurons are characteristically similar to those observed in other cell types (Geisler et al., 2010; Matsuda et al., 2010) in that these aggregates are also positive for ubiquitin. It is, however, difficult to distinguish whether enhanced ubiquitination in these aggregates is a result of Parkin's E3 ligase-mediated ubiqutination of downstream targets (Geisler et al., 2010) or a result of Parkin's auto-ubiqutination function (Matsuda et al., 2010).

Finally, we have shown that the regulatory relationships between Parkin, Pink1 and DJ-1 in primary neurons are similar, if not identical, to those observed in MEFs. This includes the fact that Pink1 is absolutely required for Parkin translocation and that DJ-1 regulates Parkin translocation and is in turn regulated by Pink1 and Parkin. It is important to note that not all modes of damage activate the Parkin-specific mitochondrial quality

control pathway. For example, TFAM deletion induced mitochondrial damage does not result in any evidence of Parkin translocation *in vivo*. In fact, multiple pathways of mitochondrial quality control have been proposed to exist (Andrade-Navarro et al., 2009).

In summary, we have clarified at least three critical issues in this report. First, we show that primary neurons can activate mitochondrial quality control-related Parkin translocation to mitochondria. Second, we demonstrate that ROS plays a central role in this process. Third, we provide evidence that DJ-1 regulates this process. Loss of DJ-1 leads to enhancement in Parkin translocation and conversely both Parkin and Pink1 deficiency block stress-mediated increase in mitochondrial DJ-1, an event previously shown to be critical for cell survival (Junn et al., 2009). Taken together, we propose that in neurons, mitochondrial health and consequent sensitivity to environmental stress is regulated by at least two interrelated and parallel pathways that are in turn regulated via feedback from mitochondrial health. These pathways include: a) the classic pathway of mitochondrial quality control involving Parkin translocation to damaged mitochondria, which are then eliminated via downstream clearance mechanisms and b) Pink1/Parkin-regulated increase in mitochondrial DJ-1. In this latter case, we hypothesize that this may limit oxidative stress-induced damage at mitochondria to improve mitochondrial health.

Materials and Methods

Transgenic mice

The generation and genotype of the Parkin, DJ-1, and Pink1 deficient mice have previously been described in detail, respectively (Itier et al., 2003; Kim et al., 2005a; Kitada et al., 2007). All procedures involving animals were approved by the University of Ottawa Animal Care Committee and were maintained in strict accordance to the Guidelines for the Use and Treatment of Animals put forth by the Animal Care Council of Canada and endorsed by the Canadian Institute of Health Research.

Cell Culture

Mouse embryonic fibroblasts (MEFs) were derived from E14.5-15.5 transgenic DJ-1 (C57BL/6), Pink1 (C57BL/6) and Parkin (mixed background) mice (Charles River Laboratories) of either sex and maintained in Dulbecco's Modified Eagle Media (DMEM) (Sigma) supplemented with 10% fetal bovine serum (FBS) (Sigma) and antibiotic/antimycotic (Sigma). All MEFs were immortalized as previously described (Aleyasin et al., 2010). Fractionation experiments were performed on near confluent (90-95%) 100mm plate and were treated with 100μM H_2O_2 for up to 6hr to induce oxidative stress. Cortical neurons were derived from E14.5-15.5 wildtype (WT) CD1 mice or C57BL/6 WT/transgenic Pink1/transgenic DJ-1 mice (Charles River Laboratories) of either sex and maintained in Neurobasal media (Invitrogen) supplemented with B27 with antioxidants (Gibco), N2 (Gibco), 0.5 mM L-glutamine (Sigma), and penicillin/ streptomycin (Gibco) as previously reported (Kim et al., 2005a). For DJ-1 studies of mitochondrial-enriched fractions, neurons were plated on poly-D-lysine-coated (Sigma)-100mm plates at a density of 4-5 $x10^6$ cells/100mm plate. For immunofluorescence of

endogenous DJ-1, neurons were plated on poly-D-lysine-coated coverslips in 24-well plates at a density of 100,000 cells per well. For all DJ-1 studies, on DIV5, media was completely changed to media identical to initial plating, with the exception of including B27 without antioxidants (Gibco). Neurons were treated with 30μM H_2O_2 for up to 6hr, 10μM MPP^+ (Sigma) for up to 24hr, or 10μM CCCP (Sigma) for up to 2hr to induce oxidative stress. All treatments finished on DIV6.

Antibodies, Plasmids and Virus

The following antibodies were used: rabbit anti-DJ-1 (Abcam), mouse anti-parkin (Santa Cruz), mouse anti-NDUFA9 (MitoSciences), mouse anti-mtHSP70 (Abcam, mouse anti-COX V (MitoSciences), mouse anti-COX I (MitoSciences), rabbit anti-TOM20 (Santa Cruz), rabbit anti-LC3 (Novus Biologicals), rabbit anti-calnexin (Abcam), mouse anti-actin (Sigma), rabbit anti-ubiquitin (Abcam), rabbit anti-Raf-1 (Santa Cruz) and anti-mouse and anti-rabbit horse radish peroxidase-conjugated secondary antibody (Bio-Rad). Construction of the FLAG-DJ-1 pcDNA3.1 has been described before (Kim et al., 2005a). FLAG-C106A mutant was generated by site directed mutagenesis of the FLAG-DJ-1. emGFP-Parkin Adeno-associated virus was generated and purified as described (Zolotukhin et al., 2002).

Infection/Transfection

For infection of mouse cortical neurons, cortical cultures were prepared as described above. 5 x 10^5 neurons were plated into 24-well plates containing coverslips that were acid treated with 1N Nitric acid and 1N HCl and pre-coated with 1X Poly D-Lysine (PDL) and Lamminin. Cultures were infected with GFP-Parkin Adeno-associated virus at the time of plating at an MOI of 5. Fresh growth media was added to the conditioned

media at the ratio of 1:1 every 3 days of culture. On DIV7, media from the wells were aspirated and replaced with fresh growth media similar to that used at the time of plating with the exception of B27. Treatments were performed on DIV8 using 10X working stocks of CCCP, rotenone (Sigma) or MPP^+.

For MEFs, 5 x 10^4 cells were seeded into 24-well plates containing poly-D-lysine pre-coated coverslips one day before the day of transfection. GFP-Parkin-pEGFP construct was transfected into the cells using Lipofectamine (Invitrogen) following manufacturer's recommendations. For co-transfections GFP-Parkin-pEGFP was co-transfected with either empty vector, WT DJ-1-FLAG or C106A-FLAG at a ratio of 1:3 using Effectene Transfection Reagent (Qiagen) as per manufacturer's recommendations. 24 hours after transfection, cells were treated with 10μM CCCP or 100μM hydrogen peroxide for indicated amounts of time. For antioxidant studies, cells were pre-treated for 3hr with either 100μM TIRON (Sigma) or 2mM N-acetyl cysteine (Sigma) prior to oxidative insult.

Immunofluorescence, quantification of Parkin translocation and mitochondrial fluorescence intensity

For endogenous DJ-1, following treatment, cells were fixed in 4% formalin in growth media at 37°C for 15min. The cells were permeablized and blocked simultaneously using 0.1% Triton X-100 and 5% normal goat serum for 1hr at room temperature. Hybridizations using the respective primary antibodies were performed overnight at 4°C. Cells were subsequently washed in 5% normal goat serum and stained with the corresponding secondary antibodies. Cells were subsequently washed in 1X PBS, stained with Hoechst, mounted and analyzed by confocal microscopy.

For Parkin translocation experiments, following drug treatments the cells were fixed in 4% formalin in growth media at 37˚C for 15min. The cells were permeabilized using 0.2% Triton X-100 for 5min at room temperature, followed by blocking using 2.5% normal goat serum for 1hr at room temperature. Hybridizations using the respective primary antibodies were performed either at 37˚C for 30min or at 4˚C overnight. Cells were subsequently washed in 1X PBS and stained with the corresponding secondary antibodies. Cells were finally stained with Hoechst, mounted and were analyzed by confocal microscopy. Quantifications of Parkin translocation were performed using an inverted fluorescence microscope. Cells displaying Parkin puncta were scored among the cells that were positive for GFP-Parkin staining.

For quantification of mitochondrial fluorescence intensity, all confocal photomicrographs were taken using identical conditions. Using NIH ImageJ software, an outline of the individual cell was drawn using the GFP staining as a cue. Mitochondrial staining intensity within this region of interest was measured, which is indicative of total mitochondrial staining intensity relative to the total area of the region of interest. At least 25 cells were counted per condition. Bar diagram is representative of two independent experiments.

Mitochondrial Fractionation

Fractionation was performed identically for both MEFs and neurons. Briefly, cells were washed once with PBS and scraped in 1.2mL of PBS into a 1.5mL Eppendorf tube. From each sample, 300uL of cell suspension was saved for whole cell lysate. Harvested cells were centrifuged at 5000rpm for 5min at 4°C in an Eppendorf Centrifuge 5417R. The cell pellet was resuspended in 250-500μL of isolation buffer (0.25M Sucrose, 10mM Tris,

pH7.5, 1mM EDTA, freshly added protease inhibitors) and passed through a 27 gauge insulin syringe 35 times. Samples were then centrifuged at 610g for 10min at 4°C. The supernatant was then transferred to a new tube and centrifuged at 10,000g for 20min at 4°C. The supernatant (cytosolic fraction) was transferred to a new tube and the pellet (mitochondrial-enriched fraction) was resuspended in 25-50μL of isolation buffer. The whole cell lysis pellet was resuspended in 50-100μL of lysis buffer (50mM Tris-HCl pH 7.5, 100mM NaCl, 1mM EDTA, 0.2% NP-40, and freshly added 1mM DTT and protease inhibitors), vortexed for 10sec at maximum setting, and incubated on ice for 30min. Samples were stored at -80°C.

Immunoblotting

Protein quantification was carried out using traditional Bradford (Bio-Rad) method. For mitochondrial-enriched blots, 10μg of each sample was electrophoresed on 12% sodium dodecyl sulfate polyacrylamide gels and transferred to polyvinylidene fluoride (PVDF) membranes (Millipore). For relative whole cell, mitochondrial-enriched fractions and cytoplasmic fractions comparisons, sample amounts were calculated based on cell number. Membranes were probed with the respective primary antibodies followed by horseradish peroxidase–conjugated secondary antibodies and developed with the Immobilon Western Chemiluminescent HRP Substrate (Millipore).

Survival Assay

For survival assay, primary cortical neurons infected with GFP-Parkin AAV were prepared as mentioned before. Following 48 hr of MPP^+ treatment, cells were fixed and stained with Hoechst and the number of GFP-positive apoptotic nuclei counted under fluorescence microscope.

Statistical Analysis

Statistical significance was determined using paired Student's t-test for related samples. Two-way ANOVA was used in select immunoblots to determine significance between WT and KO in control and treated conditions. All data are presented as mean ± standard error of the mean (SEM). Significance at $p<0.05$ (*), $p<0.01$ (**) and $p<0.001$ (***); no significance is denoted by n.s.

Funding

This work was supported by grants from Parkinson's Society Canada (PSC) to D.S.P (2011-28); the Canadian Institutes of Health Research (Grant numbers MOP-15123, MOP-43952, MOP-114868, INE-117890 to DSP); Heart and Stroke Foundation of Ontario (T6356, T6813 to DSP); Neuroscience Canada/Krembil Foundation (Brain Repair Grant); The Michael J. Fox foundation for Parkinson's research; Parkinson Research Consortium; the Canadian Stroke Network; the Heart and Stroke Foundation Centre for Stroke Recovery; World Class University program through the National Research Foundation of Korea funded by the Ministry of Education, Science and Technology, South Korea (R31-2008-000-20004-0 to DSP); the Ontario Graduate Scholarship to SJH; and the PSC Graduate Student Award to SJH.

Acknowledgements

We would like to thank Dr. Brice and Aventis Pharma for the Parkin mice, Dr. Matsumoto for the Parkin-pEGFP construct and Dr. Fon for the GFP-Parkin AAV construct. We would also like to thank Carmen Estey, Farzaneh Safarpour, Elizabeth Abdel-Messih, Dr. M. Emdadul Haque and Fadi Hage for technical assistance.

Conflict of Interest Statement

All authors declare no conflict of interest.

Supplementary Information

Figure 2.S1. Parkin expression levels in HeLa cells. HeLa cells transfected with GFP-Parkin were pretreated with 2mM n-acetyl cysteine for 3hr before treating with 10μM CCCP for 2h. Cell lysates were then analyzed by western blotting using the indicated antibodies. Images are representative of 3 independent experiments.

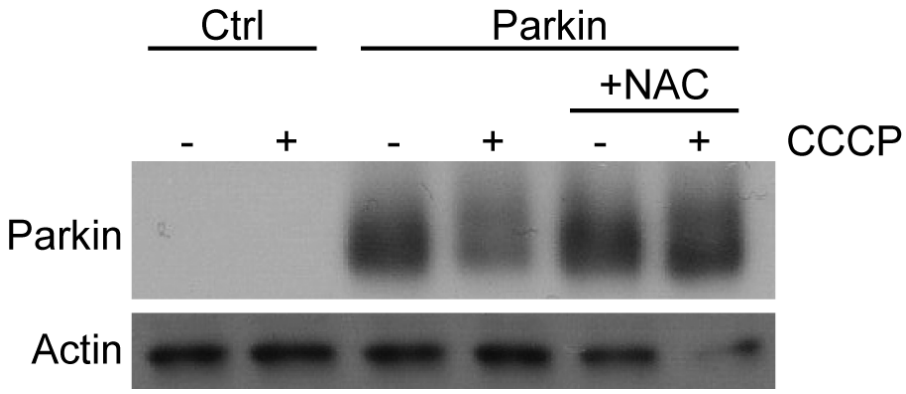
Ctrl
Parkin
+NAC
- + - + - + CCCP
Parkin
Actin

Figure 2.S2. Parkin translocation in response to hydrogen peroxide treatment. A) Representative confocal photomicrographs of WT MEFs either left untreated (0h) or treated with 100μM H_2O_2 for 5h. Fixed cells were stained using COX I antibody. White arrowheads highlight co-localized Parkin puncta B) Quantification of number of cells displaying Parkin translocation. Bar graph represents mean ± SEM with 200 cells counted in duplicates per condition. $^{**}P<0.01$; *t*-test for related samples.

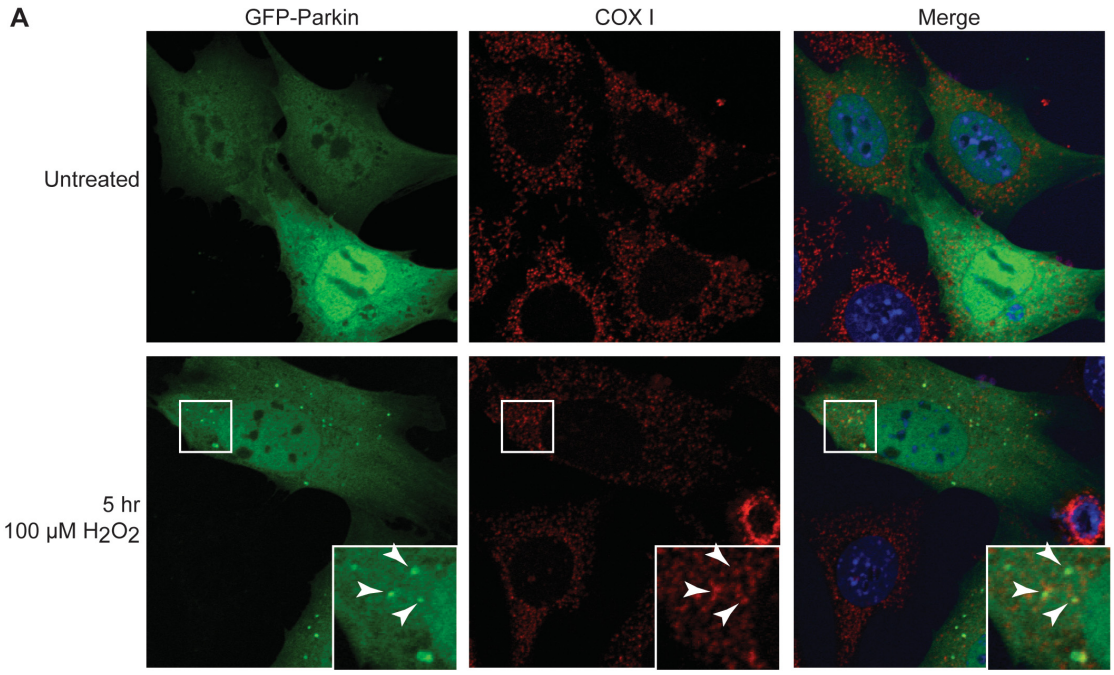
A
GFP-Parkin
COX I
Merge
Untreated
5 hr
100 μM H_2O_2

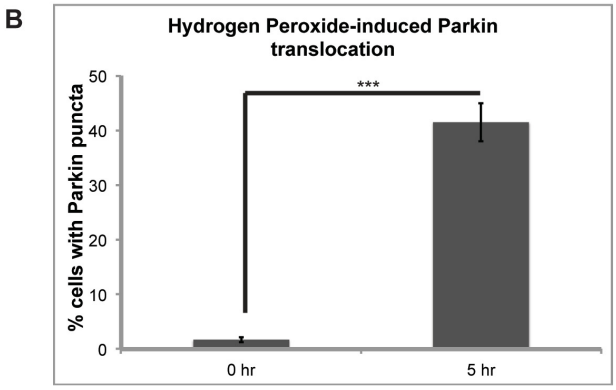
B
Hydrogen Peroxide-induced Parkin translocation
% cells with Parkin puncta
50
40
30
20
10
0
***
0 hr
5 hr

Figure 2.S3. Whole cell level of DJ-1 in mouse embryonic fibroblasts and cortical neurons. A-C) Treatment with H_2O_2, CCCP, and MPP^+ does not increase whole cell level of DJ-1. D) Pink1 and Parkin deficient MEFs have similar DJ-1 expression level to WT MEFs. E) Pink1 deficient cortical neurons have slightly increased DJ-1 levels compared to WT cortical neurons. All data is representative of n=2. K, DJ-1 KO sample.

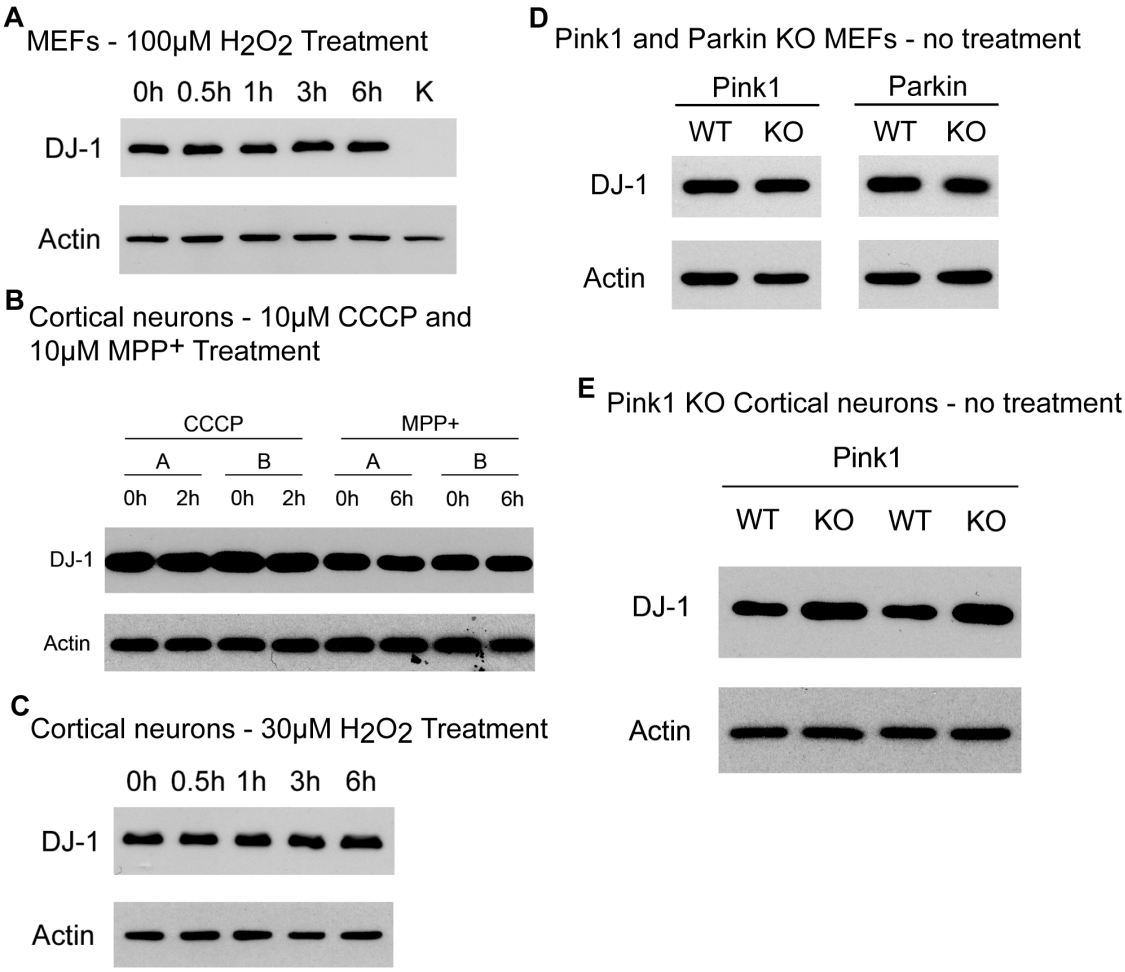
A
MEFs - 100μM H2O2 Treatment
0h 0.5h 1h 3h 6h K
DJ-1
Actin
B
Cortical neurons - 10μM CCCP and
10μM MPP+ Treatment
CCCP
MPP+
A
B
A
B
0h 2h 0h 2h 0h 6h 0h 6h
DJ-1
Actin
C
Cortical neurons - 30μM H2O2 Treatment
0h 0.5h 1h 3h 6h
DJ-1
Actin
D
Pink1 and Parkin KO MEFs - no treatment
Pink1
Parkin
WT KO WT KO
DJ-1
Actin
E
Pink1 KO Cortical neurons - no treatment
Pink1
WT KO WT KO
DJ-1
Actin

Figure 2.S4. Relative levels of DJ-1, calnexin, and Raf-1 in whole cell lysates, mitochondria and cytoplasm. The relative amount of DJ-1 in the mitochondrial-enriched and cytoplasmic fractions was determined. ER marker calnexin and cytoplasmic marker Raf-1 were assessed to check ER or cytoplasmic contamination respectively. Mitochondrial markers NDFUA9, mtHSP70 and TOM20 were also assessed. Densitometric quantification of the levels of each marker in mitochondria-enriched and cytoplasmic fractions relative to whole cell level is indicated below each blot. A) WT MEF whole cell, mitochondrial and cytoplasmic fractions. Equal amounts of whole cell and cytoplasmic fraction were loaded. 5 times as much mitochondrial enriched fractions was used (as indicated by ratio). B) CD1 whole cell, mitochondrial and cytoplasmic fractions. Equal amount of mitochondria-enriched fraction and cytoplasmic fraction were loaded relative to whole cell lysate (as indicated by ratio). W, whole cell lysate; M, mitochondrial-enriched fraction; C, cytoplasmic fraction. * band of interest.

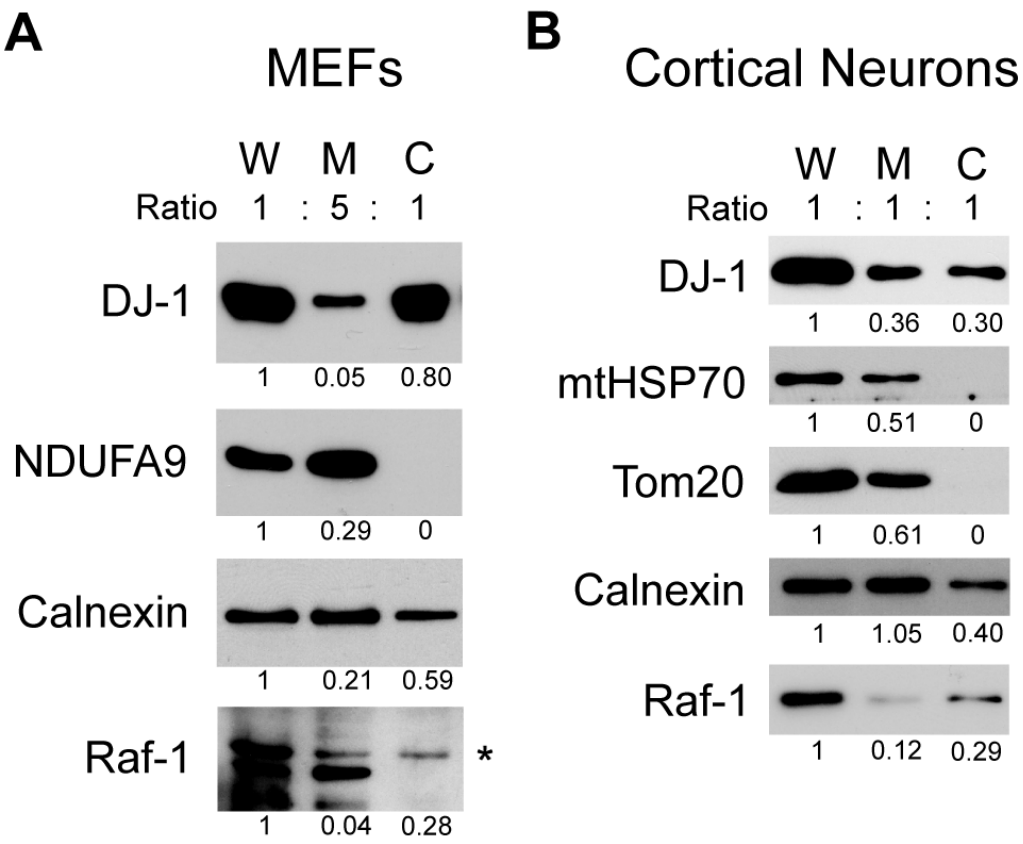
A
MEFs
W M C
Ratio 1 : 5 : 1
DJ-1
1 0.05 0.80
NDUFA9
1 0.29 0
Calnexin
1 0.21 0.59
Raf-1
*
1 0.04 0.28
B
Cortical Neurons
W M C
Ratio 1 : 1 : 1
DJ-1
1 0.36 0.30
mtHSP70
1 0.51 0
Tom20
1 0.61 0
Calnexin
1 1.05 0.40
Raf-1
1 0.12 0.29

Figure 2.S5. Immunofluorescence of endogenous DJ-1 in cortical neurons. CD1 cortical neurons were treated with vehicle, 10μM MPP^+ (6h) or 10μM CCCP (1h) in the absence of antioxidants on DIV6. White box corresponds to zoomed area of interest in control sample. Representative zoomed area of interest of MPP^+ and CCCP treated samples are shown with specific examples of co-localization demonstrated (white arrows). Images are representative of two independent experiments conducted in quadruplicate.

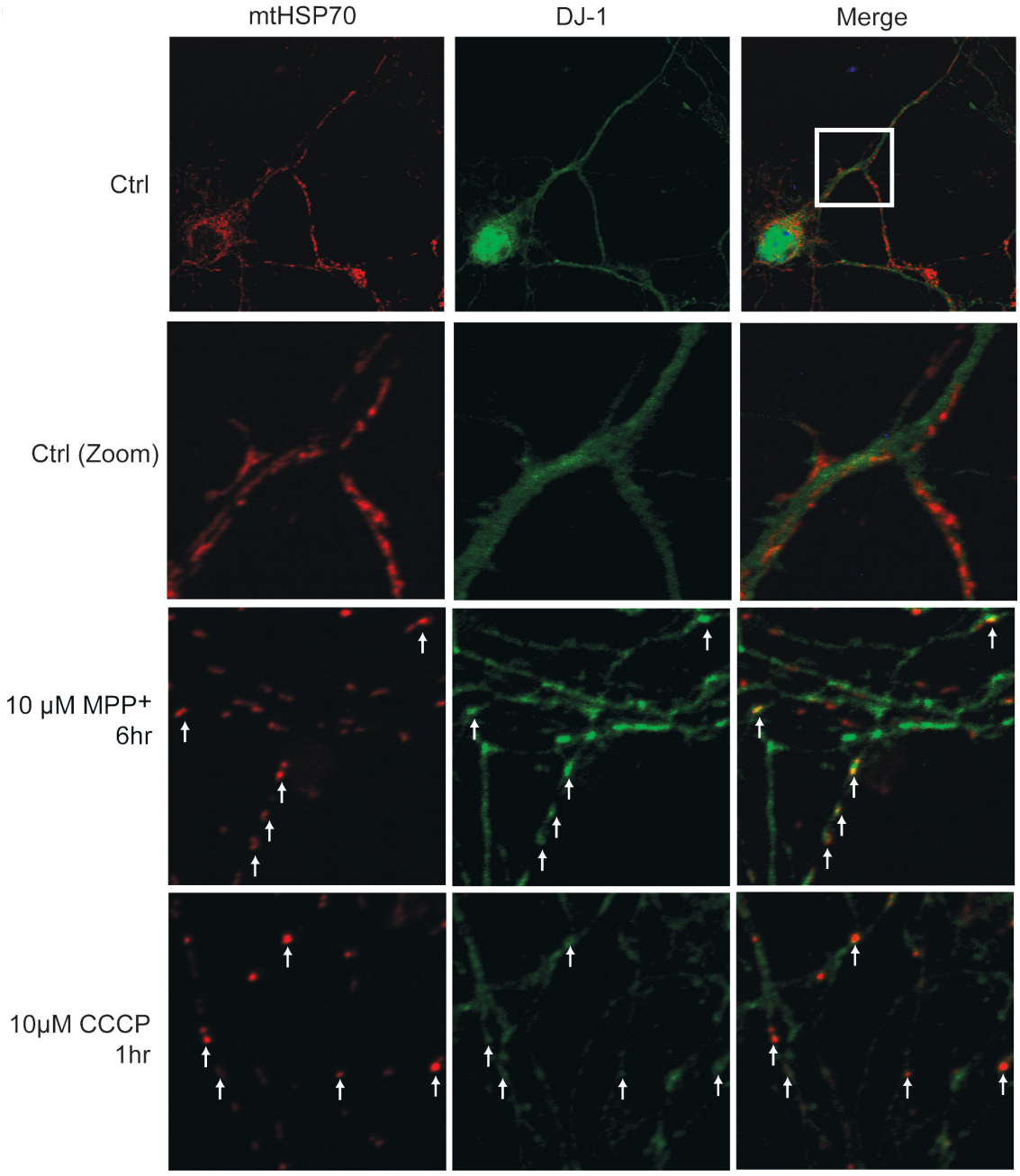
mtHSP70
DJ-1
Merge
Ctrl
Ctrl (Zoom)
10 μM MPP+
6hr
10μM CCCP
1hr

Unpublished Data Relevant to Manuscript

Following the publication of this manuscript, we were able to examine stress-induced response of DJ-1 translocation to mitochondria in Parkin KO cortical neurons. Parkin WT and KO primary cortical neurons from E14.5-15.5 were treated with 10μM MPP^+, in absence of antioxidants on DIV 6 (Figure 2.12). Equal amounts (10μg) of mitochondrial enriched fractions from each time point were loaded. At 1h of MPP^+ treatment, a significant increase (Figure 2.12B) in the level of DJ-1 at mitochondria was observed in cortical neurons. These findings are similar to what was observed in Parkin KO MEFs and therefore indicate that Parkin is important in stress-induced increase of mitochondrial DJ-1.

Figure 2.12. MPP^+-induced increase in mitochondrial DJ-1 requires Parkin in cortical neurons. Wild-type (WT) and Parkin KO cortical neurons harvested from E14.5-15.5 embryos were treated with 10μM MPP^+ for indicated time points in absence of antioxidants. Mitochondrial-enriched fractions were obtained through sub-cellular fractionation and were analyzed by immunoblot. A) Quantification of densitometry using Image J software (NIH). Data represent mean ± SEM (n=2). *P<0.05; two-way ANOVA for WT vs. KO samples. B) Representative blots for DJ-1 and mitochondrial loading control (mtHSP70).

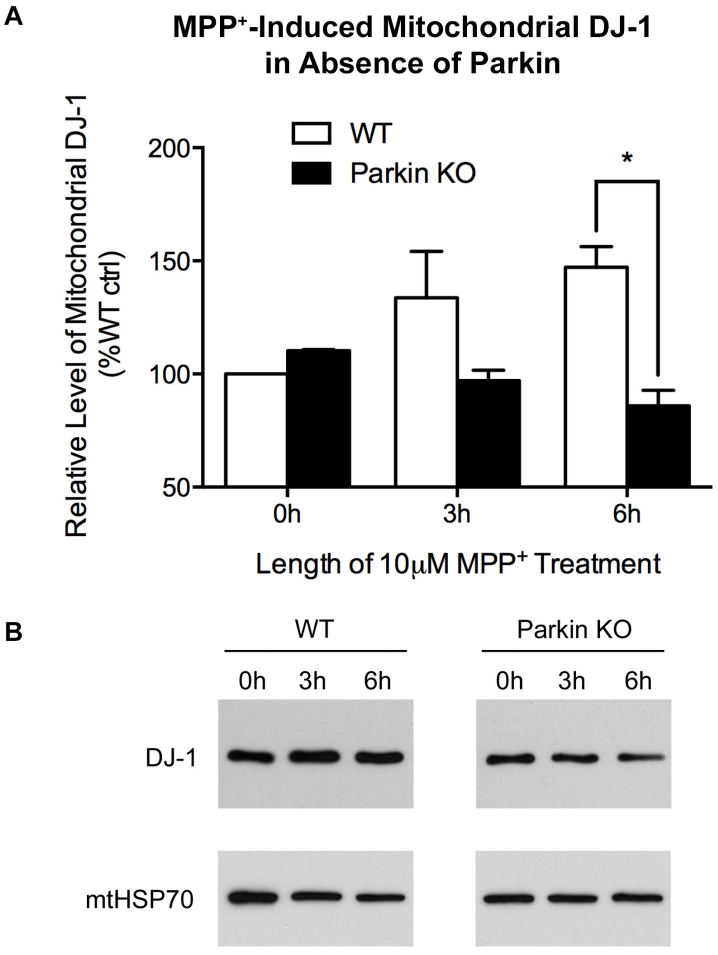
A
MPP+-Induced Mitochondrial DJ-1
in Absence of Parkin
WT
Parkin KO
*
Relative Level of Mitochondrial DJ-1
(%WT ctrl)
200
150
100
50
0h
3h
6h
Length of 10μM MPP+ Treatment
B
WT
Parkin KO
0h 3h 6h
0h 3h 6h
DJ-1
mtHSP70

CHAPTER 3

VDAC1 is important for sub-mitochondrial localization of DJ-1

Sarah J. Hewitt, Steve M. Callaghan, Marisa Brini, William J. Craigen, Daniel Figeys, Ruth S. Slack, David S. Park

This manuscript is in preparation for submission and peer-review

Statement of Author Contributions

Sarah J. Hewitt designed and conducted all experiments under the guidance of Dr. David S. Park. Steve M. Callaghan provided excellent technical support. DJ-1 constructs were a generous gift from Dr. Marisa Brini. VDAC1 MEFs and transgenic mice were a generous gift from Dr. William J. Craigen. Dr. Daniel Figeys performed the interactor screen. Dr. Ruth S. Slack provided insight into the design and implementation of experiments. **Sarah J. Hewitt** and Dr. David S. Park analyzed data and wrote the manuscript.

VDAC1 is important for sub-mitochondrial localization of DJ-1

Sarah J. Hewitt[1], Steve M. Callaghan[1], Marisa Brini[2], William J. Craigen[3,4], Daniel Figeys[5], Ruth S. Slack[1], David S. Park[1]

This manuscript is in preparation for submission and peer-review

1 Department of Cellular and Molecular Medicine, Faculty of Medicine, University of Ottawa, Ottawa, Ontario, Canada, K1H 8M5

2 Department of Biology, University of Padova, Padova, Italy 35131

3 Department of Molecular and Human Genetics, Baylor College of Medicine, Houston, Texas, USA, 77030

4 Department of Pediatrics, Baylor College of Medicine, Houston, Texas, USA, 77030

5 Ottawa Institute of Systems Biology (OISB), University of Ottawa, Ottawa, Ontario, Canada, K1H 8M5

Abstract

Loss-of-function mutations in *DJ-1* cause early-onset Parkinson's disease (PD) and are responsible for ~1-2% of all familial cases. Investigation of familial genes involved in PD gives us insight into the mechanism of degeneration, as the majority of cases are of unknown cause. While DJ-1 has many potential functions in the cell, its major role appears to be the handling of oxidative stress. In this regard, DJ-1 loss leads to hypersensitivity to exogenous oxidative insults. Others have shown that an important factor in the mechanism of DJ-1-mediated survival is its mitochondrial localization. In this study we show an interaction between DJ-1 and the mitochondrial protein voltage dependent anion channel 1 (VDAC1). We demonstrate that stress-induced increase in mitochondrial DJ-1 requires VDAC1. We also identify decreased mitochondrial health in VDAC1 deficient cortical neurons, as evidenced by reduced survival, increased ROS production following stress, fragmented mitochondria and decreased ATP production. We also show that DJ-1 requires VDAC1 for its sub-mitochondrial matrix localization. In the absence of VDAC1, DJ-1 localization to the matrix is reduced. Importantly, DJ-1 localization is responsive to reductions in mitochondrial-generated ATP. Taken together our work suggests one potential model by which VDAC1 regulates proper localization of DJ-1 in the mitochondrial matrix to regulate ATP production.

Introduction

Parkinson's disease (PD) is a common neurodegenerative disease that is caused by loss of dopaminergic neurons in the *substantia nigra pars compacta* (SNc). Approximately 90% of cases are of unknown cause, however the remaining 10% have a genetic basis. Understanding the function of these genes will lead to a better understanding of the pathogenesis in PD.

DJ-1 was originally identified as an oncogene (Nagakubo et al., 1997) and since has had a multitude of functions attributed to it, including chaperone (Shendelman et al., 2004), transcription regulator (Takahashi et al., 2001), atypical peroxireductase (Andres-Mateos et al., 2007) and most relevant to our study, oxidative stress sensor (Canet-Avilés et al., 2004). Loss-of-function mutations in *DJ-1* cause early-onset PD (Bonifati et al., 2003).

Given the wide range of functions that DJ-1 appears to regulate, it is unclear which activity(s) are relevant for PD pathogenesis. Previously we have shown that loss of DJ-1 results in hypersensitivity to oxidative stress *in vitro* and *in vivo*, as well as fragmented mitochondria and elevated ROS levels (Kim et al., 2005a; Irrcher et al., 2010). We and others have demonstrated that during oxidative stress, DJ-1 partially localizes to mitochondria (Canet-Avilés et al., 2004; Andres-Mateos et al., 2007; Junn et al., 2009; Joselin et al., 2012). This mitochondrial localization of DJ-1 has been shown to be protective during oxidative stress (Canet-Avilés et al., 2004; Junn et al., 2009). Despite these findings, the mechanism that regulates mitochondrial localization of DJ-1 remains unclear.

One major factor that plays a role in mitigating cell survival is the voltage dependent anion channel (VDAC). Mammalian cells have three isoforms of VDAC, all of which reside in the outer mitochondria membrane (OMM) (Colombini, 1980; Roos et al., 1982; Rostovtseva et al., 2000). This voltage dependent channel allows passage of anions such as pyruvate and adenine nucleotides as well as cations such as Ca^{2+} through the OMM (Shoshan-Barmatz et al., 2006). During times of stress, mitochondria can undergo a sudden permeabilization, in which the mitochondrial permeability pore (mPTP) opens and leads to apoptosis (Massari and Azzone, 1972; Haworth and Hunter, 1979; Green and Reed, 1998). Although not an essential component of the mPTP, VDAC1 can interact with numerous factors such as Bcl-$_{XL}$ and hexokinase to affect mitochondrial permeabilization and therefore influence cell survival (Azoulay-Zohar et al., 2004; Baines et al., 2007; Abu-Hamad et al., 2009; Arbel et al., 2012).

An interaction screen revealed DJ-1 as a potential binding partner of VDAC1. Given their overlapping roles in survival and mitochondrial localization, we investigated the potential role of these two factors regulating mitochondrial function and stress response.

Results

DJ-1 requires VDAC1 for stress-induced localization to mitochondria

An unbiased screen, that employed mass spectrometry to identify endogenous proteins interacting with overexpressed bait proteins, was performed. This unbiased screen suggests that overexpressed VDAC1 interacts with endogenous DJ-1. We sought to validate this interaction screen to further understand the function of DJ-1 in the cell. Both overexpressed GST-DJ-1 in HEK293 cells and endogenous DJ-1 in murine embryonic fibroblasts (MEFs) show an interaction with endogenous VDAC1 (Figure 3.S1A, B).

Based upon this data, we next investigated the potential role of these two proteins at the mitochondria. In our previous work, we demonstrated that mitochondrial DJ-1 levels increase with oxidative stress, in both MEFs and in primary cortical neurons (Joselin et al., 2012). The signal that regulates this translocation has yet to be determined. As VDAC1 is localized to the OMM and interacts with DJ-1, we investigated how its loss could affect translocation of DJ-1 to mitochondria.

Following up to 3h of 100μM H_2O_2 treatment, VDAC1 WT and KO MEFs were subjected to subcellular fractionation via differential centrifugation to obtain mitochondrial enriched fractions. Samples were analyzed by Western blot for levels of DJ-1 and the mitochondrial loading control mitochondrial heat shock protein 70 (mtHSP70). WT MEFs show an increase in mitochondrial DJ-1 levels and this increase does not occur with VDAC1 deficiency (Figure 3.1A, B). We next examined mitochondrial localization of DJ-1 in primary cortical neurons. WT and VDAC1 KO

primary cortical neurons from E14.5-15.5 embryos were cultured *in vitro* for 6 days prior to treatment with 10μM MPP^+ in absence of supplemented antioxidants for up to 24h. Mitochondrial enriched fractions were similarly obtained as mentioned above and subjected to Western blot analysis. Unlike in WT cortical neurons, there is no stress-induced increase in mitochondrial DJ-1 in absence of VDAC1 (Figure 3.1C, D). VDAC1 appears to be necessary for stress-induced increase of mitochondrial DJ-1. Interestingly, the basal level of mitochondrial DJ-1 is increased with VDAC1 deficiency in cortical neurons. This finding is suggestive that VDAC1 KO cortical neurons have increased stress, as increased mitochondrial DJ-1 occurs following exogenous stimulus of oxidative stress (Joselin et al., 2012).

Figure 3.1: Oxidative stress-induced increase in mitochondrial DJ-1 is impaired in VDAC1-deficient MEFs and primary cortical neurons. A, B) Wildtype (WT) and VDAC1 KO MEFs were treated with 100μM H_2O_2 for indicated time points. C, D) WT and VDAC1 KO cortical neurons harvested from E14.5-15.5 embryos were treated with 10μM MPP^+ for indicated time points in absence of antioxidants. Mitochondrial enriched fractions were obtained through subcellular fractionation and were analyzed by immunoblot. A, C) Quantification of densitometry using Image J software (NIH). Data represent mean ± SEM (n=3). $*P<0.05$; two-way ANOVA with Tukey post-hoc analysis for WT vs. KO samples. B, D) Representative blots for DJ-1 and mitochondrial loading control (NDUFA9 or mtHSP70).

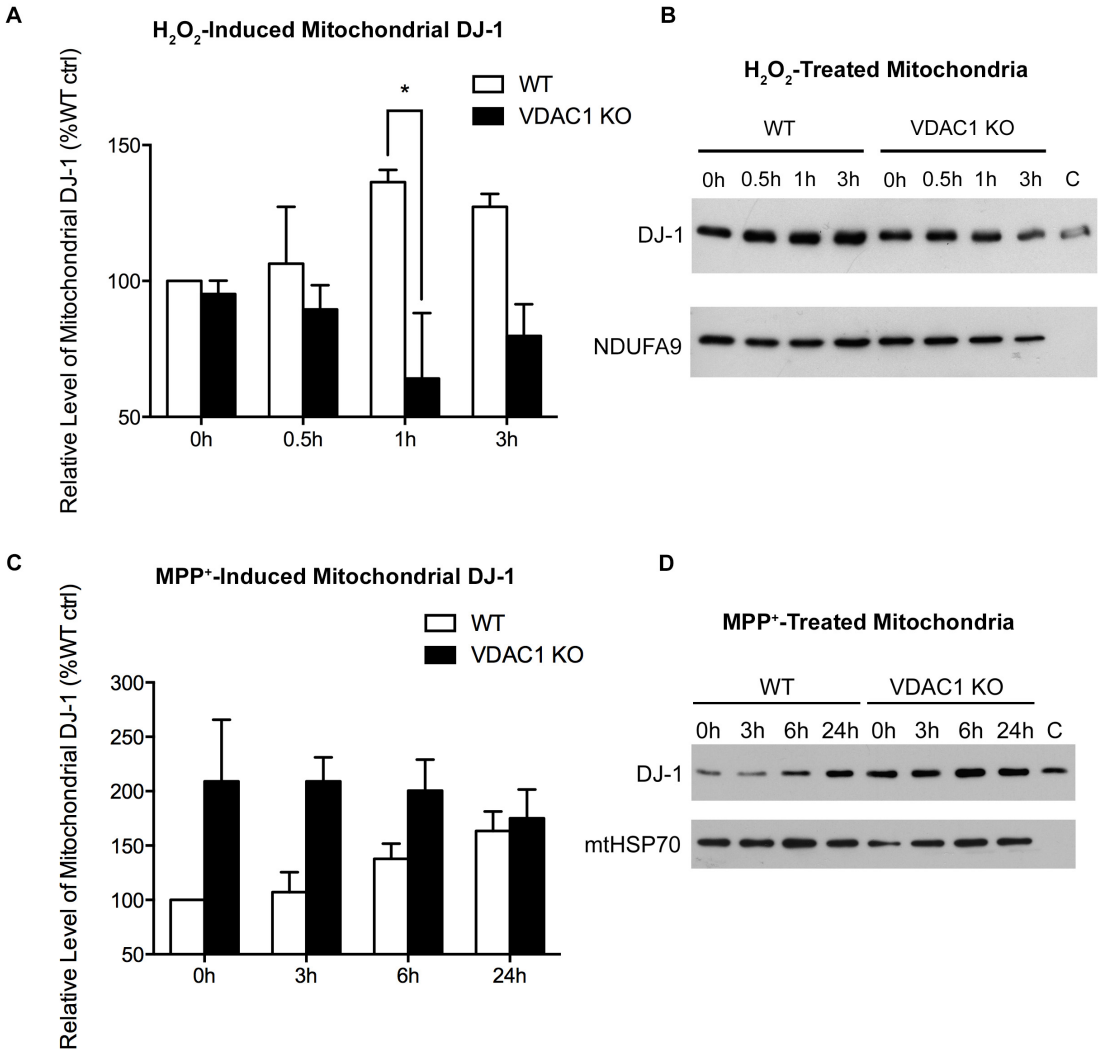
A
H_2O_2-Induced Mitochondrial DJ-1
WT
VDAC1 KO
*
Relative Level of Mitochondrial DJ-1 (%WT ctrl)
150
100
50
0h
0.5h
1h
3h
B
H_2O_2-Treated Mitochondria
WT
VDAC1 KO
0h 0.5h 1h 3h 0h 0.5h 1h 3h C
DJ-1
NDUFA9
C
MPP+-Induced Mitochondrial DJ-1
WT
VDAC1 KO
Relative Level of Mitochondrial DJ-1 (%WT ctrl)
300
250
200
150
100
50
0h
3h
6h
24h
D
MPP+-Treated Mitochondria
WT
VDAC1 KO
0h 3h 6h 24h 0h 3h 6h 24h C
DJ-1
mtHSP70

VDAC1 deficiency causes significantly decreased mitochondrial health

Given that VDAC1 KO appear, at least in neurons, to show increased DJ-1 mitochondrial localization, we sought to determine whether VDAC1 KO neurons display indices of cellular stress. Although the mitochondrial effects of VDAC1 deficiency has been investigated in multiple tissues (Wu et al., 1999; Anflous et al., 2001; Krauskopf et al., 2006; Baines et al., 2007), little work has been done characterizing neurons that lack VDAC1. As such, we question what effect VDAC1 deficiency may have on mitochondria function. Here we sought to determine how VDAC1 KO affected mitochondrial health by examining survival, ROS levels, mitochondrial length, and ATP levels in cortical neurons.

While decreased cell survival can occur via multiple pathways, increased cell death can be indicative of mitochondrial damage (Esposito et al., 1999; Fiskum et al., 2003; Lin and Beal, 2006; Lin et al., 2009). Primary cortical neurons from WT and VDAC1 KO E14.5-15.5 embryos were grown *in vitro* for 6 days prior to treatment with 10μM MPP^+ treatment for up to 6h in absence of supplemented antioxidants. Samples were fixed and nuclei were stained with Hoechst to assess nuclear integrity. Basally, VDAC1 KO cortical neurons exhibit significantly decreased survival that is not further enhanced by 10μM MPP^+ treatment (Figure 3.2A). The decreased survival of these cortical neurons basally suggests increased cellular stress.

Accordingly, we next examined levels of ROS in VDAC1 WT and KO cortical neurons. Increased ROS is also often indicative of mitochondrial dysfunction (Esposito et al., 1999; Fiskum et al., 2003; Lin and Beal, 2006; Chinta and Andersen, 2008; Lin et al., 2009). WT and VDAC1 KO primary cortical neurons were cultured *in vitro* for 6 days

prior to analysis. We employed the cell-permeable probe CM-H_2DCFDA, which fluoresces according to the level of oxidative stress within the cell. With 1h of 10μM MPP^+ treatment (in absence of antioxidants), we see a significantly smaller increase in ROS production with VDAC1 KO, compared to WT (Figure 3.2B). Interestingly, with 3h of 10μM MPP^+ (in absence of antioxidants) we observe a significantly larger increase in ROS production in the VDAC1 KO cortical neurons (Figure 3.2B). These findings suggest that VDAC1 KO cortical neurons are able to compensate with short-term stress, but fail to do so with extended stress and subsequently produce higher levels of ROS.

Next we examined mitochondrial length. Healthy mitochondria exist in tubular networks and can undergo fission and fusion. A disruption in the balance between fission and fusion is often indicative of mitochondrial damage (Chen et al., 2006; Detmer and Chan, 2007; Archer, 2013). WT and VDAC1 KO primary cortical neurons were grown *in vitro* for 6 days prior to up to 6h of 10μM MPP^+ in absence of supplemented antioxidants. Samples were fixed and stained for mitochondria (mitochondrial protein Tom20) and nuclei (Hoechst) and analyzed by confocal microscopy. Length was measured using ImageJ software (NIH). With 10μM MPP^+ treatment for 3h, WT mitochondria become more fragmented (Figure 3.2C, D; Figure 3.S2). Basally, VDAC1 KO cortical neurons have shorter mitochondria compared to WT and are further fragmented following 10μM MPP^+ treatment for 6h (Figure 3.2C, D; Figure 3.S2). A shift towards a fragmented pool of mitochondria, as we have observed here, is often indicative of mitochondrial damage (Chen and Chan, 2006; Chen and Chan, 2009; Archer, 2013; Lackner, 2014).

Finally we sought to determine ATP levels, as neurons are highly dependent on mitochondria for ATP production and a decrease would indicate a decrease in

mitochondrial health (Fiskum et al., 2003; Detmer and Chan, 2007; Mattson et al., 2008). Using a luciferase-based assay, we determined ATP levels in VDAC1 WT and KO cortical neurons. Basally, there is less ATP in VDAC1 KO versus WT neurons (Figure 3.2E). Additionally, treatment with the ATP synthase inhibitor oligomycin, which blocks mitochondrial ATP production, decreases ATP levels to similar levels in both VDAC1 WT and KO (Figure 3.2E). This finding suggests that specifically mitochondrial-produced ATP (indicated by the decrease in ATP levels with oligomycin treatment) is decreased in VDAC1 KO neurons. No significant difference was noted in ATP levels following 1h MPP^+ treatment (Figure 3.2E). VDAC1 deficiency results in decreased mitochondrial-dependent ATP production, which suggests these cortical neurons have dysfunctional mitochondria.

Figure 3.2: VDAC1 deficient cortical neurons have impaired mitochondrial health. Cortical neurons harvested from WT and VDAC KO E14.5 – E15.5 embryos were cultured 6 days *in vitro* prior to 10μM MPP^+ treatment for 1h, 3h or 6h, in absence of antioxidants. A) Survival was determined by assessment of nuclear integrity, via Hoechst stain. Arrow, live cell; arrowhead, dead cell. Data represent mean ± SEM (n=3, in quadruplicate). **P*<0.05 and ***P*<0.01; two-way ANOVA with Tukey post-hoc analysis for WT vs. KO samples. B) Cortical neurons were incubated with the cell permeable CM-H_2DCFDA (10uM), to detect ROS production. Data represent mean ± SEM (n=3-5). **P*<0.05, ****P*<0.001 and *****P*<0.0001; two-way ANOVA with Bonferroni post-hoc analysis. C) Representative confocal images of mitochondria, stained for Tom20, in WT and VDAC1 KO cortical neurons. D) Average length of mitochondria, quantified using ImageJ (NIH). Data represent mean ± SEM (n=4-5, with minimum 500 mitochondria/n). *****P*<0.0001; Two-way ANOVA with Bonferroni post-hoc analysis. E) A luciferase-based assay was used to quantify ATP levels in WT and VDAC1 KO cortical neurons. Oligomycin was used to inhibit mitochondrial-produced ATP. Data represent mean ± SEM (WT n=2; KO n=4).

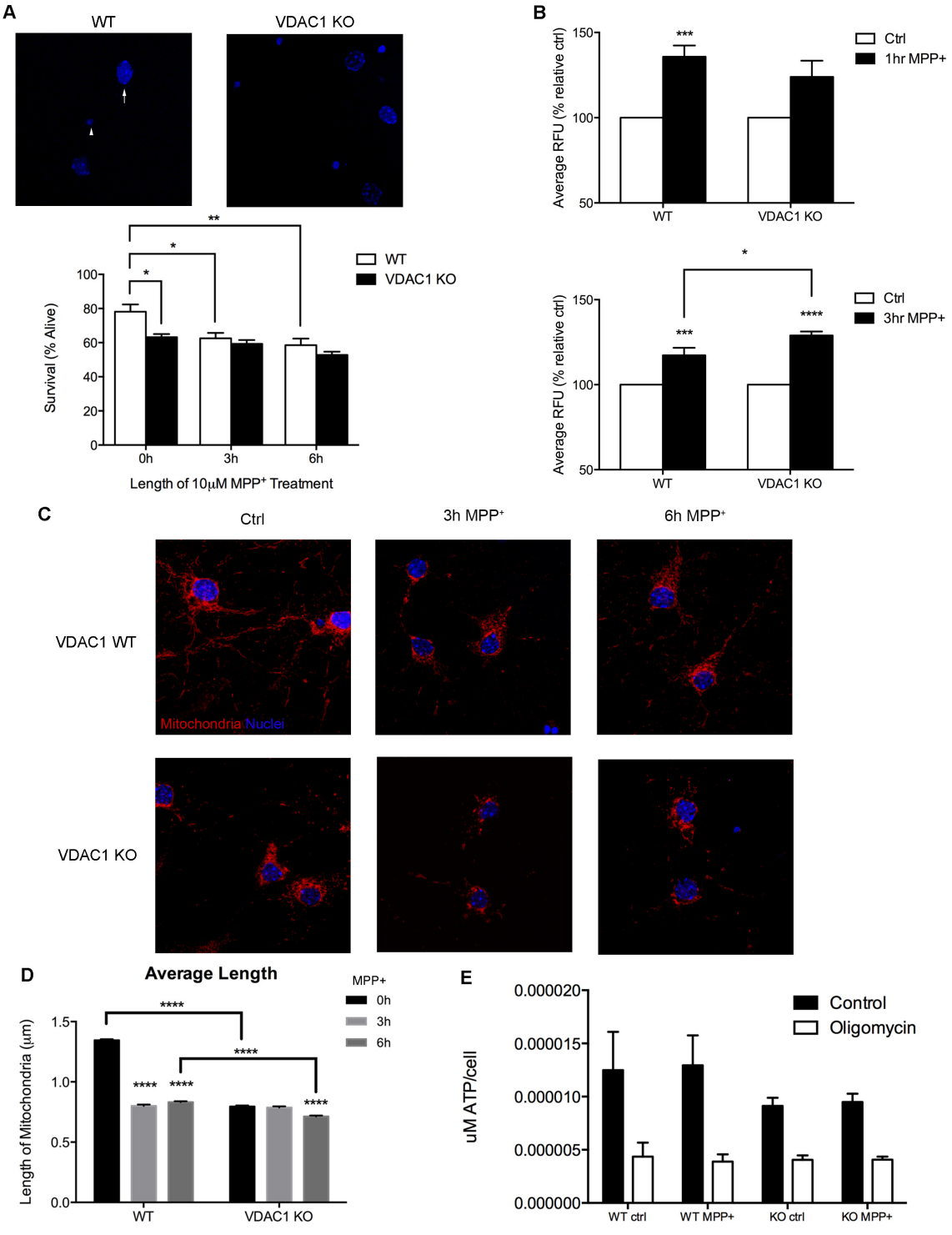
A
WT
VDAC1 KO
Survival (% Alive)
Length of 10μM MPP+ Treatment
0h
3h
6h
WT
VDAC1 KO
B
Average RFU (% relative ctrl)
Ctrl
1hr MPP+
3hr MPP+
C
Ctrl
3h MPP+
6h MPP+
VDAC1 WT
VDAC1 KO
Mitochondria Nuclei
D
Average Length
MPP+
0h
3h
6h
Length of Mitochondria (μm)
E
uM ATP/cell
Control
Oligomycin
WT ctrl
WT MPP+
KO ctrl
KO MPP+

VDAC1 KO cortical neurons exhibit reduced basal survival, produce more ROS with prolonged stress and have fragmented mitochondria that produce less ATP. These findings suggest that VDAC1 KO cortical neurons have decreased mitochondrial health, even in absence of an exogenous stressor. However, basally there is more DJ-1 localized to mitochondria - something that has been suggested to be protective in a WT scenario (Canet-Avilés et al., 2004; Junn et al., 2009). These discrepant observations suggest that perhaps DJ-1 is not properly localized to the right mitochondrial compartment critical for survival and regulation of mitochondrial function, in absence of VDAC1. Accordingly we next determined where DJ-1 is localized and how this may be affected with VDAC1 deficiency.

DJ-1 requires VDAC1 for proper sub-mitochondrial localization

While DJ-1 localization to mitochondria has been documented by a number of groups (Canet-Avilés et al., 2004; Junn et al., 2009; Joselin et al., 2012), the function that DJ-1 exerts at mitochondria is still unknown. DJ-1 contains no mitochondrial localization signal and the mechanism by which it localizes to mitochondria is also not well understood. As such, the site DJ-1 resides within mitochondria is not agreed upon, with different groups claiming OMM, IMM and/or matrix (Canet-Avilés et al., 2004; Li et al., 2005; Zhang et al., 2005; Hayashi et al., 2009). In order to better understand the potential function of DJ-1 at mitochondria, we wanted to clarify its sub-mitochondrial localization.

To assess sub-mitochondrial localization of DJ-1, we subjected mitochondrial enriched fractions to proteolytic digestion by trypsin for up to 120min. Proteins localized

at the OMM will be subjected to digestion first, and over time more internally localized proteins are exposed and able to be digested. WT MEFs have mitochondrial DJ-1 that is highly resistant to proteolytic digestion, both in control and H_2O_2-treated conditions (Figure 3.3A). The degree to which DJ-1 is digested is similar to the digestion of matrix marker mtHSP70, which suggests that DJ-1 largely resides in the matrix. VDAC1 KO MEFs appear to have a similar localization for DJ-1 in control conditions, however with H_2O_2 treatment DJ-1 is much more readily digested (Figure 3.3B). This finding suggests that during oxidative stress, in absence of VDAC1, DJ-1 is not localized to the matrix. As a control, to confirm that our proteins of interest can be degraded by proteolysis, we subjected mitochondrial enriched fractions to identical proteolytic digestion in the presence of Triton X-100, which allows for equal digestion regardless of location within mitochondria (Figure 3.S3). All proteins of interest are readily digested by trypsin. In MEFs, VDAC1 is important for sub-mitochondrial localization of DJ-1 during oxidative stress.

To further confirm the changes in DJ-1 sub-mitochondrial localization in cortical neurons, we utilized a recently devised system with bi-fluorescent complementation. In this system, complementation of GFP can occur when DJ-1 is localized either at the OMM or the matrix, depending on the plasmid employed. We analyzed the relative level of GFP fluorescence, and thus level of DJ-1 at either the OMM or matrix, compared to mitochondrial content. WT and VDAC1 KO primary cortical neurons were cultured *in vitro* for 4 days prior to transfection with either WT-DJ1-S11 and OMM-GFP1-10 or WT DJ-1 and matrix-GFP1-10. At 24h post-transfection, cortical neurons were treated with 10μM MPP^+ for 3h in absence of antioxidants. Both control and 10μM MPP^+ treated

VDAC1 WT cortical neurons exhibit strong, and similar levels of both OMM and matrix DJ-1 (Figure 3.3C). While we do not observe a change in either OMM or matrix DJ-1 levels following treatment in WT cortical neurons, this may be due to the over-expression system utilized. Notably, control VDAC1 KO cortical neurons have reduced matrix DJ-1, and this level is further decreased following 10μM MPP^+ treatment (Figure 3.3C).

Figure 3.3: Sub-mitochondrial DJ-1 is altered with VDAC1 deficiency. During oxidative stress, DJ-1 is localized more superficially within mitochondria deficient for VDAC1. Either control (A) or 3h 100μM H_2O_2–treated (B) WT and VDAC1 KO MEFs were subjected to trypsin digestion for up to 120min and subsequently analyzed by Western blot to assess degradation of mitochondrial components. Tom20 was used to identify outer mitochondrial membrane (OMM), NDUFA9 was used to identify inner mitochondrial membrane (IMM) and mtHSP70 was used to identify matrix. Blots are representative of n=3. C) Cortical neurons harvested from WT and VDAC KO E14.5 – E15.5 embryos were cultured 4 days *in vitro* prior to transfection. On DIV 5, neurons were treated with 10μM MPP^+ treatment for 3h, in absence of antioxidants. Representative confocal images with mitochondrial (Tom20, red), nuclei (Hoechst, blue) GFP signal. Quantification of corrected total cell fluorescence (as a % of WT ctrl) for ctrl and 10μM MPP^+ treatment. Data represent mean ± SEM (n=4). $^{**}P<0.01$ and $^{****}P<0.0001$; two-way ANOVA with Tukey's post-hoc analysis.

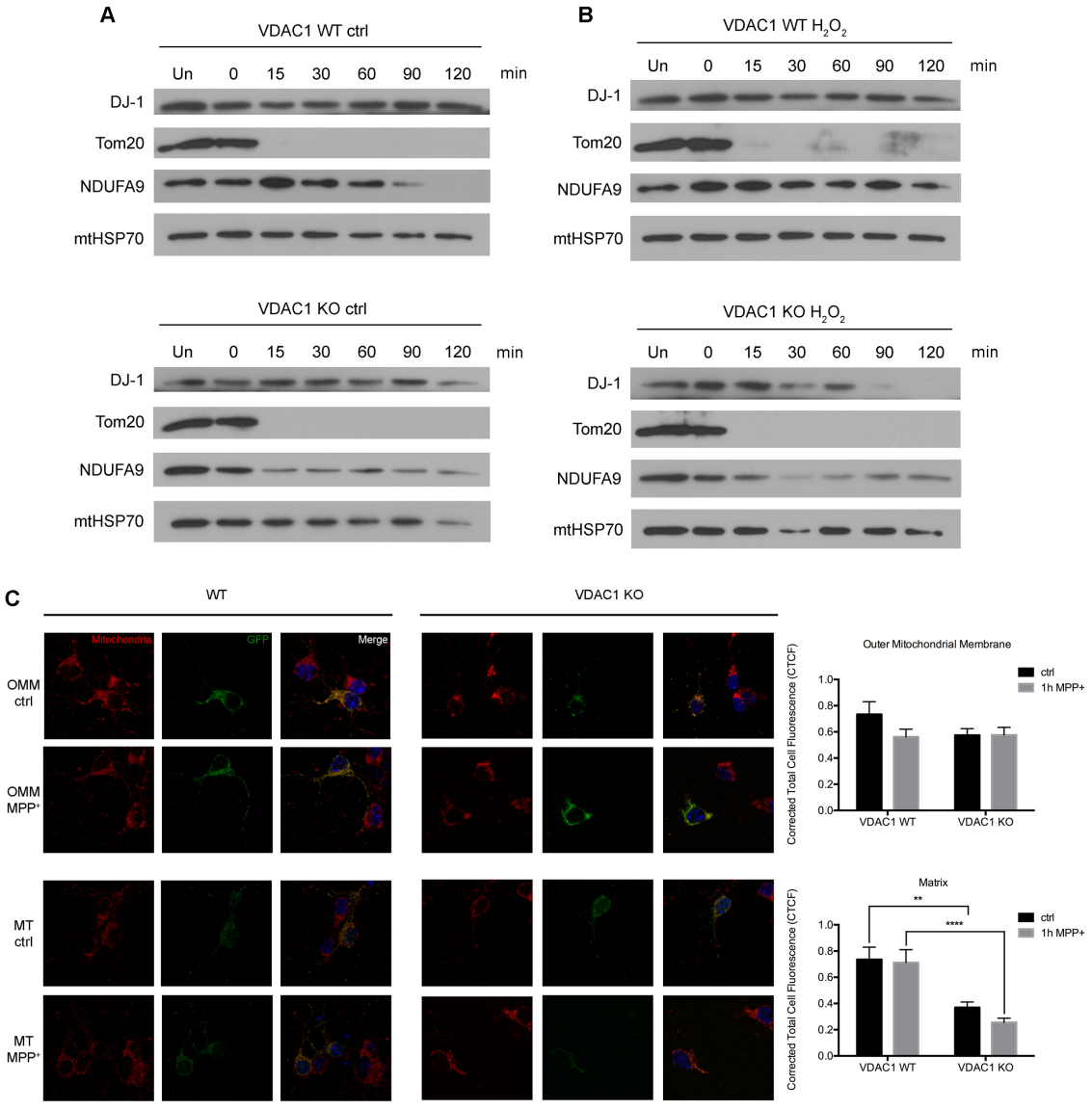
A
VDAC1 WT ctrl
Un 0 15 30 60 90 120 min
DJ-1
Tom20
NDUFA9
mtHSP70
VDAC1 KO ctrl
Un 0 15 30 60 90 120 min
DJ-1
Tom20
NDUFA9
mtHSP70
B
VDAC1 WT H2O2
Un 0 15 30 60 90 120 min
DJ-1
Tom20
NDUFA9
mtHSP70
VDAC1 KO H2O2
Un 0 15 30 60 90 120 min
DJ-1
Tom20
NDUFA9
mtHSP70
C
WT
VDAC1 KO
Mitochondria
GFP
Merge
OMM ctrl
OMM MPP+
MT ctrl
MT MPP+
Outer Mitochondrial Membrane
Corrected Total Cell Fluorescence (CTCF)
ctrl
1h MPP+
VDAC1 WT
VDAC1 KO
Matrix
**
****

Both VDAC1 KO MEFs and cortical neurons have reduced matrix-localized DJ-1 compared to WT cells. This suggests that VDAC1 is important in proper sub-mitochondrial localization of DJ-1. Improper localization of DJ-1 could result in the mitochondrial dysfunction observed in the VDAC1 null cortical neurons.

Mitochondrial DJ-1 is responsive to decreased ATP levels

Our previous work demonstrated that various stressors could cause increased localization of DJ-1 to mitochondria (Joselin et al., 2012). We sought to determine the nature of the signal that regulates this response.

While we previously showed that oxidative stressors could increase levels of mitochondrial DJ-1 (Joselin et al., 2012), we did not determine if ROS was directly the signal causing this translocation. To investigate if ROS is indeed the signal, we used two antioxidants, N-acetyl-cysteine (NAC) and Tiron to block ROS. WT primary cortical neurons from E14.5-15.5 embryos were cultured *in vitro* for 6 days prior to treatment. First we decreased ROS by pre-treating WT primary cortical neurons with NAC for 2h prior to treatment with 30μM H_2O_2 for up to 3h. Mitochondrial enriched samples were obtained as mentioned above and subjected to Western blot analysis. Treatment with NAC alone increases mitochondrial DJ-1 (Figure 3.4A). However no further increase is observed following H_2O_2 treatment (Figure 3.4A). Pre-treatment of WT cortical neurons with the anti-oxidant Tiron also basally increases mitochondrial DJ-1 with no significant increase following H_2O_2 treatment (Figure 3.4B). Therefore, while blocking ROS prevents stress-induced increase in mitochondrial DJ-1, it also basally increases

mitochondrial DJ-1 levels. This indicates that mitochondrial DJ-1 regulation by ROS, similar to VDAC1, is complex.

Neurons are highly reliant on mitochondria for ATP production (Chen and Chan, 2006). Interestingly we noted decreased ATP levels in VDAC1 null cortical neurons as well as increased mitochondrial DJ-1 levels. The signal for DJ-1 translocation to mitochondria is still present in absence of VDAC1, and perhaps even heightened. We were curious as to the role of DJ-1 and ATP and therefore investigated if ATP could serve as a signal for DJ-1 translocation to mitochondria. WT primary cortical neurons from E14.5-15.5 embryos were cultured *in vitro* for 6 days prior to treatment in absence of antioxidants. WT cortical neurons were treated with 10μM oligomycin, an ATP synthase inhibitor, for up to 60min and subjected to subcellular fractionation and Western blot analysis (Figure 3.4C). Within 5min of ATP synthase inhibition, we observe a significant increase in mitochondrial DJ-1 that is maintained with up to 60min of treatment (Figure 3.4C). We also confirmed this localization by immunofluorescence of endogenous DJ-1 in cortical neurons (Figure 3.4D). Our results demonstrate that inhibition of ATP is a strong driver of mitochondrial localization of DJ-1.

Figure 3.4: Reduced ATP levels induce translocation of DJ-1 to mitochondria. Pre-treatment of wild-type (WT) cortical neurons harvested from E14.5-15.5 embryos with the antioxidant NAC (A) or Tiron (B) prior to 3h or 6h 30μM H_2O_2 treatment. Mitochondrial enriched fractions were obtained through subcellular fractionation and were analyzed by Western blot for DJ-1 and mitochondrial loading control (mtHSP70). Quantification of densitometry using Image J software (NIH). Data represent mean ± SEM (n=2). C, cytoplasm. C) WT cortical neurons were treated with 10μM oligomycin for indicated time points in absence of antioxidants. Data represent mean ± SEM (n=5-6). *$P<0.01$; *t*-test for related samples. D) Representative confocal images of oligomycin treated cortical neurons, stained for mitochondria (COXI), endogenous DJ-1 and nuclei (Hoechst); n=2.

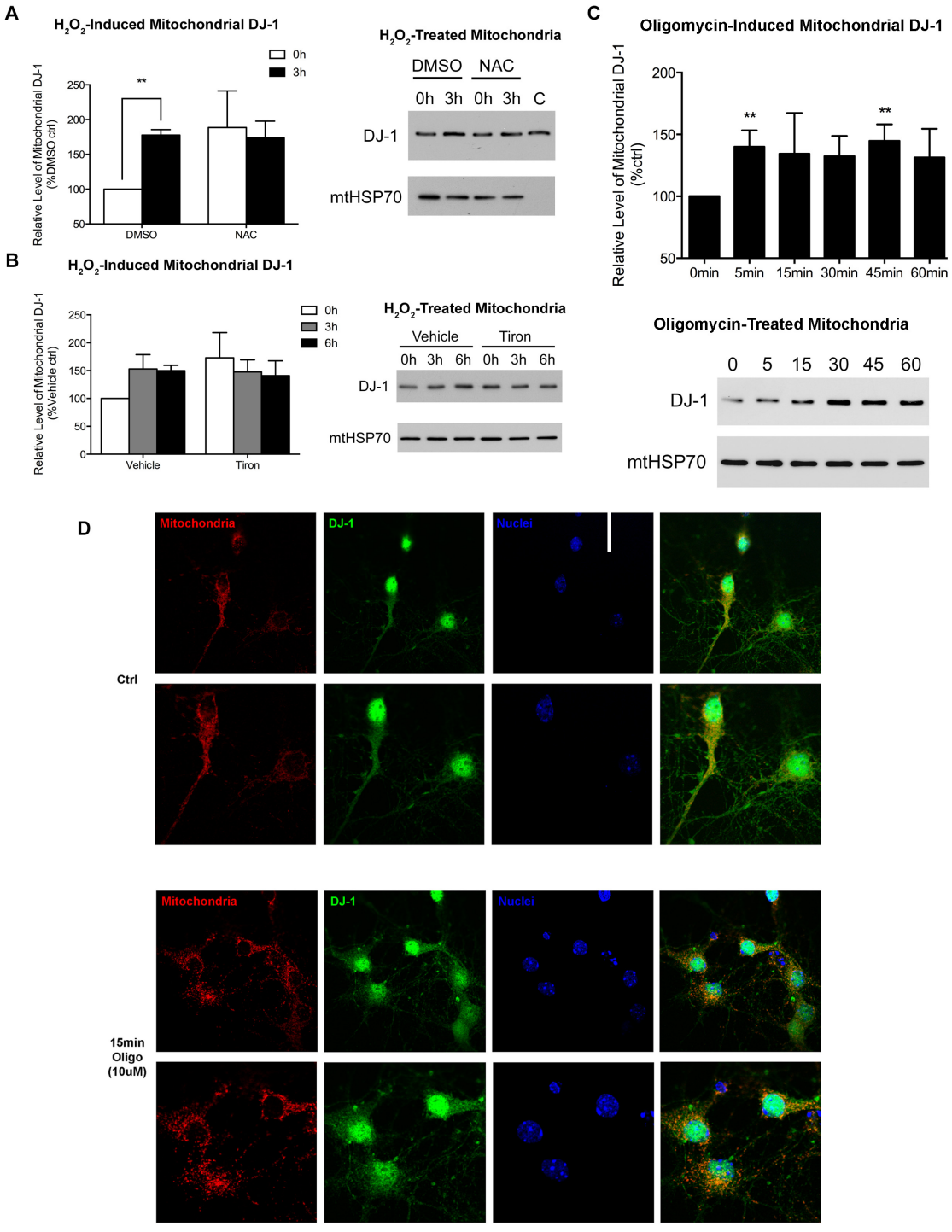
A
H_2O_2-Induced Mitochondrial DJ-1
0h
3h
Relative Level of Mitochondrial DJ-1 (%DMSO ctrl)
250
200
150
100
50
**
DMSO
NAC
H_2O_2-Treated Mitochondria
DMSO NAC
0h 3h 0h 3h C
DJ-1
mtHSP70
B
H_2O_2-Induced Mitochondrial DJ-1
0h
3h
6h
Relative Level of Mitochondrial DJ-1 (%Vehicle ctrl)
250
200
150
100
50
0
Vehicle
Tiron
H_2O_2-Treated Mitochondria
Vehicle Tiron
0h 3h 6h 0h 3h 6h
DJ-1
mtHSP70
C
Oligomycin-Induced Mitochondrial DJ-1
Relative Level of Mitochondrial DJ-1 (%ctrl)
200
150
100
50
**
**
0min 5min 15min 30min 45min 60min
Oligomycin-Treated Mitochondria
0 5 15 30 45 60
DJ-1
mtHSP70
D
Mitochondria
DJ-1
Nuclei
Ctrl
Mitochondria
DJ-1
Nuclei
15min Oligo (10uM)

Discussion

Previous studies by our group and others have reported a role for DJ-1 in mitochondrial health as well as stress-induced localization of DJ-1 to mitochondria to promote survival (Canet-Avilés et al., 2004; Junn et al., 2009; Irrcher et al., 2010; Krebiehl et al., 2010; Joselin et al., 2012). To better understand what regulates translocation of DJ-1 mitochondria, we investigated the potential interaction between DJ-1 and the mitochondrial protein VDAC1, as identified by an interactor screen.

In this regard, we provide evidence that overexpressed and endogenous DJ-1 interact with endogenous VDAC1. We also show that VDAC1 is important in regulating DJ-1 translocation, as stress-induced translocation of DJ-1 to mitochondria is impaired with VDAC1 deficiency in both MEFs and primary cortical neurons. Interestingly, VDAC1 KO cortical neurons have basally increased levels of mitochondrial DJ-1. As mitochondrial DJ-1 has previously been shown to have a protective effect (Junn et al., 2009), we questioned if perhaps VDAC1 deficiency has a negative impact on mitochondrial health.

Dysfunctional mitochondria produce more ROS and less ATP, two factors which can negatively impact neuronal survival (Esposito et al., 1999; Abou-Sleiman et al., 2006; Chen and Chan, 2006; Lin and Beal, 2006; Chinta and Andersen, 2008). Additionally, disruption in mitochondrial dynamics has been implicated in mitochondrial dysfunction and disease (Chen and Chan, 2006; Detmer and Chan, 2007; Archer, 2013). We demonstrate that in fact, VDAC1 deficient cortical neurons do have indices of mitochondrial stress including reduced ATP and fragmentation. We also observe decreased cell survival in the VDAC1 KO cortical neurons. We do note that MPP^+

treatment does not cause further cell death in the VDAC1 KO cortical neurons. Most likely, these cortical neurons are able to compensate and prevent further cell death, perhaps via VDAC2 or VDAC3. Examination of cell survival following longer treatment may show additional sensitization. VDAC1 deficiency results in cortical neurons that produce more ROS with extended stress. It appears as though, again, there is some compensation mechanism with short-term stress however VDAC1 deficient cortical neurons fail to compensate with longer MPP^+ treatment. Additionally, VDAC1 null mitochondria are more fragmented and resemble WT mitochondria that have been treated with MPP^+. Interestingly, this shift towards a fragmented phenotype was also observed with DJ-1 KO cells (Irrcher et al., 2010). There are several commonalities between VDAC1 and DJ-1 deficiency, which suggests one factor may rely on the other for proper function. What is intriguing with our results is that there is also increased mitochondrial DJ-1 in these cortical neurons. Mitochondrial-targeted DJ-1 has been shown to be protective and to drive ATP synthesis (Junn et al., 2009; Calì et al., 2014). However we show both increased mitochondrial DJ-1 and decreased ATP production in absence of VDAC1, at least in neurons. What is the explanation for this discrepancy?

We proposed that perhaps DJ-1 localization to its appropriate mitochondrial compartment might be altered with loss of VDAC1. Various studies have claimed that DJ-1 resides at the OMM, IMM and/or matrix (Canet-Avilés et al., 2004; Li et al., 2005; Zhang et al., 2005; Hayashi et al., 2009). In our hands, in WT MEFs, we show endogenous DJ-1 to reside within mitochondria, most likely at the matrix. However, with VDAC1 deficiency the level of DJ-1 in the mitochondrial matrix is dramatically reduced following oxidative stress. Consistent with the results in MEFs we also see similar results

in neurons for matrix-specific localization of DJ-1. In primary cortical neurons, we note both OMM and matrix localization of exogenously expressed DJ-1 in a GFP complementation assay. In contrast, VDAC1 deficient cortical neurons have substantially less matrix-localized DJ-1 as observed by decreased GFP complementation. Interestingly, at least with the conditions tested in this assay in neurons, we did not observe increased mitochondrial DJ-1 as we have previously shown. This difference is likely due to the differing in conditions of stress and cell type employed as well as the expressed nature of DJ-1 required for this assay.

These findings suggest a two-step model by which DJ-1 goes to mitochondria. In the first, an unknown step regulates OMM mitochondrial localization. This signal would likely be a response to stress, and drives DJ-1 localization to the OMM. One potential signal for this step may be a reduction in ATP levels (see below). It is important to note that this step is likely not simply reliant on ROS since ROS inhibition actually induces localization of DJ-1 to mitochondria. However, ROS itself is known to be involved in critical intracellular signalling (Sena and Chandel, 2012). Thus inhibition of ROS could increase stress in the cell. In the second step, DJ-1 translocates to the matrix, a process that is dependent upon VDAC1. Taken together, we suggest that in absence of VDAC1, DJ-1 is unable to localize to the matrix. Consequently, VDAC1 deficient cortical neurons have mitochondrial defects, which may explain its reduced viability.

In our two-step model of DJ-1 translocation to mitochondria, what might be the function of matrix-localized DJ-1? Previous work has demonstrated that matrix-targeted DJ-1 promotes ATP production by mitochondria (Calì et al., 2014). This works suggests that a drop in ATP production, such as with exogenous oxidative stress or MPP^+

treatment may signal DJ-1 to enter the matrix to compensate for loss of ATP. Consistent with this, we demonstrate that inhibition of ATP production by oligomycin is a strong driver of DJ-1 translocation to mitochondria. Additionally, if matrix-DJ-1 is important in ATP production, then our observation of decreased mitochondrial-produced ATP in VDAC1 KO cortical neurons fits this model. In summary, we propose that DJ-1 must localize to the matrix of mitochondria in a VDAC1-dependent manner to regulate ATP levels and perhaps to promote survival during stress. Future work will investigate aspects of this model.

Methods and Materials

Animals

The generation and genotype of DJ-1 and VDAC1 mice has been described previously (Wu et al., 1999; Weeber et al., 2002; Kim et al., 2005a). All procedures involving animals were approved by the University of Ottawa Animal Care Committee and were maintained in strict accordance to the Guidelines for the Use and Treatment of Animals put forth by the Animal Care Council of Canada and endorsed by the Canadian Institute of Health Research.

Cell culture

Mouse embryonic fibroblasts (MEFs) were derived from E14.5-15.5 transgenic DJ-1 (C57BL/6) mice and immortalized as previously described (Aleyasin et al., 2010). VDAC1 WT and KO MEFs were a generous gift from Dr. William Craigen and were immortalized by natural selection of cells that persist beyond typical senescence. All MEFs were maintained in Dulbecco's Modified Eagle Media (DMEM) (Sigma) supplemented with 10% fetal bovine serum (FBS) (Sigma) and antibiotic/antimycotic (Sigma). All MEFs were immortalized as previously described (Aleyasin et al., 2010). Cortical neurons were derived from E14.5-15.5 wildtype (WT) CD1 mice or VDAC1 transgenic mice (Charles River Laboratories) of either sex and maintained in Neurobasal media (Invitrogen) supplemented with B27 with antioxidants (Gibco), N2 (Gibco), 0.5 mM L-glutamine (Sigma), and penicillin/ streptomycin (Gibco) as previously reported (Kim et al., 2005a). Neurons were plated onto poly-D-lysine coated plates as follows: $5x10^6$ cells per 10cm plate for mitochondrial fractionation; 100,000 per well of 24-well plate for survival, or mitochondrial length; 200,000 per well of 24-well plate for GFP-

complementation assay; 500,000 per well of 12-well plate for ROS assay; and $2x10^6$ per well of 6-well plate for ATP assay.

Mitochondrial enriched fractions

Both VDAC1 WT and KO MEFs were treated for up to 3h with 100μM H_2O_2 and then subjected to fractionation via differential centrifugation as previously described (Joselin et al., 2012). Similarly, VDAC1 KO cortical neurons harvested from E14.5-15.5 mouse embryos were grown in culture for 5 days in the presence of antioxidants. On DIV5, cultures received new media containing no antioxidants. On DIV6, cultures were treated with either 10μM MPP^+ for up to 24h or 10μM oligomycin for up to 1h and then subjected to fractionation via differential centrifugation.

Trypsin digestion

VDAC1 WT and KO MEFs were treated with 100uM H_2O_2 for 3hr and subjected to a modified subcellular fractionation. Specifically, isolation buffer consisted of 200mM mannitol, 70mM sucrose, 10mM HEPES, and 1mM EGTA with pH 7.5 and no protease inhibitors were added. The mitochondrial-enriched fractions were digested with 25μg/mL trypsin (Sigma) for up to 120min. To stop the digestion, 50 μg/mL of AEBSF (Fisher) was added to the reaction. This non-specific proteolysis of mitochondria will cause a progressive loss of mitochondrial proteins, starting with OMM proteins and moving in to the matrix. To ensure that our proteins of interest can be degraded by proteolysis, we subjected mitochondria to identical digestion with trypsin in the presence of Triton X-100, which allows for equal digestion regardless of location within mitochondria.

Co-immunoprecipitation

GST immunoprecipitation was performed in human embryonic kidney (HEK) 293 cell

line. GST-DJ1 or GST alone was transiently transfected using Lipofectamine 2000 (Invitrogen) and cells were lysed 24-36hr later in lysis buffer (50 mM Tris HCl pH7.5, 100 mM NaCl, 1 mM EDTA, 1 mM DTT, 0.2% NP-40 and protease inhibitor). Lysate was incubated with 40µL of glutathione sepharose (GE Healthcare) for 4h. Samples were washed 3 times with lysis buffer. Bound proteins were eluted by boiling samples in 2X SDS-loading buffer and analyzed by Western blot.

Endogenous immunoprecipitation of DJ-1 was performed in mitochondrial-enriched fractions from either VDAC1 WT and VDAC1 KO MEFs or DJ-1 WT and DJ-1 KO MEFs. Mitochondrial-enriched fractions were resuspended in isolation buffer and pre-cleared with TrueBlot rabbit IgG beads for 6h. Cleared lysate was incubated with 5µg of DJ-1 antibody (Abcam) or normal rabbit IgG (Santa Cruz) overnight. Samples were washed 5 times with isolation buffer and eluted by boiling in 2X SDS-loading buffer.

Western blot

Protein quantification was performed using Bradford (Bio-Rad) method. Samples were electrophoresed on 12% sodium dodecyl sulfate polyacrylamide gels and transferred to polyvinylidene fluoride (PVDF) membranes (Millipore). Membranes were probed with the respective primary antibodies followed by horseradish peroxidase–conjugated secondary antibodies and developed with the Immobilon Western Chemiluminescent HRP Substrate (Millipore). Densitometry analysis was carried out using ImageJ (NIH). For mitochondrial-enriched samples 10µg of each sample was analyzed. For mitochondrial digestion samples, equal volumes of sample were assessed. Primary antibodies included: for the OMM - Tom20 (Santa Cruz, rabbit, 1:2000); for the IMM - ATPβ (Abcam, mouse, 1:1000) or NDUFA9 (Abcam, mouse, 1:2000); for the matrix and

loading control - mtHSP70 (Abcam, mouse, 1:2000); VDAC1 (Calbiochem, rabbit, 1:2000); DJ-1 (Abcam, rabbit, 1:20,000); GST (Abcam, rabbit, 1:2000).

Immunofluorescence

Following treatment, neurons were fixed in 4% formalin in growth media at room temperature for 30min. The cells were permeabilized and blocked simultaneously using 0.1% Triton X-100 and 5% normal goat serum for 1hr at room temperature. Incubation with the respective primary antibodies (DJ-1, Abcam, 1:500; Tom20, Santa Cruz, 1:500; COXI, MitoSciences, 1:300) was performed overnight at 4°C. Samples were subsequently washed in 5% normal goat serum and stained with the corresponding secondary antibodies (1:500). Following 3 washes in PBS, samples were stained with Hoechst, mounted and analyzed by confocal microscopy.

Survival assay

Following 10μM MPP^+ treatment, cortical neurons were fixed in 4% formalin in growth media at room temperature for 30min. Subsequently they were stained with Hoechst and amount of apoptotic nuclei was analyzed by fluorescence microscopy.

ROS assay

The cell-permeable fluorogenic probe 5-(and-6)-chloromethyl-2', 7'-dichlorodihydrofluorescin diacetate (CM-H2DCFDA) is oxidized rapidly by ROS to a fluorescent compound. This probe is considered a general indicator for level of oxidative stress in the cell (Halliwell and Whiteman, 2004). Prior to treatment, cortical neurons were loaded with 10μM CM-H2DCFDA (Invitrogen) for 10min. Cortical neurons were subsequently washed with PBS and then placed in unsupplemented, dye-free Neurobasal media (Invitrogen). Following 10μM MPP^+ treatment, fluorescence was determined using

a plate reader (excitation 485; emission 530) over 15min. Data is averaged and presented as % treatment versus control.

Mitochondrial length

Mitochondrial length was assessed using ImageJ (NIH) as previously described (Irrcher et al., 2010). Briefly, length of mitochondria stained for Tom20 was measured in VDAC1 WT and KO cortical neurons for control and 10μM MPP^+ treated conditions. Lengths were either averaged or binned accordingly. A minimum of 500 mitochondria were counted per sample size (n).

ATP assay

The CellTiter Glo Luminescent (Promega) assay relies on level of ATP in the cell to produce luminescence and has been previously described to assess cellular ATP levels (Khacho et al., 2014). Following 10μM MPP^+ treatment, cortical neurons were harvested by gentle trypsinization using TrypLE reagent (Invitrogen). Each sample was divided into 6 wells of an opaque 96-well plate, of which 3 wells were incubated with 10μM oligomycin for 1h to inhibit mitochondrial-produced ATP. An aliquot of each sample was used to determine cell number using a hemocytometer. Luminescence was recorded using a plate reader. A range of standard ATP concentrations was used to determine ATP concentrations in samples. Data is presented as μM of ATP, corrected for cell number.

GFP complementation system

A bi-fluorescent complementation system has been developed to examine sub-mitochondrial localization of DJ-1 (Calì et al., 2014). Specifically, one part of GFP is fused with DJ-1 and the complementing part of GFP is targeted to either the OMM or matrix. As such, GFP fluorescence occurs only when both parts of GFP are in the same

area, that is, if DJ-1 localizes to the OMM in the presence of OMM-GFP. At DIV4, we transfected primary cortical neurons with WT-DJ1-S11 and OMM-GFP1-10 (targeted to outer mitochondrial membrane) or mt-GFP1-10 (targeted to matrix) using Lipofectamine 3000 (Invitrogen). Following 24hr, media was changed to NB without AO and neurons were treated with 10μM MPP^+ for 3h and then fixed. Samples were stained with COXI to label mitochondria. We analyzed the relative level of GFP to mitochondrial fluorescence.

Statistical analysis

Statistical significance was determined using two-tailed Student's *t*-test for related samples or two-way ANOVA (with either Tukey's or Bonferroni post-hoc analysis) when comparing WT versus KO conditions. All data are presented as mean ± standard error of the mean (SEM). Significance at $P<0.05$ (*), $P<0.01$ (**), $P<0.001$ (***) and $P<0.0001$(****).

Supplementary Information

Figure 3.S1. DJ-1 interaction with VDAC1. A) GST-DJ1 but not GST alone interacts with endogenous VDAC1 in HEK293 cells, as observed by GST co-immunoprecipitation studies. Samples were analyzed by Western blot and probed for DJ-1 and GST. This is representative of two experiments. * denotes VDAC1 specific band. B) Endogenous DJ-1 interacts with endogenous VDAC1 in mitochondrial enriched fractions from VDAC1 WT MEFs. VDAC1 KO MEFs are used as a negative control. Samples were analyzed by Western blot and probed for DJ-1 and VDAC1. This is representative of three experiments.

A

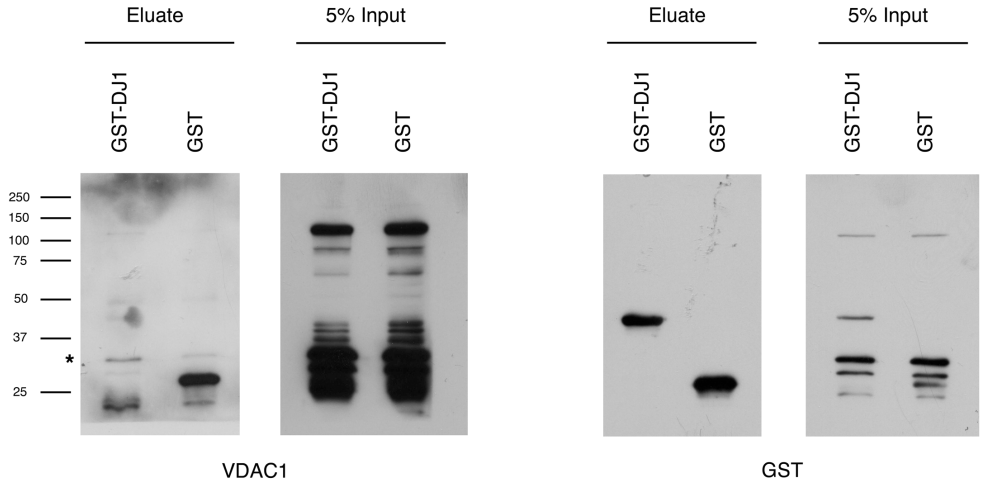
Eluate
5% Input
Eluate
5% Input
GST-DJ1
GST
GST-DJ1
GST
GST-DJ1
GST
GST-DJ1
GST
250
150
100
75
50
37
*
25
VDAC1
GST

B

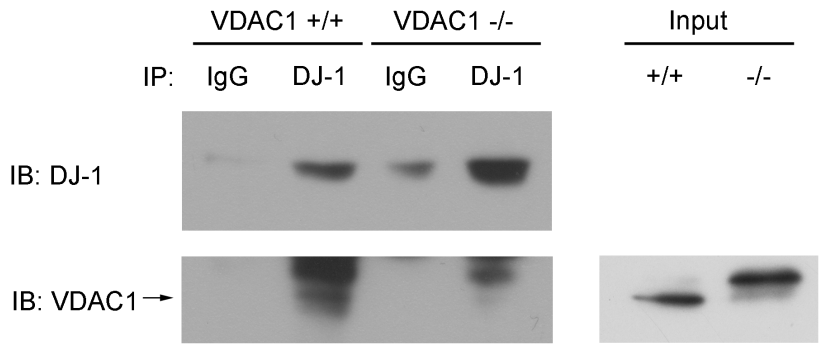
VDAC1 +/+
VDAC1 -/-
Input
IP:
IgG
DJ-1
IgG
DJ-1
+/+
-/-
IB: DJ-1
IB: VDAC1

Figure 3.S2. Mitochondria in VDAC1 KO cortical neurons are basally fragmented compared to WT mitochondria. Cortical neurons harvested from WT and VDAC1 KO E14.5-15.5 embryos were cultured for 6 days *in vitro* prior to 10μM MPP^+ for 3h or 6h, in absence of antioxidants. Mitochondrial length was calculated using Image J (NIH). Length was binned accordingly. Data represent mean ± SEM (n=4-5), minimum 500 mitochondria/n. $^{**}P<0.01$, $^{***}P<0.001$ and $^{****}P<0.0001$; two-way ANOVA with Bonferroni post-doc analysis.

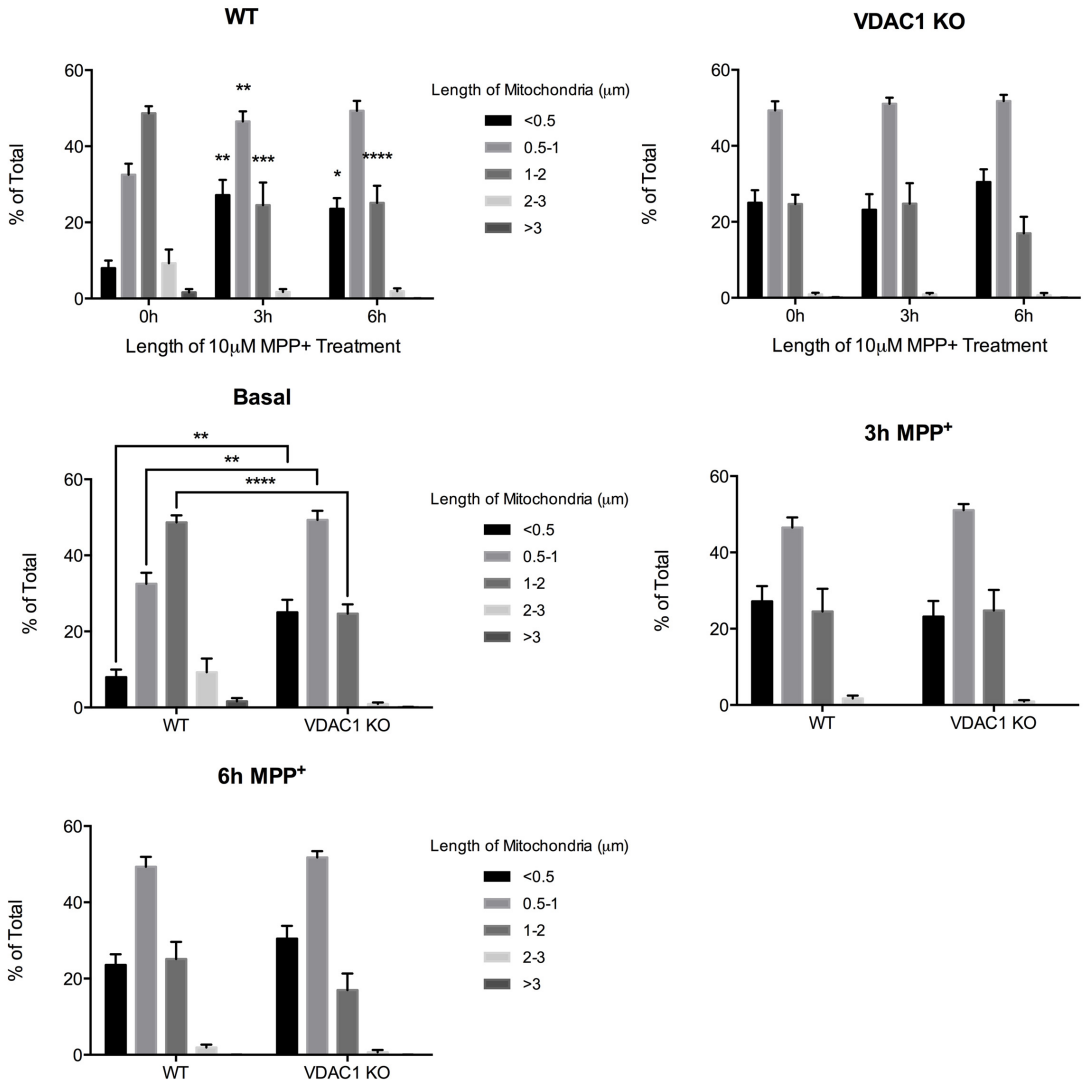
WT
VDAC1 KO
% of Total
Length of Mitochondria (μm)
<0.5
0.5-1
1-2
2-3
>3
0h
3h
6h
Length of 10μM MPP+ Treatment
Basal
3h MPP+
6h MPP+
WT
VDAC1 KO

Figure 3.S3. DJ-1 is localized to matrix and is not resistant to proteolytic digestion. WT MEFs were subjected to trypsin digestion for up to 60min and subsequently analyzed by Western blot to assess degradation of mitochondrial components (top). Addition of Triton X-100 to samples prior to digestion allows for equal digestion to all proteins, regardless of localization (bottom). Tom20 was used to identify outer mitochondrial membrane (OMM), NDUFA9 was used to identify inner mitochondrial membrane (IMM) and mtHSP70 was used to identify matrix. This is representative of three experiments.

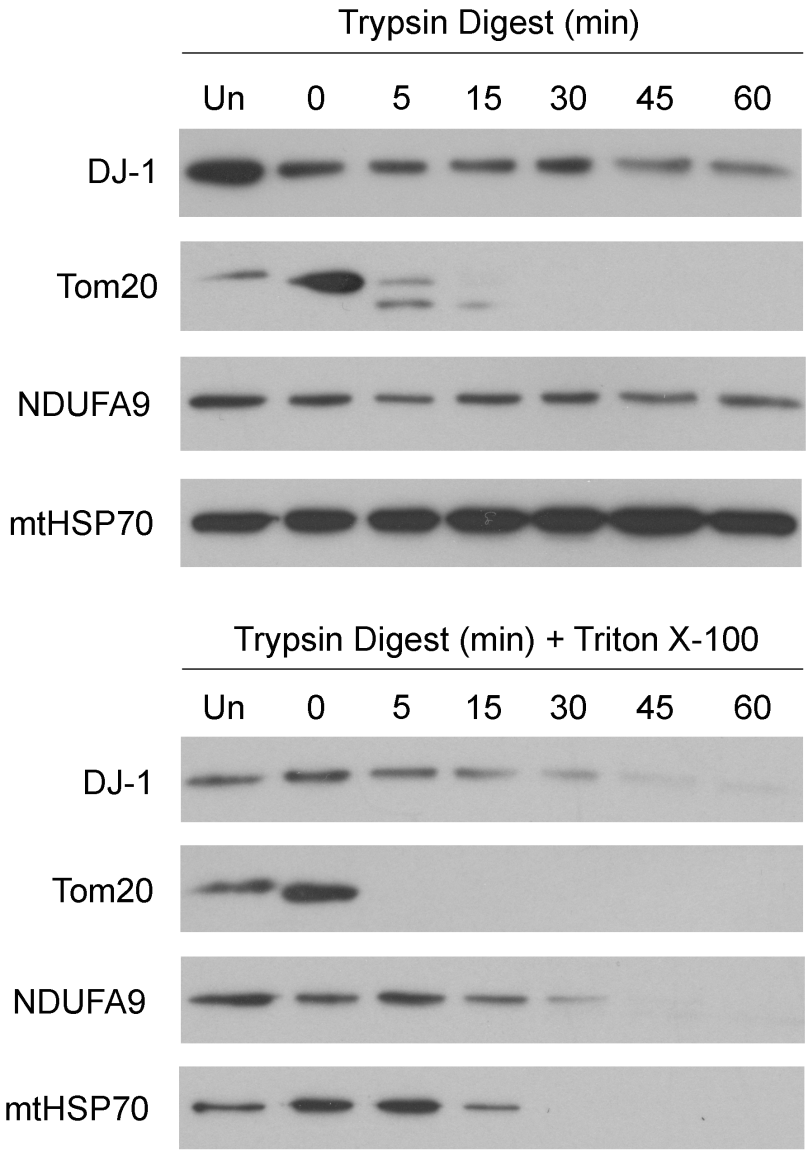
Trypsin Digest (min)
Un
0
5
15
30
45
60
DJ-1
Tom20
NDUFA9
mtHSP70
Trypsin Digest (min) + Triton X-100
Un
0
5
15
30
45
60
DJ-1
Tom20
NDUFA9
mtHSP70

CHAPTER 4

General Discussion

Parkinson's disease (PD) is the most common movement disorder and second most common neurodegenerative disease. With 90% of cases having unknown origin, it is difficult to discern the mechanism by which the degeneration occurs. There are numerous studies that suggest protein aggregation, inflammation, oxidative stress and mitochondrial dysfunction being involved in PD pathogenesis (Okazaki et al., 1961; Davis et al., 1979; McGeer et al., 1988; Dexter et al., 1989; Schapira et al., 1989; Hoozemans et al., 2007; Lira et al., 2011). Unfortunately many of the findings come from post-mortem analysis, in which cause versus consequence of the disease process cannot be determined.

With the discovery of genetic causes to PD, we can much more readily explore possible pathways involved in the pathogenesis of the disease. Loss-of-function mutations of one such gene, *DJ*-1, cause early-onset PD (Abou-Sleiman et al., 2003; Bonifati et al., 2003; Clark et al., 2004; Hering et al., 2004; Annesi et al., 2005). We and others have previously shown the pro-survival role of DJ-1 during stress and its involvement in mitochondrial health (Canet-Avilés et al., 2004; Kim et al., 2005a; Andres-Mateos et al., 2007; Junn et al., 2009; Irrcher et al., 2010; Krebiehl et al., 2010). Further understanding of the regulation of mitochondrial-localized DJ-1 is the subject of this dissertation.

Endogenous DJ-1 translocation to mitochondria

Numerous studies have examined mitochondrial localization of DJ-1 following induction of stress (Canet-Avilés et al., 2004; Blackinton et al., 2005; Junn et al., 2009). However, none of these studies have been conducted in primary neurons. Additionally,

some groups have examined the effects/consequences of exogenously expressed DJ-1, which may not be representative of endogenous mechanisms. Here we show for the first time that endogenous DJ-1 translocates to mitochondria in primary cortical neurons, using various stressors such as H_2O_2, MPP^+ and CCCP. We also investigated the importance of the PD genes *Parkin* and *Pink1* in translocation of DJ-1 to mitochondria. We demonstrate that in both Parkin KO MEFs and cortical neurons, this translocation does not occur. Interestingly, in absence of DJ-1, Parkin translocation to mitochondria is enhanced. It is also interesting to note that the mitochondria membrane uncoupler, CCCP, which induces Parkin translocation to mitochondria, also induces DJ-1 translocation to mitochondria. Further investigation into the role of Parkin in DJ-1 translocation to mitochondria would provide additional insight into the regulation of mitochondrial DJ-1. As Parkin is an E3 ubiquitin ligase (Imai et al., 2000), the impact of this function on mitochondrial DJ-1 could be determined as well as whether it is cytosolic or mitochondrial localized Parkin that is important. We also found that no stress-induced increase in mitochondrial DJ-1 was observed with Pink1 deficiency in MEFs or cortical neurons. Notably, basal level of mitochondrial DJ-1 was increased in both cell types. While this could indicate that the amount of DJ-1 at mitochondria is saturated, it could also suggest that Pink1 is important in the stress-induced localization of DJ-1. Further inquiry into the importance of Pink1 and its kinase activity into DJ-1 translocation to mitochondria will giver further insights into this pathway. Intriguingly, loss of either Parkin or Pink1 causes mitochondrial defects (Palacino et al., 2004; Wood-Kaczmar et al., 2008). Parkin null mice have decreased ETC complexes, decreased respiratory capacity and increased oxidative stress (Palacino et al., 2004). Pink1 deficiency decreases

survival, alters mitochondrial morphology and increases ROS production in a human dopaminergic neuron model (Wood-Kaczmar et al., 2008). As stress-induced DJ-1 translocation is absent with loss of either Parkin or Pink1, it would be interesting to investigate the importance of mitochondrial DJ-1 in regards to these noted defects. Additionally both Parkin and Pink1 are involved in mitochondrial quality control (MQC) (Narendra et al., 2008; Geisler et al., 2010). While not directly involved in this process itself, DJ-1 appears to require both Parkin/Pink1 for proper mitochondrial localization during oxidative stress. The interplay between these PD genes gives us better insight into the complexity in familial PD and the importance of mitochondrial health. We suggest that mitochondrial health is regulated by at least two pathways that act in parallel. First, there is the classic mechanism by which Parkin is recruited to damaged mitochondria that are then cleared by mitophagy. Second, there is a pathway by which Parkin and Pink1 regulate stress-induced increase in mitochondrial DJ-1. These two pathways, involving DJ-1, Parkin and Pink1, help maintain mitochondrial integrity. However, the actual signal and mechanism for translocation of DJ-1 to mitochondria remain unclear. Accordingly, we further explored the mechanisms of DJ-1 localization to mitochondria in Chapter 3.

Interaction of DJ-1 and VDAC1

An unbiased interactor screen suggests that DJ-1 interacts with the outer mitochondrial membrane (OMM) protein VDAC1. We investigated this interaction in hopes of better understanding the regulation of mitochondrial DJ-1. We were able to confirm the interaction between DJ-1 and VDAC1. We next explored the effect of

VDAC1 deficiency on mitochondrial localization of DJ-1. Specifically we queried whether VDAC1 signals for DJ-1 translocation to mitochondria.

Both VDAC1 null MEFs and cortical neurons show no stress-induced increase in mitochondrial DJ-1. VDAC1 is required for stress-induced increase of mitochondrial DJ-1. However, as DJ-1 is able to localize to VDAC1 deficient mitochondria, we do not believe that VDAC1 is the central signal for translocation to the OMM. Instead, we propose that VDAC1 is critical for sub-compartmentalization of DJ-1 to inner compartments such as the matrix (see below). Interestingly, similar to Pink1 KO conditions, VDAC1 KO cortical neurons exhibit basally increased level of mitochondrial DJ-1. Why would basal level of mitochondrial DJ-1 be increased in cortical neurons, but not MEFs that lack VDAC1? Without knowing the role of DJ-1 at mitochondria, it is difficult to identify why this difference is observed. However, comparing the two cell models may give us some insight. MEFs are actively dividing cells that are maintained in high glucose media. This media gears cells towards higher levels of glycolysis, therefore relying minimally on mitochondria for ATP production (Ibsen, 1961). Primary cortical neurons are terminally differentiated and rely much more heavily on mitochondria for ATP production (Bolaños et al., 2010). This reliance on mitochondria may add additional stress to the cell, specifically to the mitochondria themselves. If there is a mitochondrial defect, it could be exacerbated by oxidative phosphorylation, which is at a much higher level in cortical neurons versus MEFs. As such, we investigated the affect of VDAC1 deficiency on mitochondrial health in neurons.

Role of VDAC1 on mitochondrial health

VDAC1 deficiency has been characterized in numerous mouse cell types. Muscle from VDAC1 KO mice has altered mitochondrial morphology (Anflous et al., 2001). Isolated mitochondria from VDAC1 KO mouse liver undergo normal permeability transition following induction of apoptosis (Krauskopf et al., 2006). VDAC1 KO mouse embryonic stem cells have decreased oxygen consumption and decreased activity of complex IV of the ETC (Wu et al., 1999). MEFs lacking VDAC1 have altered mitochondrial morphology, but normal permeability transition and no altered sensitivity to stress (Baines et al., 2007).

Given the noted mitochondrial dysfunction with VDAC1 deficiency, it is surprising at the lack of studies in neural populations. We therefore investigated the consequences of VDAC1 KO on primary cortical neurons. Common indications of mitochondrial health include cell survival, level of cellular ROS, mitochondrial length and level of mitochondrial ATP production (Esposito et al., 1999; Abou-Sleiman et al., 2003; Chen and Chan, 2006; Lin and Beal, 2006; Detmer and Chan, 2007; Chinta and Andersen, 2008; Archer, 2013). We clearly demonstrate that VDAC1 KO cortical neurons have mitochondrial impairment. Specifically, there is reduced cell survival basally, increased ROS production following extended stress, basally fragmented mitochondria and decreased basal ATP production by mitochondria with VDAC1 deficiency. Interestingly, there is significant overlap between VDAC1 KO and DJ-1 KO cortical neuron phenotype (Kim et al., 2005a; Irrcher et al., 2010). DJ-1 null cortical neurons show hypersensitivity to oxidative stress (Kim et al., 2005a). With VDAC1 deficiency, cortical neurons have basally increased cell death. DJ-1 null cortical neurons

have fragmented mitochondria (Irrcher et al., 2010) similar to what we observed with VDAC1 deficiency. Isolated mitochondria from DJ-1 KO mouse whole brain lysates produced more ROS (Irrcher et al., 2010). We also show increased ROS production with VDAC1 KO cortical neurons following extended stress. Other groups have demonstrated reduced ATP production in DJ-1 KO MEFs and in a DJ-1 null dopaminergic cell line (Giaime et al., 2012; Heo et al., 2012), coinciding with our findings of decreased ATP production with VDAC1 deficiency.

Sub-mitochondrial localization of DJ-1

The sub-mitochondrial localization of DJ-1 has been studied, however OMM, inner mitochondrial membrane (IMM), and/or matrix localization have all been suggested (Canet-Avilés et al., 2004; Li et al., 2005; Zhang et al., 2005; Hayashi et al., 2009). It is important to note the variation in methods utilized in these studies – some rely purely on interaction with proteins in known mitochondrial compartments (Li et al., 2005; Hayashi et al., 2009). Recently a bi-fluorescent complementation system, which uses a split-GFP methodology, was employed to demonstrate DJ-1 localization to both the OMM and matrix (Calì et al., 2014). In conditions of stress, the matrix pool, but not the OMM pool, of DJ-1 increases (Calì et al., 2014). We investigated the sub-mitochondrial localization of DJ-1 in our hands. We found that in WT MEFs, mitochondrial DJ-1 is highly resistant to proteolytic digestion, suggesting it resides within the mitochondria, most likely at the matrix. While we noted a similar sub-mitochondrial localization of DJ-1 in untreated VDAC1 KO MEFs, but with H_2O_2 treatment, DJ-1 is much more readily digested. This

suggests that during times of stress, DJ-1 exists more externally within VDAC1 null mitochondria, perhaps at the OMM.

Using the above-mentioned GFP complementation system, we demonstrate a similar finding in cortical neurons. VDAC1 KO cortical neurons exhibit highly reduced matrix, but not OMM, localized DJ-1 that is further decreased following stress induction. We suggest that in absence of VDAC1, sub-mitochondrial localization of DJ-1 is altered in neurons. This finding coincides with the finding that more DJ-1 is localized to mitochondria in VDAC1 deficient cortical neurons. We suggest that the signal exists for DJ-1 to translocate to mitochondria however DJ-1 fails to enter mitochondria and remains at the OMM. As the signal persists in the VDAC1 null cells, more DJ-1 is recruited to the outside of mitochondria and total mitochondrial DJ-1 level is increased. Interestingly, we did not observe an increase in matrix DJ-1 in treated WT cortical neurons using expressed DJ-1. This observation may be due to the use of expressed DJ-1. We can conclude, however, that VDAC1 is required for proper sub-mitochondrial localization of DJ-1, especially during times of stress. With VDAC1 deficiency, DJ-1 cannot localize to the matrix and this specific sub-mitochondrial localization may be important in its pro-survival function.

Future work will investigate if we can rescue the observed mitochondrial defects in VDAC1 KO cortical neurons by expressing DJ-1 that is specifically targeted to mitochondria. We expect that matrix-targeted, but not OMM-targeted DJ-1 will rescue the observed defects. DJ-1 targeted to the matrix would bypass the VDAC1-dependent facilitated import of DJ-1 into mitochondria. While matrix localization of DJ-1 appears to be important, we still do not know the functional consequence of this localization.

Regulation and function of mitochondrial DJ-1

There have been numerous studies suggesting potential roles of DJ-1 at mitochondria. Earlier work suggested that DJ-1 could act as an atypical peroxiredoxin-like peroxidase to locally quench ROS (Taira et al., 2004; Andres-Mateos et al., 2007). The degree to which DJ-1 can quench ROS is debated, as is the role that this potential peroxidase activity has in promoting survival (Shendelman et al., 2004; Yang et al., 2005; Andres-Mateos et al., 2007). The oxidation of DJ-1, specifically at C106, has been implicated in localization of DJ-1 to mitochondria (Canet-Avilés et al., 2004). However another study reported that while C106 can be oxidized, this oxidations is not necessary for mitochondrial localization of DJ-1 (Maita et al., 2013). Given this ROS link, we questioned if ROS could perhaps be the signal for DJ-1 to translocate to mitochondria. Interestingly, pre-treatment of cells with an antioxidant in cortical neurons increases basal level of mitochondrial DJ-1. While no stress-induced increase is observed, the involvement of ROS as a signal for DJ-1 translocation to mitochondria appears complex. We have shown that ROS can induce translocation of DJ-1 to mitochondria, however it is most likely an indirect effect.

Neurons have higher energetic demands and rely significantly on mitochondria for ATP production (Chen and Chan, 2006). We noted decreased ATP levels in VDAC1 null cortical neurons as well as increased mitochondrial DJ-1 levels. These findings suggest that the signal for translocation of DJ-1 to the outside of mitochondria still exists and is potentially even higher with VDAC1 deficiency in cortical neurons. We were curious about the connection between ATP and DJ-1 and therefore investigated if decreased ATP could serve as a signal for DJ-1 translocation to mitochondria. A direct

mechanism to inhibit mitochondrial ATP production is to inhibit ATP synthase using the compound oligomycin (Bertina et al., 1974; Penefsky, 1985). Indeed, inhibition of ATP synthase induces DJ-1 translocation to mitochondria. The robust nature of the response of DJ-1 to oligomycin treatment is encouraging to the idea that cellular ATP level could in fact be a signal for translocation. As such, we propose a two-step model in which DJ-1 translocates to mitochondria. The first step relies on a signal, such as decreased ATP levels, for translocation of DJ-1 to the outside of mitochondria. The second step allows for DJ-1 to localize to the matrix in a VDAC1-dependent manner.

In this two-step model, what may be the role of matrix-localized DJ-1? We noted a decrease in ATP production by mitochondria in VDAC1 KO cortical neurons. Previous work has shown that DJ-1 specifically targeted to mitochondria is protective, more so than untargeted DJ-1 (Junn et al., 2009). More importantly, DJ-1 targeted to the matrix increases ATP production (Calì et al., 2014). Given that DJ-1 is localized to the matrix and responds to decreased ATP levels, we propose that DJ-1 is somehow involved in modulating ATP production.

In summary, understanding the role of DJ-1 at mitochondria during oxidative stress is important in understanding which pathways are important in promoting survival. Here we show that DJ-1 translocates to the matrix of mitochondria following induction of stress in a two-step process. We suggest that DJ-1 is involved in sensing ATP levels during times of oxidative stress. We also show that VDAC1 is important in the proper sub-mitochondrial localization of DJ-1, and this lack of proper localization appears to negatively impact the health of mitochondria. We demonstrate the complex interaction between DJ-1 and two other PD genes, Parkin and Pink1. Loss of one PD gene can

clearly negatively affect the function of another PD gene, which sheds some light on the complicated nature of this disease. Elucidating the mechanisms of action of the various PD genes is important in progressing our understanding of the disease. Our findings contribute to a growing pool of knowledge that will assist in discerning the mechanisms by which neurons degenerate in PD. We cannot hope to truly prevent or cure the disease without understanding how and why this degeneration occurs.

APPENDIX I

References

Aarsland D, Andersen K, Larsen JP, Lolk A, Nielsen H, Kragh-Sørensen P (2001) Risk of dementia in Parkinson's disease: a community-based, prospective study. Neurology 56:730-736.

Abbott RD, Petrovitch H, White LR, Masaki KH, Tanner CM, Curb JD, Grandinetti A, Blanchette PL, Popper JS, Ross GW (2001) Frequency of bowel movements and the future risk of Parkinson's disease. Neurology 57:456-462.

Abou-Sleiman PM, Muqit MMK, Wood NW (2006) Expanding insights of mitochondrial dysfunction in Parkinson's disease. Nature Reviews Neuroscience 7:207-219.

Abou-Sleiman PM, Healy DG, Quinn N, Lees AJ, Wood NW (2003) The role of pathogenic DJ-1 mutations in Parkinson's disease. Annals of Neurology 54:283-286.

Abu-Hamad S, Zaid H, Israelson A, Nahon E, Shoshan-Barmatz V (2008) Hexokinase-I protection against apoptotic cell death is mediated via interaction with the voltage-dependent anion channel-1: mapping the site of binding. The Journal of Biological Chemistry 283:13482-13490.

Abu-Hamad S, Arbel N, Calo D, Arzoine L, Israelson A, Keinan N, Ben-Romano R, Friedman O, Shoshan-Barmatz V (2009) The VDAC1 N-terminus is essential both for apoptosis and the protective effect of anti-apoptotic proteins. Journal of Cell Science 122:1906-1916.

Ahlskog JE, Muenter MD (2001) Frequency of levodopa-related dyskinesias and motor fluctuations as estimated from the cumulative literature. Movement Disorders 16:448-458.

Alberico SL, Cassell MD, Narayanan NS (2015) The vulnerable ventral tegmental area in Parkinson's disease. Basal Ganglia 5:51-55.

Aleyasin H, Rousseaux MWC, Marcogliese PC, Hewitt SJ, Irrcher I, Joselin AP, Parsanejad M, Kim RH, Rizzu P, Callaghan SM, Slack RS, Mak TW, Park DS (2010) DJ-1 protects the nigrostriatal axis from the neurotoxin MPTP by modulation of the AKT pathway. Proceedings Of The National Academy Of Sciences Of The United States Of America 107:3186-3191.

Alves G, Forsaa EB, Pedersen KF, Dreetz Gjerstad M, Larsen JP (2008) Epidemiology of Parkinson's disease. Journal of Neurology 255 Suppl 5:18-32.

Andrade-Navarro MA, Sanchez-Pulido L, McBride HM (2009) Mitochondrial vesicles: an ancient process providing new links to peroxisomes. Current Opinion in Cell Biology 21:560-567.

Andres-Mateos E, Perier C, Zhang L, Blanchard-Fillion B, Greco TM, Thomas B, Ko HS, Sasaki M, Ischiropoulos H, Przedborski S, Dawson TM, Dawson VL (2007) DJ-1 gene deletion reveals that DJ-1 is an atypical peroxiredoxin-like peroxidase. Proceedings Of The National Academy Of Sciences Of The United States Of America 104:14807-14812.

Anflous K, Armstrong D, Craigen W (2001) Altered mitochondrial sensitivity for ADP and maintenance of creatine-stimulated respiration in oxidative striated muscles from VDAC1-deficient mice. Journal of Biological Chemistry 276:1954-1960.

Angot E, Steiner JA, Lema Tomé CM, Ekström P, Mattsson B, Björklund A, Brundin P (2012) Alpha-synuclein cell-to-cell transfer and seeding in grafted dopaminergic neurons in vivo. PLoS ONE 7:e39465.

Annesi G, Savettieri G, Pugliese P, D'Amelio M, Tarantino P, Ragonese P, La Bella V, Piccoli T, Civitelli D, Annesi F, Fierro B, Piccoli F, Arabia G, Caracciolo M, Cirò Candiano IC, Quattrone A (2005) DJ-1 mutations and parkinsonism-dementia-amyotrophic lateral sclerosis complex. Annals of Neurology 58:803-807.

Arbel N, Shoshan-Barmatz V (2010) Voltage-dependent anion channel 1-based peptides interact with Bcl-2 to prevent antiapoptotic activity. The Journal of Biological Chemistry 285:6053-6062.

Arbel N, Ben-Hail D, Shoshan-Barmatz V (2012) Mediation of the antiapoptotic activity of Bcl-xL protein upon interaction with VDAC1 protein. Journal of Biological Chemistry 287:23152-23161.

Archer SL (2013) Mitochondrial dynamics--mitochondrial fission and fusion in human diseases. The New England Journal of Medicine 369:2236-2251.

Arnoult D, Grodet A, Lee Y-J, Estaquier J, Blackstone C (2005) Release of OPA1 during apoptosis participates in the rapid and complete release of cytochrome c and subsequent mitochondrial fragmentation. The Journal of Biological Chemistry 280:35742-35750.

Ashrafi G, Schwarz TL (2012) The pathways of mitophagy for quality control and clearance of mitochondria. Cell Death and Differentiation.

Azoulay-Zohar H, Israelson A, Abu-Hamad S, Shoshan-Barmatz V (2004) In self-defence: hexokinase promotes voltage-dependent anion channel closure and prevents mitochondria-mediated apoptotic cell death. The Biochemical Journal 377:347-355.

Baba M, Nakajo S, Tu PH, Tomita T, Nakaya K, Lee VM, Trojanowski JQ, Iwatsubo T (1998) Aggregation of alpha-synuclein in Lewy bodies of sporadic Parkinson's disease and dementia with Lewy bodies. The American Journal of Pathology 152:879-884.

Baines CP, Kaiser RA, Sheiko T, Craigen WJ, Molkentin JD (2007) Voltage-dependent anion channels are dispensable for mitochondrial-dependent cell death. Nature Cell Biology 9:550-555.

Baines CP, Kaiser RA, Purcell NH, Blair NS, Osinska H, Hambleton MA, Brunskill EW, Sayen MR, Gottlieb RA, Dorn GW, Robbins J, Molkentin JD (2005) Loss of cyclophilin D reveals a critical role for mitochondrial permeability transition in cell death. Nature 434:658-662.

Balaban RS, Nemoto S, Finkel T (2005) Mitochondria, Oxidants, and Aging. Cell.

Banati RB, Daniel SE, Blunt SB (1998) Glial pathology but absence of apoptotic nigral neurons in long-standing Parkinson's disease. Movement Disorders 13:221-227.

Basso E, Fante L, Fowlkes J, Petronilli V, Forte MA, Bernardi P (2005) Properties of the permeability transition pore in mitochondria devoid of Cyclophilin D. The Journal of Biological Chemistry 280:18558-18561.

Batchelor PE, Liberatore GT, Wong JY, Porritt MJ, Frerichs F, Donnan GA, Howells DW (1999) Activated macrophages and microglia induce dopaminergic sprouting in the injured striatum and express brain-derived neurotrophic factor and glial cell line-derived neurotrophic factor. The Journal of Neuroscience 19:1708-1716.

Bathori G, Csordas G, Garcia-Perez C, Davies E, Hajnoczky G (2006) Ca2+-dependent Control of the Permeability Properties of the Mitochondrial Outer Membrane and

Voltage-dependent Anion-selective Channel (VDAC). Journal of Biological Chemistry 281:17347-17358.

Bayrhuber M, Meins T, Habeck M, Becker S, Giller K, Villinger S, Vonrhein C, Griesinger C, Zweckstetter M, Zeth K (2008) Structure of the human voltage-dependent anion channel. Proceedings Of The National Academy Of Sciences Of The United States Of America 105:15370-15375.

Beal MF (2005) Mitochondria take center stage in aging and neurodegeneration. Annals of Neurology 58:495-505.

Benabid AL, Pollak P, Louveau A, Henry S, de Rougemont J (1987) Combined (thalamotomy and stimulation) stereotactic surgery of the VIM thalamic nucleus for bilateral Parkinson disease. Applied Neurophysiology 50:344-346.

Bennett J, Weeds A (1986) Calcium and the cytoskeleton. British Medical Bulletin 42:385-390.

Benz R (1994) Permeation of hydrophilic solutes through mitochondrial outer membranes: review on mitochondrial porins. Biochimica et Biophysica Acta 1197:167-196.

Benz R, Kottke M, Brdiczka D (1990) The cationically selective state of the mitochondrial outer membrane pore: a study with intact mitochondria and reconstituted mitochondrial porin. Biochimica et Biophysica Acta 1022:311-318.

Benz R, Wojtczak L, Bosch W, Brdiczka D (1988) Inhibition of adenine nucleotide transport through the mitochondrial porin by a synthetic polyanion. FEBS Letters 231:75-80.

Berardelli A, Rothwell JC, Thompson PD, Hallett M (2001) Pathophysiology of bradykinesia in Parkinson's disease. Brain 124:2131-2146.

Berchtold MW, Brinkmeier H, Müntener M (2000) Calcium ion in skeletal muscle: its crucial role for muscle function, plasticity, and disease. Physiological Reviews 80:1215-1265.

Bernardi P (1999) Mitochondrial transport of cations: channels, exchangers, and permeability transition. Physiological Reviews 79:1127-1155.

Bernardi P, Krauskopf A, Basso E, Petronilli V (2006) The mitochondrial permeability transition from in vitro artifact to disease target. FEBS.

Bernheimer H, Birkmayer W, Hornykiewicz O, Jellinger K, Seitelberger F (1973) Brain dopamine and the syndromes of Parkinson and Huntington. Clinical, morphological and neurochemical correlations. Journal of the Neurological Sciences 20:415-455.

Bertina RM, Steenstra JA, Slater EC (1974) The mechanism of inhibition by oligomycin of oxidative phosphorylation in mitochondria. Biochimica et Biophysica Acta 368:279-297.

Betarbet R, Sherer TB, MacKenzie G, Garcia-Osuna M, Panov AV, Greenamyre JT (2000) Chronic systemic pesticide exposure reproduces features of Parkinson's disease. Nature Neuroscience 3:1301-1306.

Blackinton J, Ahmad R, Miller DW, van der Brug MP, Canet-Avilés RM, Hague SM, Kaleem M, Cookson MR (2005) Effects of DJ-1 mutations and polymorphisms on protein stability and subcellular localization. Brain Research Molecular Brain Research 134:76-83.

Blackinton J, Lakshminarasimhan M, Thomas KJ, Ahmad R, Greggio E, Raza AS, Cookson MR, Wilson MA (2009) Formation of a stabilized cysteine sulfinic acid is critical for the mitochondrial function of the parkinsonism protein DJ-1. The Journal of Biological Chemistry 284:6476-6485.

Blonder LX, Slevin JT (2011) Emotional dysfunction in Parkinson's disease. Behavioural Neurology 24:201-217.

Boise LH, González-García M, Postema CE, Ding L, Lindsten T, Turka LA, Mao X, Nuñez G, Thompson CB (1993) bcl-x, a bcl-2-related gene that functions as a dominant regulator of apoptotic cell death. Cell 74:597-608.

Bolaños JP, Almeida A, Moncada S (2010) Glycolysis: a bioenergetic or a survival pathway? Trends in Biochemical Sciences 35:145-149.

Bonifati V (2014) Genetics of Parkinson's disease--state of the art, 2013. Parkinsonism & Related Disorders 20 Suppl 1:S23-28.

Bonifati V, Rizzu P, van Baren MJ, Schaap O, Breedveld GJ, Krieger E, Dekker MCJ, Squitieri F, Ibanez P, Joosse M, van Dongen JW, Vanacore N, van Swieten JC, Brice A, Meco G, van Duijn CM, Oostra BA, Heutink P (2003) Mutations in the DJ-1 gene associated with autosomal recessive early-onset parkinsonism. Science 299:256-259.

Bonifati V et al. (2005) Early-onset parkinsonism associated with PINK1 mutations: frequency, genotypes, and phenotypes. Neurology 65:87-95.

Boustany NN, Drezek R, Thakor NV (2002) Calcium-induced alterations in mitochondrial morphology quantified in situ with optical scatter imaging. Biophysical Journal 83:1691-1700.

Bower JH, Maraganore DM, McDonnell SK, Rocca WA (1999) Incidence and distribution of parkinsonism in Olmsted County, Minnesota, 1976-1990. Neurology 52:1214-1220.

Braak H, Rüb U, Gai WP, Del Tredici K (2003) Idiopathic Parkinson's disease: possible routes by which vulnerable neuronal types may be subject to neuroinvasion by an unknown pathogen. Journal of Neural Transmission 110:517-536.

Braak H, Ghebremedhin E, Rüb U, Bratzke H, Del Tredici K (2004) Stages in the development of Parkinson's disease-related pathology. Cell and Tissue Research 318:121-134.

Braak H, Del Tredici K, Bratzke H, Hamm-Clement J, Sandmann-Keil D, Rüb U (2002) Staging of the intracerebral inclusion body pathology associated with idiopathic Parkinson's disease (preclinical and clinical stages). Journal of Neurology 249 Suppl 3:1-5.

Bras J, Guerreiro R, Hardy J (2015) SnapShot: Genetics of Parkinson's Disease. Cell 160:570-570.e571.

Butow RA, Avadhani NG (2004) Mitochondrial Signaling: The Retrograde Response. Molecular Cell.

Calì T, Ottolini D, Soriano ME, Brini M (2014) A new split-GFP based probe reveals DJ-1 translocation into the mitochondrial matrix to sustain ATP synthesis upon nutrient deprivation. Human Molecular Genetics.

Canet-Avilés RM, Wilson MA, Miller DW, Ahmad R, McLendon C, Bandyopadhyay S, Baptista MJ, Ringe D, Petsko GA, Cookson MR (2004) The Parkinson's disease protein DJ-1 is neuroprotective due to cysteine-sulfinic acid-driven mitochondrial

localization. Proceedings Of The National Academy Of Sciences Of The United States Of America 101:9103-9108.

Cash R, Dennis T, L'Heureux R, Raisman R, Javoy-Agid F, Scatton B (1987) Parkinson's disease and dementia: norepinephrine and dopamine in locus ceruleus. Neurology 37:42-46.

Cenci MA (2007) Dopamine dysregulation of movement control in L-DOPA-induced dyskinesia. Trends in Neurosciences 30:236-243.

Chan CS, Gertler TS, Surmeier DJ (2010) A molecular basis for the increased vulnerability of substantia nigra dopamine neurons in aging and Parkinson's disease. Movement Disorders 25 Suppl 1:S63-70.

Chan CS, Guzman JN, Ilijic E, Mercer JN, Rick C, Tkatch T, Meredith GE, Surmeier DJ (2007) 'Rejuvenation' protects neurons in mouse models of Parkinson's disease. Nature 447:1081-1086.

Chan-Palay V, Asan E (1989) Alterations in catecholamine neurons of the locus coeruleus in senile dementia of the Alzheimer type and in Parkinson's disease with and without dementia and depression. The Journal of Comparative Neurology 287:373-392.

Chartier-Harlin M-C, Kachergus J, Roumier C, Mouroux V, Douay X, Lincoln S, Levecque C, Larvor L, Andrieux J, Hulihan M, Waucquier N, Defebvre L, Amouyel P, Farrer M, Destée A (2004) Alpha-synuclein locus duplication as a cause of familial Parkinson's disease. Lancet 364:1167-1169.

Chase TN (1998) Levodopa therapy: consequences of the nonphysiologic replacement of dopamine. Neurology 50:S17-25.

Chaudhuri KR, Naidu Y (2008) Early Parkinson's disease and non-motor issues. Journal of Neurology.

Chen AI, de Nooij JC, Jessell TM (2006) Graded activity of transcription factor Runx3 specifies the laminar termination pattern of sensory axons in the developing spinal cord. Neuron 49:395-408.

Chen H, Chan DC (2004) Mitochondrial dynamics in mammals. Current Topics in Developmental Biology 59:119-144.

Chen H, Chan D (2006) Critical dependence of neurons on mitochondrial dynamics. Current Opinion in Cell Biology 18:453-459.

Chen H, Chan DC (2009) Mitochondrial dynamics-fusion, fission, movement, and mitophagy-in neurodegenerative diseases. Human Molecular Genetics 18:R169-R176.

Chinta SJ, Andersen JK (2008) Redox imbalance in Parkinson's disease. Biochimica et Biophysica Acta 1780:1362-1367.

Choi J, Sullards MC, Olzmann JA, Rees HD, Weintraub ST, Bostwick DE, Gearing M, Levey AI, Chin L-S, Li L (2006) Oxidative damage of DJ-1 is linked to sporadic Parkinson and Alzheimer diseases. The Journal of Biological Chemistry 281:10816-10824.

Choi W-S, Kruse SE, Palmiter RD, Xia Z (2008) Mitochondrial complex I inhibition is not required for dopaminergic neuron death induced by rotenone, MPP+, or paraquat. Proceedings of the National Academy of Sciences 105:15136-15141.

Clapham DE (2007) Calcium signaling. Cell 131:1047-1058.

Clark LN, Afridi S, Mejia-Santana H, Harris J, Louis ED, Cote LJ, Andrews H, Singleton A, Wavrant De-Vrieze F, Hardy J, Mayeux R, Fahn S, Waters C, Ford B, Frucht S, Ottman R, Marder K (2004) Analysis of an early-onset Parkinson's disease cohort for DJ-1 mutations. Movement Disorders 19:796-800.

Clements CM, McNally RS, Conti BJ, Mak TW, Ting JPY (2006) DJ-1, a cancer- and Parkinson's disease-associated protein, stabilizes the antioxidant transcriptional master regulator Nrf2. Proceedings of the National Academy of Sciences 103:15091-15096.

Colombini M (1980) Structure and mode of action of a voltage dependent anion-selective channel (VDAC) located in the outer mitochondrial membrane. Annals of the New York Academy of Sciences 341:552-563.

Colombini M (1987) Characterization of channels isolated from plant mitochondria. Methods in Enzymology 148:465-475.

Connolly BS, Lang AE (2014) Pharmacological treatment of Parkinson disease: a review. JAMA 311:1670-1683.

Cooper IS (1956) Neurosurgical alleviation of parkinsonism. Bulletin of the New York Academy of Medicine 32:713.

Crompton M (1999) The mitochondrial permeability transition pore and its role in cell death. The Biochemical Journal 341 (Pt 2):233-249.

Csordás G, Renken C, Várnai P, Walter L, Weaver D, Buttle KF, Balla T, Mannella CA, Hajnóczky G (2006) Structural and functional features and significance of the physical linkage between ER and mitochondria. The Journal of Cell Biology 174:915-921.

Dagda RK, Cherra SJ, Kulich SM, Tandon A, Park D, Chu CT (2009) Loss of PINK1 function promotes mitophagy through effects on oxidative stress and mitochondrial fission. Journal of Biological Chemistry 284:13843-13855.

Dauer W, Przedborski S (2003) Parkinson's disease: mechanisms and models. Neuron 39:889-909.

Davis GC, Williams AC, Markey SP, Ebert MH, Caine ED, Reichert CM, Kopin IJ (1979) Chronic Parkinsonism secondary to intravenous injection of meperidine analogues. Psychiatry Research 1:249-254.

de Lau LML, Breteler MMB (2006) Epidemiology of Parkinson's disease. Lancet Neurology 5:525-535.

de Rijk MC, Breteler MM, Graveland GA, Ott A, Grobbee DE, van der Meché FG, Hofman A (1995) Prevalence of Parkinson's disease in the elderly: the Rotterdam Study. Neurology 45:2143-2146.

Detmer SA, Chan DC (2007) Functions and dysfunctions of mitochondrial dynamics. Nature Reviews Molecular Cell Biology 8:870-879.

Dexter D, Carter C, Wells F, Javoyagid F, Agid Y, Lees A, Jenner P, Marsden C (1989) Basal lipid-peroxidation in substantia nigra is inreased in Parkinson's disease. Journal of Neurochemistry 52:381-389.

Dick FD, De Palma G, Ahmadi A, Scott NW, Prescott GJ, Bennett J, Semple S, Dick S, Counsell C, Mozzoni P, Haites N, Wettinger SB, Mutti A, Otelea M, Seaton A, Söderkvist P, Felice A, group Gs (2007) Environmental risk factors for Parkinson's disease and parkinsonism: the Geoparkinson study. Occupational and Environmental Medicine 64:666-672.

Ding W-X, Ni H-M, Li M, Liao Y, Chen X, Stolz DB, Dorn Ii GW, Yin X-M (2010) Nix is critical to two distinct phases of mitophagy: reactive oxygen species (ROS)-mediated autophagy induction and Parkin-ubiqutin-p62-mediated mitochondria priming. Journal of Biological Chemistry:1-31.

Disease MDSTFoRSfPas (2003) The Unified Parkinson's Disease Rating Scale (UPDRS): status and recommendations. Movement Disorders 18:738-750.

Doty RL, Deems DA, Stellar S (1988) Olfactory dysfunction in parkinsonism: a general deficit unrelated to neurologic signs, disease stage, or disease duration. Neurology 38:1237-1244.

Duchen MR (1999) Contributions of mitochondria to animal physiology: from homeostatic sensor to calcium signalling and cell death. The Journal of Physiology 516 (Pt 1):1-17.

Duchen MR (2004) Mitochondria and calcium: from cell signalling to cell death. The Journal of Physiology 529:57-68.

Dymecki J, Lechowicz W, Bertrand E, Szpak GM (1996) Changes in dopaminergic neurons of the mesocorticolimbic system in Parkinson's disease. Folia Neuropathologica 34:102-106.

Edvardson S, Cinnamon Y, Ta-Shma A, Shaag A, Yim Y-I, Zenvirt S, Jalas C, Lesage S, Brice A, Taraboulos A, Kaestner KH, Greene LE, Elpeleg O (2012) A deleterious mutation in DNAJC6 encoding the neuronal-specific clathrin-uncoating co-chaperone auxilin, is associated with juvenile parkinsonism. PLoS ONE 7:e36458.

Edwards LL, Pfeiffer RF, Quigley E (1991) Gastrointestinal symptoms in Parkinson's disease. Movement Disorders 6:151-156.

Ekert PG, Vaux DL (2005) The mitochondrial death squad: hardened killers or innocent bystanders? Current Opinion in Cell Biology 17:626-630.

Ekstrand MI, Galter D (2009) The MitoPark Mouse - an animal model of Parkinson's disease with impaired respiratory chain function in dopamine neurons. Parkinsonism & Related Disorders 15 Suppl 3:S185-188.

Esposito LA, Melov S, Panov A, Cottrell BA, Wallace DC (1999) Mitochondrial disease in mouse results in increased oxidative stress. Proceedings Of The National Academy Of Sciences Of The United States Of America 96:4820-4825.

Fan J, Yu H, Lv Y, Yin L (2015) Diagnostic and prognostic value of serum thioredoxin and DJ-1 in non-small cell lung carcinoma patients. Tumour Biology.

Fearnley JM, Lees AJ (1991) Ageing and Parkinson's disease: substantia nigra regional selectivity. Brain 114 (Pt 5):2283-2301.

Feng Y, Jankovic J, Wu Y-C (2014) Epigenetic mechanisms in Parkinson's disease. Journal of the Neurological Sciences.

Finsterer J (2008) Leigh and Leigh-like syndrome in children and adults. Pediatric Neurology 39:223-235.

Fischer F, Hamann A, Osiewacz HD (2012) Mitochondrial quality control: an integrated network of pathways. Trends in Biochemical Sciences 37:284-292.

Fiskum G, Starkov A, Polster BM, Chinopoulos C (2003) Mitochondrial mechanisms of neural cell death and neuroprotective interventions in Parkinson's disease. Annals of the New York Academy of Sciences 991:111-119.

Foix C, Nicolesco J (1925) Anatomie cérébrale: les noyaux gris centraux et la région mésencéphalo-sous-optique. Journal of the American Medical Association 87:1148.

Forno LS (1996) Neuropathology of Parkinson's disease. Journal of Neuropathology and Experimental Neurology 55:259-272.

Friel DD (2000) Mitochondria as regulators of stimulus-evoked calcium signals in neurons. Cell Calcium 28:307-316.

Fuchs J, Nilsson C, Kachergus J, Munz M, Larsson E-M, Schüle B, Langston JW, Middleton FA, Ross OA, Hulihan M, Gasser T, Farrer MJ (2007) Phenotypic variation in a large Swedish pedigree due to SNCA duplication and triplication. Neurology 68:916-922.

Gagnon J-F, Postuma RB, Mazza S, Doyon J, Montplaisir J (2006) Rapid-eye-movement sleep behaviour disorder and neurodegenerative diseases. The Lancet Neurology 5:424-432.

García-Lorenzo D, Longo-Dos Santos C, Ewenczyk C, Leu-Semenescu S, Gallea C, Quattrocchi G, Pita Lobo P, Poupon C, Benali H, Arnulf I, Vidailhet M, Lehéricy S (2013) The coeruleus/subcoeruleus complex in rapid eye movement sleep behaviour disorders in Parkinson's disease. Brain 136:2120-2129.

Gaspar P, Gray F (1984) Dementia in idiopathic Parkinson's disease. Acta Neuropathologica 64:43-52.

Gegg ME, Cooper JM, Chau K-Y, Rojo M, Schapira AHV, Taanman J-W (2010) Mitofusin 1 and mitofusin 2 are ubiquitinated in a PINK1/parkin-dependent manner upon induction of mitophagy. Human Molecular Genetics 19:4861-4870.

Geisler S, Holmström KM, Skujat D, Fiesel FC, Rothfuss OC, Kahle PJ, Springer W (2010) PINK1/Parkin-mediated mitophagy is dependent on VDAC1 and p62/SQSTM1. Nature Cell Biology 12:119-131.

Gellerich FN, Wagner M, Kapischke M, Wicker U, Brdiczka D (1993) Effect of macromolecules on the regulation of the mitochondrial outer membrane pore and the activity of adenylate kinase in the inter-membrane space. Biochimica et Biophysica Acta 1142:217-227.

German DC, Manaye K, Smith WK, Woodward DJ, Saper CB (1989) Midbrain dopaminergic cell loss in Parkinson's disease: computer visualization. Annals of Neurology 26:507-514.

German DC, Manaye KF, White CL, Woodward DJ, McIntire DD, Smith WK, Kalaria RN, Mann DM (1992) Disease-specific patterns of locus coeruleus cell loss. Annals of Neurology 32:667-676.

Giaime E, Yamaguchi H, Gautier CA, Kitada T, Shen J (2012) Loss of DJ-1 does not affect mitochondrial respiration but increases ROS production and mitochondrial permeability transition pore opening. PLoS ONE 7:e40501.

Gincel D, Zaid H, Shoshan-Barmatz V (2001) Calcium binding and translocation by the voltage-dependent anion channel: a possible regulatory mechanism in mitochondrial function. The Biochemical journal 358:147-155.

Goetz CG, Poewe W, Rascol O, Sampaio C (2005) Evidence-based medical review update: pharmacological and surgical treatments of Parkinson's disease: 2001 to 2004. Movement Disorders 20:523-539.

Goker-Alpan O, Schiffmann R, LaMarca ME, Nussbaum RL, McInerney-Leo A, Sidransky E (2004) Parkinsonism among Gaucher disease carriers. Journal of Medical Genetics 41:937-940.

Gorell JM, Johnson CC, Rybicki BA, Peterson EL, Richardson RJ (1998) The risk of Parkinson's disease with exposure to pesticides, farming, well water, and rural living. Neurology 50:1346-1350.

Görner K, Holtorf E, Waak J, Pham T-T, Vogt-Weisenhorn DM, Wurst W, Haass C, Kahle PJ (2007) Structural determinants of the C-terminal helix-kink-helix motif essential for protein stability and survival promoting activity of DJ-1. The Journal of Biological Chemistry 282:13680-13691.

Gray MW, Burger G, Lang BF (1999) Mitochondrial evolution. Science 283:1476-1481.

Gray MW, Burger G, Lang BF (2001) The origin and early evolution of mitochondria. Genome Biology 2:REVIEWS1018.

Green DR, Reed JC (1998) Mitochondria and apoptosis. Science 281:1309-1312.

Green DR, Kromer G (2004) The pathophysiology of mitochondrial cell death. Science 305:626-629.

Greenamyre JT, MacKenzie G, Peng TI, Stephans SE (1999) Mitochondrial dysfunction in Parkinson's disease. Biochemical Society Symposium 66:85-97.

Greenfield JG, Bosanquet FD (1953) The brain-stem lesions in Parkinsonism. Journal of Neurology, Neurosurgery, and Psychiatry 16:213-226.

Greffard S, Verny M, Bonnet A-M, Beinis J-Y, Gallinari C, Meaume S, Piette F, Hauw J-J, Duyckaerts C (2006) Motor score of the Unified Parkinson Disease Rating

Scale as a good predictor of Lewy body-associated neuronal loss in the substantia nigra. Archives of Neurology 63:584-588.

Grenier K, McLelland G-L, Fon EA (2013) Parkin- and PINK1-Dependent Mitophagy in Neurons: Will the Real Pathway Please Stand Up? Frontiers in Neurology 4:100.

Guzman JN, Sanchez-Padilla J, Wokosin D, Kondapalli J, Ilijic E, Schumacker PT, Surmeier DJ (2010) Oxidant stress evoked by pacemaking in dopaminergic neurons is attenuated by DJ-1. Nature.

Haehner A, Hummel T, Reichmann H (2011) Olfactory loss in Parkinson's disease. Parkinson's Disease 2011:450939.

Halestrap AP, Davidson AM (1990) Inhibition of Ca2(+)-induced large-amplitude swelling of liver and heart mitochondria by cyclosporin is probably caused by the inhibitor binding to mitochondrial-matrix peptidyl-prolyl cis-trans isomerase and preventing it interacting with the adenine nucleotide translocase. The Biochemical Journal 268:153-160.

Halliwell B, Whiteman M (2004) Measuring reactive species and oxidative damage in vivo and in cell culture: how should you do it and what do the results mean? British Journal of Pharmacology 142:231-255.

Hanisch U-K, Kettenmann H (2007) Microglia: active sensor and versatile effector cells in the normal and pathologic brain. Nature Neuroscience 10:1387-1394.

Hao L-Y, Giasson BI, Bonini NM (2010) DJ-1 is critical for mitochondrial function and rescues PINK1 loss of function. Proceedings Of The National Academy Of Sciences Of The United States Of America 107:9747-9752.

Haque ME, Thomas KJ, D'Souza C, Callaghan S, Kitada T, Slack RS, Fraser P, Cookson MR, Tandon A, Park DS (2008) Cytoplasmic Pink1 activity protects neurons from dopaminergic neurotoxin MPTP. Proceedings Of The National Academy Of Sciences Of The United States Of America 105:1716-1721.

Hardy J (2010) Genetic analysis of pathways to Parkinson disease. Neuron 68:201-206.

Haworth RA, Hunter DR (1979) The Ca2+-induced membrane transition in mitochondria. Archives of Biochemistry and Biophysics 195:460-467.

Hayashi T, Ishimori C, Takahashi-Niki K, Taira T, Kim Y-C, Maita H, Maita C, Ariga H, Iguchi-Ariga SM (2009) DJ-1 binds to mitochondrial complex I and maintains its activity. Biochemical and Biophysical Research Communications:6.

Healy DG et al. (2008) Phenotype, genotype, and worldwide genetic penetrance of LRRK2-associated Parkinson's disease: a case-control study. The Lancet Neurology 7:583-590.

Heikkila R, Hess A, Duvoisin R (1984) Dopaminergic neurotoxicity of 1-methyl-4-phenyl-1,2,5,6-tetradyropyridine in mice. Science 224:1451-1453.

Heikkila RE, Nicklas WJ, Vyas I, Duvoisin RC (1985) Dopaminergic toxicity of rotenone and the 1-methyl-4-phenylpyridinium ion after their stereotaxic administration to rats: implication for the mechanism of 1-methyl-4-phenyl-1,2,3,6-tetrahydropyridine toxicity. Neuroscience Letters 62:389-394.

Heneka MT, Kummer MP, Latz E (2014) Innate immune activation in neurodegenerative disease. Nature Reviews Immunology 14:463-477.

Heo JY, Park JH, Kim SJ, Seo KS, Han JS, Lee SH, Kim JM, Park JI, Park SK, Lim K, Hwang BD, Shong M, Kweon GR (2012) DJ-1 null dopaminergic neuronal cells

exhibit defects in mitochondrial function and structure: Involvement of mitochondrial complex I assembly. PLoS ONE 7:e32629.

Hering R, Strauss KM, Tao X, Bauer A, Woitalla D, Mietz E-M, Petrovic S, Bauer P, Schaible W, Müller T, Schöls L, Klein C, Berg D, Meyer PT, Schulz JB, Wollnik B, Tong L, Krüger R, Riess O (2004) Novel homozygous p.E64D mutation in DJ1 in early onset Parkinson disease (PARK7). Human Mutation 24:321-329.

Hernán MA, Takkouche B, Caamaño-Isorna F, Gestal-Otero JJ (2002) A meta-analysis of coffee drinking, cigarette smoking, and the risk of Parkinson's disease. Annals of Neurology 52:276-284.

Herrera AJ, Castaño A, Venero JL, Cano J, Machado A (2000) The single intranigral injection of LPS as a new model for studying the selective effects of inflammatory reactions on dopaminergic system. Neurobiology of Disease 7:429-447.

Hilker R, Schweitzer K, Coburger S, Ghaemi M, Weisenbach S, Jacobs AH, Rudolf J, Herholz K, Heiss W-D (2005) Nonlinear progression of Parkinson disease as determined by serial positron emission tomographic imaging of striatal fluorodopa F 18 activity. Archives of Neurology 62:378-382.

Hiller S, Garces RG, Malia TJ, Orekhov VY, Colombini M, Wagner G (2008) Solution structure of the integral human membrane protein VDAC-1 in detergent micelles. Science 321:1206-1210.

Hod Y, Pentyala S, Whyard T, El-Maghrabi M (1999) Identification and characterization of a novel protein that regulates RNA-protein interaction. Journal Of Cellular Biochemistry 72:435-444.

Hoehn MM, Yahr MD (1967) Parkinsonism: onset, progression and mortality. Neurology 17:427-442.

Holdorff B (2002) Friedrich Heinrich Lewy (1885-1950) and his work.

Honbou K, Suzuki NN, Horiuchi M, Niki T, Taira T, Ariga H, Inagaki F (2003) The crystal structure of DJ-1, a protein related to male fertility and Parkinson's disease. The Journal of Biological Chemistry 278:31380-31384.

Hoozemans JJM, van Haastert ES, Eikelenboom P, de Vos RAI, Rozemuller JM, Scheper W (2007) Activation of the unfolded protein response in Parkinson's disease. Biochemical and Biophysical Research Communications 354:707-711.

Hruska KS, LaMarca ME, Scott CR, Sidransky E (2008) Gaucher disease: mutation and polymorphism spectrum in the glucocerebrosidase gene (GBA). Human Mutation 29:567-583.

Huai Q (2003) Crystal structure of DJ-1/RS and implication on familial Parkinson's disease. FEBS Letters 549:171-175.

Huang H, Hu X, Eno CO, Zhao G, Li C, White C (2013) An interaction between Bcl-xL and the voltage-dependent anion channel (VDAC) promotes mitochondrial Ca2+ uptake. Journal of Biological Chemistry 288:19870-19881.

Hughes AJ, Daniel SE, Blankson S, Lees AJ (1993) A clinicopathologic study of 100 cases of Parkinson's disease. Archives of Neurology 50:140-148.

Hughes AJ, Daniel SE, Ben-Shlomo Y, Lees AJ (2002) The accuracy of diagnosis of parkinsonian syndromes in a specialist movement disorder service. Brain 125:861-870.

Hunot S, Dugas N, Faucheux B, Hartmann A, Tardieu M, Debré P, AGID Y, Dugas B, Hirsch EC (1999) FcepsilonRII/CD23 is expressed in Parkinson's disease and induces, in vitro, production of nitric oxide and tumor necrosis factor-alpha in glial cells. The Journal of Neuroscience 19:3440-3447.

Hunter DR, Haworth RA (1979) The Ca2+-induced membrane transition in mitochondria. III. Transitional Ca2+ release. Archives of Biochemistry and Biophysics 195:468-477.

Ibáñez P, Bonnet A-M, Débarges B, Lohmann E, Tison F, Pollak P, AGID Y, Dürr A, Brice A (2004) Causal relation between alpha-synuclein gene duplication and familial Parkinson's disease. Lancet 364:1169-1171.

Ibáñez P, Lesage S, Janin S, Lohmann E, Durif F, Destée A, Bonnet A-M, Brefel-Courbon C, Heath S, Zelenika D, Agid Y, Durr A, Brice A, Group FPsDGS (2009) Alpha-synuclein gene rearrangements in dominantly inherited parkinsonism: frequency, phenotype, and mechanisms. Archives of Neurology 66:102-108.

Ibsen KH (1961) The Crabtree Effect: A Review. 21:829-841.

Imai Y, Soda M, Takahashi R (2000) Parkin suppresses unfolded protein stress-induced cell death through its E3 ubiquitin-protein ligase activity. The Journal of Biological Chemistry 275:35661-35664.

Imamura K, Hishikawa N, Sawada M, Nagatsu T, Yoshida M, Hashizume Y (2003) Distribution of major histocompatibility complex class II-positive microglia and cytokine profile of Parkinson's disease brains. Acta Neuropathologica 106:518-526.

Irrcher I et al. (2010) Loss of the Parkinson's Disease-linked gene DJ-1 perturbs mitochondrial dynamics. Human Molecular Genetics.

Ishikawa S, Ishikawa S, Taira T, Taira T, Takahashi-Niki K, Takahashi-Niki K, Niki T, Niki T, Ariga H, Ariga H, Iguchi-Ariga SMM, Iguchi-Ariga SMM (2010) Human DJ-1-specific transcriptional activation of tyrosine hydroxylase gene. Journal of Biological Chemistry 285:39718-39731.

Itier J-M et al. (2003) Parkin gene inactivation alters behaviour and dopamine neurotransmission in the mouse. Human Molecular Genetics 12:2277-2291.

Jakovcevski M, Akbarian S (2012) Epigenetic mechanisms in neurological disease. Nature Medicine 18:1194-1204.

Jankovic J (2005) Motor fluctuations and dyskinesias in Parkinson's disease: Clinical manifestations. Movement Disorders 20:S11-S16.

Jankovic J (2008) Parkinson's disease: clinical features and diagnosis. Journal of Neurology, Neurosurgery, and Psychiatry 79:368-376.

Jenner P (2001) Parkinson's disease, pesticides and mitochondrial dysfunction. Trends in Neurosciences 24:245-247.

Jenner P (2008) Molecular mechanisms of L-DOPA-induced dyskinesia. Nature Reviews Neuroscience 9:665-677.

Jeong H, Kim M-S, Kwon J, Kim KS, Seol W (2006) Regulation of the transcriptional activity of the tyrosine hydroxylase gene by androgen receptor. Neuroscience letters 396:57-61.

Joselin AP, Hewitt SJ, Callaghan SM, Kim RH, Chung Y-H, Mak TW, Shen J, Slack RS, Park DS (2012) ROS-dependent regulation of Parkin and DJ-1 localization during oxidative stress in neurons. Human Molecular Genetics.

Jouaville LS, Pinton P, Bastianutto C, Rutter GA, Rizzuto R (1999) Regulation of mitochondrial ATP synthesis by calcium: evidence for a long-term metabolic priming. Proceedings Of The National Academy Of Sciences Of The United States Of America 96:13807-13812.

Junn E, Jang WH, Zhao X, Jeong BS, Mouradian MM (2009) Mitochondrial localization of DJ-1 leads to enhanced neuroprotection. Journal of Neuroscience Research 87:123-129.

Junn E, Taniguchi H, Jeong BS, Zhao X, Ichijo H, Mouradian MM (2005) Interaction of DJ-1 with Daxx inhibits apoptosis signal-regulating kinase 1 activity and cell death. Proceedings Of The National Academy Of Sciences Of The United States Of America 102:9691-9696.

Kang S, Cooper G, Dunne SF, Dusel B, Luan C-H, Surmeier DJ, Silverman RB (2012) CaV1.3-selective L-type calcium channel antagonists as potential new therapeutics for Parkinson's disease. Nature Communications 3:1146.

Kaufman RJ (1999) Stress signaling from the lumen of the endoplasmic reticulum: coordination of gene transcriptional and translational controls. Genes & Development 13:1211-1233.

Khacho M, Tarabay M, Patten D, Khacho P, MacLaurin JG, Guadagno J, Bergeron R, Cregan SP, Harper M-E, Park DS, Slack RS (2014) Acidosis overrides oxygen

deprivation to maintain mitochondrial function and cell survival. Nature Communications 5:1-15.

Kim RH, Smith PD, Aleyasin H, Hayley S, Mount MP, Pownall S, Wakeham A, You-Ten AJ, Kalia SK, Horne P, Westaway D, Lozano AM, Anisman H, Park DS, Mak TW (2005a) Hypersensitivity of DJ-1-deficient mice to 1-methyl-4-phenyl-1,2,3,6-tetrahydropyrindine (MPTP) and oxidative stress. Proceedings Of The National Academy Of Sciences Of The United States Of America 102:5215-5220.

Kim RH, Peters M, Jang Y, Shi W, Pintilie M, Fletcher GC, DeLuca C, Liepa J, Zhou L, Snow B, Binari RC, Manoukian AS, Bray MR, Liu F-F, Tsao M-S, Mak TW (2005b) DJ-1, a novel regulator of the tumor suppressor PTEN. Cancer Cell 7:263-273.

Kim Y, Park J, Kim S, Song S, Kwon SK, Lee SH, Kitada T, Kim JM, Chung J (2008) PINK1 controls mitochondrial localization of Parkin through direct phosphorylation. Biochem Biophys Research Communications 377:975-980.

Kitada T, Asakawa S, Hattori N, Matsumine H, Yamamura Y, Minoshima S, Yokochi M, Mizuno Y, Shimizu N (1998) Mutations in the parkin gene cause autosomal recessive juvenile parkinsonism. Nature 392:605-608.

Kitada T, Pisani A, Porter DR, Yamaguchi H, Tscherter A, Martella G, Bonsi P, Zhang C, Pothos EN, Shen J (2007) Impaired dopamine release and synaptic plasticity in the striatum of PINK1-deficient mice. Proceedings Of The National Academy Of Sciences Of The United States Of America 104:11441-11446.

Klein C, Lohmann-Hedrich K (2007) Impact of recent genetic findings in Parkinson's disease. Current Opinion in Neurology 20:453-464.

Klein C, Westenberger A (2012) Genetics of Parkinson's disease. Cold Spring Harbor Perspectives in Medicine 2:a008888.

Klionsky DJ et al. (2008) Guidelines for the use and interpretation of assays for monitoring autophagy in higher eukaryotes. Autophagy 4:151-175.

Kluck RM, Esposti MD, Perkins G, Renken C, Kuwana T, Bossy-Wetzel E, Goldberg M, Allen T, Barber MJ, Green DR, Newmeyer DD (1999) The pro-apoptotic proteins, Bid and Bax, cause a limited permeabilization of the mitochondrial outer membrane that is enhanced by cytosol. The Journal of Cell Biology 147:809-822.

Kokoszka JE, Waymire KG, Levy SE, Sligh JE, Cai J, Jones DP, MacGregor GR, Wallace DC (2004) The ADP/ATP translocator is not essential for the mitochondrial permeability transition pore. Nature 427:461-465.

Koller WC, Glatt S, Vetere-Overfield B, Hassanein R (1989) Falls and Parkinson's disease. Clinical Neuropharmacology 12:98-105.

Kordower JH, Chu Y, Hauser RA, Freeman TB, Olanow CW (2008) Lewy body-like pathology in long-term embryonic nigral transplants in Parkinson's disease. Nature Medicine 14:504-506.

Kostyuk PG (2007) Key role of calcium signaling in synaptic transmission. Neurophysiology 39:248-250.

Krauskopf A, Eriksson O, Craigen WJ, Forte MA, Bernardi P (2006) Properties of the permeability transition in VDAC1(-/-) mitochondria. Biochimica et Biophysica Acta 1757:590-595.

Krebiehl G, Ruckerbauer S, Burbulla LF, Kieper N, Maurer B, Waak J, Wolburg H, Gizatullina Z, Gellerich FN, Woitalla D, Riess O, Kahle PJ, Proikas-Cezanne T,

Krüger R (2010) Reduced basal autophagy and impaired mitochondrial dynamics due to loss of Parkinson's disease-associated protein DJ-1. PLoS ONE 5:e9367.

Krebs CE, Karkheiran S, Powell JC, Cao M, Makarov V, Darvish H, Di Paolo G, Walker RH, Shahidi G-A, Buxbaum JD, De Camilli P, Yue Z, Paisán-Ruíz C (2013) The Sac1 domain of SYNJ1 identified mutated in a family with early-onset progressive Parkinsonism with generalized seizures. Human Mutation 34:1200-1207.

Kringelbach ML, Jenkinson N, Owen SLF, Aziz TZ (2007) Translational principles of deep brain stimulation. Nature Reviews Neuroscience 8:623-635.

Krüger R, Kuhn W, Müller T, Woitalla D, Graeber M, Kösel S, Przuntek H, Epplen JT, Schöls L, Riess O (1998) Ala30Pro mutation in the gene encoding alpha-synuclein in Parkinson's disease. Nature Publishing Group 18:106-108.

Kuwana T, Mackey MR, Perkins G, Ellisman MH, Latterich M, Schneiter R, Green DR, Newmeyer DD (2002) Bid, Bax, and lipids cooperate to form supramolecular openings in the outer mitochondrial membrane. Cell 111:331-342.

Lackner LL (2014) Shaping the dynamic mitochondrial network. BMC Biology 12:35.

Lang AE, Lozano AM (1998) Parkinson's disease. First of two parts. The New England Journal of Medicine 339:1044-1053.

Lang AE, Lees A (2002) Management of Parkinson's disease: an evidence-based review. Movement Disorders 17:S1-S166.

Langston J, Ballard P, Tetrud J, Irwin I (1983) Chronic parkinsonism in humans due to a product of meperidine-analog syntehsis. Science 219:979-980.

Larsson NG, Wang J, Wilhelmsson H, Oldfors A, Rustin P, Lewandoski M, Barsh GS, Clayton DA (1998) Mitochondrial transcription factor A is necessary for mtDNA maintenance and embryogenesis in mice. Nature Genetics 18:231-236.

Le Naour F, Misek DE, Krause MC, Deneux L, Giordano TJ, Scholl S, Hanash SM (2001) Proteomics-based identification of RS/DJ-1 as a novel circulating tumor antigen in breast cancer. Clinical Cancer Research 7:3328-3335.

Lee AC, Zizi M, Colombini M (1994) Beta-NADH decreases the permeability of the mitochondrial outer membrane to ADP by a factor of 6. The Journal of Biological Chemistry 269:30974-30980.

Lesage S, Durr A, Tazir M, Lohmann E, Leutenegger A-L, Janin S, Pollak P, Brice A, Group FPsDGS (2006) LRRK2 G2019S as a cause of Parkinson's disease in North African Arabs. The New England Journal of Medicine 354:422-423.

Li HM, Niki T, Taira T, Iguchi-Ariga SMM, Ariga H (2005) Association of DJ-1 with chaperones and enhanced association and colocalization with mitochondrial Hsp70 by oxidative stress. Free Radical Research 39:1091-1099.

Li P, Nijhawan D, Budihardjo I, Srinivasula SM, Ahmad M, Alnemri ES, Wang X (1997) Cytochrome c and dATP-Dependent Formation of Apaf-1/Caspase-9 Complex Initiates an Apoptotic Protease Cascade. Cell 91:479-489.

Lin MT, Beal MF (2006) Mitochondrial dysfunction and oxidative stress in neurodegenerative diseases. Nature 443:787-795.

Lin T-K, Liou C-W, Chen S-D, Chuang Y-C, Tiao M-M, Wang P-W, Chen J-B, Chuang J-H (2009) Mitochondrial dysfunction and biogenesis in the pathogenesis of Parkinson's disease. Chang Gung Medical Journal 32:589-599.

Lindén M, Gellerfors P (1983) Hydrodynamic properties of porin isolated from outer membranes of rat liver mitochondria. Biochimica et Biophysica Acta 736:125-129.

Lira A, Kulczycki J, Slack R, Anisman H, Park DS (2011) Involvement of the Fc gamma receptor in a chronic N-methyl-4-phenyl-1,2,3,6-tetrahydropyridine mouse model of dopaminergic loss. The Journal of Biological Chemistry 286:28783-28793.

Liu MY, Colombini M (1992) Regulation of mitochondrial respiration by controlling the permeability of the outer membrane through the mitochondrial channel, VDAC. Biochimica et Biophysica Acta 1098:255-260.

Liu S, Lu B (2010) Reduction of protein translation and activation of autophagy protect against PINK1 pathogenesis in Drosophila melanogaster. PLoS Genetics 6:e1001237.

Lohmann E et al. (2003) How much phenotypic variation can be attributed to parkin genotype? Annals of Neurology 54:176-185.

Lücking CB et al. (2000) Association between early-pnset Parkinson's disease and mutations in the Parkin gene. The New England Journal of Medicine 342:1560-1567.

Ludwig O, De Pinto V, Palmieri F, Benz R (1986) Pore formation by the mitochondrial porin of rat brain in lipid bilayer membranes. Biochimica et Biophysica Acta 860:268-276.

Luk KC, Kehm V, Carroll J, Zhang B, O'Brien P, Trojanowski JQ, Lee VM-Y (2012) Pathological α-synuclein transmission initiates Parkinson-like neurodegeneration in nontransgenic mice. Science 338:949-953.

Lwin A, Orvisky E, Goker-Alpan O, LaMarca ME, Sidransky E (2004) Glucocerebrosidase mutations in subjects with parkinsonism. Molecular Genetics and Metabolism 81:70-73.

Macedo MG, Anar B, Bronner IF, Cannella M, Squitieri F, Bonifati V, Hoogeveen A, Heutink P, Rizzu P (2003) The DJ-1L166P mutant protein associated with early onset Parkinson's disease is unstable and forms higher-order protein complexes. Human Molecular Genetics 12:2807-2816.

Maita C, Maita H, Iguchi-Ariga SMM, Ariga H (2013) Monomer DJ-1 and its N-terminal sequence are necessary for mitochondrial localization of DJ-1 mutants. PLoS ONE 8:e54087.

Manning-Boğ AB, Caudle WM, Perez XA, Reaney SH, Paletzki R, Isla MZ, Chou VP, McCormack AL, Miller GW, Langston JW, Gerfen CR, Dimonte DA (2007) Increased vulnerability of nigrostriatal terminals in DJ-1-deficient mice is mediated by the dopamine transporter. Neurobiology of Disease 27:141-150.

Marder K, Tang MX, Cote L, Stern Y, Mayeux R (1995) The frequency and associated risk factors for dementia in patients with Parkinson's disease. Archives of Neurology 52:695-701.

Maries E, Dass B, Collier TJ, Kordower JH, Steece-Collier K (2003) The role of alpha-synuclein in Parkinson's disease: insights from animal models. Nature Reviews Neuroscience 4:727-738.

Massano J, Bhatia KP (2012) Clinical approach to Parkinson's disease: features, diagnosis, and principles of management. Cold Spring Harbor Perspectives in Medicine 2:a008870.

Massari S, Azzone GF (1972) The equivalent pore radius of intact and damaged mitochondria and the mechanism of active shrinkage. Biochimica et Biophysica Acta 283:23-29.

Matsuda N, Sato S, Shiba K, Okatsu K, Saisho K, Gautier CA, Sou Y-S, Saiki S, Kawajiri S, Sato F, Kimura M, Komatsu M, Hattori N, Tanaka K (2010) PINK1 stabilized by mitochondrial depolarization recruits Parkin to damaged mitochondria and activates latent Parkin for mitophagy. The Journal of Cell Biology 189:211-221.

Matsumoto K, Shichijo F, Fukami T (1984) Long-term follow-up review of cases of Parkinson's disease after unilateral or bilateral thalamotomy. Journal of neurosurgery 60:1033-1044.

Mattson MP, Gleichmann M, Cheng A (2008) Mitochondria in neuroplasticity and neurological disorders. Neuron 60:748-766.

McGeer PL, Itagaki S, Boyes BE, McGeer EG (1988) Reactive microglia are positive for HLA-DR in the substantia nigra of Parkinson's and Alzheimer's disease brains. Neurology 38:1285-1291.

Medina L, Chi TL, DeVivo DC, Hilal SK (1990) MR findings in patients with subacute necrotizing encephalomyelopathy (Leigh syndrome): correlation with biochemical defect. American journal of Roentgenology 154:1269-1274.

Mertins B, Psakis G, Grosse W, Back KC, Salisowski A, Reiss P, Koert U, Essen L-O (2012) Flexibility of the N-terminal mVDAC1 segment controls the channel's gating behavior. PLoS ONE 7:e47938.

Meyers R (1940) Surgical procedure for postencephalitic tremor, with notes on the physiology of premotor fibers. Archives of Neurology and Psychiatry 44:455-459.

Mitsumoto A, Nakagawa Y, Takeuchi A, Okawa K, Iwamatsu A, Takanezawa Y (2001) Oxidized forms of peroxiredoxins and DJ-1 on two-dimensional gels increased in response to sublethal levels of paraquat. Free Radical Research 35:301-310.

Miyajima Y, Schmidt ML, Sato Y, Lee VM, Oka H, Trojanowski JQ, Utsuki S, Jakes R, Kondo K, Goedert M, Tanizaki Y, Nagashio R, Tsuchiya B, Okayasu I, Fujii K (2010) Prognostic significance of nuclear DJ-1 expression in astrocytoma. Anticancer Research 30:265-269.

Mogi M, Harada M, Kondo T, Riederer P, Nagatsu T (1996) Interleukin-2 but not basic fibroblast growth factor is elevated in parkinsonian brain. Journal of Neural Transmission 103:1077-1081.

Mogi M, Harada M, Kondo T, Riederer P, Inagaki H, Minami M, Nagatsu T (1994) Interleukin-1 beta, interleukin-6, epidermal growth factor and transforming growth factor-alpha are elevated in the brain from parkinsonian patients. Neuroscience Letters 180:147-150.

Mosley RL, Hutter-Saunders JA, Stone DK, Gendelman HE (2012) Inflammation and adaptive immunity in Parkinson's disease. Cold Spring Harbor Perspectives in Medicine 2:a009381.

Mount MP, Lira A, Grimes D, Smith PD, Faucher S, Slack R, Anisman H, Hayley S, Park DS (2007) Involvement of interferon-gamma in microglial-mediated loss of dopaminergic neurons. The Journal of Neuroscience 27:3328-3337.

Muller F (2000) The nature and mechanism of superoxide production by the electron transport chain: Its relevance to aging. AGE 23:227-253.

Murphy MP (2009) How mitochondria produce reactive oxygen species. The Biochemical Journal 417:1-13.

Nagakubo D, Taira T, Kitaura H, Ikeda M, Tamai K, Iguchi-Ariga SM, Ariga H (1997) DJ-1, a novel oncogene which transforms mouse NIH3T3 cells in cooperation with ras. Biochemical and Biophysical Research Communications 231:509-513.

Narendra D, Tanaka A, Suen D-F, Youle RJ (2008) Parkin is recruited selectively to impaired mitochondria and promotes their autophagy. Journal Of Cell Biology 183:795-803.

Narendra D, Kane LA, Hauser DN, Fearnley IM, Youle RJ (2010a) p62/SQSTM1 is required for Parkin-induced mitochondrial clustering but not mitophagy; VDAC1 is dispensable for both. Autophagy 6:1090-1106.

Narendra DP, Jin SM, Tanaka A, Suen D-F, Gautier CA, Shen J, Cookson MR, Youle RJ (2010b) PINK1 Is Selectively Stabilized on Impaired Mitochondria to Activate Parkin. PLoS Biology 8:e1000298.

Narhi L, Wood SJ, Steavenson S, Jiang Y, Wu GM, Anafi D, Kaufman SA, Martin F, Sitney K, Denis P, Louis JC, Wypych J, Biere AL, Citron M (1999) Both familial Parkinson's disease mutations accelerate alpha-synuclein aggregation. The Journal of Biological Chemistry 274:9843-9846.

Navarro A, Boveris A (2009) Brain mitochondrial dysfunction and oxidative damage in Parkinson's disease. Journal of Bioenergetics and Biomembranes 41:517-521.

Navarro A, Boveris A, Bández MJ, Sánchez-Pino MJ, Gómez C, Muntané G, Ferrer I (2009) Human brain cortex: mitochondrial oxidative damage and adaptive response in Parkinson disease and in dementia with Lewy bodies. Free Radical Biology & Medicine 46:1574-1580.

Newmeyer DD, Ferguson-Miller S (2003) Mitochondria: releasing power for life and unleashing the machineries of death. Cell 112:481-490.

Novo E, Parola M (2008) Redox mechanisms in hepatic chronic wound healing and fibrogenesis. Fibrogenesis & Tissue Repair 1:5.

Nuytemans K, Theuns J, Cruts M, Van Broeckhoven C (2010) Genetic etiology of Parkinson disease associated with mutations in the SNCA, PARK2, PINK1, PARK7, and LRRK2 genes: a mutation update. Human Mutation 31:763-780.

Nyberg P, Nordberg A, Wester P, Winblad B (1983) Dopaminergic deficiency is more pronounced in putamen than in nucleus caudatus in Parkinson's disease. Neurochemical Pathology 1:193-202.

Okazaki H, Lipkin LE, Aronson SM (1961) Diffuse intracytoplasmic ganglionic inclusions (Lewy type) associated with progressive dementia and quadrparesis in flexion. Journal of Neuropathology and Experimental Neurology 20:237.

Ozelius LJ, Senthil G, Saunders-Pullman R, Ohmann E, Deligtisch A, Tagliati M, Hunt AL, Klein C, Henick B, Hailpern SM, Lipton RB, Soto-Valencia J, Risch N, Bressman SB (2006) LRRK2 G2019S as a cause of Parkinson's disease in Ashkenazi Jews. The New England Journal of Medicine 354:424-425.

Paisán-Ruíz C, Bhatia KP, Li A, Hernandez D, Davis M, Wood NW, Hardy J, Houlden H, Singleton A, Schneider SA (2009) Characterization of PLA2G6 as a locus for dystonia-parkinsonism. Annals of Neurology 65:19-23.

Palacino JJ, Sagi D, Goldberg MS, Krauss S, Motz C, Wacker M, Klose J, Shen J (2004) Mitochondrial dysfunction and oxidative damage in parkin-deficient mice. The Journal of Biological Chemistry 279:18614-18622.

Pankratz N, Pauciulo MW, Elsaesser VE, Marek DK, Halter CA, Wojcieszek J, Rudolph A, Shults CW, Foroud T, Nichols WC, Investigators PSG-P (2006) Mutations in DJ-1 are rare in familial Parkinson disease. Neuroscience Letters 408:209-213.

Parker WD, Oley CA, Parks JK (1989) A defect in mitochondrial electron-transport activity (NADH-coenzyme Q oxidoreductase) in Leber's hereditary optic neuropathy. The New England Journal of Medicine 320:1331-1333.

Parkinson J (1817) An essay on the shaking palsy. Sherwood, Neely, and Jones:80.

Pastorino JG, Hoek JB, Shulga N (2005) Activation of glycogen synthase kinase 3beta disrupts the binding of hexokinase II to mitochondria by phosphorylating voltage-dependent anion channel and potentiates chemotherapy-induced cytotoxicity. Cancer Research 65:10545-10554.

Peeraully T, Tan E-K (2012) Genetic variants in sporadic Parkinson's disease: East vs West. Parkinsonism & Related Disorders 18 Suppl 1:S63-65.

Penefsky HS (1985) Mechanism of inhibition of mitochondrial adenosine triphosphatase by dicyclohexylcarbodiimide and oligomycin: relationship to ATP synthesis. Proceedings Of The National Academy Of Sciences Of The United States Of America 82:1589-1593.

Peng S, Blachly-Dyson E, Colombini M, Forte M (1992) Determination of the number of polypeptide subunits in a functional VDAC channel from Saccharomyces cerevisiae. Journal of Bioenergetics and Biomembranes 24:27-31.

Pivovarova NB, Andrews SB (2010) Calcium-dependent mitochondrial function and dysfunction in neurons. FEBS Journal 277:3622-3636.

Poewe W (2008) Non-motor symptoms in Parkinson's disease. European Journal of Neurology 15 Suppl 1:14-20.

Polymeropoulos MH, Lavedan C, Leroy E, Ide SE, Dehejia A, Dutra A, Pike B, Root H, Rubenstein J, Boyer R, Stenroos ES, Chandrasekharappa S, Athanassiadou A, Papapetropoulos T, Johnson WG, Lazzarini AM, Duvoisin RC, Di Iorio G, Golbe LI, Nussbaum RL (1997) Mutation in the alpha-synuclein gene identified in families with Parkinson's disease. Science 276:2045-2047.

Ponsen MM, Stoffers D, Booij J, van Eck-Smit BLF, Wolters EC, Berendse HW (2004) Idiopathic hyposmia as a preclinical sign of Parkinson's disease. Annals of Neurology 56:173-181.

Poole AC, Thomas RE, Yu S, Vincow ES, Pallanck L (2010) The mitochondrial fusion-promoting factor mitofusin is a substrate of the PINK1/parkin pathway. PLoS ONE 5:e10054.

Portela A, Esteller M (2010) Epigenetic modifications and human disease. Nature Biotechnology 28:1057-1068.

Porter B, Macfarlane R, Walker R (2008) The frequency and nature of sleep disorders in a community-based population of patients with Parkinson's disease. European Journal of Neurology 15:50-54.

Pounds JG, Rosen JF (1988) Cellular Ca2+ homeostasis and Ca2+-mediated cell processes as critical targets for toxicant action: Conceptual and methodological pitfalls. Toxicology and Applied Pharmacology 94:331-341.

Priyadarshi A, Khuder SA, Schaub EA, Priyadarshi SS (2001) Environmental risk factors and Parkinson's disease: a metaanalysis. Environmental Research 86:122-127.

Qin L, Wu X, Block ML, Liu Y, Breese GR, Hong J-S, Knapp DJ, Crews FT (2007) Systemic LPS causes chronic neuroinflammation and progressive neurodegeneration. Glia 55:453-462.

Quigley PM, Korotkov K, Baneyx F, Hol WGJ (2003) The 1.6-A crystal structure of the class of chaperones represented by Escherichia coli Hsp31 reveals a putative catalytic triad. Proceedings Of The National Academy Of Sciences Of The United States Of America 100:3137-3142.

Rakovic A, Grünewald A, Seibler P, Ramirez A, Kock N, Orolicki S, Lohmann K, Klein C (2010) Effect of endogenous mutant and wild-type PINK1 on Parkin in fibroblasts from Parkinson disease patients. Human Molecular Genetics 19:3124-3137.

Ramirez A, Heimbach A, Gründemann J, Stiller B, Hampshire D, Cid LP, Goebel I, Mubaidin AF, Wriekat A-L, Roeper J, Al-Din A, Hillmer AM, Karsak M, Liss B, Woods CG, Behrens MI, Kubisch C (2006) Hereditary parkinsonism with dementia is caused by mutations in ATP13A2, encoding a lysosomal type 5 P-type ATPase. Nature Publishing Group 38:1184-1191.

Rankin CA, Joazeiro CA, Floor E, Hunter T (2001) E3 ubiquitin-protein ligase activity of Parkin is dependent on cooperative interaction of RING finger (TRIAD) elements. Journal of Biomedical Science 8:421-429.

Rapizzi E, Pinton P, Szabadkai G, Wieckowski MR, Vandecasteele G, Baird G, Tuft RA, Fogarty KE, Rizzuto R (2002) Recombinant expression of the voltage-dependent anion channel enhances the transfer of Ca2+ microdomains to mitochondria. The Journal of Cell Biology 159:613-624.

Rhoads DM, Umbach AL, Subbaiah CC, Siedow JN (2006) Mitochondrial reactive oxygen species. Contribution to oxidative stress and interorganellar signaling. Plant Physiology 141:357-366.

Ritz B, Ascherio A, Checkoway H, Marder KS, Nelson LM, Rocca WA, Ross GW, Strickland D, Van Den Eeden SK, Gorell J (2007) Pooled analysis of tobacco use and risk of Parkinson disease. Archives of Neurology 64:990-997.

Rogaeva E et al. (2004) Analysis of the PINK1 gene in a large cohort of cases with Parkinson disease. Archives of Neurology 61:1898-1904.

Roos N, Benz R, Brdiczka D (1982) Identification and characterization of the pore-forming protein in the outer membrane of rat liver mitochondria. Biochimica et Biophysica Acta 686:204-214.

Ross CA, Poirier MA (2005) Opinion: What is the role of protein aggregation in neurodegeneration? Nature Reviews Molecular Cell Biology 6:891-898.

Ross GW, Abbott RD, Petrovitch H, Morens DM, Grandinetti A, Tung KH, Tanner CM, Masaki KH, Blanchette PL, Curb JD, Popper JS, White LR (2000) Association of

coffee and caffeine intake with the risk of Parkinson disease. JAMA 283:2674-2679.

Rostovtseva T, Colombini M (1997) VDAC channels mediate and gate the flow of ATP: implications for the regulation of mitochondrial function. Biophysical Journal 72:1954-1962.

Rostovtseva TK, Liu TT, Colombini M, Parsegian VA, Bezrukov SM (2000) Positive cooperativity without domains or subunits in a monomeric membrane channel. Proceedings Of The National Academy Of Sciences Of The United States Of America 97:7819-7822.

Rowland AA, Voeltz GK (2012) Endoplasmic reticulum-mitochondria contacts: function of the junction. Nature Reviews Molecular Cell Biology 13:607-625.

Rugarli EI, Langer T (2012) Mitochondrial quality control: a matter of life and death for neurons. The EMBO journal 31:1336-1349.

Russo SJ, Nestler EJ (2013) The brain reward circuitry in mood disorders. Nature Reviews Neuroscience 14:609-625.

Ryu EJ, Harding HP, Angelastro JM, Vitolo OV, Ron D, Greene LA (2002) Endoplasmic reticulum stress and the unfolded protein response in cellular models of Parkinson's disease. The Journal of Neuroscience 22:10690-10698.

Sakakibara R, Shinotoh H, Uchiyama T, Sakuma M, Kashiwado M, Yoshiyama M, Hattori T (2001) Questionnaire-based assessment of pelvic organ dysfunction in Parkinson's disease. Autonomic Neuroscience : Basic & Clinical 92:76-85.

Samii A, Nutt JG, Ransom BR (2004) Parkinson's disease. Lancet 363:1783-1793.

Sampson MJ, Lovell RS, Craigen WJ (1997) The murine Voltage-dependent anion channel gene gamily: Conserved structure and function. Journal of Biological Chemistry 272:18966-18973.

Schapira A, Cooper J, Dexter D, Jenner P, Clark J, Marsden C (1989) Mitochondrial complex I deficiency in Parkinson's disease. Lancet 1:1269-1269.

Schenck CH, Bundlie SR, Mahowald MW (1996) Delayed emergence of a parkinsonian disorder in 38% of 29 older men initially diagnosed with idiopathic rapid eye movement sleep behaviour disorder. Neurology 46:388-393.

Scherman D, Desnos C, Darchen F, Pollak P, Javoy-Agid F, AGID Y (1989) Striatal dopamine deficiency in Parkinson's disease: role of aging. Annals of Neurology 26:551-557.

Schrier SA, Falk MJ (2011) Mitochondrial disorders and the eye. Current Opinion in Ophthalmology 22:325-331.

Sena LA, Chandel NS (2012) Physiological roles of mitochondrial reactive oxygen species. Molecular Cell 48:158-167.

Sharma S, Singh S, Sharma V, Singh VP, Deshmukh R (2015) Neurobiology of l-DOPA induced dyskinesia and the novel therapeutic strategies. Biomedicine & Pharmacotherapy 70:283-293.

Shendelman S, Jonason A, Martinat C, Leete T, Abeliovich A (2004) DJ-1 is a redox-dependent molecular chaperone that inhibits alpha-synuclein aggregate formation. PLoS Biology 2:e362.

Sherer TB, Betarbet R, Greenamyre JT (2002) Environment, mitochondria, and Parkinson's disease. The Neuroscientist 8:192-197.

Shi Y, Chen J, Weng C, Chen R, Zheng Y, Chen Q, Tang H (2003) Identification of the protein-protein contact site and interaction mode of human VDAC1 with Bcl-2 family proteins. Biochemical and Biophysical Research Communications 305:989-996.

Shimizu S, Narita M, Tsujimoto Y (1999) Bcl-2 family proteins regulate the release of apoptogenic cytochrome c by the mitochondrial channel VDAC. Nature 399:483-487.

Shinbo Y, Niki T, Taira T, Ooe H, Takahashi-Niki K, Maita C, Seino C, Iguchi-Ariga SMM, Ariga H (2006) Proper SUMO-1 conjugation is essential to DJ-1 to exert its full activities. Cell Death and Differentiation 13:96-108.

Shojaee S, Sina F, Banihosseini SS, Kazemi MH, Kalhor R, Shahidi G-A, Fakhrai-Rad H, Ronaghi M, Elahi E (2008) Genome-wide linkage analysis of a Parkinsonian-pyramidal syndrome pedigree by 500 K SNP arrays. American Journal of Human Genetics 82:1375-1384.

Shoshan-Barmatz V, Keinan N, Zaid H (2008) Uncovering the role of VDAC in the regulation of cell life and death. Journal of Bioenergetics and Biomembranes 40:183-191.

Shoshan-Barmatz V, Zalk R, Gincel D, Vardi N (2004) Subcellular localization of VDAC in mitochondria and ER in the cerebellum. Biochimica et Biophysica Acta 1657:105-114.

Shoshan-Barmatz V, Israelson A, Brdiczka D, Sheu S (2006) The voltage-dependent anion channel (VDAC): Function in intracellular signalling, cell life and cell death. Current Pharmaceutical Design 12:2249-2270.

Shoshan-Barmatz V, Keinan N, Abu-Hamad S, Tyomkin D, Aram L (2010) Apoptosis is regulated by the VDAC1 N-terminal region and by VDAC oligomerization: release of cytochrome c, AIF and Smac/Diablo. Biochimica et Biophysica Acta.

Sidransky E et al. (2009) Multicenter analysis of glucocerebrosidase mutations in Parkinson's disease. The New England Journal of Medicine 361:1651-1661.

Sileikyte J, Petronilli V, Zulian A, Dabbeni-Sala F, Tognon G, Nikolov P, Bernardi P, Ricchelli F (2011) Regulation of the inner membrane mitochondrial permeability transition by the outer membrane translocator rrotein (peripheral benzodiazepine receptor). Journal of Biological Chemistry 286:1046-1053.

Šileikytė J, Blachly-Dyson E, Sewell R, Carpi A, Menabò R, Di Lisa F, Ricchelli F, Bernardi P, Forte M (2014) Regulation of the mitochondrial permeability transition pore by the outer membrane does not involve the peripheral benzodiazepine receptor (Translocator Protein of 18 kDa (TSPO)). Journal of Biological Chemistry 289:13769-13781.

Silvestri L, Caputo V, Bellacchio E, Atorino L, Dallapiccola B, Valente EM, Casari G (2005) Mitochondrial import and enzymatic activity of PINK1 mutants associated to recessive parkinsonism. Human Molecular Genetics 14:3477-3492.

Simuni T, Sethi K (2008) Nonmotor manifestations of Parkinson's disease. Annals of Neurology 64 Suppl 2:S65-80.

Singer C, Weiner WJ, Sanchez-Ramos JR (1992) Autonomic dysfunction in men with Parkinson's disease. European Neurology 32:134-140.

Smith WW, Jiang H, Pei Z, Tanaka Y, Morita H, Sawa A, Dawson VL, Dawson TM, Ross CA (2005) Endoplasmic reticulum stress and mitochondrial cell death

pathways mediate A53T mutant alpha-synuclein-induced toxicity. Human Molecular Genetics 14:3801-3811.

Spillantini MG, Schmidt ML, Lee VM, Trojanowski JQ, Jakes R, Goedert M (1997) Alpha-synuclein in Lewy bodies. Nature 388:839-840.

Stacy M (2002) Sleep disorders in Parkinson's disease: epidemiology and management. Drugs & Aging 19:733-739.

Sterky FH, Lee S, Wibom R, Olson L, Larsson N-G (2011) Impaired mitochondrial transport and Parkin-independent degeneration of respiratory chain-deficient dopamine neurons in vivo. Proceedings Of The National Academy Of Sciences Of The United States Of America 108:12937-12942.

Struhal W, Presslauer S, Spielberger S, Zimprich A, Auff E, Bruecke T, Poewe W, Ransmayr G, Team AV-I (2014) VPS35 Parkinson's disease phenotype resembles the sporadic disease. Journal of neural Transmission 121:755-759.

Susin SA, Lorenzo HK, Zamzami N, Marzo I, Snow BE, Brothers GM, Mangion J, Jacotot E, Costantini P, Loeffler M, Larochette N, Goodlett DR, Aebersold R, Siderovski DP, Penninger JM, Kroemer G (1999) Molecular characterization of mitochondrial apoptosis-inducing factor. Nature 397:441-446.

Swinn L, Schrag A, Viswanathan R (2003) Sweating dysfunction in Parkinson's disease. Movement Disorders 18:1459-1463.

Szabó I, Zoratti M (1993) The mitochondrial permeability transition pore may comprise VDAC molecules: I. Binary structure and voltage dependence of the pore. FEBS Letters 330:201-205.

Szabó I, De Pinto V, Zoratti M (1993) The mitochondrial permeability transition pore may comprise VDAC molecules. II. The electrophysiological properties of VDAC are compatible with those of the mitochondrial megachannel. FEBS Letters 330:206-210.

Taira T, Saito Y, Niki T, Iguchi-Ariga SMM, Takahashi K, Ariga H (2004) DJ-1 has a role in antioxidative stress to prevent cell death. EMBO Reports 5:213-218.

Takahashi K, Taira T, Niki T, Seino C, Iguchi-Ariga SM, Ariga H (2001) DJ-1 positively regulates the androgen receptor by impairing the binding of PIASx alpha to the receptor. The Journal of Biological Chemistry 276:37556-37563.

Tanner CM, Langston JW (1990) Do environmental toxins cause Parkinson's disease? A critical review. Neurology 40:17-30.

Tanner CM et al. (2005) The Parkinson's disease-associated DJ-1 protein is a transcriptional co-activator that protects against neuronal apoptosis. Human Molecular Genetics 14:1231-1241.

Tao X, Tong L (2003) Crystal structure of human DJ-1, a protein associated with early onset Parkinson's disease. The Journal of Biological Chemistry 278:31372-31379.

Tasker RR (1998) Deep brain stimulation is preferable to thalamotomy for tremor suppression. Surgical Neurology 49:145-153- discussion 153-144.

Tatsuta T, Langer T (2008) Quality control of mitochondria: protection against neurodegeneration and ageing. The EMBO Journal 27:306-314.

Thomas KJ, McCoy MK, Blackinton J, Beilina A, van der Brug M, Sandebring A, Miller D, Maric D, Cedazo-Minguez A, Cookson MR (2011) DJ-1 acts in parallel to the

PINK1/parkin pathway to control mitochondrial function and autophagy. Human Molecular Genetics 20:40-50.

Tillman JE, Yuan J, Gu G, Fazli L, Ghosh R, Flynt AS, Gleave M, Rennie PS, Kasper S (2007) DJ-1 binds androgen receptor directly and mediates its activity in hormonally treated prostate cancer cells. Cancer Research 67:4630-4637.

Trump BF, Berezesky IK (1995) Calcium-mediated cell injury and cell death. The FASEB Journal 9:219-228.

Tsujimoto Y, Cossman J, Jaffe E, Croce C (1985) Involvement of the bcl-2 gene in human follicular lymphoma. Science 228:1440-1443.

Turrens JF (2003) Mitochondrial formation of reactive oxygen species. The Journal of Physiology 552:335-344.

Uhl GR, Hedreen JC, Price DL (1985) Parkinson's disease: loss of neurons from the ventral tegmental area contralateral to therapeutic surgical lesions. Neurology 35:1215-1218.

Ujwal R, Cascio D, Colletier JP, Faham S, Zhang J, Toro L, Ping P, Abramson J (2008) The crystal structure of mouse VDAC1 at 2.3 A resolution reveals mechanistic insights into metabolite gating. Proceedings of the National Academy of Sciences 105:17742-17747.

Urdinguio RG, Sanchez-Mut JV, Esteller M (2009) Epigenetic mechanisms in neurological diseases: genes, syndromes, and therapies. Lancet Neurology 8:1056-1072.

Valente EM et al. (2004) Hereditary early-onset Parkinson's disease caused by mutations in PINK1. Science 304:1158-1160.

Valko M, Leibfritz D, Moncol J, Cronin MTD, Mazur M, Telser J (2007) Free radicals and antioxidants in normal physiological functions and human disease. The International Journal of Biochemistry & Cell Biology 39:44-84.

Van Laar VS, Arnold B, Cassady SJ, Chu CT, Burton EA, Berman SB (2010) Bioenergetics of neurons inhibit the translocation response of Parkin following rapid mitochondrial depolarization. Human Molecular Genetics.

Vander Heiden MG, Li XX, Gottleib E, Hill RB, Thompson CB, Colombini M (2001) Bcl-xL promotes the open configuration of the voltage-dependent anion channel and metabolite passage through the outer mitochondrial membrane. The Journal of Biological Chemistry 276:19414-19419.

Vaux DL, Cory S, Adams JM (1988) Bcl-2 gene promotes haemopoietic cell survival and cooperates with c-myc to immortalize pre-B cells. Nature 335:440-442.

Verbaan D, Marinus J, Visser M, van Rooden SM, Stiggelbout AM, van Hilten JJ (2007) Patient-reported autonomic symptoms in Parkinson disease. Neurology 69:333-341.

Verhagen AM, Ekert PG, Pakusch M, Silke J, Connolly LM, Reid GE, Moritz RL, Simpson RJ, Vaux DL (2000) Identification of DIABLO, a mammalian protein that promotes apoptosis by binding to and antagonizing IAP proteins. Cell 102:43-53.

Verkhratsky A (2005) Physiology and pathophysiology of the calcium store in the endoplasmic reticulum of neurons. Physiological Reviews 85:201-279.

Vilariño-Güell C et al. (2011) VPS35 mutations in Parkinson disease. American Journal of Human Genetics 89:162-167.

Vives-Bauza C, Zhou C, Huang Y, Cui M, de Vries RLA, Kim J, May J, Tocilescu MA, Liu W, Ko HS, Magrané J, Moore DJ, Dawson VL, Grailhe R, Dawson TM, Li C, Tieu K, Przedborski S (2010) PINK1-dependent recruitment of Parkin to mitochondria in mitophagy. Proceedings Of The National Academy Of Sciences Of The United States Of America 107:378-383.

Volpicelli-Daley LA, Luk KC, Patel TP, Tanik SA, Riddle DM, Stieber A, Meaney DF, Trojanowski JQ, Lee VM-Y (2011) Exogenous α-synuclein fibrils induce Lewy body pathology leading to synaptic dysfunction and neuron death. Neuron 72:57-71.

Weeber EJ, Levy M, Sampson MJ, Anflous K, Armstrong DL, Brown SE, Sweatt JD, Craigen WJ (2002) The role of mitochondrial porins and the permeability transition pore in learning and synaptic plasticity. The Journal of Biological Chemistry 277:18891-18897.

Williams DR, Watt HC, Lees AJ (2006) Predictors of falls and fractures in bradykinetic rigid syndromes: a retrospective study. Journal of Neurology, Neurosurgery, and Psychiatry 77:468-473.

Wilson JM, Levey AI, Rajput A, Ang L, Guttman M, Shannak K, Niznik HB, Hornykiewicz O, Pifl C, Kish SJ (1996) Differential changes in neurochemical markers of striatal dopamine nerve terminals in idiopathic Parkinson's disease. Neurology 47:718-726.

Wilson MA, Collins JL, Hod Y, Ringe D, Petsko GA (2003) The 1.1-A resolution crystal structure of DJ-1, the protein mutated in autosomal recessive early onset

Parkinson's disease. Proceedings Of The National Academy Of Sciences Of The United States Of America 100:9256-9261.

Wood-Kaczmar A, Gandhi S, Yao Z, Abramov AY, Abramov ASY, Miljan EA, Keen G, Stanyer L, Hargreaves I, Klupsch K, Deas E, Downward J, Mansfield L, Jat P, Taylor J, Heales S, Duchen MR, Latchman D, Tabrizi SJ, Wood NW (2008) PINK1 is necessary for long term survival and mitochondrial function in human dopaminergic neurons. PLoS ONE 3:e2455.

Wu S, Sampson MJ, Decker WK, Craigen WJ (1999) Each mammalian mitochondrial outer membrane porin protein is dispensable: effects on cellular respiration. Biochimica et Biophysica Acta 1452:68-78.

Xiong H, Wang D, Chen L, Choo YS, Ma H, Tang C, Xia K, Jiang W, Ronai Zae, Zhuang X, Zhang Z (2009) Parkin, PINK1, and DJ-1 form a ubiquitin E3 ligase complex promoting unfolded protein degradation. The Journal of Clinical Investigation 119:650-660.

Yang Y, Gehrke S, Haque ME, Imai Y, Kosek J, Yang L, Beal MF, Nishimura I, Wakamatsu K, Ito S, Takahashi R, Lu B (2005) Inactivation of Drosophila DJ-1 leads to impairments of oxidative stress response and phosphatidylinositol 3-kinase/Akt signaling. Proceedings Of The National Academy Of Sciences Of The United States Of America 102:13670-13675.

Youle RJ, Strasser A (2008) The BCL-2 protein family: opposing activities that mediate cell death. Nature Reviews Molecular Cell Biology 9:47-59.

Zalk R, Israelson A, Garty ES, Azoulay-Zohar H, Shoshan-Barmatz V (2005) Oligomeric states of the voltage-dependent anion channel and cytochrome c release from mitochondria. The Biochemical Journal 386:73-83.

Zarow C, Lyness SA, Mortimer JA, Chui HC (2003) Neuronal loss is greater in the locus coeruleus than nucleus basalis and substantia nigra in Alzheimer and Parkinson diseases. Archives of Neurology 60:337-341.

Zhang L, Shimoji M, Thomas B, Moore DJ, Yu S-W, Marupudi NI, Torp R, Torgner IA, Ottersen OP, Dawson TM, Dawson VL (2005) Mitochondrial localization of the Parkinson's disease related protein DJ-1: implications for pathogenesis. Human Molecular Genetics 14:2063-2073.

Zhong N, Xu J (2008) Synergistic activation of the human MnSOD promoter by DJ-1 and PGC-1alpha: regulation by SUMOylation and oxidation. Human Molecular Genetics 17:3357-3367.

Zhong N, Kim CY, Rizzu P, Geula C, Porter DR, Pothos EN, Squitieri F, Heutink P, Xu J (2006) DJ-1 transcriptionally up-regulates the human tyrosine hydroxylase by inhibiting the sumoylation of pyrimidine tract-binding protein-associated splicing factor. The Journal of Biological Chemistry 281:20940-20948.

Zhou C, Huang Y, Shao Y, May J, Prou D, Perier C, Dauer W, Schon EA, Przedborski S (2008) The kinase domain of mitochondrial PINK1 faces the cytoplasm. Proc Natl Acad Sci USA 105:12022-12027.

Zhou W, Zhu M, Wilson MA, Petsko GA, Fink AL (2006) The oxidation state of DJ-1 regulates its chaperone activity toward alpha-synuclein. Journal of Molecular Biology 356:1036-1048.

Zimprich A et al. (2004) Mutations in LRRK2 cause autosomal-dominant parkinsonism with pleomorphic pathology. Neuron 44:601-607.

Zimprich A et al. (2011) A mutation in VPS35, encoding a subunit of the retromer complex, causes late-onset Parkinson disease. American Journal of Human Genetics 89:168-175.

Ziviani E, Tao RN, Whitworth AJ (2010) Drosophila Parkin requires PINK1 for mitochondrial translocation and ubiquitinates Mitofusin. Proceedings Of The National Academy Of Sciences Of The United States Of America 107:5018-5023.

Zolotukhin S, Potter M, Zolotukhin I, Sakai Y, Loiler S, Fraites TJ, Chiodo VA, Phillipsberg T, Muzyczka N, Hauswirth WW, Flotte TR, Byrne BJ, Snyder RO (2002) Production and purification of serotype 1, 2, and 5 recombinant adeno-associated viral vectors. Methods 28:158-167.

Zorov DB, Juhaszova M, Sollott SJ (2014) Mitochondrial reactive oxygen species (ROS) and ROS-induced ROS release. Physiological Reviews 94:909-950.

APPENDIX II

Permission to Reprint Published Manuscripts

Rights and Permissions

Requests for Permission to Reprint

Requests for permission should be made in writing. For the fastest response time, please send your request via email to PNASPermissions@nas.edu. If necessary, requests may be faxed to 202-334-2739 or mailed to:

PNAS Permissions Editor
500 Fifth Street, NW
NAS 340
Washington, DC 20001 USA

Anyone may, without requesting permission, use original figures or tables published in PNAS for noncommercial and educational use (i.e., in a review article, in a book that is not for sale) provided that the original source and the applicable copyright notice are cited.

For permission to reprint material in volumes 1–89 (1915–1992), requests should be addressed to the original authors, who hold the copyright. The full journal reference must be cited.

For permission to reprint material in volumes 90–present (1993–present), requests must be sent via email, fax, or mail and include the following information about the original material:

1. Your full name, affiliation, and title
2. Your complete mailing address, phone number, fax number, and email address
3. PNAS volume number, issue number, and issue date
4. PNAS article title
5. PNAS authors' names
6. Page numbers of items to be reprinted
7. Figure/table number or portion of text to be reprinted

Also include the following information about the intended use of the material:

1. Title of work in which PNAS material will appear
2. Authors/editors of work
3. Publisher of work
4. Retail price of work

5. Number of copies of work to be produced
6. Intended audience
7. Whether work is for nonprofit or commercial use

PNAS authors need not obtain permission for the following cases: (1) to use their original figures or tables in their future works; (2) to make copies of their papers for their own personal use, including classroom use, or for the personal use of colleagues, provided those copies are not for sale and are not distributed in a systematic way; (3) to include their papers as part of their dissertations; or (4) to use all or part of their articles in printed compilations of their own works. Citation of the original source must be included and copies must include the applicable copyright notice of the original report.

Authors whose work will be reused should be notified. PNAS cannot supply original artwork. Use of PNAS material must not imply any endorsement by PNAS or the National Academy of Sciences. The full journal reference must be cited and, for articles published in Volumes 90–105 (1993–2008), "Copyright (copyright year) National Academy of Sciences, USA."

Requests for Permission to Photocopy

For permission to photocopy beyond that permitted by Section 107 or 108 of the US Copyright Law, contact:

Copyright Clearance Center
222 Rosewood Drive
Danvers, MA 01923 USA
Phone: 1-978-750-8400
Fax: 1-978-750-4770
Email: info@copyright.com

Authorization to photocopy items for the internal or personal use of specific clients is granted by The National Academy of Sciences provided that the proper fee is paid directly to CCC.

[12/14]

License Details

This is a License Agreement between Sarah J Hewitt ("You") and Oxford University Press ("Oxford University Press"). The license consists of your order details, the terms and conditions provided by Oxford University Press, and the payment terms and conditions.

Get the printable license.

License Number	3707720499818
License date	Sep 14, 2015
Licensed Content Publisher	Oxford University Press
Licensed Content Publication	Human Molecular Genetics
Licensed Content Title	Loss of the Parkinson's disease-linked gene DJ-1 perturbs mitochondrial dynamics:
Licensed Content Author	I. Irrcher, H. Aleyasin, E.L. Seifert, S.J. Hewitt, S. Chhabra, M. Phillips, A.K. Lutz, M.W.C. Rousseaux, L. Bevilacqua, A. Jahani-Asl, S. Callaghan, J.G. MacLaurin, K.F. Winklhofer, P. Rizzu, P. Rippstein, R.H. Kim, C.X. Chen, E.A. Fon, R.S. Slack, M.E. Harper, H.M. McBride, T.W. Mak, D.S. Park
Licensed Content Date	10/01/2010
Volume number	19
Issue number	19
Type of Use	Thesis/Dissertation
Requestor type	Academic/Educational institute
Format	Print and electronic
Portion	Text Extract
Number of pages requested	17
Will you be translating?	No
Author of this OUP article	Yes
Order reference number	None
Title of your thesis / dissertation	Understanding DJ-1: Role of mitochondria and VDAC1
Expected completion date	Sep 2015
Estimated size(pages)	200
Publisher VAT ID	GB 125 5067 30
Total	**0.00 USD**

BACK

License Details

This is a License Agreement between Sarah J Hewitt ("You") and Oxford University Press ("Oxford University Press"). The license consists of your order details, the terms and conditions provided by Oxford University Press, and the payment terms and conditions.

Get the printable license.

License Number	3707720455489
License date	Sep 14, 2015
Licensed Content Publisher	Oxford University Press
Licensed Content Publication	Human Molecular Genetics
Licensed Content Title	Loss of the Parkinson's disease-linked gene DJ-1 perturbs mitochondrial dynamics:
Licensed Content Author	I. Irrcher, H. Aleyasin, E.L. Seifert, S.J. Hewitt, S. Chhabra, M. Phillips, A.K. Lutz, M.W.C. Rousseaux, L. Bevilacqua, A. Jahani-Asl, S. Callaghan, J.G. MacLaurin, K.F. Winklhofer, P. Rizzu, P. Rippstein, R.H. Kim, C.X. Chen, E.A. Fon, R.S. Slack, M.E. Harper, H.M. McBride, T.W. Mak, D.S. Park
Licensed Content Date	10/01/2010
Volume number	19
Issue number	19
Type of Use	Thesis/Dissertation
Requestor type	Academic/Educational institute
Format	Print and electronic
Portion	Figure/table
Number of figures/tables	13
Will you be translating?	No
Author of this OUP article	Yes
Order reference number	None
Title of your thesis / dissertation	Understanding DJ-1: Role of mitochondria and VDAC1
Expected completion date	Sep 2015
Estimated size(pages)	200
Publisher VAT ID	GB 125 5067 30
Total	**0.00 USD**

BACK

License Details

This is a License Agreement between Sarah J Hewitt ("You") and Oxford University Press ("Oxford University Press"). The license consists of your order details, the terms and conditions provided by Oxford University Press, and the payment terms and conditions.

Get the printable license.

License Number	3707720184610
License date	Sep 14, 2015
Licensed Content Publisher	Oxford University Press
Licensed Content Publication	Human Molecular Genetics
Licensed Content Title	ROS-dependent regulation of Parkin and DJ-1 localization during oxidative stress in neurons:
Licensed Content Author	Alvin P. Joselin, Sarah J. Hewitt, Steve M. Callaghan, Raymond H. Kim, Young-Hwa Chung, Tak W. Mak, Jie Shen, Ruth S. Slack, David S. Park
Licensed Content Date	11/15/2012
Volume number	21
Issue number	22
Type of Use	Thesis/Dissertation
Requestor type	Academic/Educational institute
Format	Print and electronic
Portion	Abstract
Will you be translating?	No
Author of this OUP article	Yes
Order reference number	None
Title of your thesis / dissertation	Understanding DJ-1: Role of mitochondria and VDAC1
Expected completion date	Sep 2015
Estimated size(pages)	200
Publisher VAT ID	GB 125 5067 30
Total	**0.00 USD**

BACK

License Details

This is a License Agreement between Sarah J Hewitt ("You") and Oxford University Press ("Oxford University Press"). The license consists of your order details, the terms and conditions provided by Oxford University Press, and the payment terms and conditions.

Get the printable license.

License Number	3707720151269
License date	Sep 14, 2015
Licensed Content Publisher	Oxford University Press
Licensed Content Publication	Human Molecular Genetics
Licensed Content Title	ROS-dependent regulation of Parkin and DJ-1 localization during oxidative stress in neurons:
Licensed Content Author	Alvin P. Joselin, Sarah J. Hewitt, Steve M. Callaghan, Raymond H. Kim, Young-Hwa Chung, Tak W. Mak, Jie Shen, Ruth S. Slack, David S. Park
Licensed Content Date	11/15/2012
Volume number	21
Issue number	22
Type of Use	Thesis/Dissertation
Requestor type	Academic/Educational institute
Format	Print and electronic
Portion	Text Extract
Number of pages requested	23
Will you be translating?	No
Author of this OUP article	Yes
Order reference number	None
Title of your thesis / dissertation	Understanding DJ-1: Role of mitochondria and VDAC1
Expected completion date	Sep 2015
Estimated size(pages)	200
Publisher VAT ID	GB 125 5067 30
Total	**0.00 USD**

BACK

License Details

This is a License Agreement between Sarah J Hewitt ("You") and Oxford University Press ("Oxford University Press"). The license consists of your order details, the terms and conditions provided by Oxford University Press, and the payment terms and conditions.

Get the printable license.

License Number	3707711478555
License date	Sep 14, 2015
Licensed Content Publisher	Oxford University Press
Licensed Content Publication	Human Molecular Genetics
Licensed Content Title	ROS-dependent regulation of Parkin and DJ-1 localization during oxidative stress in neurons:
Licensed Content Author	Alvin P. Joselin, Sarah J. Hewitt, Steve M. Callaghan, Raymond H. Kim, Young-Hwa Chung, Tak W. Mak, Jie Shen, Ruth S. Slack, David S. Park
Licensed Content Date	11/15/2012
Volume number	21
Issue number	22
Type of Use	Thesis/Dissertation
Requestor type	Academic/Educational institute
Format	Print and electronic
Portion	Figure/table
Number of figures/tables	16
Will you be translating?	No
Author of this OUP article	Yes
Order reference number	None
Title of your thesis / dissertation	Understanding DJ-1: Role of mitochondria and VDAC1
Expected completion date	Sep 2015
Estimated size(pages)	200
Publisher VAT ID	GB 125 5067 30
Total	**0.00 USD**

BACK

APPENDIX III

Additional Publications

DJ-1 protects the nigrostriatal axis from the neurotoxin MPTP by modulation of the AKT pathway

Hossein Aleyasin[a,1], Maxime W. C. Rousseaux[a,1], Paul C. Marcogliese[a], Sarah J. Hewitt[a], Isabella Irrcher[a], Alvin P. Joselin[a], Mohammad Parsanejad[a], Raymond H. Kim[b], Patrizia Rizzu[c], Steve M. Callaghan[a], Ruth S. Slack[a], Tak W. Mak[b,2], and David S. Park[a,d,2]

[a]Department of Cellular and Molecular Medicine, University of Ottawa, Ottawa, ON K1H 8M5, Canada; [b]Campbell Family Institute for Breast Cancer Research, Toronto, ON M5G 2C1, Canada; [c]Section Medical Genomics, Department of Clinical Genetics, Vrije Universiteit University Medical Center, Van der Boechorststraat 7, 1081 BT, Amsterdam, The Netherlands; and [d]Department of Cogno-Mechatronics Engineering, Pusan National University, Geumjeong GU, Busan 609 735 South Korea

Contributed by Tak Wah Mak, December 24, 2009 (sent for review December 15, 2009)

Loss-of-function DJ-1 (PARK7) mutations have been linked with a familial form of early onset Parkinson disease. Numerous studies have supported the role of DJ-1 in neuronal survival and function. Our initial studies using DJ-1-deficient neurons indicated that DJ-1 specifically protects the neurons against the damage induced by oxidative injury in multiple neuronal types and degenerative experimental paradigms, both in vitro and in vivo. However, the manner by which oxidative stress-induced death is ameliorated by DJ-1 is not completely clear. We now present data that show the involvement of DJ-1 in modulation of AKT, a major neuronal pro-survival pathway induced upon oxidative stress. We provide evidence that DJ-1 promotes AKT phosphorylation in response to oxidative stress induced by H_2O_2 in vitro and in vivo following 1-methyl-4-phenyl-1,2,3,6-tetrahydropyridine (MPTP) treatment. Moreover, we show that DJ-1 is necessary for normal AKT-mediated protective effects, which can be bypassed by expression of a constitutively active form of AKT. Taken together, these data suggest that DJ-1 is crucial for full activation of AKT upon oxidative injury, which serves as one explanation for the protective effects of DJ-1.

neurodegeneration | Parkinson disease | reactive oxygen species

Individuals with homozygous loss-of-function mutations of DJ-1 (PARK7) have been clinically characterized with familial early onset Parkinson disease (PD) (1, 2). Although the physiological role of DJ-1 is not completely understood, several lines of evidence indicate a protective role for DJ-1 in multiple models of neuronal and nonneuronal oxidative stress-induced cell death (3–7). For example, we have previously shown that genetic ablation of DJ-1 in mice hypersensitizes dopamine neurons to the toxic effects induced by the mitochondrial toxin, 1-methyl-4-phenyl-1,2,3,6-tetrahydropyridine (MPTP). This sensitivity was reversed by the induction of virally delivered human DJ-1 (8). These observations are in line with data by other groups showing sensitivity of dopaminergic neurons in DJ-1–deficient *Drosophila* models, as well as increased susceptibility to oxidative stress in vitro (9–11). To further support the importance of DJ-1 in managing oxidative stress, we provided evidence showing that DJ-1 protects the brain against ischemic injury that models clinical stroke. Moreover, our data indicated a direct correlation between DJ-1 neuroprotective activity and the reduced levels of oxidized DNA nucleotide species, 8-oxo guanine, a marker of oxidative damage (12).

Despite the fact that the neuroprotective role of DJ-1 has been consistently shown in multiple models of neurodegeneration, the exact mechanism of the neuroprotective function has not been fully elucidated. A direct antioxidant property of DJ-1 as a reactive oxygen species (ROS) scavenger has been proposed as a mechanism to overcome oxidative stress (7, 13). In fact, recombinant human DJ-1 confers some ROS scavenging activity; however, this activity is much weaker than any known peroxidase, thus not fully explaining its neuroprotective function (10, 13). Several alternative mechanisms to account for the neuroprotective function of DJ-1 have been suggested. For example, via its putative role in transcription regulation (14), DJ-1 up-regulates the expression of other antioxidant genes, such as glutathione synthase, during oxidative stress (15). Interestingly, it has also been reported that DJ-1 enhances the activity of the transcription factor Nrf2, a master regulator of antioxidant genes (16, 17). Alternatively, DJ-1 has also been shown to modulate key signaling pathways (3, 10). One signaling pathway implicated with DJ-1 function and relevant to the present work is AKT (10, 18).

AKT is a member of a larger class of serine/threonine kinases called AGC [protein kinase A (AMP protein kinase), PKG (GMP protein kinase), and PKC]. AKT has an N-terminus pleckstrin homology domain that mediates the interaction of AKT with a plasma membrane phospholipid, phophatidylinositol 3,4,5-triphosphate (PIP3). Extensive studies have shown that recruitment of AKT to the plasma membrane, and its association with PIP3, is crucial for its activation (19, 20). Phosphatase and tensin homolog deleted on chromosome 10 (PTEN) is particularly known for its action to convert PIP3 to phosphatidylinositol-4, 5- biphosphate (PIP2). This function of PTEN directly antagonizes PI3K to eventually down-regulate AKT (21, 22). Several lines of evidence indicated that the AKT signaling pathway responds to oxidative stress (23) and exerts a neuroprotective function (24, 25). Moreover, a large number of studies in vitro have illustrated that pharmacological compounds that protect cells against oxidative stress exert their neuroprotective effects through activation of the AKT pathway (26–30).

Early studies described DJ-1 as a negative regulator of PTEN using a *Drosophila* genetic screen (31). Evidence to confirm this negative regulation was demonstrated via down-regulation of DJ-1 using small interfering RNA, which resulted in the inhibition of endogenous AKT phosphorylation in cancer cell lines as well as in the *Drosophila* brain (10, 31, 32). Furthermore, loss of DJ-1 has been shown to reduce AKT activation in response to hypoxia in murine embryonic fibroblasts (MEFs) (33). However, the relevance of this pathway has yet to be shown in the context of neurons either in vitro or in vivo. Evidence to support a role for DJ-1 in the regulation of the AKT pathway would be particularly important when one considers the genetic linkage of DJ-1 to familial PD. Presently, we provide direct evidence, both in vitro and in vivo, that DJ-1 exerts an important role in the regulation of the AKT pathway in response to oxidative stress and neuronal protection. In

Author contributions: H.A., M.W.C.R., R.H.K., R.S.S., T.W.M., and D.S.P. designed research; H.A., M.W.C.R., P.C.M., S.J.H., I.I., A.P.J., and M.P. performed research; R.H.K., P.R., S.C., R.S.S., and T.W.M. contributed new reagents/analytic tools; H.A., M.W.C.R., P.C.M., S.J.H., A.P.J., M.P., and D.S.P. analyzed data; and H.A., M.W.C.R., I.I., and D.S.P. wrote the paper.

The authors declare no conflict of interest.

Freely available online through the PNAS open access option.

[1]H.A. and M.W.C.R. contributed equally to this work.

[2]To whom correspondence should be addressed. E-mail: dpark@uottawa.ca or tmak@uhnresearch.ca.

This article contains supporting information online at www.pnas.org/cgi/content/full/0914876107/DCSupplemental.

addition, based on our results, we propose a mechanism suggesting that DJ-1 acts as an upstream regulator of AKT through membrane recruitment to confer neuroprotection.

Results

Phosphorylation of AKT in Response to Oxidative Stress Is Reduced in the Absence of DJ-1 in Vitro and in Vivo. To examine the role of DJ-1 on AKT signaling, we first determined whether lack of DJ-1 affects AKT phosphorylation following hydrogen peroxide (H_2O_2) treatment. To test this, neurons harvested from DJ-$1^{-/-}$ or DJ-$1^{+/+}$ embryos were treated with 100-μM H_2O_2 for indicated time points. As demonstrated in Fig. 1*A*, phosphorylation of AKT peaked in wild-type neurons at 15 min, whereas in the knockout there was a reduction in AKT phosphorylation. Quantification of three independent experiments revealed a significant reduction in p-AKT 15 min following treatment (3.67 ± 0.17 in DJ-$1^{+/+}$ vs. 1.49 ± 0.76 in DJ-$1^{-/-}$), as demonstrated in Fig. 1*B*. To further support this observation and to examine this response in a more clinically relevant model of PD, we examined AKT phosphorylation in dopaminergic neurons of the *substantia nigra* (SNc) in response to MPTP treatment. As indicated in Fig. 1*C*, and quantified in Fig. 1*D*, AKT phosphorylation in response to MPTP was reduced in the SNc cells of DJ-$1^{-/-}$ compared to wild-type controls (1.19 ± 0.10 vs. 1.52 ± 0.14, respectively). There was no significant increase in AKT phosphorylation when comparing saline and MPTP treated DJ-$1^{-/-}$ animals (1.00 ± 0.2 vs. 1.19 ± 0.10, respectively). To further confirm these results, we also examined AKT phosphorylation in response to H_2O_2 in human lymphoblasts from human PD patients harboring DJ-1 mutations. As demonstrated in Fig. 1*E*, AKT response was significantly attenuated in L166P mutated cells compared to the controls.

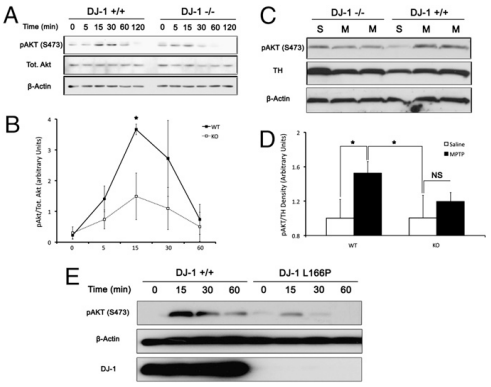

Fig. 1. AKT activation is suppressed in the absence of DJ-1. (*A*) Cortical neurons from DJ-$1^{+/+}$ and DJ-$1^{-/-}$ embryos were harvested, plated, and treated with H_2O_2 (100 μM) in a time-dependent fashion. Extracts were probed for pAKT (S473), total AKT, and β-actin by Western blot. (*B*) Quantification of *A* from three independent experiments. Values are presented as mean optical density relative to total AKT. (*C*) Eight- to 10-week-old C57Bl6 mice of WT and DJ-1 knockout genotype were treated with two 30-mg/kg doses of MPTP (M), or saline (S), given 24 h apart. Three hours following the second injection, mice brains were quickly dissected for SNc and samples were processed for Western blot analysis. (*D*) Quantification of *C*. $n = 3$–6 per group. (*E*) Immortalized lymphoblasts derived from patients with the DJ-1 L166P mutation or healthy control lymphoblasts were treated with H_2O_2 in a time dependant manner. Analysis of cell lysates was carried out by Western blot. Blot presented is representative of two independent experiments. Data are presented as mean ± SEM.

DJ-1 Is Necessary for AKT-Mediated Neuroprotective Function in Vitro and in Vivo. We next evaluated the functional role of DJ-1 in the protective effects of AKT following oxidative stress. First, we examined the role of AKT in protecting neurons against oxidative stress induced by H_2O_2 in vitro. Neurons, transfected with HA-tagged wild-type AKT along with GFP expression vectors as a marker of transfection (or GFP/empty vector transfection as control) were treated with H_2O_2, 24 h after transfection, and survival was assessed as described in *Materials and Methods* (Fig.2*A*). As shown in Fig. 2*B*, induction of exogenous wild-type AKT confers protection in DJ-$1^{+/+}$ neuronal cells in response to H_2O_2. Next, DJ-$1^{-/-}$ cortical neurons were tested to examine whether induction of wild-type AKT could provide similar protection in DJ-1-deficient cells. Surprisingly, induction of exogenous AKT failed to protect DJ-$1^{-/-}$ neurons against H_2O_2-induced death (Fig. 2*C*). To confirm these observations, we cultured neurons harvested from DJ-$1^{-/-}$ and DJ-$1^{+/+}$ litters at the same time. Three days after plating, the cells were transiently transfected with wild-type AKT together with or without a DJ-1

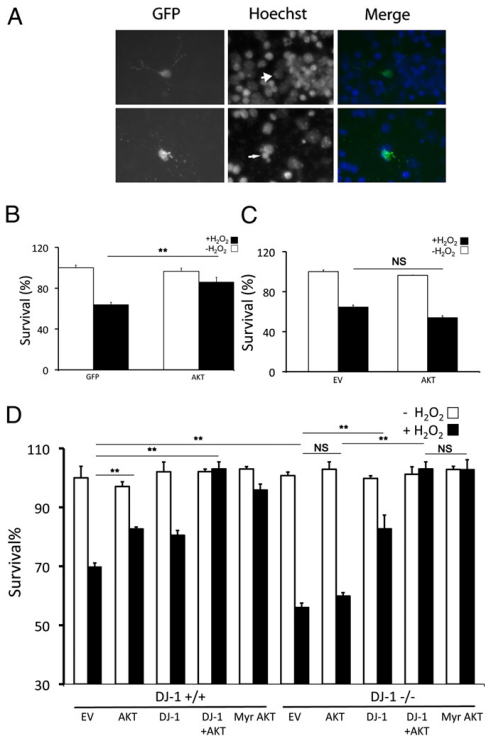

Fig. 2. AKT requires DJ-1 to exert its neuroprotective function in vitro. (*A*) Representative pictures of alive (*Upper*, large arrowhead) and dead (*Lower*, thin arrowhead) neurons. Neuronal survival was measured by identifying GFP-positive cells and determining their nuclear integrity by Hoechst stain. (*B–D*) Cortical neurons from either DJ-$1^{+/+}$ or DJ-$1^{-/-}$ embryos were harvested, plated, and transfected with empty vector (EV), AKT, DJ-1, or Myr AKT. Cells were treated with H_2O_2 (30 μM) or vehicle control ($-H_2O_2$) for 3 h. Quantification was assessed as in *A*. Data are presented as mean ± SEM. **, $P < 0.01$; NS, no significant difference.

expression vector, DJ-1 only, or myristoylated AKT, a membrane-anchored constitutively active form of AKT (34). After treatment with H_2O_2, cell survival was assessed. The results of this experiment clearly verified our findings in Fig. 2*C*, indicating the protective role of wildtype AKT expressed in DJ-$1^{+/+}$ neurons but not in DJ-$1^{-/-}$ cells (82.65 ± 0.65% DJ-$1^{+/+}$ vs. 59.88 ± 1.18% DJ-$1^{-/-}$) (Fig. 2*D*). Interestingly, myristoylated AKT significantly protects neurons against oxidative damage induced by H_2O_2 regardless of DJ-1 genotype (95.85 ± 2.02% DJ-$1^{+/+}$ vs. 102.77 ± 3.38% DJ-$1^{-/-}$).

Suppression of AKT Abolishes the Neuroprotective Function of DJ-1 in Vitro and in Vivo. The observations that DJ-1 deficiency reduces AKT activation and that wild-type AKT requires DJ-1 to effectively protect neurons against oxidative stress suggests DJ-1 acts as an upstream activator of AKT. We next determined whether DJ-1 exerts its neuroprotective effects, at least partially, through the AKT pathway. To examine this, we first used a conventional pharmacological inhibitor of AKT, LY294002 (LY) (35). Because the basal activity of AKT is essential for the long-term health of cultured neurons, we determined the optimal dose of inhibitor that suppressed AKT with minimal toxicity to the cultured neurons (Fig. 3*A*). We next infected cultured cortical neurons with adenoviral vectors expressing GFP only or DJ-1 and GFP on separate promoters at the time of plating. Thirty-six hours after plating, we pretreated the cells with 10-μM LY or vehicle for 30 min before application of H_2O_2 or vehicle for 3 h. Cells were then assessed for survival. As shown in Fig. 3*B*, the neuroprotective activity of DJ-1 is significantly reduced upon suppression of AKT phosphorylation by LY (52.78 ± 0.20% vs. 40.55 ± 0.55%, respectively). We also used a more specific molecular strategy to validate our results by transiently transfecting a phosphorylation mutant, dominant-negative form (DN-AKT) of AKT (AAA-AKT) into cortical neurons. In this mutant, all phosphorylation sites of AKT have been mutated to alanine; therefore, this artificial mutant of AKT is incapable of being phosphorylated and displays dominant-negative properties toward endogenous AKT (21). As shown in Fig. 3*C*, the results of this experiment confirmed that suppression of AKT diminished the neuroprotective function of DJ-1 (84.46 ± 2.90% without DN-AKT vs. 59.26 ± 2.01% with DN-AKT).

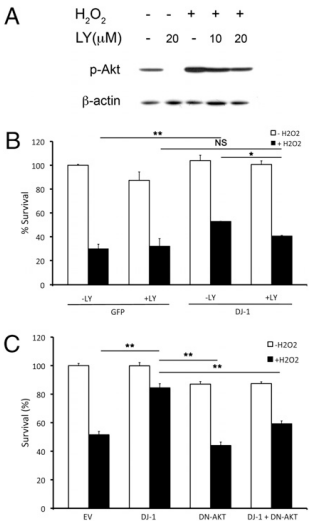

Fig. 3. DJ-1 requires AKT activation to promote cellular survival in vitro. (*A*) Cortical neurons were treated for either 10 or 20 μM of LY with and without H_2O_2 (100 μM, 15 min) to determine the effective dose of LY. (*B*) Cortical neurons were infected with either GFP or DJ-1 with GFP. Cells were then pretreated with LY followed by H_2O_2 treatment for survival assessment. (*C*) Cortical neurons were cotransfected with GFP and empty vector (EV), DJ-1, DN-AKT, or a DJ-1/DN-AKT combination followed by H2O2 treatment. Survival was assessed as in *B*. Data are presented as mean ± SEM. *, $P < 0.05$; **, $P < 0.01$; NS, no significant difference.

DJ-1 Is Necessary for AKT-Mediated Neuroprotection in Vivo Following MPTP Treatment. In vitro experiments indicated that DJ-1 is necessary for AKT activation and is neuroprotective in response to H_2O_2. To confirm these results and to test this hypothesis in a more clinically relevant paradigm, we examined whether induction of wild-type AKT can protect nigrostriatal neurons against the dopaminergic specific neurotoxin MPTP in vivo. To achieve this, we injected adenoviral vectors harboring HA-tagged wild-type AKT or myristoylated AKT into the striatum of DJ-$1^{+/+}$ and DJ-$1^{-/-}$ age-matched mice. β-gal expressing adenoviruses

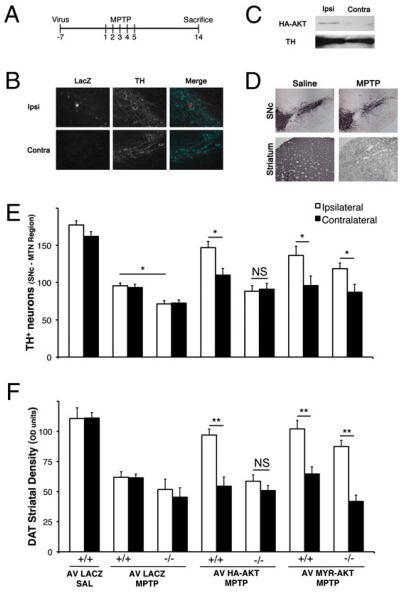

Fig. 4. AKT requires DJ-1 to exert its neuroprotective function in an in vivo model of PD. (*A*) Schematic representation of treatment course. Mice were injected ipsilaterally in the striatum with adenovirus (LacZ, HA-AKT, Myr-AKT) 7 d before commencement of MPTP injections. MPTP was injected for 5 consecutive days and brains were collected 14 days following the first MPTP injection. (*B*) Confirmation of virus expression was performed by immunohistochemistry. Dual labeling of both TH and protein of interest in the SNc. (*C*) HA expression was tested in the SNc by Western blot analysis. (*D*) Representative pictures of both striatum and SNc of mice treated with MPTP or saline. SNc and striatum were stained for TH and DAT, respectively. (*E*) Quantification of TH-immunoreactive neurons was performed at the MTN region of the SNc where virus expression was highest. "Ipsi" denotes the side of the brain ipsilateral to the virus injection, whereas "contra" denotes the contralateral side. (*F*) Quantification of DAT-positive fibers normalized to cortex (DAT-negative). Data are presented as mean ± SEM. *, $P < 0.05$; **, $P < 0.01$; NS, no significant difference.

were used as control. As shown in Fig. 4 *B* and *C*, the virus localizes specifically to the ipsilateral side in dopamine neurons. One week after virus injection, we performed a subchronic MPTP treatment paradigm as indicated in Fig. 4*A*. Two weeks after the initial MPTP injection, animals in all groups were sacrificed and prepared for histological analysis. We first assessed survival by counting the number TH+ neurons of SNc at the level of the medial terminal nucleus (MTN) (Fig. 4*E*). Consistent with our in vitro observations, DJ-$1^{+/+}$ animals that received wild-type HA-tagged AKT and were subjected to MPTP treatments showed larger number of surviving TH+ neurons in the ipsilateral side of virus injection, compared to the contralateral side (146.9 ± 8.5 vs. 109.9 ± 9.2, respectively). Meanwhile, there was no significant difference between ipsi- and contralateral sides of the SNc in the knockout animals that received HA-AKT. (88.2 ± 7.4 vs. 90.9 ± 8.0, respectively). To verify whether the loss of TH immunoreactivity was in fact a result of the death of dopaminergic neurons and not loss of expression, we stained for cresyl violet and assessed neuronal survival in the MTN region of the SNc. Similarly, a substantial rescue was observed in the wild-type mice (62.8 ± 1.9% vs. 50.7 ± 3.0%, ipsilateral vs. contralateral), whereas no protective effect was observed when injecting HA-AKT in the DJ-$1^{-/-}$ mice (48.9 ± 3.0% vs. 51.9 ± 4.0% ipsilateral vs. contralateral) (Fig. S1). To further substantiate the SNc neuronal survival results, we examined whether prophylactic administration of virus could rescue dopaminergic terminals in the striatum of the animals subjected to MPTP injection in each group using expression of dopamine transporter (DAT) as a marker of dopaminergic terminals. Consistent with SNc results, higher densities, and thus greater survival of dopaminergic terminals, were observed following MPTP treatment in the striatum of virus-injected sides compared to the contralateral sides in the AKT-expressing group (97.0 ± 5.0 vs. 54.5 ± 7.6 for HA-AKT, respectively) (Fig. 4*F*). Such protection was not observed in DJ-$1^{-/-}$ animals, which signifies that the AKT-mediated neuroprotection is dependent upon the presence of DJ-1. In line with our observations in vitro and in vivo, myristoylated AKT (Myr-AKT) provides protection to both DJ-$1^{-/-}$ and DJ-$1^{+/+}$ animals (87.5 ± 5.0 ipsilateral vs. 41.9 ± 5.2 contralateral, and 102.0 ± 7.1 ipsilateral vs. 64.7 ± 6.0 contralateral, respectively). All viruses were also injected without MPTP treatment to note effects of virus toxicity. No significant death of SNc neurons was attributed to viral vectors.

DJ-1 Modulates AKT Translocation to Membranous Fractions. Our results in vitro and in vivo demonstrated specifically that myristoylated rather than a wild-type form of AKT promotes protection in DJ-$1^{-/-}$ neurons. We therefore tested whether DJ-1 was affecting AKT translocation to membranous compartments following oxidative stress. This was done by determining the subcellular localization of AKT following H_2O_2 treatment in DJ-$1^{+/+}$ and DJ-$1^{-/-}$ neurons and MEFs. As shown in Fig. 5*A*, the H_2O_2-induced AKT localization to the membrane fraction is greatly decreased in the DJ-$1^{-/-}$ compared with the DJ-$1^{+/+}$ MEFs. Quantification revealed AKT translocation to the membrane fraction following treatment that was 4-fold greater in the DJ-$1^{+/+}$ than in DJ-$1^{-/-}$ cells (2.94 ± 1.14 vs. 0.78 ± 0.30, respectively). Similarly, in DJ-$1^{-/-}$ neurons, no AKT translocation was observed following H_2O_2 (0.58 ± 0.10-fold increase), whereas DJ-$1^{+/+}$ neurons showed an AKT translocation 5 min post-treatment (1.55 ± 0.37 fold increase) No significant differences were observed in levels of total AKT in the cytoplasmic fraction.

Discussion

DJ-1 was first discovered as a weak oncogene with an unclear mechanism of action (36). Since then, putative roles for DJ-1 have been proposed, which include functions in transcriptional regulation either via binding to and modulating an androgen receptor inhibitor, PIASx-alpha (37), as well as RNA–protein

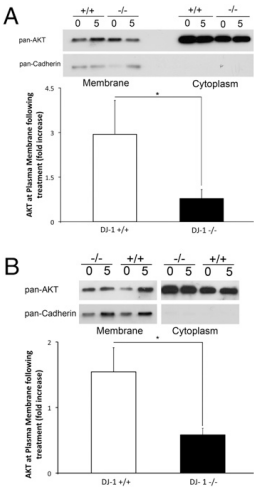

Fig. 5. AKT requires DJ-1 to localize to membranous fractions following oxidative insult. (*A*) DJ-$1^{+/+}$ and DJ-$1^{-/-}$ MEFs were treated with 500 μM of H_2O_2 for 5 min or with media control. Western blot analysis by probing pan-AKT and pan-Cadherin as membranous fraction control. Quantification of membranous fractions was performed in the lower panel by calculating relative AKT density normalized to Cadherin levels and normalizing treatment group to control. Data are representative of $n = 4$ experiments. (*B*) DJ-$1^{+/+}$ and DJ-$1^{-/-}$ cortical neurons were subjected to 100 μM of H_2O_2 for 5 min or media control. Quantification was performed as in *A*. Data are presented as mean ± SEM. *, $P < 0.05$.

interactions (38). The DJ-1 protein also displayed some homology to the proteins of the ThiJ/PfpI family of bacterial proteases (39, 40), suggesting a putative chaperone function. Interestingly, DJ-1 was also noted to display an isoelectric pH shift upon induction of oxidative stress, potentially placing DJ-1 within the oxidative stress-response pathway. Despite these important implications, its physiological relevance was not entirely clear until its genetic linkage to PD. To this end, several themes regarding DJ-1 have now emerged that link this protein to neurodegeneration, PD, and oxidative stress. These themes include, but are not limited to the following: (*i*) DJ-1 protects neurons against oxidative stress (4, 9, 11, 41–44); (*ii*) Loss of DJ-1 on its own does not lead to dopamine neuron death, at least in mice, but DJ-1-deficient animals are sensitized to environmental stress and exhibit impaired dopamine signaling (45–48); and (*iii*) DJ-1 modulates signaling pathways critical to cell survival such as PTEN and AKT, at least in select nonneuronal contexts (31).

In the present study, we more carefully characterized the necessity of DJ-1 for activation of the AKT pathway in response to oxidative injury, particularly in neurons. We first demonstrated that the absence of DJ-1 significantly attenuates AKT phosphorylation in vitro and in vivo, as well as in human lymphoblasts derived from PD patients harboring pathogenic DJ-1 mutations. Importantly, even though AKT phosphorylation is not completely abolished by loss of DJ-1, we also demonstrated that the significant attenuation in AKT signaling brought about by DJ-1 deficiency resulted in enhanced cell death both in vitro and in vivo. These data not only highlighted an important functional role for DJ-1 in AKT-mediated cell survival, but also indicated that the AKT pathway is integral to the mechanism of protection conferred by DJ-1 and suggested that DJ-1 could be an upstream regulator of AKT.

In light of our findings above, together with the knowledge that AKT is considered to be part of the survival pathway, we sought to further investigate the nature of the DJ-1/AKT relationship. We first demonstrated that overexpression of AKT alone protects cultured neurons exposed to oxidative stress in vitro as well as dopamine neurons exposed to MPTP in vivo. Furthermore, inhibition of the PI3K/Akt pathway significantly reduces the protection that is conferred by DJ-1. Importantly, we also demonstrated that wild-type AKT required DJ-1 to exert its protective effect as DJ-1 deficiency abrogated the effect of AKT on cell survival. Interestingly, the protective effects of AKT in a DJ-1-deficient background can be bypassed using myristoylated AKT, its membrane-anchored constitutively active form. This latter observation is consistent with reports that membrane-bound AKT is sufficient to provide protection following MPP^+ treatment both in vitro (49) as well as 6-OHDA treatment in vivo (50). Because AKT recruitment to the membrane is a prior event to its phosphorylation and activation (51, 52), these results, in addition to the cell fractionation experiments presented in our study, suggested that DJ-1 permits AKT translocation to the membrane fractions.

Our study therefore proposes a working model in which DJ-1 acts upstream of AKT, thereby facilitating its activation following neuronal injury via oxidative stress. We propose that DJ-1 may be involved in fine-tuning the response of neurons to ROS and modulation of signaling pathways that mediate survival. In this regard, it will be critical in future studies to address the possible mechanisms underlying the ROS-mediated, DJ-1-dependent activation of AKT. One might consider the possibility that DJ-1 regulates AKT by modulating its recruitment to the membrane in a ROS-dependent manner. It is noteworthy that the AKT response to H_2O_2 can be altered depending on antioxidant protein activity within the cell (53–55). Thus, further studies in models that permit well-controlled ROS levels are needed to address these questions. However, other possibilities exist. For example, a recent study has suggested that DJ-1 interacts with PTEN to permit AKT activation, although this needs to be further investigated in more physiologically relevant models (56). Additionally, DJ-1 may interact with other PI3K pathway kinases, such as mTOR and PDK, to permit AKT phosphorylation. Finally, while DJ-1 plays a significant role in facilitating AKT phosphorylation, other factors may also each play a role (21, 57, 58). Thus, additional studies should be performed to investigate the nature of the DJ-1/AKT interdependence.

Finally, it is interesting to note that even though it is clear that DJ-1 is linked to familial PD, there is a report of an epidemiological association with certain haplotype of AKT1 and a reduced risk of PD (59). This observation provides further strength to the notion that the DJ-1/AKT signaling axis may be important in regulating dopaminergic function or death. Elucidation of these mechanisms may provide an eventual basis for neuroprotective therapies.

Materials and Methods

Cell culture, Western blot analysis, and in vivo stereotaxic injections and MPTP administration were performed as previously described (60). All procedures involving animals were approved by the University of Ottawa Animal Care Committee and were maintained in strict accordance with the Guidelines for the Use and Treatment of Animals put forth by the Animal Care Council of Canada and endorsed by the Canadian Institutes of Health Research. For additional in vivo and in vitro procedures, see *SI Materials and Methods.*

Subcellular Fractionation. Membrane fractions were obtained similarly for MEFs and DIV 6 cortical neurons using differential centrifugation. Briefly, cells were harvested in cold PBS and centrifuged at 1,200 × *g* for 3 min. The cell pellet was resuspended in 200 μL of hypo-osmolar buffer [50 mM Tris-HCl, pH 7.4; 50 mM NaCl; protease inhibitor complex (Roche)] and homogenized for 30 s. Samples were centrifuged at 20,000 × *g*, at 4 °C for 20 min. Supernatants (cellular debris) were transferred to 1.5-mL ultracentrifuge tubes (Beckman) and centrifuged at 100,000 × *g*, at 4 °C for 3 h. The pellets (microsomal enriched) were resuspended in RIPA buffer (150 mM NaCl; 1% Nonidet P-40; 0.5% deoxycholic acid; 0.1% SDS; 50 mM Tris-HCl, pH 8.0) and sonicated briefly for subsequent Western blot analysis. Supernatants from final spin were used as a cytoplasmic control.

Statistical Analysis. Statistical significance was either determined by Student's *t*-test or one-way ANOVA followed by Tukey's post hoc test. All data are presented as mean ± SEM. Significance at $P < 0.05$ (*) and $P < 0.01$ (**), and NS denotes no significant difference.

ACKNOWLEDGMENTS. This work was supported by grants from Canadian Institutes of Health Research, Heart and Stroke Foundation of Ontario, the Canadian Stroke Network, The Centre for Stroke Recovery, Parkinson Society Canada, and Parkinson's Disease Foundation (to D.S.P), Heart and Stroke Foundation of Canada (to H.A.), Heart and Stroke Foundation of Ontario (to M.W.C.R.), Canadian Institutes of Health Research (to I.I.), and the Parkinson Society Canada (to S.J.H.), and the World Class University program through the National Research Foundation of Korea (Grant R31-2008-000-20004-0). Adenoviral constructs were provided by Dr. J. Albrecht at the Hennepin County Medical Center (Minneapolis, MN).

1. Bonifati V, et al. (2003) Mutations in the DJ-1 gene associated with autosomal recessive early-onset parkinsonism. *Science* 299:256–259.
2. Abou-Sleiman PM, Healy DG, Quinn N, Lees AJ, Wood NW (2003) The role of pathogenic DJ-1 mutations in Parkinson's disease. *Ann Neurol* 54:283–286.
3. Gu L, et al. (2009) Involvement of ERK1/2 signaling pathway in DJ-1-induced neuroprotection against oxidative stress. *Biochem Biophys Res Commun* 383:469–474.
4. Inden M, et al. (2006) PARK7 DJ-1 protects against degeneration of nigral dopaminergic neurons in Parkinson's disease rat model. *Neurobiol Dis* 24:144–158.
5. Lev N, et al. (2009) DJ-1 protects against dopamine toxicity. *J Neural Transm* 116: 151–160.
6. Canet-Avilés RM, et al. (2004) The Parkinson's disease protein DJ-1 is neuroprotective due to cysteine-sulfinic acid-driven mitochondrial localization. *Proc Natl Acad Sci USA* 101:9103–9108.
7. Taira T, et al. (2004) DJ-1 has a role in antioxidative stress to prevent cell death. *EMBO Rep* 5:213–218.
8. Kim RH, et al. (2005) Hypersensitivity of DJ-1-deficient mice to 1-methyl-4-phenyl-1,2,3,6-tetrahydropyrindine (MPTP) and oxidative stress. *Proc Natl Acad Sci USA* 102:5215–5220.
9. Lavara-Culebras E, Paricio N (2007) *Drosophila* DJ-1 mutants are sensitive to oxidative stress and show reduced lifespan and motor deficits. *Gene* 400:158–165.
10. Yang Y, et al. (2005) Inactivation of *Drosophila* DJ-1 leads to impairments of oxidative stress response and phosphatidylinositol 3-kinase/Akt signaling. *Proc Natl Acad Sci USA* 102:13670–13675.
11. Martinat C, et al. (2004) Sensitivity to oxidative stress in DJ-1-deficient dopamine neurons: an ES- derived cell model of primary Parkinsonism. *PLoS Biol* 2:e327.
12. Aleyasin H, et al. (2007) The Parkinson's disease gene DJ-1 is also a key regulator of stroke-induced damage. *Proc Natl Acad Sci USA* 104:18748–18753.
13. Andres-Mateos E, et al. (2007) DJ-1 gene deletion reveals that DJ-1 is an atypical peroxiredoxin-like peroxidase. *Proc Natl Acad Sci USA* 104:14807–14812.
14. Xu J, et al. (2005) The Parkinson's disease-associated DJ-1 protein is a transcriptional co-activator that protects against neuronal apoptosis. *Hum Mol Genet* 14:1231–1241.
15. Zhou W, Freed CR (2005) DJ-1 up-regulates glutathione synthesis during oxidative stress and inhibits A53T alpha-synuclein toxicity. *J Biol Chem* 280:43150–43158.
16. Malhotra D, et al. (2008) Decline in NRF2-regulated antioxidants in chronic obstructive pulmonary disease lungs due to loss of its positive regulator, DJ-1. *Am J Respir Crit Care Med* 178:592–604.
17. Clements CM, McNally RS, Conti BJ, Mak TW, Ting JP (2006) DJ-1, a cancer- and Parkinson's disease-associated protein, stabilizes the antioxidant transcriptional master regulator Nrf2. *Proc Natl Acad Sci USA* 103:15091–15096.
18. van der Brug MP, et al. (2008) RNA binding activity of the recessive Parkinsonism protein DJ-1 supports involvement in multiple cellular pathways. *Proc Natl Acad Sci USA* 105:10244–10249.
19. Klippel A, Kavanaugh WM, Pot D, Williams LT (1997) A specific product of phosphatidylinositol 3-kinase directly activates the protein kinase Akt through its pleckstrin homology domain. *Mol Cell Biol* 17:338–344.
20. Kohn AD, Takeuchi F, Roth RA (1996) Akt, a pleckstrin homology domain containing kinase, is activated primarily by phosphorylation. *J Biol Chem* 271:21920–21926.
21. Stambolic V, et al. (1998) Negative regulation of PKB/Akt-dependent cell survival by the tumor suppressor PTEN. *Cell* 95:29–39.
22. Sun H, et al. (1999) PTEN modulates cell cycle progression and cell survival by regulating phosphatidylinositol 3,4,5,-trisphosphate and Akt/protein kinase B signaling pathway. *Proc Natl Acad Sci USA* 96:6199–6204.
23. Crossthwaite AJ, Hasan S, Williams RJ (2002) Hydrogen peroxide-mediated phosphorylation of ERK1/2, Akt/PKB and JNK in cortical neurones: dependence on Ca(2+) and PI3-kinase. *J Neurochem* 80:24–35.
24. Sun X, et al. (2009) Insulin/PI3K signaling protects dentate neurons from oxygen-glucose deprivation in organotypic slice cultures. *J Neurochem*112:377–388.

25. Lee HJ, Kim MK, Kim HJ, Kim SU (2009) Human neural stem cells genetically modified to overexpress Akt1 provide neuroprotection and functional improvement in mouse stroke model. *PLoS One* 4:e5586.
26. Li Z, Hu Y, Zhu Q, Zhu J (2008) Neurotrophin-3 reduces apoptosis induced by 6-OHDA in PC12 cells through Akt signaling pathway. *Int J Dev Neurosci* 26:635–640.
27. Dudek H, et al. (1997) Regulation of neuronal survival by the serine-threonine protein kinase Akt. *Science* 275:661–665.
28. Malagelada C, Jin ZH, Greene LA (2008) RTP801 is induced in Parkinson's disease and mediates neuron death by inhibiting Akt phosphorylation/activation. *J Neurosci* 28: 14363–14371.
29. Heo SR, Han AM, Kwon YK, Joung I (2009) p62 protects SH-SY5Y neuroblastoma cells against H2O2-induced injury through the PDK1/Akt pathway. *Neurosci Lett* 450: 45–50.
30. Liu JH, Yin F, Guo LX, Deng XH, Hu YH (2009) Neuroprotection of geniposide against hydrogen peroxide induced PC12 cells injury: involvement of PI3 kinase signal pathway. *Acta Pharmacol Sin* 30:159–165.
31. Kim RH, et al. (2005) DJ-1, a novel regulator of the tumor suppressor PTEN. *Cancer Cell* 7:263–273.
32. Sitaram RT, et al. (2009) The PTEN regulator DJ-1 is associated with hTERT expression in clear cell renal cell carcinoma. *Int J Cancer* 125:783–790.
33. Vasseur S, et al. (2009) DJ-1/PARK7 is an important mediator of hypoxia-induced cellular responses. *Proc Natl Acad Sci USA* 106:1111–1116.
34. Meier R, Alessi DR, Cron P, Andjelković M, Hemmings BA (1997) Mitogenic activation, phosphorylation, and nuclear translocation of protein kinase Bbeta. *J Biol Chem* 272: 30491–30497.
35. Taylor JM, et al. (2004) Akt phosphorylation and NFkappaB activation are counterregulated under conditions of oxidative stress. *Exp Cell Res* 300:463–475.
36. Nagakubo D, et al. (1997) DJ-1, a novel oncogene which transforms mouse NIH3T3 cells in cooperation with ras. *Biochem Biophys Res Commun* 231:509–513.
37. Takahashi K, et al. (2001) DJ-1 positively regulates the androgen receptor by impairing the binding of PIASx alpha to the receptor. *J Biol Chem* 276:37556–37563.
38. Hod Y, Pentyala SN, Whyard TC, El-Maghrabi MR (1999) Identification and characterization of a novel protein that regulates RNA-protein interaction. *J Cell Biochem* 72:435–444.
39. Mitsumoto A, et al. (2001) Oxidized forms of peroxiredoxins and DJ-1 on two-dimensional gels increased in response to sublethal levels of paraquat. *Free Radic Res* 35:301–310.
40. Wilson MA, St Amour CV, Collins JL, Ringe D, Petsko GA (2004) The 1.8-A resolution crystal structure of YDR533Cp from *Saccharomyces cerevisiae*: a member of the DJ-1/ThiJ/PfpI superfamily. *Proc Natl Acad Sci USA* 101:1531–1536.
41. Liu M, et al. (2008) Parkin regulates Eg5 expression by Hsp70 ubiquitination-dependent inactivation of c-Jun NH2-terminal kinase. *J Biol Chem* 283:35783–35788.
42. Paterna JC, Leng A, Weber E, Feldon J, Büeler H (2007) DJ-1 and Parkin modulate dopamine-dependent behavior and inhibit MPTP-induced nigral dopamine neuron loss in mice. *Mol Ther* 15:698–704.
43. Meulener M, et al. (2005) *Drosophila* DJ-1 mutants are selectively sensitive to environmental toxins associated with Parkinson's disease. *Curr Biol* 15:1572–1577.
44. Yokota T, et al. (2003) Down regulation of DJ-1 enhances cell death by oxidative stress, ER stress, and proteasome inhibition. *Biochem Biophys Res Commun* 312: 1342–1348.
45. Yamaguchi H, Shen J (2007) Absence of dopaminergic neuronal degeneration and oxidative damage in aged DJ-1-deficient mice. *Mol Neurodegener* 2:10.
46. Pisani A, et al. (2006) Enhanced sensitivity of DJ-1-deficient dopaminergic neurons to energy metabolism impairment: role of Na+/K+ ATPase. *Neurobiol Dis* 23:54–60.
47. Park J, et al. (2005) *Drosophila* DJ-1 mutants show oxidative stress-sensitive locomotive dysfunction. *Gene* 361:133–139.
48. Goldberg MS, et al. (2005) Nigrostriatal dopaminergic deficits and hypokinesia caused by inactivation of the familial Parkinsonism-linked gene DJ-1. *Neuron* 45:489–496.
49. Salinas M, Martin D, Alvarez A, Cuadrado A (2001) Akt1/PKBalpha protects PC12 cells against the parkinsonism-inducing neurotoxin 1-methyl-4-phenylpyridinium and reduces the levels of oxygen-free radicals. *Mol Cell Neurosci* 17:67–77.
50. Ries V, et al. (2006) Oncoprotein Akt/PKB induces trophic effects in murine models of Parkinson's disease. *Proc Natl Acad Sci USA* 103:18757–18762.
51. James SR, et al. (1996) Specific binding of the Akt-1 protein kinase to phosphatidylinositol 3,4,5-trisphosphate without subsequent activation. *Biochem J* 315:709–713.
52. Franke TF, Kaplan DR, Cantley LC, Toker A (1997) Direct regulation of the Akt proto-oncogene product by phosphatidylinositol-3,4-bisphosphate. *Science* 275:665–668.
53. Taylor JM, Ali U, Iannello RC, Hertzog P, Crack PJ (2005) Diminished Akt phosphorylation in neurons lacking glutathione peroxidase-1 (Gpx1) leads to increased susceptibility to oxidative stress-induced cell death. *J Neurochem* 92: 283–293.
54. Endo H, Nito C, Kamada H, Yu F, Chan PH (2007) Reduction in oxidative stress by superoxide dismutase overexpression attenuates acute brain injury after subarachnoid hemorrhage via activation of Akt/glycogen synthase kinase-3beta survival signaling. *J Cereb Blood Flow Metab* 27:975–982.
55. Handy DE, et al. (2009) Glutathione peroxidase-1 regulates mitochondrial function to modulate redox-dependent cellular responses. *J Biol Chem* 284:11913–11921.
56. Kim YC, Kitaura H, Taira T, Iguchi-Ariga SM, Ariga H (2009) Oxidation of DJ-1-dependent cell transformation through direct binding of DJ-1 to PTEN. *Int J Oncol* 35: 1331–1341.
57. Alessi DR, et al. (1997) Characterization of a 3-phosphoinositide-dependent protein kinase which phosphorylates and activates protein kinase Balpha. *Curr Biol* 7: 261–269.
58. Sarbassov DD, Guertin DA, Ali SM, Sabatini DM (2005) Phosphorylation and regulation of Akt/PKB by the rictor-mTOR complex. *Science* 307:1098–1101.
59. Xiromerisiou G, et al. (2008) Association between AKT1 gene and Parkinson's disease: a protective haplotype. *Neurosci Lett* 436:232–234.
60. Qu D, et al. (2007) Role of Cdk5-mediated phosphorylation of Prx2 in MPTP toxicity and Parkinson's disease. *Neuron* 55:37–52.

Human Molecular Genetics, 2010, Vol. 19, No. 19 **3734–3746**
doi:10.1093/hmg/ddq288
Advance Access published on July 16, 2010

Loss of the Parkinson's disease-linked gene DJ-1 perturbs mitochondrial dynamics

I. Irrcher[1], H. Aleyasin[1], E.L. Seifert[2], S.J. Hewitt[1], S. Chhabra[1], M. Phillips[1], A.K. Lutz[4], M.W.C. Rousseaux[1], L. Bevilacqua[2], A. Jahani-Asl[1], S. Callaghan[1], J.G. MacLaurin[1], K.F. Winklhofer[4], P. Rizzu[5], P. Rippstein[3], R.H. Kim[6], C.X. Chen[7], E.A. Fon[7], R.S. Slack[1], M.E. Harper[2], H.M. McBride[3], T.W. Mak[6] and D.S. Park[1,8,*]

[1]Department of Cellular and Molecular Medicine, [2]Department of Biochemistry, Microbiology, and Immunology and [3]Ottawa Heart Institute, University of Ottawa, Ottawa, Canada, [4]Adolf Butenandt Institute, Neurobiochemistry, Ludwig Maximillians University, Munich, Germany, [5]Department of Clinical Genetics, Medical Genomics VU University Medical Center, Amsterdam, The Netherlands, [6]The Campbell Family Institute for Breast Cancer Research, University of Toronto, Toronto, Canada, [7]Department of Biochemistry, McGill University, Montreal, Canada and [8]Department of Cogno-Mechatronics Engineering, Pusan National University, Korea

Received June 2, 2010; Revised and Accepted July 7, 2010

Growing evidence highlights a role for mitochondrial dysfunction and oxidative stress as underlying contributors to Parkinson's disease (PD) pathogenesis. DJ-1 (PARK7) is a recently identified recessive familial PD gene. Its loss leads to increased susceptibility of neurons to oxidative stress and death. However, its mechanism of action is not fully understood. Presently, we report that DJ-1 deficiency in cell lines, cultured neurons, mouse brain and lymphoblast cells derived from DJ-1 patients display aberrant mitochondrial morphology. We also show that these DJ-1-dependent mitochondrial defects contribute to oxidative stress-induced sensitivity to cell death since reversal of this fragmented mitochondrial phenotype abrogates neuronal cell death. Reactive oxygen species (ROS) appear to play a critical role in the observed defects, as ROS scavengers rescue the phenotype and mitochondria isolated from DJ-1 deficient animals produce more ROS compared with control. Importantly, the aberrant mitochondrial phenotype can be rescued by the expression of Pink1 and Parkin, two PD-linked genes involved in regulating mitochondrial dynamics and quality control. Finally, we show that DJ-1 deficiency leads to altered autophagy in murine and human cells. Our findings define a mechanism by which the DJ-1-dependent mitochondrial defects contribute to the increased sensitivity to oxidative stress-induced cell death that has been previously reported.

INTRODUCTION

Parkinson's disease (PD), the second most common neurodegenerative disorder, is characterized by the progressive loss of neurons within the substantia nigra *pars compacta* (1,2). Though the pathogenic mechanisms underlying PD are not well understood, growing evidence supports a role for mitochondrial dysfunction, oxidative stress and more recently autophagy.

Mitochondrial dysfunction was initially tied to PD in studies demonstrating the presence of aberrant mitochondrial function in idiopathic PD patients (3,4). Moreover, several dopaminergic toxins acted as mitochondrial toxins by inhibiting the electron transport chain, producing toxic-free radicals in the process (5,6). Since this time, several familial PD genes, including, Parkin (PARK2), Pink1 (PARK6) and DJ-1 (PARK7), have been linked to mitochondria. Their loss results in abnormal mitochondrial morphology (7,8). Interestingly, the interplay of Pink1 and Parkin dynamically regulates mitochondrial morphology via mitochondrial fission/fusion and also affects mitochondrial quality control (9–11). As the function of Pink1 and Parkin in these contexts continues to be elucidated, the role(s) of DJ-1 is less understood.

*To whom correspondence should be addressed at: Faculty of Medicine, Department Of Cellular and Molecular Medicine (CMM), University of Ottawa, 451 Smyth Road, Ottawa, Ontario, Canada K1H 8M5. Tel: +1 6135625800 ext. 8816; Fax: +1 6135625403; Email: dpark@uottawa.ca

Homozygous loss-of-function mutations in DJ-1 (PARK7) result in early onset PD (12). Several lines of evidence, including our own, indicate that DJ-1 protects neurons against oxidative stress-induced cell death (13,14). It has been postulated that DJ-1 exerts its protective function by regulating mitochondrial homeostasis or participating in the oxidative stress response either serving as an antioxidant scavenger or a redox sensor (14–17). More recently, DJ-1 was found to affect mitochondrial quality control (18,19). Given the importance of reactive oxygen species (ROS) in regulating mitochondrial dynamics and the observations that loss of Pink1 and Parkin has also been linked to mitochondrial dysfunction, we wanted to address whether DJ-1 also affects mitochondrial dynamics and function.

Here we examined mitochondrial morphology and function in DJ-1 deficient tissues and hypothesized that loss of DJ-1 would produce a fragmented mitochondrial phenotype, accounting increased sensitivity to cell death of DJ-1 deficient neurons previously reported (14). We demonstrate that DJ-1 deficiency leads to a fragmented mitochondrial phenotype in multiple contexts including neurons and human DJ-1 patient cells. Second, we provide evidence that ROS plays a critical role in this fragmentation phenotype and that DJ-1 deficiency results in elevated ROS levels. Third, we show that this mitochondrial phenotype is an important contributor to the sensitivity to oxidative stress caused by the loss of DJ-1. Fourth, we show that Pink1 and Parkin can rescue the mitochondrial fragmentation induced by the loss of DJ-1. Finally, we also show that the loss of DJ-1 results in increased autophagic activity.

RESULTS

Loss of DJ-1 alters mitochondrial morphology and dynamics

Based upon the growing evidence for mitochondrial morphology and dynamics as underlying contributors to PD, we first investigated a role for DJ-1 in mitochondrial remodeling. Primary cortical neurons and mouse embryonic fibroblasts (MEFs) from DJ-$1^{+/+}$ or DJ-$1^{-/-}$ embryos (E15.5) were cultured. Mitochondria were quantified and binned according to length, as done previously (20). As shown in Figure 1A and quantified in Figure 1B, mitochondrial lengths in DJ-$1^{+/+}$ primary cortical neurons at 3 days *in vitro* were significantly longer and less fragmented than in DJ-$1^{-/-}$ neurons. This fragmented mitochondrial phenotype was also evident in MEFs (Fig. 1C and D) and *in vivo* in the striatum of DJ-$1^{+/+}$ and DJ-$1^{-/-}$ mice (Fig. 1E and F). Thus, the fragmented morphology appears to be a more generalized phenomenon rather than restricted to a specific cell type, occurring both *in vitro* and *in vivo*. These data demonstrate that mitochondrial morphology is altered with the loss of DJ-1.

To address whether the DJ-1-dependent mitochondrial fragmentation was related to alterations in mitochondrial fusion rates, DJ-$1^{+/+}$ or DJ-$1^{-/-}$ MEFs were transduced with a matrix-targeted photoactivatable GFP lentivirus (PA-GFP). PA-GFP was activated in ~10% of the cell using a 405 nm laser line at 75% intensity (21). Upon photoactivation, the spread of the GFP signal throughout the mitochondrial reticulum was assessed immediately post-activation and following 20 min (Fig. 2A). The data in Figure 2B demonstrate that mitochondrial fusion in MEFs is decreased by 30% DJ-$1^{-/-}$ when compared with DJ-$1^{+/+}$. Steady-state levels of the mitochondrial fission and fusion proteins, Dynamin Related Protein-1 (Drp1) and mitofusin 1 (MFN1) were also measured to determine whether the loss of DJ-1 would result in altered expression. As shown in Figure 2C, Drp1 levels were not altered, while decreases in the levels of MFN1 were observed.

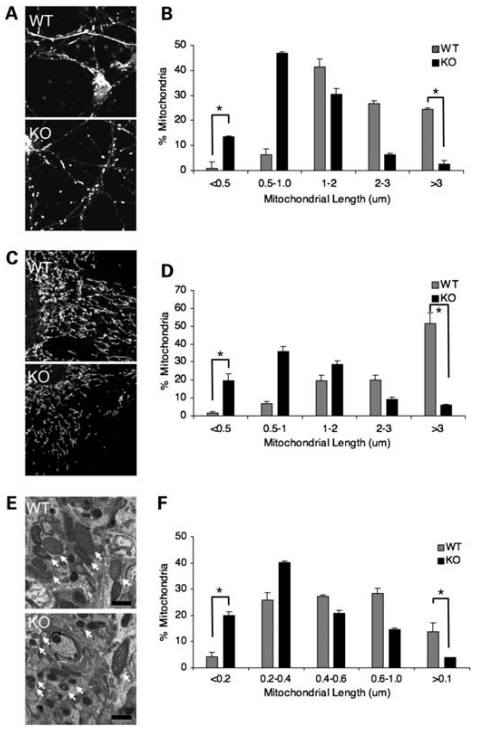

Figure 1. DJ-1 deficiency results in altered mitochondrial morphology *in vitro* and *in vivo*. (**A**) Primary cortical neurons (3 DIV) and (**C**) MEFs from wild-type (WT) and knockout (KO) DJ-1 embryos were harvested and fixed as described under Materials and Methods and immunostained with antibodies to Tom20 to visualize mitochondria. Quantification of mitochondrial lengths in (**B**) primary cortical neurons and (**D**) MEFs was done as described previously [Jahani-Asl *et al*. (20); $n = 4$ independent experiments with a minimum of 500 mitochondria/experiment counted]. Scale Bar = 2 μm. $^*P < 0.05$ versus respective +/+ control. (**E**) Electron microscopic images of WT and KO DJ-1 striatum prepared as described in Materials and Methods. (**F**) Quantification of mitochondrial diameters in the striatum of WT and KO DJ-1 mice from three mice/genotype. Scale bar = 500 nm. $^*P < 0.05$ versus respective WT DJ-1 control. DIV, days *in vitro*. White arrows in (E) depict mitochondria.

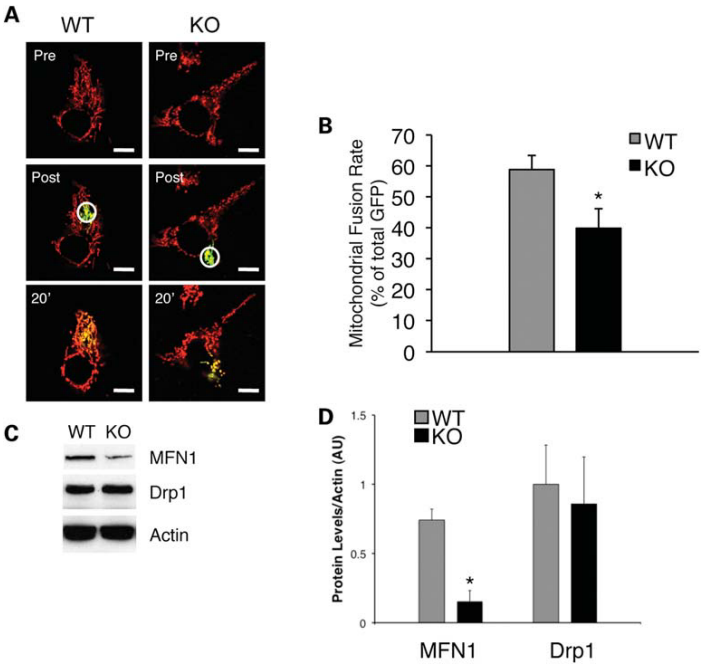

Figure 2. Mitochondrial fusion is decreased with DJ-1 deficiency. (**A**) Confocal images of mitochondria from DJ-$1^{+/+}$ (WT) and DJ-$1^{-/-}$ (KO) MEFs transduced with mitochondrial matrix-targeted DS-red and PA-GFP lentiviruses as described in the Supplementary Information. Images shown are from pre-activation (Pre), immediately following activation (Post) in a small region of interest (indicated by open white circles) as well as following 20 min (20′) of activation. (**B**) Quantification of mitochondrial fusion 20 min post-activation from DJ-$1^{+/+}$ ($n = 14$ cells) and DJ-$1^{-/-}$ ($n = 12$ cells) MEFs. (**C**) Protein extracts were made from DJ-$1^{+/+}$ and DJ-$1^{-/-}$ MEFs and subjected to western blotting for Drp-1, Mfn1 and actin (for loading control). Data shown are representative of at least three independent experiments. (**D**) Quantification of Drp1 and MFN1 protein levels, corrected with actin for loading in DJ-1 WT and KO MEFs. $^{*}P < 0.05$.

Rescue of mitochondrial length in DJ-$1^{-/-}$ neurons abrogates neuronal cell death

Our previous work has shown that overexpression of DJ-1 protects primary cortical neurons from oxidative stress (14). Here we report that DJ-1 deficiency promotes mitochondrial fragmentation. To determine whether these phenomena are linked, primary cortical neurons from DJ-$1^{+/+}$ and DJ-$1^{-/-}$ embryos were infected with dominant-negative dynamin-related protein 1 (DRP1K38E), a mutant form of the mitochondrial fission factor that promotes an elongated mitochondrial reticulum when expressed in cells. Expression levels of Drp1 K38E are shown in Figure 3A and were previously described (21). When primary cortical neurons were subjected to oxidative stress in the form of MPP^{+} (10 μM), a metabolite of the parkinsonism-inducing drug MPTP (22) for 48 h, the hypersensitive DJ-$1^{-/-}$ neurons showed an increase in cell death. However, DJ-$1^{-/-}$ cortical neurons infected with DRP1K38E were completely protected from the toxic effects of MPP^{+} suggesting that mitochondrial fragmentation contributes to oxidative stress-induced sensitivity to cell death (Fig. 3B).

NAC treatment rescues the mitochondrial phenotype in DJ-$1^{-/-}$ neurons

ROS can significantly influence mitochondrial morphology, producing a fragmented phenotype (23). Thus, to assess whether the DJ-1-dependent mitochondrial morphology is related to ROS, we determined whether quenching with N-acetyl-L-cysteine (NAC) might affect mitochondrial fragmentation observed in DJ-1 deficient cells. DJ-$1^{+/+}$ and DJ-$1^{-/-}$ primary cortical neurons were incubated with the ROS scavenger NAC (1 mM) for 48 h (Fig. 4A). Quantification of mitochondrial lengths in vehicle-treated (VEH) DJ-$1^{+/+}$ and DJ-$1^{-/-}$ neurons revealed a similar pattern of mitochondrial morphology deficits as described in Figure 1. While treatment with NAC did not significantly alter mitochondrial length in the DJ-$1^{+/+}$ neurons, treatment of DJ-$1^{-/-}$ neurons with NAC completely reversed the mitochondrial fragmentation where the percentage of mitochondria exhibiting lengths greater than 3 μm increased (i.e. $1.14 \pm 0.305\%$ in KO-VEH to $32.144 \pm 3.141\%$ in KO-NAC; Fig. 2B) and the percentage of fragmented mitochondria decreased (i.e.

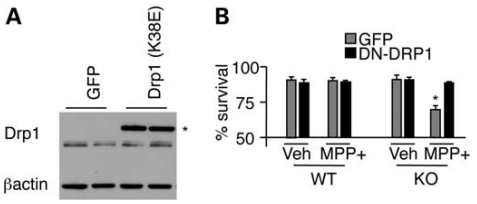

Figure 3. Mitochondrial length is critical for neuronal cell survival. (**A**) Primary cortical neurons infected with either GFP or DN-Drp1 were treated with vehicle (Veh) or MPP+ (10 μM) for 24 h. (**B**) Cell survival was assessed by counting infected cells with intact or dead nuclei plotting the ratio of live:dead cells in treated and untreated DJ-$1^{+/+}$ and DJ-$1^{-/-}$ ($n = 3$ independent experiments, each experiment was performed in triplicate).

<0.5 μm; 15.928 ± 3.03% in KO-VEH versus 0.198 ± 0.038% in KO-NAC; Fig. 4B), suggesting that elevated levels of ROS can cause mitochondrial fragmentation, which can be reversed if ROS levels are reduced.

Wild-type DJ-1 but not the DJ-1 C106A mutant rescue mitochondrial morphology defects

It has been previously reported that DJ-1 exerts its effect on oxidative stress via an isoelectric pH shift resulting in a more acidic molecule (24). Importantly, the residue that appears to be sensitive to oxidative modification, in particular hydrogen peroxide-induced oxidation, is a cysteine residue in position 106 (25,26). Thus, to provide additional relevance for the role of ROS and the importance of DJ-1 and oxidative stress in the regulation of mitochondrial morphology, we investigated whether DJ-1 itself actively regulates mitochondrial morphology and to further ascertain whether the DJ-1 mutant that is defective in handling ROS would fail to rescue the DJ-1 deficient phenotype. DJ-$1^{+/+}$ and DJ-$1^{-/-}$ cortical neurons were infected with adenoviruses encoding GFP (as a control), wild-type DJ-1 (DJ-1) or an oxidant mutant form of DJ-1 (C106A). This DJ-1 mutant harbors a cysteine to alanine point mutation at amino acid 106 rendering the oxidative capacity of DJ-1 non-functional. Expression levels of viruses are shown in Supplementary Material, Fig. S1. As shown in Figure 5A and quantified in Figure 5B, DJ-$1^{+/+}$ or DJ-$1^{-/-}$ cortical neurons infected with GFP virus alone display the wild-type mitochondrial phenotype as shown in Figure 1, demonstrating that viral expression of GFP alone does not significantly alter mitochondrial length. Next, while overexpression of DJ-1 had no effect on mitochondrial morphology in DJ-$1^{+/+}$ neurons, DJ-1 expression in DJ-$1^{-/-}$ neurons increased the percentage of mitochondria exhibiting lengths greater than 3 μm (5.15 ± 0.826% in KO-GFP versus 47.97 ± 12.51% in KO DJ-1) and decreased the percentage of fragmented mitochondria (42.00 ± 2.56% in KO-GFP versus 1.403 ± 1.4% in KO DJ-1) supporting the idea that wild-type DJ-1 plays a role in regulating mitochondrial morphology. On the other hand, the oxidant mutant C106A cannot recapitulate the full rescue displayed by WT DJ-1 indicating that the redox function of DJ-1 is critical in promoting a fused mitochondrial reticulum.

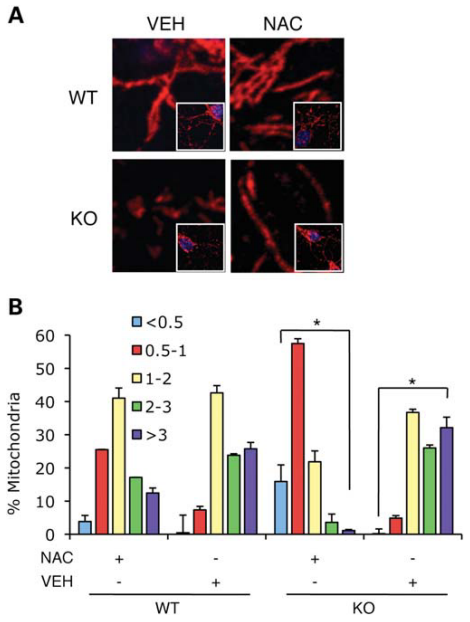

Figure 4. NAC rescues the mitochondrial morphology in DJ-1-deficient primary cortical neurons. (**A**) Confocal images of neurons taken from vehicle- (VEH) and NAC-treated (NAC) WT and KO neurons. Neurons were harvested and fixed 48 h post-treatment and immunostained with antibodies to Tom20 (red) to visualize mitochondria. Scale bar = 2 μm. Inset: lower magnification images. (**B**) Quantification of mitochondrial lengths as described previously [Jahani-Asl *et al.* (20); $n = 3$ independent experiments with a minimum of 500 mitochondria/experiment were counted]. Scale bar = 2 μm. *$P < 0.05$ versus respective controls.

DJ-1 deficiency alters ROS production

If ROS were indeed important in promoting the fragmented mitochondrial phenotype induced by DJ-1 deficiency, we would expect that ROS production would be elevated in mitochondria isolated from DJ-$1^{-/-}$ mice when compared with DJ-$1^{+/+}$ controls. Accordingly, we isolated mitochondrial fractions from brain and skeletal muscle; tissues typically associated with high metabolic requirements and mitochondria and are therefore significant sources of ROS. As predicted, we observed that H_2O_2 production in mitochondria isolated from DJ-$1^{-/-}$ mice is increased 1.4-fold ($P < 0.05$) compared with DJ-$1^{+/+}$ controls in both brain (Fig. 6) and skeletal muscle (Supplementary Material, Fig. S2A), respectively. In either tissue, H_2O_2 production in the DJ-$1^{-/-}$ animals was not further increased with the addition of the mitochondrial Complex I inhibitor rotenone, suggesting that ROS production in DJ-1 deficient mitochondria is generated primarily via Complex I. Despite the increased H_2O_2 production, we did not observe gross differences in mitochondrial function

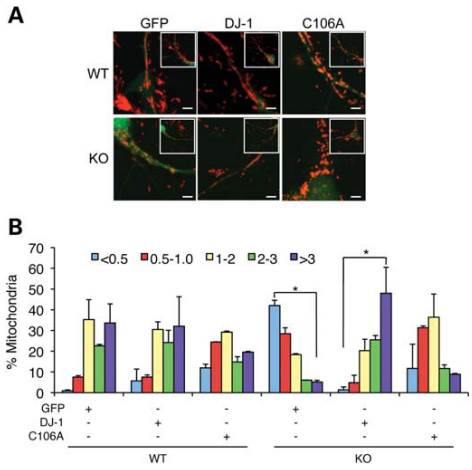

Figure 5. Restoration of wild-type mitochondrial phenotype upon re-expression of DJ-1 *in vitro*. (**A**) Confocal images from WT and KO DJ-1 primary cortical neurons infected with GFP, GFP-DJ-1 and GFP-DJ-1 C106A adenoviruses as described in Materials and Methods. Neurons were harvested and fixed 48 h post-infection and immunostained with antibodies to Tom20 (red) to visualize mitochondria. Inset: lower magnification images. (**B**) Quantification of mitochondrial lengths as described previously [Jahani-Asl *et al.* (20); $n = 3$ independent experiments with a minimum of 500 mitochondria/experiment that were counted per condition]. $^{*}P < 0.05$ versus respective controls.

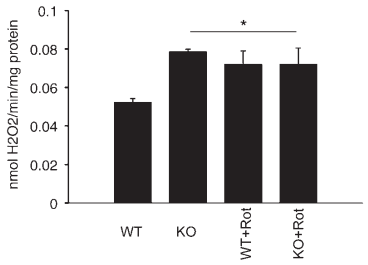

Figure 6. Brain mitochondria isolated from DJ-1 deficient animals produce more ROS. H_2O_2 production was measured in mitochondria isolated from WT and KO DJ-1 brains. $^{*}P < 0.05$ versus WT DJ-1 (P/M, pyruvate/malate; Rot, rotenone).

measurements that were performed such as mitochondrial respiration and citrate synthase activity in DJ-1$^{-/-}$ mice, at least in the brain (Supplementary Material, Fig. S2B and S2C). However, it should be noted that both mitochondrial respiration and citrate synthase activity were decreased in skeletal muscle (Supplementary Material, Fig. S2D and S2E).

Pink1 and Parkin rescue mitochondrial length in DJ-1$^{-/-}$ primary cortical neurons

Previous work conducted in *Drosophila* has demonstrated that Pink1 and Parkin participate in mitochondrial remodeling and are part of the same genetic pathway where Pink1 is upstream of Parkin (9–11,27–29). More recent evidence in mammalian cells is supportive of this notion and also implicates Parkin and Pink1 in the regulation of autophagy, a lysosomal degradation pathway responsible for the degradation of damaged proteins and organelles, including mitochondria (29–31). Thus, we determined whether Pink1 and Parkin could rescue the mitochondrial phenotype in DJ-1$^{-/-}$ primary cortical neurons. Accordingly, we infected DJ-1$^{+/+}$ and DJ-1$^{-/-}$ primary cortical neurons with Pink1 and Parkin viruses, and quantified mitochondrial length as before. Viral expression of Parkin was confirmed in Supplementary Material, Fig. S3. Viral expression of Pink1 was previously described (32). As shown in Figure 7A and C and quantified in Figure 7B and D, overexpression of either Pink1 or Parkin in DJ-1$^{-/-}$ primary cortical neurons promoted an increase in the percentage of mitochondria that were greater than 3 μm in length (5.151 ± 0.826% in KO-GFP versus 44.08 ± 1.646% in KO-Pink; Fig. 7B and 1.686 ± 0.133% in KO-GFP versus 30.126 ± 8.068% in KO-Parkin; Fig. 7D) and decreased the percentage of fragmented mitochondrial (i.e. <0.5 μm; 42.00 ± 2.562%; Fig. 7B in KO-GFP versus 0.948 ± .271% in KO-Pink1 and 34.108 ± 5.50% in KO-GFP versus 4.888 ± 2.924% in KO-Parkin; Fig. 7D) respectively, suggesting that both Pink1 and Parkin can rescue the fragmentation phenotype observed with the loss of DJ-1.

To further confirm these findings, we also quantified the percentage of cells that contained fragmented mitochondria a dopaminergic cell line (SH-5Y5Y) in which DJ-1 was transiently knocked down and subsequently overexpressed with Parkin or Pink1. Confirmation of DJ-1, Pink1 and Parkin overexpression is shown in Supplementary Material, Fig. S4A, S4B and S4C, respectively. As seen in DJ-1$^{-/-}$ primary cortical neurons, transient knockdown of DJ-1 produced a significant increase in cells exhibiting fragmented mitochondria and this phenotype could be prevented with overexpression of DJ-1, Pink1 or Parkin (Fig. 7E and F).

DJ-1 deficiency results in enhanced autophagic flux

As mentioned above, Pink1 and Parkin have both been implicated in the regulation of autophagy in response to mitochondrial damage (9–11,30,31). Our present data show that the loss of DJ-1 leads to increased mitochondrial ROS production and fragmentation. Since both of these parameters are linked with autophagy, we evaluated whether a downstream autophagic response might also be altered with DJ-1 deficiency. To this end, we employed conventional autophagy assays including the evaluation of steady-state microtubule-associated protein light chain 3-II (LC3-II) and the LC3-associated protein p62, under basal conditions as well as GFP-LC3 puncta formation (33). As shown in Figure 8A, the markers

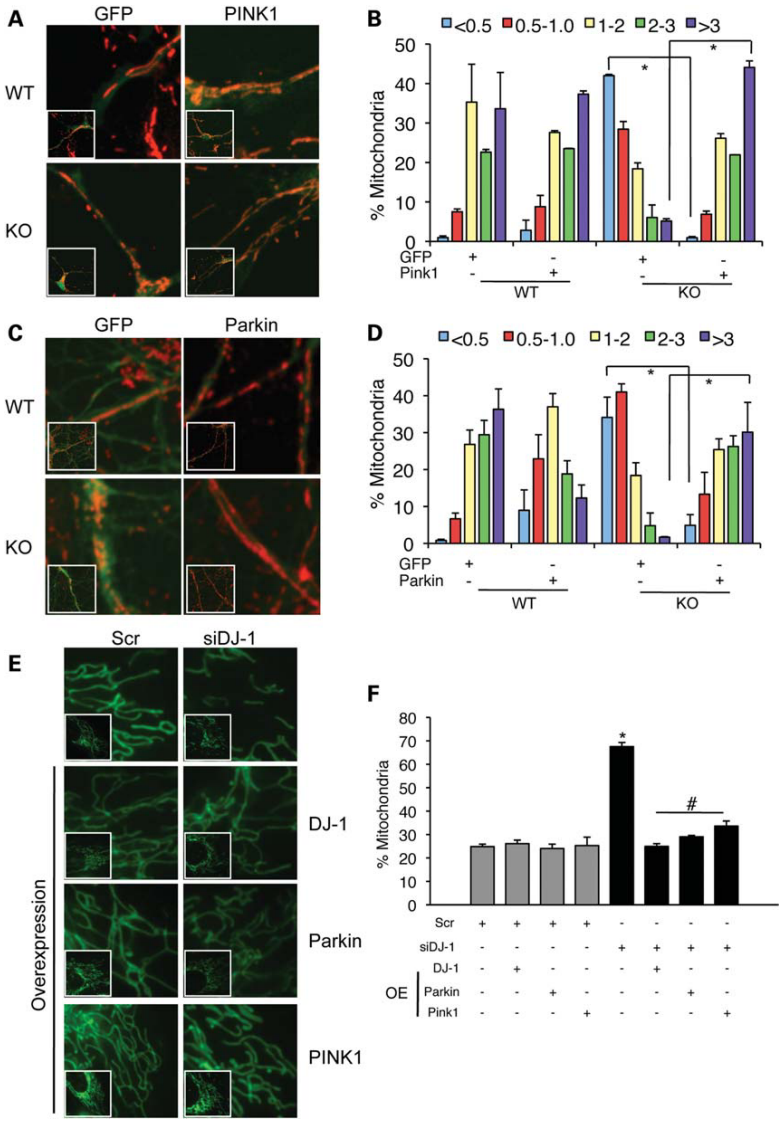

Figure 7. Rescue of mitochondrial morphology with Pink1 and Parkin in a DJ-1-deficient background. (**A**) Confocal images from WT and KO DJ-1 primary cortical neurons infected with GFP or GFP-PINK1 adenoviruses as described in Materials and Methods. Neurons were harvested and fixed 48 h post-infection and immunostained with antibodies to Tom20 (red) to visualize mitochondria. Inset: lower magnification images. (**B**) Quantification of mitochondrial lengths as described previously [Jahani-Asl *et al.* (20); $n = 3$ independent experiments with a minimum of 500 mitochondria/experiment that were counted per condition]. Scale bar = 5 μm. $^{*}P < 0.05$ versus respective controls. (**C**) Confocal images from WT and KO DJ-1 primary cortical neurons infected with eGFP or eGFP-Parkin adeno-associated viruses as described in Materials and Methods. Neurons were harvested and fixed 4 days post-infection and immunostained with

of autophagy p62 and LC3-II levels in DJ-$1^{-/-}$ mouse embryonic fibroblasts (MEFs) are decreased compared with DJ-$1^{+/+}$ controls, indicating that the loss of DJ-1 results in a reduction in autophagosomes since levels of LC3-II correlate with autophagosome number (34,35). This reduction can either be attributed to the downregulation of autophagosome formation or enhanced autophagic degradation (34). The use of bafilomycin A1, a late inhibitor of autophagy (34), restores steady-state p62 as well as LC3-II protein levels suggesting that the loss of DJ-1 enhances autophagic degradation, in other words autophagic activity is overactive. Next, we made use of the H1299 cell line in which GFP-LC3 is stably expressed and transiently reduced DJ-1 protein levels via siRNA to confirm the DJ-1-dependent perturbations in the autophagic pathway. As shown in Figure 8B, at 48 h post-transfection, the level of DJ-1 was significantly reduced upon transfection of a siRNA specifically targeted to DJ-1. The effect of DJ-1 knockdown was accompanied by a significant decrease in p62 levels, and an increased accumulation of cleaved GFP demonstrating that autophagic activity is enhanced by transient knockdown of DJ-1 (Fig. 8B). This was further observed with immunofluorescence where GFP puncta formation was increased by 1.5-fold ($P < 0.05$) with transient knockdown of DJ-1 (Fig. 8C and D). Given the recent involvement of Parkin and PINK1 in the regulation of mitochondria specific autophagy (mitophagy), we also assessed the steady-state levels of mitochondrial markers to determine whether DJ-1 may also play a role. As shown in Figure 8E, loss of DJ-1 does not induce significantly altering the expression of *cytochrome c* oxidase (COX) subunits of complex I or complex V. Furthermore, expression of the outer mitochondrial membrane marker Tom20 was also unchanged. This suggests that mitophagy, at least at a gross level, is not affected by the loss of DJ-1. This theory is supported by initial observations that Parkin is not significantly recruited to mitochondria in DJ-1 KO cells under basal conditions (Joselin *et al*., unpublished data).

Mitochondrial morphology and autophagy are also perturbed in human DJ-1-linked Parkinson's disease

Finally, to provide evidence that the DJ-1-dependent perturbations in mitochondrial homeostasis also extend to a human model of DJ-1-linked PD, we obtained human lymphoblasts isolated from control and PD patients. The PD lymphoblasts were obtained from an Italian and Dutch family, respectively (12). The previously described L166P pathogenic mutation found in the Italian family consists of a leucine to proline substitution at amino acid 166, while the Deletion (Del) mutation, found in a Dutch family, results from a complete loss of exons 1–5 (12). As shown in Figure 9A, similar to the pattern of mitochondrial morphology observed in DJ-$1^{+/+}$ and DJ-$1^{-/-}$ murine tissues, electron microscopic analysis of lymphoblasts isolated from human PD patients (L166P, DEL) contained a greater percentage of fragmented mitochondria compared with control lymphoblasts (i.e. <0.5 μm; $41.578 \pm 2.41\%$ and $48.316 \pm 6.02\%$ in PD versus $12.62 \pm 3.03\%$ and $9.755 \pm 2.23\%$ in controls) and a smaller percentage of mitochondria that were longer than >1.0 μm ($23.019 \pm 0.84\%$ and $23.997 \pm 0.94\%$ in PD versus $41.578 \pm 2.41\%$ and $48.316 \pm 6.02\%$ in controls; Fig. 9B). We also evaluated whether autophagy was similarly affected in human DJ-1-linked PD and observed that p62 was decreased in both PD patient cell lines when compared with CTRL lymphoblasts (Fig. 9C). These data confirm that the mitochondrial morphology as well as changes in autophagic markers observed in DJ-$1^{+/+}$ and DJ-$1^{-/-}$ are also present in human DJ-1-linked PD.

DISCUSSION

Mitochondrial dysfunction appears to contribute to the progression of sporadic PD and it has been postulated that excess ROS produced as the result of mitochondrial dysfunction may be an important reason for which neurons exhibit increased sensitivity to oxidative stress-induced neuronal cell death (36,37). Emerging evidence points to underlying defects in mitochondrial morphology and dynamics as a potential mechanism to explain this increased sensitivity (38). In PD, this relationship is significant since several PD-linked genes (DJ-1, Parkin, Pink1) have been found to reside or translocate to the mitochondrial compartments (7,8,29,39–42), participate in mitochondrial remodeling (7,9–11) and actively regulate mitochondrial quality control (18,19,41–43). Of the three PD-linked genes that have been associated with mitochondria, the least is known regarding the role of DJ-1.

Mitochondrial morphology, dynamics and ROS production are altered by the loss of DJ-1

We first began our investigation by characterizing the impact of DJ-1 deficiency on mitochondrial morphology and function under steady-state conditions in a variety of experimental systems. We demonstrated both *in vitro* and *in vivo* neuronal and non-neuronal cells, as well as in brain tissue that mitochondria are significantly more fragmented with the loss of DJ-1. Importantly, we also extended these findings to human DJ-1-linked PD to convincingly implicate that an aberrant DJ-1-dependent mitochondrial phenotype in a more disease relevant model. We also demonstrated that the mitochondrial phenotype produced by the loss of DJ-1 contributes to the

antibodies to Tom20 (red) to visualize mitochondria. Inset: lower magnification images. (**D**) Quantification of mitochondrial lengths as described previously [Jahani-Asl *et al*. (20); $n = 3$ independent experiments with a minimum of 500 mitochondria/experiment that were counted per condition]. Scale bar = 5 μm. $^{*}P < 0.05$ versus respective controls. (**E**) Confocal images from SH-5Y5Y cells in which DJ-1 has been knocked down via siRNA, and transfected with DJ-1, Parkin or PINK1 as described in the Materials and Methods. Inset: lower magnification images. (**F**) Quantification of at least 300 cells/condition was performed as described in the Materials and Methods. Data are representative of at least three independent experiments where each condition was done in triplicate. OE, overexpression. Scale bar = 5 μm. $^{*}P < 0.05$ versus siDJ-1- and $^{\#}P < 0.05$ versus siDJ-1.

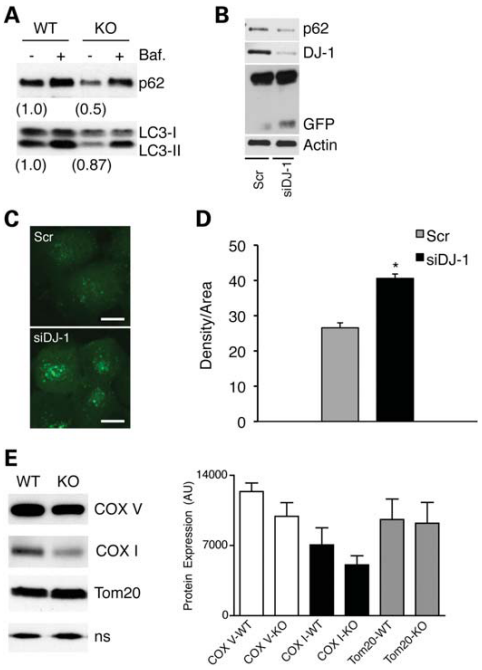

Figure 8. Cells deficient for DJ-1 undergo enhanced autophagic activity. (**A**) Proteins were extracted from WT and KO DJ-1 MEFs treated with (+) or without (−) Bafilomycin (10 μg/ml, 3 h) and subjected to western blotting for p62 and LC3-I and LC3-II levels. Numbers below representative images refer to fold changes versus WT (-Baf) after correction for actin. Data are representative of three independent experiments. (**B**) Total cell lysates from H1299 cells stably expressing GFP-LC3 and transfected with either scrambled (Scr) or a siRNA against DJ-1 (siDJ-1) were analyzed by western blotting for DJ-1, p62 and free GFP. Data are representative of at least three independent experiments. (**C**) Confocal images of H1299 cells stably expressing GFP-LC3 cells transfected with either scrambled (Scr) or a siRNA against DJ-1 (siDJ-1). (**D**) The density of GFP puncta in Scr versus siDJ-1 conditions was analyzed in at least 150 cells/condition. Data are representative of three independent experiments $^{*}P < 0.05$, siDJ-1 versus. Scr. control. Scale bar = 2 μm. (**E**) Total cell lysates from DJ-1 WT and KO MEFs were subjected to western blotting for COX V, COX I and Tom20 levels (n.s., non-specific band was used as a loading control). Data are representative of five to seven independent experiments.

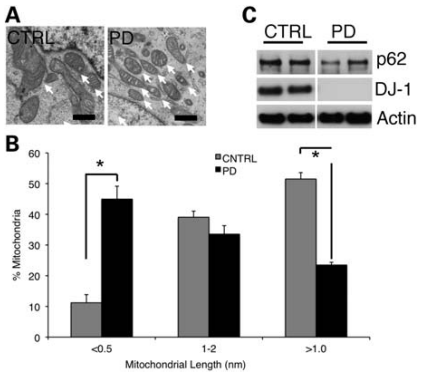

Figure 9. Mitochondrial morphology and autophagy are also perturbed in human DJ-1-linked PD. (**A**) EM images of mitochondria from human lymphoblasts isolated from healthy control (C48 and GEPA) and PD (L166P and Del) patients. (**B**) Quantification of mitochondrial diameters in human lymphoblasts ($n = 4$; at least 200 mitochondria/experiment were counted). Scale bar = 500 nm. $^{*}P < 0.05$, PD versus control. (**C**) Total protein was extracted from human control (CTRL), and PD (L166P and Del) lymphoblasts were subjected to western blotting for DJ-1, p62 and actin. Data are quantified as the relative changes in steady state protein levels corrected for loading using actin. Five independent experiments are represented. $^{*}P < 0.05$, PD versus control. White arrows in (A) depict mitochondria.

oxidative stress-induced sensitivity to cell death since reversal of the mitochondrial phenotype by overexpression of DN-Drp1 to rescue mitochondrial fragmentation abrogated neuronal cell death induced by MPP+. Is the fragmented phenotype a result of increased fission or decreased fusion? Since mitochondrial fusion rates and the steady state levels of the mitochondrial fusion protein MFN1 are decreased in DJ-1 deficient cells, we would be tempted to speculate that mitochondrial fusion is decreased. However, our results also do not rule out that an increase in mitochondrial fission is also a possibility. Indeed, during the preparation of this manuscript, Krebiehl *et al.* (44) demonstrated that altered mitochondrial morphology induced by the loss of DJ-1 could be attributed to changes in mitochondrial fission. The implications of decreased or increased mitochondrial fusion or fission that occurs with DJ-1 deficiency could readily explain the increased sensitivity of these cells to oxidative stress (14), as it is known that fragmented mitochondria precedes apoptosis, or alternatively renders mitochondria more susceptible to death-inducing stimuli (20,45–48).

ROS is important in establishing the DJ-1-dependent phenotype

Based on the known impact of excess ROS on mitochondrial morphology (23), we suspected that the increased ROS produced by mitochondria from DJ-$1^{-/-}$ animals could be responsible for the fragmented phenotype. Indeed, we confirmed this hypothesis by first demonstrating that scavenging ROS with the use of NAC or WT DJ-1 (itself a suspected free radical scavenger), but not an oxidant mutant of DJ-1 (C106A), was able to rescue the fragmented phenotype observed in DJ-1 deficient primary cortical neurons. Our data also show that while the excess H_2O_2 produced within mitochondria by the loss of DJ-1 is sufficient to alter mitochondrial morphology, they are not produced in sufficient concentrations to cause overt changes in mitochondrial oxygen consumption and citrate synthase activity, at least in the

brain. In all likelihood, these factors contribute to the lack of any gross neuronal abnormalities including dopaminergic neuron numbers in the substantia nigra, fiber densities and dopamine levels in the striatum and the absence of any behavioral deficits in untreated DJ-1 deficient mice (14). It is therefore more likely that DJ-1 deficiency compromises the sub-cellular milieu rendering them more vulnerable to additional stress. Indeed, the observation that DJ-1 deficiency does not seem to grossly affect mitophagy leading to the accumulation, instead of the removal of fragmented mitochondria further adds to this possibility. This theory is also supported by initial observations that Parkin is not significantly recruited to mitochondria in DJ-1 KO cells under basal conditions (Joselin *et al*., unpublished data).

Indeed, as we have previously demonstrated, DJ-1 deficient animals/cells are hypersensitive to MPTP or hydrogen peroxide treatment and this hypersensitization results in the previously described dopaminergic cell death and behavioral deficits, effectively recapitulating some pathological and clinical features of human PD (14).

Pink1 and Parkin can rescue DJ-1 deficient mitochondrial fragmentation

We also assessed the relationship of DJ-1 with Parkin and Pink1, two recessively linked PD genes, as they have all been implicated in regulating aspects of mitochondrial morphology and/or dynamics. Previous studies using the *Drosophila melanogaster* model have shown that the loss of Pink1 and Parkin independently compromise mitochondrial integrity (9,11,28,49). Since double mutants produce an identical phenotype to each mutant alone, and overexpression of Parkin rescues Pink1 deficits but not *vice versa*, it was postulated that they function in the same pathway with Pink1 positioned upstream of Parkin (9,11,28,49). More recently, it has been shown that Pink1 and Parkin actively participate in mitochondrial quality control (18,19,41–43). Given that DJ-1 deficiency induces oxidative stress and mitochondrial defects, we hypothesized that overexpression of these mitochondrial quality control factors would rescue the DJ-1 deficient mitochondrial phenotype. We confirmed this hypothesis using two different models. First, Pink1 and Parkin were overexpressed in DJ-1 deficient primary cortical neurons. In this model, overexpression of either Pink1 or Parkin rescued the fragmented mitochondrial phenotype in DJ-1 deficient cells. Second, we used a dopaminergic cell line to overexpress Pink1 and Parkin in cells where DJ-1 levels were reduced down by siRNA. Similar to our findings in primary cortical neurons, the DJ-1-induced fragmentation phenotype produced by knockdown of DJ-1 was reversed with overexpression of either Pink1 or Parkin. It is important to stress that the exact mechanistic link between DJ-1 and Pink/Parkin is not clear. However, we would propose that DJ-1 somehow modulates the actions or activity of Pink1 and/or Parkin, possibly via its effect on the ROS environment. Given the effects of Parkin and PINK1 deficiency on antioxidant capacity and ROS production (50–52), it is also tempting to speculate that overexpression of either gene could potentially ameliorate that ROS milieu of the DJ-1 deficient cells, thereby reversing the fragmented phenotype. Alternatively, a more direct regulation is also possible.

DJ-1 deficiency increases autophagic activity

Increasing evidence has implicated several PD-linked genes including Pink and Parkin in the process of autophagy (18,19,41–43). Two recently published studies have now implicated DJ-1 (19,44). We also pursued this phenomenon in the present manuscript and suggest that the loss of DJ-1 promotes enhanced autophagy resulting in increased turnover. According to Mizushima and Yoshimori (34) and Rubinsztein *et al*. (35), a loss in the levels of the autophagy markers LC3-II and p62 at a given time is either attributed to a downregulation of autophagosome formation or enhanced degradation. If the level of LC3-II or p62 rises following incubation with autophagy inhibitors such as Bafilomycin A1, as was seen in the present study, it is considered that during the course of the experimental time frame that the number of molecules degraded exceeds the number being produced. We further assessed the effect of transient DJ-1 knockdown on autophagic activity and found that within 48 h of DJ-1 knockdown, the autophagy was increased, as measured by the decrease in p62 levels and the increase in LC3 puncta formation. It has previously been shown that following acute starvation, autophagy is increased and that prolonged starvation leads to excessive activity and turnover (35). Acute starvation led to decreased p62 levels and LC3 puncta formation, whereas a complete loss of LC3-II levels was observed during prolonged starvation. By analogy, one could interpret that acute DJ-1 knockdown results increase autophagic activity, while germline deletion is associated with excessive autophagic activity resulting in increased turnover. In either condition, autophagic activity is enhanced with DJ-1 deficiency. Future studies will more carefully evaluate the nature of this phenomenon. Additionally, whether DJ-1 more directly regulates the autophagic response or merely influences the ROS environment leading to increased flux is unknown and warrants further study. The evidence suggesting that ROS triggers autophagy would be in keeping with the latter suggestion (53–55). Furthermore, the idea that DJ-1 participates in the Pink1/Parkin pathway temptingly suggests the possibility that DJ-1 could modulate Pink1/Parkin activity and thereby regulate autophagic activity. Alternatively, DJ-1 may more directly regulate additional upstream activators of autophagy, including mTOR and AMPK, which has been suggested previously (19). More careful analyses will be required to validate these possibilities.

In conclusion, this study demonstrates that DJ-1 plays an active role in the remodeling of mitochondria and regulation of autophagy. Cells lacking DJ-1 display a fragmented mitochondrial morphology that can be rescued with ROS scavengers, wild-type DJ-1, Parkin and Pink1. This DJ-1-dependent mitochondrial morphology contributes to oxidative stress-induced sensitivity to cell death since reversal of this mitochondrial phenotype abrogates neuronal cell death. Finally, we also show that DJ deficiency leads to altered autophagy in DJ-1-deficient murine and human cells. We propose that under conditions of oxidative stress, these derangements may account for the reported increased sensitivity to cell death of DJ-1 deficient neurons.

MATERIALS AND METHODS

Antibodies

The following antibodies were used in this study: mouse anti-Drp-1 (BD Transduction), chicken anti-MFN1 (Novus Biological), rabbit anti-MFN2 (Santa Cruz), mouse anti-COX V (Mitosciences), mouse anti-COX I (Mitosciences), rabbit anti-Tom20 (Santa Cruz), rabbit anti-LC3 (Novus Biologicals), guinea pig anti-p62 (ARP), mouse anti-p62 (Santa Cruz), mouse anti DJ-1 (Stressgen), mouse anti-parkin mouse PRK8 (Santa Cruz), anti-PINK1 polyclonal antibody (Novus Biologicals), anti-DJ1 polyclonal antibody (Abcam),mouse anti-&β-cactin (Sigma), horseradish peroxidase-conjugated secondary antibodies (Bio-Rad).

Cell lines, transfections, viral infections and plasmids

MEFs and primary cortical neurons were derived from E14.5–15.5 transgenic DJ-1 animals as previously described (14). Immortalized human lymphoblasts obtained from DJ-1-linked PD (Del or L166P) or healthy controls were cultured as described previously (56). H1299 cell line stably expressing GFP-LC3 cultured as previously described (57). SH-5Y5Y cells were cultivated as previously described (58). For RNA interference, SH-5Y5Y or H1299 cells were reverse-transfected with Stealth siRNA (Invitrogen) using Lipofectamine RNAiMAX (Invitrogen) or siRNA (Santa Cruz) using siLentFect (Bio-Rad), respectively, according to the manufacturer's instructions. *DNA Constructs (SH-5Y5Y cells)*: Human wild-type (wt) parkin and human wild-type PINK1 were described earlier (49,59). Human wild-type DJ was amplified from a human brain cDNA library and inserted into the pcDNA3.1 vector (Invitrogen). *Viral plasmids and infections (primary cortical neurons)*: for rescue studies, cortical neurons were harvested from DJ-$1^{+/+}$ or DJ-$1^{-/-}$ littermate embryos (produced by a heterozygote cross) at E15.5 and plated at a density of 150 000 cells per well (24-well dish) on glass cover slips coated with 1XPoly-D-Lysine. Viral particles expressing GFP, DJ-1, DJ-1 C106A, Pink1 or Parkin were administered at a multiplicity of infection (MOI) of 30 at the time of plating. Cortical neurons infected with DJ-1, DJ-1C106A and Pink1 were harvested 48 h following infection. Cortical neurons infected with Parkin were harvested 4 days post-infection and plating. For cell survival studies, cortical neurons harvested as described above were infected with either control (EGFP) adenovirus or dominant-negative Drp-1 (ECFP-C1 DLVP K38E) adenoviruses at MOI of 40 and then immediately seeded into 24-well plates at an approximate density of 350 000 neurons/well. Neurons were cultured for 3 days and then treated with 10 μM MPP^+ for 24 h.

Cell survival

Neuronal survival was evaluated by assessing nuclear integrity of GFP/CFP-positive neurons as done previously (14).

Citrate synthase activity

Maximal activity of citrate synthase (EC 4.1.3.7) was measured at 25°C in previously frozen homogenate and mitochondria from brain and skeletal as previously described (60).

Confocal microscopy/immunofluoresence/mitochondrial fusion rates

Confocal images were acquired with a 63× objective (1.4) by an inverted Laser Scanning Microscope (LSM510 META, Zeiss). Mitochondrial fusion rates were calculated as previously described (21).

Generation and genotyping of DJ-1 mice

The generation and genotype of the DJ-1 deficient mice has previously been described in detail (61).

H_2O_2 generation

Mitochondrial H_2O_2 production rate was determined in freshly isolated mitochondria from sketelal muscle and brain using the *p*-hydroxyphenylacetate (PHPA) fluorometric assay (62). Mitochondria (0.1 mg/ml) were incubated in standard incubation medium (IM: 120 mM KCl, 1 mM EGTA, 5 mM KH_2PO_4, 2 mM $MgCl_2$ and 3 mM HEPES; pH 7.4) supplemented with 0.3% defatted BSA. H_2O_2 production was monitored for up to 25 min using a temperature-controlled fluorimeter (BioTek, FLx800) at 37°C. Fluorescence readings were converted to H_2O_2 production rates by use of a standard curve.

Immunofluoresence (primary cortical neurons and MEFs)

Cortical neurons or MEFs were fixed with 4% PFA diluted in cell culture medium for 15 min at 37°C. Cells were then washed 3× with 1XPBS. Immediately following this, cells were permeabilized and blocked with 10% normal goat serum-0.1% Triton X/PBS for 1 h at room temperature. Cells were then stained with Tom-20 (1:100, a kind gift from Dr Gordon Shore or from Santa Cruz) or *cytochrome c* (1:100, BD Biosciences, in 5% normal goat serum overnight at 4°C) for the visualization of mitochondria. The following day, cells were washed 3× with 5% normal goat serum/PBS and then incubated for 1 h with the appropriate Alexa conjugated fluorophores in 5% normal goat serum/PBS. Cells were then washed 3× with 1XPBS, rinsed in sterile H_2O and mounted onto microscope slides using Gel Mount (Sigma).

Fluorescent staining of mitochondria and western blot analysis (SH-5Y5Y cells)

SH-5Y5Y cells were grown on 15 mm glass cover slips. Cells were fluorescently labeled with 0.1 μM $DiOC_6$ (3) in cell culture medium for 15 min. After washing the cover slips with medium, living cells were analyzed for mitochondrial morphology by fluorescence microscopy using a Leica DMRB microscope (Leica, Wetzlar, Germany). Cells were categorized in two classes according to their mitochondrial morphology: tubular or fragmented. Cells displaying an intact network of tubular mitochondria were classified as tubular. When this network was disrupted and mitochondria appeared predominantly spherical or rod-like, they were classified as fragmented. The mitochondrial morphology of at least 300 cells per plate was determined in a blinded manner, i.e. the researcher was blind to the transfection status.

Quantifications were based on triplicates of at least three independent experiments. Proteins were analyzed by SDS–PAGE and western blotting using polyvinylidene difluoride membranes (Millipore, Schwalbach, Germany). The membranes were blocked with 5% non-fat dry milk in TBS containing 0.1% Tween 20 (TBS-T) for 1 h at room temperature and then incubated with the primary antibody in blocking solution for 16 h at 4°C. After extensive washing with TBS-T, the membranes were incubated with HRP-conjugated secondary antibody for 60 min at room temperature. Following washing with TBS-T, the antigen was detected with the enhanced chemiluminescence (ECL) detection system or ECL plus detection system (Amersham Biosciences, Freiburg, Germany).

Immunoblotting

Cell lysis was carried out identically for both MEFs and neurons. Cells were washed twice with PBS, scraped in lysis buffer containing 50 mM Tris–HCl pH 7.5, 100 mM NaCl, 0.4% Triton X-100, 1 mM DTT and 1× protease inhibitor cocktail (Roche). Samples were kept on ice for 20 min and then spun with maximal speed at 20 000*g* at 4°C for 5 min. Protein quantification was carried out using both Bradford (Bio-Rad) and BCA (Pierce) methods. Fifteen micrograms of each lysate was electrophoresed on 12% SDS–polyacrylamide gels, or 4–20% gradient gels (Invitrogen) and transferred to polyvinylidene fluoride (PVDF) or nitrocellulose membranes (Millipore). For tissue lysates, 15 μg of each tissue lysate was electrophoresed on 12% SDS–PAGE gels and transferred to polyvinylidene fluoride (PVDF) or nitrocellulose membranes (Millipore).

Isolation of mitochondria

DJ-$1^{+/+}$ or DJ-$1^{-/-}$ mice (4–6 months old) were euthanized by decapitation for isolation of skeletal muscle and brain mitochondria. Isolation of skeletal muscle mitochondria was performed using a modified method of Chappell and Perry (63), as previously described in detail (64). Brain mitochondria were isolated as described (50).

Lentivirus production and transduction

Lentiviral vectors were generated by transient transfection in 293T cells using PEI. The constructs for manufacturing the lentiviruses were obtained from Addgene.org. Protocols used to manufacture and purify lentiviruses were done according to Tronolab's protocols (www.tronolab.com).

Oxygen consumption

Oxygen consumption was measured in isolated brain mitochondria (0.3 mg/ml) at 37°C using a Clark-type oxygen electrode (Hansatech, Norfolk, UK), incubated in standard incubation medium (IM: 120 mM KCl, 1 mM EGTA, 5 mM KH_2PO_4, 2 mM $MgCl_2$ and 3 mM HEPES; pH 7.4) containing 0.3% defatted BSA and assumed to contain 406 nmol O/ml at 37°C (65). State 3 (maximum phosphorylating) respiration was determined using 5 mM glutamate/5 mM malate as substrate, and 500 μM ADP. State 4 (non-phosphorylating or maximal leak-dependent respiration) was determined following addition of oligomycin (8 μg/ml). All measurements were performed in duplicate.

Statistical analyses

Unless otherwise described, data analysis was carried out using independent two-tailed *t*-tests. Significance was marked by * when $P < 0.05$. All data are presented as means ± SEM.

SUPPLEMENTARY MATERIAL

Supplementary Material is available at *HMG* online.

ACKNOWLEDGEMENTS

The authors would like to thank Dr Gordon Shore (McGill University, Montreal, Canada) for the provision of the GFP-LC3 stable cell line and the α-Tom20 antibody. The authors also wish to thank Paul Marcogliese and Viola Mugamba for technical assistance, and Dr Marc Germain for helpful insights on the manuscript.

Conflict of Interest statement. None declared.

FUNDING

This work was supported by grants from the Canadian Institutes of Health Research (CIHR), Heart and Stroke Foundation of Ontario (HSFO), Neuroscience Canada (Brain Repair Grant), Parkinson's Society Canada (PSC), Parkinson's Disease Foundation (PDF) and World Class University program through the National Research Foundation of Korea funded by the Ministry of Education, Science and Technology, South Korea (R31-2008-000-20004-0) to D.S.P. I.I. was supported by a CIHR Postdoctoral fellowship. H.A. was supported by a Heart and Stroke Foundation of Canada doctoral award. E.L.S. was supported by a Canadian Diabetes Association (CDA) Postdoctoral fellowship. A.J.-A. was supported by a CIHR doctoral award. M.W.C.R. was supported by a Heart and Stroke Foundation of Ontario Master's student award; S.C. was supported by a summer student award from the centre for stroke recovery (CSR); S.J.H. was supported by PSC Master's Student award.

REFERENCES

1. Abou-Sleiman, P.M., Muqit, M.M. and Wood, N.W. (2006) Expanding insights of mitochondrial dysfunction in Parkinson's disease. *Nat. Rev.*, **7**, 207–219.
2. Schapira, A.H. (1998) Mitochondrial dysfunction in neurodegenerative disorders. *Biochim. Biophys. Acta*, **1366**, 225–233.
3. Mann, V.M., Cooper, J.M., Krige, D., Daniel, S.E., Schapira, A.H. and Marsden, C.D. (1992) Brain, skeletal muscle and platelet homogenate mitochondrial function in Parkinson's disease. *Brain*, **115**, 333–342.
4. Bindoff, L.A., Birch-Machin, M.A., Cartlidge, N.E., Parker, W.D. Jr and Turnbull, D.M. (1991) Respiratory chain abnormalities in skeletal muscle from patients with Parkinson's disease. *J. Neurol. Sci.*, **104**, 203–208.

5. Drechsel, D.A. and Patel, M. (2008) Role of reactive oxygen species in the neurotoxicity of environmental agents implicated in Parkinson's disease. *Free Radic. Biol. Med.*, **44**, 1873–1886.
6. Cleeter, M.W., Cooper, J.M. and Schapira, A.H. (1992) Irreversible inhibition of mitochondrial complex I by 1-methyl-4-phenylpyridinium: evidence for free radical involvement. *J. Neurochem.*, **58**, 786–789.
7. Silvestri, L., Caputo, V., Bellacchio, E., Atorino, L., Dallapiccola, B., Valente, E.M. and Casari, G. (2005) Mitochondrial import and enzymatic activity of PINK1 mutants associated to recessive parkinsonism. *Hum. Mol. Genet.*, **14**, 3477–3492.
8. Zhou, C., Huang, Y., Shao, Y., May, J., Prou, D., Perier, C., Dauer, W., Schon, E.A. and Przedborski, S. (2008) The kinase domain of mitochondrial PINK1 faces the cytoplasm. *Proc. Natl Acad. Sci. USA*, **105**, 12022–12027.
9. Poole, A.C., Thomas, R.E., Andrews, L.A., McBride, H.M., Whitworth, A.J. and Pallanck, L.J. (2008) The PINK1/Parkin pathway regulates mitochondrial morphology. *Proc. Natl Acad. Sci. USA*, **105**, 1638–1643.
10. Deng, H., Dodson, M.W., Huang, H. and Guo, M. (2008) The Parkinson's disease genes pink1 and parkin promote mitochondrial fission and/or inhibit fusion in Drosophila. *Proc. Natl Acad. Sci. USA*, **105**, 14503–14508.
11. Clark, I.E., Dodson, M.W., Jiang, C., Cao, J.H., Huh, J.R., Seol, J.H., Yoo, S.J., Hay, B.A. and Guo, M. (2006) Drosophila pink1 is required for mitochondrial function and interacts genetically with parkin. *Nature*, **441**, 1162–1166.
12. Bonifati, V., Rizzu, P., van Baren, M.J., Schaap, O., Breedveld, G.J., Krieger, E., Dekker, M.C., Squitieri, F., Ibanez, P., Joosse, M. *et al.* (2003) Mutations in the DJ-1 gene associated with autosomal recessive early-onset parkinsonism. *Science*, **299**, 256–259.
13. Aleyasin, H., Rousseaux, M.W., Phillips, M., Kim, R.H., Bland, R.J., Callaghan, S., Slack, R.S., During, M.J., Mak, T.W. and Park, D.S. (2007) The Parkinson's disease gene DJ-1 is also a key regulator of stroke-induced damage. *Proc. Natl Acad. Sci. USA*, **104**, 18748–18753.
14. Kim, R.H., Smith, P.D., Aleyasin, H., Hayley, S., Mount, M.P., Pownall, S., Wakeham, A., You-Ten, A.J., Kalia, S.K., Horne, P. *et al.* (2005) Hypersensitivity of DJ-1-deficient mice to 1-methyl-4-phenyl-1,2,3,6-tetrahydropyrindine (MPTP) and oxidative stress. *Proc. Natl Acad. Sci. USA*, **102**, 5215–5220.
15. Andres-Mateos, E., Perier, C., Zhang, L., Blanchard-Fillion, B., Greco, T.M., Thomas, B., Ko, H.S., Sasaki, M., Ischiropoulos, H., Przedborski, S. *et al.* (2007) DJ-1 gene deletion reveals that DJ-1 is an atypical peroxiredoxin-like peroxidase. *Proc. Natl Acad. Sci. USA*, **104**, 14807–14812.
16. Taira, T., Saito, Y., Niki, T., Iguchi-Ariga, S.M., Takahashi, K. and Ariga, H. (2004) DJ-1 has a role in antioxidative stress to prevent cell death. *EMBO Rep.*, **5**, 213–218.
17. Park, J., Kim, S.Y., Cha, G.H., Lee, S.B., Kim, S. and Chung, J. (2005) Drosophila DJ-1 mutants show oxidative stress-sensitive locomotive dysfunction. *Gene*, **361**, 133–139.
18. Gonzalez-Polo, R., Niso-Santano, M., Moran, J.M., Ortiz-Ortiz, M.A., Bravo-San Pedro, J.M., Soler, G. and Fuentes, J.M. (2009) Silencing DJ-1 reveals its contribution in paraquat-induced autophagy. *J. Neurochem.*, **109**, 889–898.
19. Vasseur, S., Afzal, S., Tardivel-Lacombe, J., Park, D.S., Iovanna, J.L. and Mak, T.W. (2009) DJ-1/PARK7 is an important mediator of hypoxia-induced cellular responses. *Proc. Natl Acad. Sci. USA*, **106**, 1111–1116.
20. Jahani-Asl, A., Cheung, E.C., Neuspiel, M., MacLaurin, J.G., Fortin, A., Park, D.S., McBride, H.M. and Slack, R.S. (2007) Mitofusin 2 protects cerebellar granule neurons against injury-induced cell death. *J. Biol. Chem.*, **282**, 23788–23798.
21. Zunino, R., Schauss, A., Rippstein, P., Andrade-Navarro, M. and McBride, H.M. (2007) The SUMO protease SENP5 is required to maintain mitochondrial morphology and function. *J. Cell Sci.*, **120**, 1178–1188.
22. Kopin, I.J. and Markey, S.P. (1988) MPTP toxicity: implications for research in Parkinson's disease. *Annu. Rev. Neurosci.*, **11**, 81–96.
23. Barsoum, M.J., Yuan, H., Gerencser, A.A., Liot, G., Kushnareva, Y., Graber, S., Kovacs, I., Lee, W.D., Waggoner, J., Cui, J. *et al.* (2006) Nitric oxide-induced mitochondrial fission is regulated by dynamin-related GTPases in neurons. *EMBO J.*, **25**, 3900–3911.
24. Mitsumoto, A., Nakagawa, Y., Takeuchi, A., Okawa, K., Iwamatsu, A. and Takanezawa, Y. (2001) Oxidized forms of peroxiredoxins and DJ-1 on two-dimensional gels increased in response to sublethal levels of paraquat. *Free Radic. Res.*, **35**, 301–310.
25. Canet-Aviles, R.M., Wilson, M.A., Miller, D.W., Ahmad, R., McLendon, C., Bandyopadhyay, S., Baptista, M.J., Ringe, D., Petsko, G.A. and Cookson, M.R. (2004) The Parkinson's disease protein DJ-1 is neuroprotective due to cysteine-sulfinic acid-driven mitochondrial localization. *Proc. Natl Acad. Sci. USA*, **101**, 9103–9108.
26. Meulener, M.C., Xu, K., Thomson, L., Ischiropoulos, H. and Bonini, N.M. (2006) Mutational analysis of DJ-1 in Drosophila implicates functional inactivation by oxidative damage and aging. *Proc. Natl Acad. Sci. USA*, **103**, 12517–12522.
27. Whitworth, A.J. and Pallanck, L.J. (2009) The PINK1/Parkin pathway: a mitochondrial quality control system? *J. Bioenerg. Biomembr.*, **41**, 499–503.
28. Park, J., Lee, G. and Chung, J. (2009) The PINK1-Parkin pathway is involved in the regulation of mitochondrial remodeling process. *Biochem. Biophys. Res. Commun.*, **378**, 518–523.
29. Vives-Bauza, C., Zhou, C., Huang, Y., Cui, M., de Vries, R.L., Kim, J., May, J., Tocilescu, M.A., Liu, W., Ko, H.S. *et al.* (2010) PINK1-dependent recruitment of Parkin to mitochondria in mitophagy. *Proc. Natl Acad. Sci. USA*, **107**, 378–383.
30. Geisler, S., Holmstrom, K.M., Skujat, D., Fiesel, F.C., Rothfuss, O.C., Kahle, P.J. and Springer, W. (2010) PINK1/Parkin-mediated mitophagy is dependent on VDAC1 and p62/SQSTM1. *Nat. Cell Biol.*, **12**, 119–131.
31. Narendra, D.P., Jin, S.M., Tanaka, A., Suen, D.F., Gautier, C.A., Shen, J., Cookson, M.R. and Youle, R.J. (2010) PINK1 is selectively stabilized on impaired mitochondria to activate parkin. *PLoS Biol.*, **8**, e1000298.
32. Haque, M.E., Thomas, K.J., D'Souza, C., Callaghan, S., Kitada, T., Slack, R.S., Fraser, P., Cookson, M.R., Tandon, A. and Park, D.S. (2008) Cytoplasmic Pink1 activity protects neurons from dopaminergic neurotoxin MPTP. *Proc. Natl Acad. Sci. USA*, **105**, 1716–1721.
33. Klionsky, D.J., Abeliovich, H., Agostinis, P., Agrawal, D.K., Aliev, G., Askew, D.S., Baba, M., Baehrecke, E.H., Bahr, B.A., Ballabio, A. *et al.* (2008) Guidelines for the use and interpretation of assays for monitoring autophagy in higher eukaryotes. *Autophagy*, **4**, 151–175.
34. Mizushima, N. and Yoshimori, T. (2007) How to interpret LC3 immunoblotting. *Autophagy*, **3**, 542–545.
35. Rubinsztein, D.C., Cuervo, A.M., Ravikumar, B., Sarkar, S., Korolchuk, V., Kaushik, S. and Klionsky, D.J. (2009) In search of an 'autophagomometer'. *Autophagy*, **5**, 585–589.
36. Giasson, B.I., Ischiropoulos, H., Lee, V.M. and Trojanowski, J.Q. (2002) The relationship between oxidative/nitrative stress and pathological inclusions in Alzheimer's and Parkinson's diseases. *Free Radic. Biol. Med.*, **32**, 1264–1275.
37. Perkins, G., Bossy-Wetzel, E. and Ellisman, M.H. (2009) New insights into mitochondrial structure during cell death. *Exp. Neurol.*, **218**, 183–192.
38. Knott, A.B., Perkins, G., Schwarzenbacher, R. and Bossy-Wetzel, E. (2008) Mitochondrial fragmentation in neurodegeneration. *Nat. Rev.*, **9**, 505–518.
39. Lev, N., Ickowicz, D., Melamed, E. and Offen, D. (2008) Oxidative insults induce DJ-1 upregulation and redistribution: implications for neuroprotection. *Neurotoxicology*, **29**, 397–405.
40. Junn, E., Jang, W.H., Zhao, X., Jeong, B.S. and Mouradian, M.M. (2009) Mitochondrial localization of DJ-1 leads to enhanced neuroprotection. *J. Neurosci. Res.*, **87**, 123–129.
41. Narendra, D., Tanaka, A., Suen, D.F. and Youle, R.J. (2009) Parkin-induced mitophagy in the pathogenesis of Parkinson disease. *Autophagy*, **5**, 706–708.
42. Narendra, D., Tanaka, A., Suen, D.F. and Youle, R.J. (2008) Parkin is recruited selectively to impaired mitochondria and promotes their autophagy. *J. Cell Biol.*, **183**, 795–803.
43. Cherra, S.J. 3rd, Dagda, R.K., Tandon, A. and Chu, C.T. (2009) Mitochondrial autophagy as a compensatory response to PINK1 deficiency. *Autophagy*, **5**, 1213–1214.
44. Krebiehl, G., Ruckerbauer, S., Burbulla, L.F., Kieper, N., Maurer, B., Waak, J., Wolburg, H., Gizatullina, Z., Gellerich, F.N., Woitalla, D. *et al.* (2010) Reduced basal autophagy and impaired mitochondrial dynamics due to loss of Parkinson's disease-associated protein DJ-1. *PLoS ONE*, **5**, e9367.
45. Delivani, P., Adrain, C., Taylor, R.C., Duriez, P.J. and Martin, S.J. (2006) Role for CED-9 and Egl-1 as regulators of mitochondrial fission and fusion dynamics. *Mol. Cell*, **21**, 761–773.
46. Frank, S., Gaume, B., Bergmann-Leitner, E.S., Leitner, W.W., Robert, E.G., Catez, F., Smith, C.L. and Youle, R.J. (2001) The role of dynamin-related

protein 1, a mediator of mitochondrial fission, in apoptosis. *Dev. Cell*, **1**, 515–525.
47. Karbowski, M., Arnoult, D., Chen, H., Chan, D.C., Smith, C.L. and Youle, R.J. (2004) Quantitation of mitochondrial dynamics by photolabeling of individual organelles shows that mitochondrial fusion is blocked during the Bax activation phase of apoptosis. *J. Cell Biol.*, **164**, 493–499.
48. Lee, Y.J., Jeong, S.Y., Karbowski, M., Smith, C.L. and Youle, R.J. (2004) Roles of the mammalian mitochondrial fission and fusion mediators Fis1, Drp1 and Opa1 in apoptosis. *Mol. Biol. Cell*, **15**, 5001–5011.
49. Exner, N., Treske, B., Paquet, D., Holmstrom, K., Schiesling, C., Gispert, S., Carballo-Carbajal, I., Berg, D., Hoepken, H.H., Gasser, T. *et al.* (2007) Loss-of-function of human PINK1 results in mitochondrial pathology and can be rescued by parkin. *J. Neurosci.*, **27**, 12413–12418.
50. Palacino, J.J., Sagi, D., Goldberg, M.S., Krauss, S., Motz, C., Wacker, M., Klose, J. and Shen, J. (2004) Mitochondrial dysfunction and oxidative damage in parkin-deficient mice. *J. Biol. Chem.*, **279**, 18614–18622.
51. Wood-Kaczmar, A., Gandhi, S., Yao, Z., Abramov, A.Y., Miljan, E.A., Keen, G., Stanyer, L., Hargreaves, I., Klupsch, K., Deas, E. *et al.* (2008) PINK1 is necessary for long term survival and mitochondrial function in human dopaminergic neurons. *PLoS ONE*, **3**, e2455.
52. Gegg, M.E., Cooper, J.M., Schapira, A.H. and Taanman, J.W. (2009) Silencing of PINK1 expression affects mitochondrial DNA and oxidative phosphorylation in dopaminergic cells. *PLoS ONE*, **4**, e4756.
53. Chen, Y. and Gibson, S.B. (2008) Is mitochondrial generation of reactive oxygen species a trigger for autophagy? *Autophagy*, **4**, 246–248.
54. Martindale, J.L. and Holbrook, N.J. (2002) Cellular response to oxidative stress: signaling for suicide and survival. *J. Cell Physiol.*, **192**, 1–15.
55. Scherz-Shouval, R., Shvets, E., Fass, E., Shorer, H., Gil, L. and Elazar, Z. (2007) Reactive oxygen species are essential for autophagy and specifically regulate the activity of Atg4. *EMBO J.*, **26**, 1749–1760.
56. Macedo, M.G., Anar, B., Bronner, I.F., Cannella, M., Squitieri, F., Bonifati, V., Hoogeveen, A., Heutink, P. and Rizzu, P. (2003) The DJ-1L166P mutant protein associated with early onset Parkinson's disease is unstable and forms higher-order protein complexes. *Hum. Mol. Genet.*, **12**, 2807–2816.
57. Chang, N.C., Nguyen, M., Germain, M. and Shore, G.C. (2010) Antagonism of Beclin 1-dependent autophagy by BCL-2 at the endoplasmic reticulum requires NAF-1. *EMBO J.*, **29**, 606–618.
58. Lutz, A.K., Exner, N., Fett, M.E., Schlehe, J.S., Kloos, K., Lammermann, K., Brunner, B., Kurz-Drexler, A., Vogel, F., Reichert, A.S. *et al.* (2009) Loss of parkin or PINK1 function increases Drp1-dependent mitochondrial fragmentation. *J. Biol. Chem.*, **284**, 22938–22951.
59. Winklhofer, K.F., Henn, I.H., Kay-Jackson, P.C., Heller, U. and Tatzelt, J. (2003) Inactivation of parkin by oxidative stress and C-terminal truncations: a protective role of molecular chaperones. *J. Biol. Chem.*, **278**, 47199–47208.
60. Matlib, M.A., Shannon, W.A. Jr and Srere, P.A. (1979) Measurement of matrix enzyme activity in situ in isolated made permeable with toluene. *Methods Enzymol.*, **56**, 544–550.
61. Kim, R.H., Peters, M., Jang, Y., Shi, W., Pintilie, M., Fletcher, G.C., DeLuca, C., Liepa, J., Zhou, L., Snow, B. *et al.* (2005) DJ-1, a novel regulator of the tumor suppressor PTEN. *Cancer Cell*, **7**, 263–273.
62. Hyslop, P.A. and Sklar, L.A. (1984) A quantitative fluorimetric assay for the determination of oxidant production by polymorphonuclear leukocytes: its use in the simultaneous fluorimetric assay of cellular activation processes. *Anal. Biochem.*, **141**, 280–286.
63. Chappell, J.B. and Perry, S.V. (1954) Biochemical and osmotic properties of skeletal muscle mitochondria. *Nature*, **173**, 1094–1095.
64. Seifert, E.L., Bezaire, V., Estey, C. and Harper, M.E. (2008) Essential role for uncoupling protein-3 in mitochondrial adaptation to fasting but not in fatty acid oxidation or fatty acid anion export. *J. Biol. Chem.*, **283**, 25124–25131.
65. Reynafarje, B., Costa, L.E. and Lehninger, A.L. (1985) O2 solubility in aqueous media determined by a kinetic method. *Anal. Biochem.*, **145**, 406–418.

Progressive dopaminergic cell loss with unilateral-to-bilateral progression in a genetic model of Parkinson disease

Maxime W. C. Rousseaux[a], Paul C. Marcogliese[a], Dianbo Qu[a], Sarah J. Hewitt[a], Sarah Seang[a], Raymond H. Kim[b], Ruth S. Slack[a], Michael G. Schlossmacher[c,d], Diane C. Lagace[a], Tak W. Mak[b], and David S. Park[a,e,1]

[a]Department of Cellular and Molecular Medicine, University of Ottawa, Ottawa, ON, Canada, K1H 8M5; [b]Campbell Family Institute for Breast Cancer Research, Department of Medical Biophysics, University of Toronto, Toronto, ON, Canada, M5G 2C1; [c]Division of Neurology, Department of Medicine, Ottawa Hospital, Ottawa, ON, Canada, K1H 8M5; [d]Division of Neuroscience, Ottawa Hospital Research Institute, Ottawa, ON, Canada, K1H 8M5; and [e]Department of Cogno-Mechatronics Engineering, Pusan National University, Geumjeong-gu, Busan 609-735, South Korea

Edited by Thomas C. Südhof, Stanford University School of Medicine, Stanford, CA, and approved August 10, 2012 (received for review March 26, 2012)

DJ-1 mutations cause autosomal recessive early-onset Parkinson disease (PD). We report a model of PD pathology: the DJ1-C57 mouse. A subset of DJ-1–nullizygous mice, when fully backcrossed to a C57BL/6J background, display dramatic early-onset unilateral loss of dopaminergic (DA) neurons in their *substantia nigra pars compacta*, progressing to bilateral degeneration of the nigrostriatal axis with aging. In addition, these mice exhibit age-dependent bilateral degeneration at the *locus ceruleus* nucleus and display mild motor behavior deficits at aged time points. These findings effectively recapitulate the early stages of PD. Therefore, the DJ1-C57 mouse provides a tool to study the preclinical aspects of neurodegeneration. Importantly, by exome sequencing, we identify candidate modifying genes that segregate with the phenotype, providing potentially critical clues into how certain genes may influence the penetrance of DJ-1–related degeneration in mice.

animal model | PARK7 | neuritic beading | neuronal death | neuroinflammation

Parkinson disease (PD) is a progressive neurodegenerative disorder with complex symptomology and etiology affecting an ever-increasing number of individuals. Although multifactorial in nature, increasing insight has been gained with regard to the pathogenesis of PD through investigation of genes linked to the disease. Because monogenic forms of PD can be modeled in a laboratory, numerous animal models have been created to recapitulate the disease. For instance, loss-of-function mutations in the *DJ-1* (*PARK7*) gene cause early-onset autosomal recessive PD (1, 2). Patients harboring *DJ-1* mutations exhibit certain key characteristics principally in early-onset PD and may lack certain neuropathological attributes present in sporadic PD cases such as Lewy bodies (LBs) (3). However, generation of DJ-1–nullizygous mice (DJ-$1^{-/-}$) on mixed background by various laboratories, including our own, failed to detect any basal levels of neurodegeneration even in aged mice (4–11) (see Table S1). Similarly, a number of PD-related, genetically manipulated mice have been created in attempts to recapitulate the disease process, whereas little or none has shown clear or robust neurodegeneration specific to the *substantia nigra pars compacta* (SNc) (reviewed in ref. 12). Therefore, the creation of murine PD models that demonstrate significant dopaminergic (DA) loss remains an acute need in the field. The need for an early-onset model of PD is made more pressing given that no postmortem analyses of human DJ-1 mutant-carrying patients have been reported. This is particularly critical if we are to understand how specific signaling pathways govern DA loss in monogenic forms of early-onset human PD. Presently, most mechanistic studies of DA loss rely on acute toxin models of Parkinsonism. However, the relevance of such studies to the human condition remains uncertain, because acute neurotoxins are rarely the culprit in the majority of PD cases. This potential discrepancy is highlighted by a number of failed clinical trials that have heavily relied on toxin models as preclinical evidence for efficacy (13–16). A more representative model of DA loss that uses known factors in human PD is likely vital to develop better therapeutic outcomes.

Results

In the course of our studies examining the effects of environmental perturbations in DJ-$1^{-/-}$ mice, we continued to examine the long-term effects of DJ-1 deficiency on DA neuron loss. Importantly, this was accomplished in animals completely backcrossed onto a C57BL/6J background (14× backcrossed, DJ-$1^{-/-}$; herein, referred to as DJ1-C57). Intriguingly, unilateral SNc degeneration in a subset of these DJ1-C57 knockout mice is observed as early as 2 mo of age (Fig. 1*A*, Fig. S1, and Table S2). This phenotype is not observed in animals younger than 2 mo ($n = 8$; Fig. S1), thus indicating that this defect is unlikely to be developmental in origin. Moreover, this phenotype is not observed in any of the wild-type (WT) mice examined ($n = 71$). In addition, the ventral tegmental area (VTA) of these mice is mostly spared (Fig. 1*D*). This latter finding is particularly interesting given the observation that in postmortem brains from PD patients, VTA neurons remain relatively protected compared with their nigral counterparts (17).

To objectively assess this phenotype, mice in this study are classified as either "affected" (unilateral phenotype: having a greater than 40% unilateral reduction of DA cells in the SNc compared with the other side) or "unaffected" (no unilateral phenotype: having similar bilateral DA cell numbers). No clear side or sex specificity is observed (right, 53%; female, 67%, respectively). Thus, to maintain consistency, "side A" is the term given for the side of the brain with the least number of neurons, regardless of the genotype (side B being the side with more DA neurons). When quantified, affected DJ1-C57 mice exhibit a dramatic reduction of neurons in their SNc, as visualized by tyrosine hydroxylase (TH) and cresyl violet (CV) staining (Fig. 1*B* and *C* and see Fig. 3*A*). Upon closer magnification of the SNc, the affected DJ1-C57 mice exhibit TH-positive fiber

Author contributions: M.W.C.R. and D.S.P. designed research; M.W.C.R., P.C.M., D.Q., S.J.H., and S.S. performed research; R.H.K., R.S.S., M.G.S., D.C.L., and T.W.M. contributed new reagents/analytic tools; M.W.C.R. and P.C.M. analyzed data; and M.W.C.R. and D.S.P. wrote the paper.

The authors declare no conflict of interest.

This article is a PNAS Direct Submission.

Freely available online through the PNAS open access option.

Data deposition: The sequences reported in this paper have been deposited in the Mouse Genome Informatics (MGI) database, ftp://ftp.informatics.jax.org/pub/datasets/index.html.

[1]To whom correspondence should be addressed. E-mail: dpark@uottawa.ca.

This article contains supporting information online at www.pnas.org/lookup/suppl/doi:10.1073/pnas.1205102109/-/DCSupplemental.

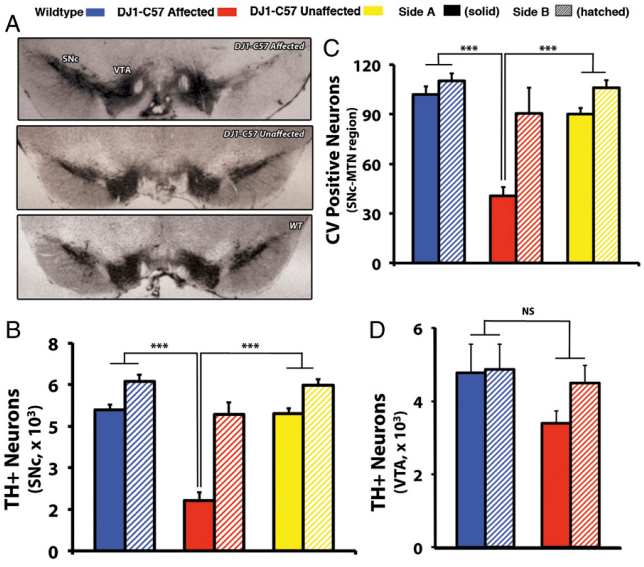

Fig. 1. Young affected DJ1-C57 mice exhibit selective unilateral degeneration in their SNc. (*A*) Representative midbrain sections of DJ1-C57 affected (*Top*), DJ1-C57 Unaffected (*Middle*), and WT (*Bottom*) mice depicting TH staining in the SNc and VTA. (*B* and *C*) Quantification of *A* by stereology of total number of TH-positive cells in the SNc (*B*) and of CV-stained cells at the level of the MTN in the SNc (*C*). (*D*) Quantification of TH-positive neurons in the VTA of WT and DJ-1 affected mice. Note that WT, DJ1-C57 affected and DJ1-C57 unaffected are represented by blue, red, and yellow bars, respectively. Side A is depicted as solid shading and side B as hatched shading. NS, not significant ($P > 0.05$); ***$P < 0.001$; ANOVA, followed by Tukey's LSD post hoc tests. Data are represented as means (n = 7–80 per group) ± SEM.

staining but with clear neuronal process disruption. When quantified, the remaining fibers at the level of the SNc in the affected DJ1-C57 mice display an elevated number of shortened processes with obvious neuritic beading (Fig. 2*A*) compared with unaffected DJ1-C57 or control mice. Consistent with this finding, an increase in CD11b-positive microglia is noted in young, affected animals (Fig. 3*B*), whereas no clear increase in astrocytosis on the affected side is observed (Fig. S2).

To assess whether this histopathological phenotype corresponds with a functional outcome, we subjected animals to behavioral testing. However, DJ1-C57 affected mice do not exhibit a clear decrease in gross motor function at 2, 6, or 12 mo of age (Fig. S3 *A*–*C*) or any differences in drug-induced rotational behavior (Fig. S3*D*). The lack of behavioral differences may be accounted for by two observations. First, examination of the striatal DA terminals revealed no clear loss in striatal fibers in young animals (Fig. 2*B*). This finding raised the possibility that sprouting of neurites within the nigrostriatal pathway may be compensatory in young mice. This is of marked interest because we note significant sprouting of dysmorphic neurites (as seen in Fig. 2*A*) in the SNc, which may be compensating for the loss of cell bodies as reported previously (18, 19). Second, an increase in the striatal postsynaptic marker ΔFBJ murine osteosarcoma viral oncogene homolog B (ΔFosB) is observed in affected DJ1-C57 mice (Fig. 2*C*). PD patients have been shown to have up-regulated ΔFosB in their caudate/putamen (20). Moreover, ΔFosB has been shown previously to be up-regulated in toxin models of neurodegeneration such as 1-methyl-4-phenyl-1,2,3,6-tetrahydropyrindine (MPTP) and 6-hydroxydopamine (6-OHDA) as a compensatory response to a loss of DA innervation (21, 22).

With aging of DJ-1–deficient animals, an increase in the prevalence of the DJ1-C57 affected unilateral phenotype was observed over time, peaking at 12 mo of age (42.9% penetrance, Fig. 4*A* and Table S2). When only affected unilateral DJ1-C57 animals are considered, there was a clear loss in total number of SNc DA neurons even at early time points (Fig. S4). However, if all (affected and unaffected) DJ-1–deficient animals were evaluated together, the total number of DA neurons was not significantly reduced until later aging stages (15 mo). At this time, the unilateral phenotype dissipated and a more bilateral phenotype of nerve cell loss was observed (Fig. 4 *A* and *B* and Table S2). Interestingly, these aged mice, unlike at the earlier times, exhibited a decrease in DA-synthesizing TH-positive striatal terminals (Fig. 4*C*). Upon evaluation of any neuritic beading in these aged animals, we noted that although process length itself did not further change between young and aged DJ1-C57 mice (Fig. S5 *A* and *B*), aged DJ1-C57 mice exhibited a decreased number of sprouting processes in the SNc region (Fig. S5*C*). Moreover, long-term behavior testing revealed a mild motor defect in the aged (14–16 mo) DJ1-C57 mice when examined by both the grid test (Fig. 4*E*) and the pole test (males; Fig. 4*F*).

The neuropathology of PD encompasses degeneration not only of the SNc but also of other nuclei in the brainstem including the *locus ceruleus* (LC) (23). Therefore, LC of DJ1-C57 mice were examined for TH-immunoreactive cell bodies. A significant reduction in TH-positive cells of the LC was observed in aged DJ1-C57 mice compared with WT controls (Fig. 4*D*). Furthermore, because α-synuclein aberrant processing is a hallmark of idiopathic PD, we examined whether our DJ1-C57 mice exhibited altered expression or localization of the protein. No visible changes were noted in the expression of endogenous α-synuclein between DJ1-C57 mice and littermate controls (Fig. S6 *A* and *B*). In addition, upon examination of leucine-rich repeat kinase 2 (LRRK2) expression (another autosomal dominant PD-linked protein), we did not note any significant changes in expression or localization of the protein (Fig. S6*B*).

Finally, to elucidate potential mechanism(s) through which this selective neurodegeneration occurs in a subset of these DJ1-C57 mice, we performed whole-exome sequencing on affected (n = 3) and unaffected (n = 3) DJ-1-C57 mice as an approach to identify candidate modifiers (Fig. 5*A*). After filtering for coding regions and for variants found in all three affected but none of the three unaffected mice, only five candidates in coding regions were

NEUROSCIENCE

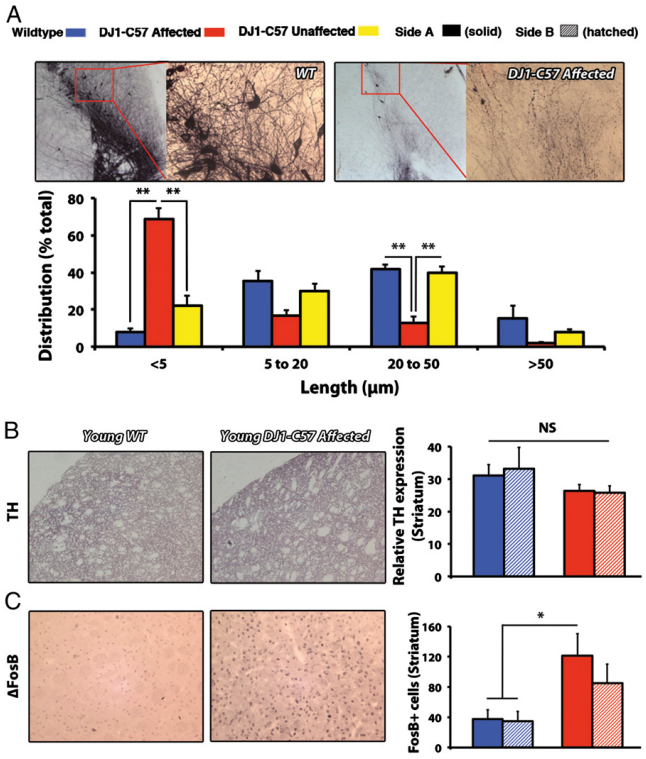

Fig. 2. Widespread process disruption and aberrant striatal innervation in young affected DJ1-C57 mice. (*A*) Fiber sprouting in WT (*Upper Left*) and DJ1-C57 affected animals (*Upper Right*). Distribution of quantified uninterrupted process (TH^+) length in a single vision plain (in microns) is presented (*Lower*). (*B*) Representative sections of striatum stained for ΔFosB in young WT (*Left*) and DJ1-C57 affected (*Center*) mice. (*Right*) Quantification of ΔFosB-positive puncta in the striatum. (*C*) Representative sections of the striatum stained for TH as in *B*. Quantification of striatal TH density is shown (*Right*). WT, DJ1-C57 affected, and DJ1-C57 unaffected are represented by blue, red, and yellow bars, respectively. Side A is depicted as solid shading and side B as hatched shading. NS, not significant ($P > 0.05$); $*P < 0.05$; $**P < 0.01$; ANOVA, followed by Tukey's LSD post hoc tests. Data are represented as means ($n = 3$–11 per group) ± SEM.

identified as potential modifiers of the phenotype [signal regulatory protein β (Sirbp)1A, 2610203C20Rik, zinc finger, SWIM domain containing 6 (Zswim6), kinesin family member (Kif) C5b, and SWI5-dependent recombination repair 1 (Sfr1); Fig. 5*B*]. Moreover, because exome sequencing also covers flanking intronic sequences, an additional 23 candidates were identified in noncoding regions (Table S3), although none of these were in known intron–exon splice sites. Together, these results suggest the segregation of several genomic loci with the phenotype.

Discussion

In our DJ1-C57 mice, we have uncovered an early PD-type phenotype that progressed with age and showed incomplete penetrance. In backcrossing and extensively interbreeding DJ-1–null mice, we obtained a subset of DJ1-C57 mice that exhibited robust unilateral nigral degeneration as early as 8 wk of age: a finding potentially consistent with the early-onset pathogenicity of DJ-1 loss in human carriers of DJ-1 mutations (1). This cell loss was accompanied with compensatory sprouting and the appearance of dysmorphic and beading neurites, as well as microgliosis, a result congruent with the notion that microglia may induce neuritic beading during neuronal dysfunction (24). Furthermore, findings of compensatory sprouting upon cell loss, dysmorphic neurites, and an increase in proinflammatory responses are all present in postmortem samples from PD patients (25–30). Therefore, given the early age of onset of degeneration in these mice, our findings are of particular significance and may correlate with features of autosomal recessive PD. This loss-of-function phenotype has not yet been modeled successfully in rodents, with the possible exception of a partial reduction in LC neurons in one *parkin*$^{-/-}$ mouse model (31).

We also noted that although DJ-1 loss–mediated neurodegeneration will invariably lead to PD in humans, this might not be as dramatic in mice with a relatively short lifespan of ∼24 mo. However, early pathological changes associated with this genetic form of PD are nonetheless observed. Thus, much like preclinical PD, where no clear clinicopathological correlate may be apparent until over 80% of the nigral cell population has been lost, a compensatory mechanism such as neuritic sprouting or postsynaptic sensitization may account for the lack of motor defects in these young animals. Furthermore, the relevance of this model is made even more apparent as the DJ1-C57 mice

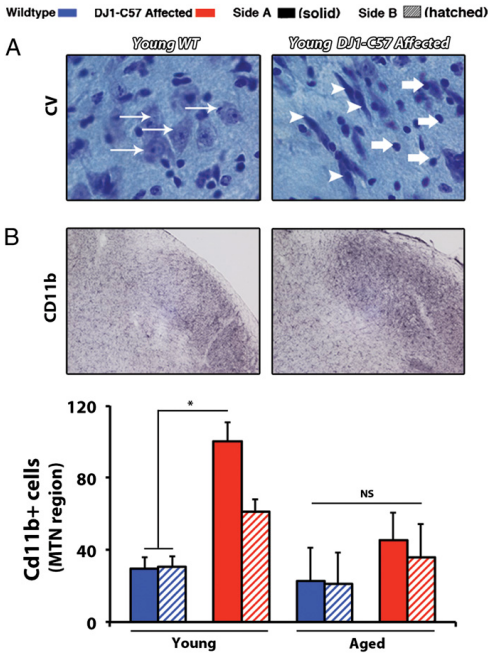

Fig. 3. Focal microgliosis in young affected DJ1-C57 mice. (*A*) Representative midbrain sections stained for CV in young WT and DJ1-C57 affected mice (1000× magnification). Thin arrows denote typical morphology of DA neurons of the SNc; thick arrows denote shrunken, dead nuclei; and arrowheads denote appearance of cells with altered morphology. (*B*) CD11b staining in the midbrain of young WT (*Left*) and DJ1-C57 affected (*Right*) mice was quantified and represented as the number of Cd11b-positive cells in the MTN region of the SNc. WT and DJ1-C57 affected are represented by blue and red bars, respectively. Side A is depicted as solid shading and side B as hatched shading. NS, not significant ($P > 0.05$); *$P < 0.05$; ANOVA, followed by Tukey's LSD post hoc tests. Data are represented as means (n = 3–9 per group) ± SEM.

age. Aged DJ1-C57 mice progressed to bilateral degeneration of their SNc, as well as of their nigrostriatal projections to the forebrain. Thus, this preclinical phenotype likely first occurs at 2 mo and progresses over the course of the following 10–12 mo. In addition, at this older stage, these mice exhibited cell loss at the level of the LC, a pathological characteristic of the human condition. Finally, aged mice beyond 12 mo start to show basal behavioral deficits. Therefore, our DJ1-C57 mouse model presents a potentially important role in filling the gap in our understanding of early-onset preclinical PD in humans.

The reason behind the observed phenotype remains unknown. To begin to explore this issue, we performed whole-exome sequencing to identify potential genes that may contain polymorphisms in affected but not unaffected mice. Surprisingly, the list of genes that met these criteria was limited to five candidates with exon-containing changes. One potential modifier gene candidate, *Sirbp1a*, was particularly interesting given the increase in microglial activation observed in the affected DJ1-C57 mice. SIRBP1A has been associated with a role in promoting phagocytosis in macrophages and monocytes (32). It is possible that disruption of this function may result in aberrant microglial activity. Future studies will seek to elucidate the putative relationship between DJ-1 and SIRBP1A, as well as with other coding modifiers. These exon candidates, although intriguing, are not the only factors that may account for the degenerative phenotype. Other possibilities include intron changes, particularly at loci-flanking

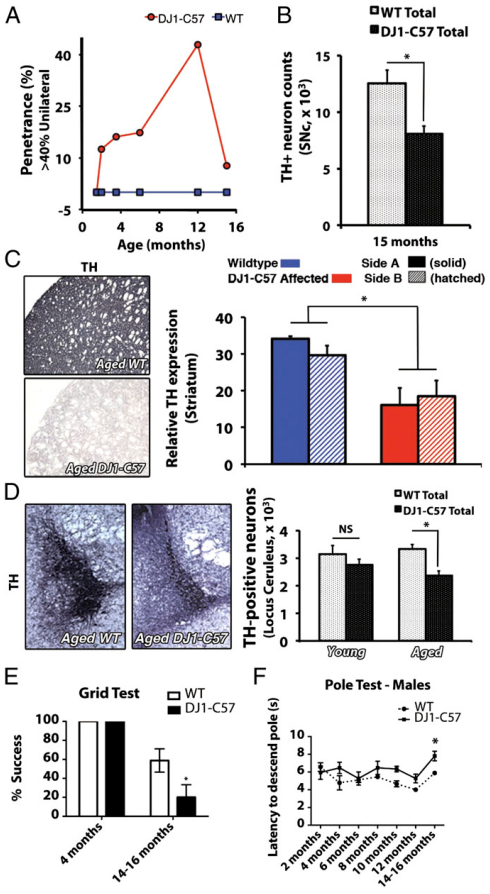

Fig. 4. Aged DJ1-C57 mice exhibit bilateral DA and noradrenergic denervation in the brainstem. (*A*) Penetrance of unilateral phenotype over time. Penetrant threshold: greater than 40% loss of DA neurons on one side (side A) vs. the other (side B). (*B*) Total stereological counts of DA neurons in the SNc of WT and DJ1-C57 aged (15-mo) animals. (*C*) Representative striatal sections of aged (12–15 mo) WT (*Upper Left*) and DJ1-C57 (*Lower Left*) mice stained for TH. Quantification of TH expression in the striatum relative to the *corpus callosum* was performed in young and aged animals (*Right*). (*D*) Representative micrographs of LC sections in the pons stained for TH for either aged WT (*Left*) or aged DJ1-C57 (*Center*). Quantification of TH-positive neurons for both young and aged animals is shown (*Right*). (*E*) The grip test evaluated the capacity of the mouse to stay on an inverted metal grid for 60 s. (*F*) The pole test evaluated the latency of mice to descend a gauze-wrapped pole (in seconds). NS, not significant ($P > 0.05$); *$P < 0.05$; ANOVA, followed by Tukey's LSD post hoc tests. Data are represented as means (n = 3–13 per group) ± SEM.

NEUROSCIENCE

A

Genomic DNA isolation from affected/unaffected DJ1-C57 → Targeted Exome Capture (Agilent SureSelect^{XT}) → Illumina HiSeq2000 Paired end sequencing (2x100bp) → Alignment (C57Bl/6J genome) → Variant Calling (Genome Analysis Toolkit) → Identify Putative Mutations: Segregation by group

B

Gene name	Gene description	Position	Chromosome	Mutation type	Codon	Effect	Amino Acid	Function	Presence	
									Affected (/3)	Unaffected (/3)
Sirpb1a	signal-regulatory protein beta 1A	15,417,016	3	SNP	tCc/tTc	Missense Mutation	S84F	Phagocytosis	3	0
Sirpb1a	signal-regulatory protein beta 1A	15,417,020	3	SNP	Cat/Tat	Missense Mutation	H83Y	Phagocytosis	3	0
2610203C20Rik	RIKEN cDNA 2610203C20 gene	41,389,287	9	SNP	Acc/Ccc	Missense Mutation	T59P	Unknown	3	0
2610203C20Rik	RIKEN cDNA 2610203C20 gene	41,389,294	9	SNP	cAc/cCc	Missense Mutation	H61P	Unknown	3	0
Zswim6	zinc finger, SWIM domain containing 6	108,679,774	13	SNP	gCg/gGg	Missense Mutation	A157G	Unknown	3	0
Kifc5b	kinesin family member C5B	27,061,155	17	SNP	Gtc/Atc	Missense Mutation	V319I	Chromosomal segregation	3	0
Sfr1	SWI5 dependent recombination repair 1	47,807,383	19	SNP	Ccc/Acc	Missense Mutation	P93T	DNA recombination	3	0

Fig. 5. List of exonic variants unique to affected DJ1-C57 mice. (*A*) Schematic workflow of exome sequencing to determine candidate mutations in affected DJ1-C57 mice (vs. unaffected littermate controls). (*B*) Table of variants present in all three examined affected animals and no unaffected littermates. See *Experimental Procedures* for selection criteria.

exons. In this regard, we observed that 23 intronic modifiers segregated with the phenotype. The specific role of these polymorphisms/indels remains unclear, because they do not correspond to splice donor/acceptor sites. Finally, it is possible that a combination of all of these factors may contribute to the phenotype. Therefore, more careful analyses must be performed to examine among these possibilities. What is important, however, is that our studies demonstrate that a defined group of polymorphisms can segregate with our phenotype. How these factors regulate DA loss in DJ-1–deficient mice will require further analyses.

Collectively, we present a murine model that reproduces a clinically detectable phenotype owing to the modification of a PD-related gene. Affected DJ1-C57 mice display: (*i*) unilateral DA cell loss with a predilection for the SNc versus VTA as early as 2 mo of age; (*ii*) development of aberrant neuritic processes with ensuing microgliosis in the SNc and increased ΔFosB staining in the striatum at a young age; and (*iii*) progression to bilateral degeneration of the nigrostriatal axis and of the LC at an older age (model; Fig. 6), which are associated with mild motoric changes. This progression to a bilateral phenotype is of particular interest to us given the typical unilateral-to-bilateral progression of the disease in humans (33). Interestingly, no significant changes were noted in α-synuclein or LRRK2 expression, suggesting a disease process independent of Lewy body generation. These results strongly suggest that this murine model of early parkinsonism mimics autosomal recessive early-onset PD pathology, rather than that of sporadic PD (3). It, thus, provides a tool to elucidate the cascade of pathogenic changes that occurs in autosomal recessive, early-onset PD, as well as a platform to explore neuroprotective interventions in the future.

Experimental Procedures

DJ1-C57 Mouse Creation. DJ-1$^{-/-}$ mice were generated as described previously (9). Mice were subsequently backcrossed 14 times onto a pure C57BL/6J background (Charles River) to obtain DJ1-C57 mice. Animals were then interbred extensively for colony maintenance and experimentation. Animals were kept at 25 °C on a light (12 h)/dark (12 h) cycle with ad libitum access to standard rodent laboratory chow and water. Animal care was carried out in accordance with the guidelines of the Canadian Council and Care of Animals in Research and the Canadian Institutes of Health Research and was approved by the University of Ottawa Animal Care Veterinary Services.

Histology. After being perfused transcardially, mouse brains were fixed in 4% paraformaldehyde and cryoprotected as described elsewhere (34). Midbrain sections containing the SNc (40 μm), pontine sections containing LC (40 μμ), and striatal (14 μm) sections were immunostained via avidin–biotin complex staining as described previously (26).

DA Cell Survival Quantification. DA neuron survival in the SNc was blindly assessed by stereology using Stereo Investigator as described previously (26). Striatal TH quantification was performed at 200×. For each picture, five samples of striatum and one sample of corpus callosum were used for densitometric analysis. Relative intensity of immunodetection was calculated using ImageJ v.1.41o (National Institutes of Health). For each sample, three slices of striatum were used to calculate the mean striatal density.

Neuritic Beading Measurement. Neuritic beading was measured using ImageJ. Briefly, average length of uninterrupted process in a visually focused plane

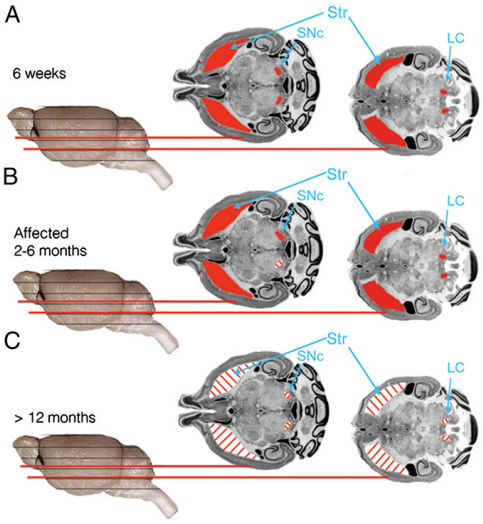

Fig. 6. DJ1-C57 preclinical model of DA neurodegeneration. (*A*) Altered representative micrographs reproduced with permission from the Mouse Brain Library [www.mbl.org; Rosen et al. (36)] depicting healthy (red) SNc, striatum, and LC in 6-wk-old DJ1-C57 mice or all WT groups examined. (*B*) Affected DJ1-C57 mice demonstrate unilateral DA cell loss in the SNc but not in the LC. (*C*) Aged DJ1-C57 mice exhibit widespread degeneration in their nigrostriatal tract, as well as their LC.

was measured as 20 measurements/section and measuring three sections per animal. Raw data were then binned into five categories of length and represented as percentage distribution.

ΔFosB and CD11b Measurement. Striatal (ΔFosB) and midbrain [cluster of differentiation (CD)11b] sections were stained, and three pictures were taken per animal, per side. Puncta in a given visual field were assessed blindly using ImageJ v1.41o.

Locus Ceruleus Neuron Quantification. Noradrenergic cell survival in the LC was measured by counting four representative sections and projecting their counts to a total value as described previously (35).

CV Quantification. CV staining and quantification were performed as described previously (26). Briefly, cell viability in the medial terminal nucleus (MTN) region of the midbrain was assessed as per the nuclear integrity of the cells present.

Antibodies Used. CD11b (1:200; AbD Serotec), FosB (1:250; Santa Cruz Biotechnologies), glial fibrillary acidic protein (GFAP) (1:1,000; Cell Signaling), DJ-1 (1:50,000; Abcam), α-synuclein (1:1,000; BD Transduction), LRRK2 (1:50,000; Epitomics), and TH (1:10,000; Immunostar or 1:2,000; Chemicon) were used for either avidin–biotin complex (ABC) visualization by 3,3′-diaminobenzidine (DAB) or via fluorophore-conjugated secondary antibody.

Motor Behavior Testing. The grid test was carried out by placing DJ1-C57 affected, unaffected, and WT mice on a metal grid (0.5-cm spacing between metal wires) and then turning the grid over for 60 s. If a mouse could hold on for the entire 60 s, it was scored as "success," whereas if it fell before the set time, it was scored as a "fail." The pole test was used to measure the latency to descent an 18-inch pole wrapped in gauze.

Exome Sequencing. Genomic DNA (6 μg) was isolated from ear samples of affected/unaffected mice using the DNeasy Blood and Tissue kit (Qiagen). Samples underwent targeted exome capture using the Agilent SureSelectXT Mouse All Exon kit and subsequently underwent next-generation sequencing via an Illumina HiSeq 2000 sequencer. Raw data were aligned to the mouse genome, and variants were called using the Broad Institute GATK (Genome Analysis ToolKit).

Statistical Analysis. Data throughout the paper are expressed as averages ± SEM for a given sample size (*n*). Statistical analysis for histological and behavioral data were performed by means of either a paired *t* test or one-way ANOVA, followed by Tukey's least significant difference (LSD) post hoc test, as indicated in *SI Text* and the figure legends.

ACKNOWLEDGMENTS. We thank the University of Ottawa Faculty of Medicine Behavior Core Facility for use of their equipment; Daniele Merico (Centre for Applied Genomics, Hospital for Sick Children) for assistance with bioinformatics analysis of the exome data; and Linda Jui, Mirela Hasu, Steve M. Callaghan, Carmen Estey, Elizabeth Abdel-Messih, and Hossein Aleyasin for technical assistance and scientific input. This work was supported by grants from Parkinson Society Canada; the Canadian Institutes of Health Research; the Centres of Excellence in Neurodegeneration (COEN); the Heart and Stroke Foundation of Ontario (HSFO); the Neuroscience Canada/Krembil Foundation; the Parkinson's Disease Foundation; The Michael J. Fox Foundation for Parkinson's Research; the Parkinson Research Consortium (PRC); the Canadian Stroke Network; the Heart and Stroke Foundation of Canada (HSFC) for Stroke Recovery; and the World Class University Program through the National Research Foundation of Korea, funded by Ministry of Education, Science, and Technology, South Korea Grant R31-2008-000-20004-0 (to D.S.P.). D.S.P. is a recipient of the HSFO Career Investigator Award. M.W.C.R. is a recipient of the HSFC Focus on Stroke Award, as well as the Canadian Institutes of Health Research (CIHR) Training Program in Neurodegenerative Lipidomics Supplement Scholarship. P.C.M. is a recipient of The PRC Toth Family Fellowship in Parkinson's Research.

1. Bonifati V, et al. (2003) Mutations in the DJ-1 gene associated with autosomal recessive early-onset parkinsonism. *Science* 299:256–259.
2. Hague S, et al. (2003) Early-onset Parkinson's disease caused by a compound heterozygous DJ-1 mutation. *Ann Neurol* 54:271–274.
3. Kitada T, Tomlinson JJ, Ao HS, Grimes DA, Schlossmacher MG (2012) Considerations regarding the etiology and future treatment of autosomal recessive versus idiopathic Parkinson disease. *Curr Treat Options Neurol* 14:230–240.
4. Ramsey CP, Tsika E, Ischiropoulos H, Giasson BI (2010) DJ-1 deficient mice demonstrate similar vulnerability to pathogenic Ala53Thr human alpha-syn toxicity. *Hum Mol Genet* 19:1425–1437.
5. Andres-Mateos E, et al. (2007) DJ-1 gene deletion reveals that DJ-1 is an atypical peroxiredoxin-like peroxidase. *Proc Natl Acad Sci USA* 104:14807–14812.
6. Chandran JS, et al. (2008) Progressive behavioral deficits in DJ-1-deficient mice are associated with normal nigrostriatal function. *Neurobiol Dis* 29:505–514.
7. Chen L, et al. (2005) Age-dependent motor deficits and dopaminergic dysfunction in DJ-1 null mice. *J Biol Chem* 280:21418–21426.
8. Goldberg MS, et al. (2005) Nigrostriatal dopaminergic deficits and hypokinesia caused by inactivation of the familial Parkinsonism-linked gene DJ-1. *Neuron* 45:489–496.
9. Kim RH, et al. (2005) Hypersensitivity of DJ-1-deficient mice to 1-methyl-4-phenyl-1,2,3,6-tetrahydropyrindine (MPTP) and oxidative stress. *Proc Natl Acad Sci USA* 102:5215–5220.
10. Manning-Boğ AB, et al. (2007) Increased vulnerability of nigrostriatal terminals in DJ-1-deficient mice is mediated by the dopamine transporter. *Neurobiol Dis* 27:141–150.
11. Pham TT, et al. (2010) DJ-1-deficient mice show less TH-positive neurons in the ventral tegmental area and exhibit non-motoric behavioural impairments. *Genes Brain Behav* 9:305–317.
12. Dawson TM, Ko HS, Dawson VL (2010) Genetic animal models of Parkinson's disease. *Neuron* 66:646–661.
13. Parkinson Study Group PRECEPT Investigators (2007) Mixed lineage kinase inhibitor CEP-1347 fails to delay disability in early Parkinson disease. *Neurology* 69:1480–1490.
14. Waldmeier P, Bozyczko-Coyne D, Williams M, Vaught JL (2006) Recent clinical failures in Parkinson's disease with apoptosis inhibitors underline the need for a paradigm shift in drug discovery for neurodegenerative diseases. *Biochem Pharmacol* 72:1197–1206.
15. Snow BJ, et al.; Protect Study Group (2010) A double-blind, placebo-controlled study to assess the mitochondria-targeted antioxidant MitoQ as a disease-modifying therapy in Parkinson's disease. *Mov Disord* 25:1670–1674.
16. Marks WJ, Jr., et al. (2010) Gene delivery of AAV2-neurturin for Parkinson's disease: A double-blind, randomised, controlled trial. *Lancet Neurol* 9:1164–1172.
17. Perl DP (2011) *Neuropathologic Involvement of the Dopaminergic Neuronal Systems in Parkinson's Disease* (Blackwell, Oxford), Chap 2, pp 8–10.
18. Song DD, Haber SN (2000) Striatal responses to partial dopaminergic lesion: Evidence for compensatory sprouting. *J Neurosci* 20:5102–5114.
19. Pritzel M, Huston JP, Sarter M (1983) Behavioral and neuronal reorganization after unilateral substantia nigra lesions: Evidence for increased interhemispheric nigrostriatal projections. *Neuroscience* 9:879–888.
20. Tekumalla PK, et al. (2001) Elevated levels of DeltaFosB and RGS9 in striatum in Parkinson's disease. *Biol Psychiatry* 50:813–816.
21. Doucet JP, et al. (1996) Chronic alterations in dopaminergic neurotransmission produce a persistent elevation of deltaFosB-like protein(s) in both the rodent and primate striatum. *Eur J Neurosci* 8:365–381.
22. Pérez-Otaño I, Mandelzys A, Morgan JI (1998) MPTP-Parkinsonism is accompanied by persistent expression of a delta-FosB-like protein in dopaminergic pathways. *Brain Res Mol Brain Res* 53:41–52.
23. Forno LS, Alvord EC, Jr. (1974) Depigmentation in the nerve cells of the substantia nigra and locus ceruleus in Parkinsonism. *Adv Neurol* 5:195–202.
24. Takeuchi H, et al. (2005) Neuritic beading induced by activated microglia is an early feature of neuronal dysfunction toward neuronal death by inhibition of mitochondrial respiration and axonal transport. *J Biol Chem* 280:10444–10454.
25. Greenwood CE, Tatton WG, Seniuk NA, Biddle FG (1991) Increased dopamine synthesis in aging substantia nigra neurons. *Neurobiol Aging* 12:557–565.
26. Mount MP, et al. (2007) Involvement of interferon-gamma in microglial-mediated loss of dopaminergic neurons. *J Neurosci* 27:3328–3337.
27. Ouchi Y, et al. (2005) Microglial activation and dopamine terminal loss in early Parkinson's disease. *Ann Neurol* 57:168–175.
28. McGeer PL, Itagaki S, Boyes BE, McGeer EG (1988) Reactive microglia are positive for HLA-DR in the substantia nigra of Parkinson's and Alzheimer's disease brains. *Neurology* 38:1285–1291.
29. Whitton PS (2007) Inflammation as a causative factor in the aetiology of Parkinson's disease. *Br J Pharmacol* 150:963–976.
30. Nagatsu T, Sawada M (2005) Inflammatory process in Parkinson's disease: Role for cytokines. *Curr Pharm Des* 11:999–1016.
31. Von Coelln R, et al. (2004) Loss of locus coeruleus neurons and reduced startle in parkin null mice. *Proc Natl Acad Sci USA* 101:10744–10749.
32. Hayashi A, et al. (2004) Positive regulation of phagocytosis by SIRPbeta and its signaling mechanism in macrophages. *J Biol Chem* 279:29450–29460.
33. Pahwa RLK, Koller WC (2003) *Handbook of Parkinson's Disease* (CRC, Boca Raton, FL), 3rd Ed, 597 pp.
34. Crocker SJ, et al. (2001) c-Jun mediates axotomy-induced dopamine neuron death in vivo. *Proc Natl Acad Sci USA* 98:13385–13390.
35. German DC, Liang CL, Manaye KF, Lane K, Sonsalla PK (2000) Pharmacological inactivation of the vesicular monoamine transporter can enhance 1-methyl-4-phenyl-1,2,3,6-tetrahydropyridine-induced neurodegeneration of midbrain dopaminergic neurons, but not locus coeruleus noradrenergic neurons. *Neuroscience* 101:1063–1069.
36. Rosen GD, et al. (2003) Informatics center for mouse genomics: The dissection of complex traits of the nervous system. *Neuroinformatics* 1:327–342.